Laboratory Evaluation of the Constant Rate of Strain and Constant Head Techniques for Measurement of the Hydraulic Conductivity of Fine Grained Soils

by

Amy Lynn Adams

Honours Bachelor of Applied Science in Geological Engineering, Cooperative Program
University of Waterloo, Waterloo, Ontario, Canada (2008)

Submitted to the Department of Civil and Environmental Engineering
in Partial Fulfillment of the Requirements for the Degree of

Masters of Science in Civil and Environmental Engineering

at the

MASSACHUSSETTS INSTITUTE OF TECHNOLOGY

June 2011

Signature of Author.....
Department of Civil and Environmental Engineering
May 6, 2011

Certified by.....
John T. Germaine
Senior Research Associate and Senior Lecturer of Civil and Environmental Engineering
Thesis Supervisor

Accepted by.....
Heidi M. Nepf
Chair, Departmental Committee for Graduate Students

Laboratory Evaluation of the Constant Rate of Strain and Constant Head Techniques for Measurement of the Hydraulic Conductivity of Fine Grained Soils

by

Amy Lynn Adams

Submitted to the Department of Civil and Environmental Engineering on May 6, 2011
in Partial Fulfillment of the Requirements for the Degree of
Masters of Science in Civil and Environmental Engineering

ABSTRACT

This thesis evaluates the constant rate of strain and constant head techniques for measurement of the hydraulic conductivity of fine grained soils. A laboratory program compares hydraulic conductivity measurements made using both measurement techniques on a total of 12 specimens.

Both resedimented and intact materials covering a wide range of plasticity are investigated. Specific material types include Boston Blue Clay, San Francisco Bay Mud, Maine Clay, Ugnu Clay and Kaolinite.

Constant rate of strain (CRS) and constant head tests were conducted in a standard Trautwein CRS device modified to allow control of the base pore pressure for constant head testing. A flexible wall permeameter device was used to perform constant head hydraulic conductivity testing on two specimens; this allowed for comparison with the constant head measurements made in the CRS device.

A bottom seating error was found in the CRS device. Bottom seating error occurs during set up when the top of the base porous stone is not flush with the bottom of the rigid specimen ring, causing a gap to form between the specimen and the porous stone. A bottom seating error translates into a strain error, which affects both the measured CRS compression and hydraulic conductivity results. Bottom seating error can be avoided using a modified set up procedure.

Void ratio errors are sometimes noted between the void ratio measured in the CRS device and that measured upon removal from the CRS device. These errors are likely resultant from specimen swelling following load removal.

Based on comparison to the results of an interlaboratory study into the reproducibility of the saturated hydraulic conductivity measured in a flexible wall permeameter, the CRS and constant head techniques were found to measure the same hydraulic conductivity. This conclusion is independent of specimen origin, i.e. resedimented or intact. The CRS and constant head techniques measure the same average hydraulic conductivity even when non uniformities are present, provided the non uniformities are continuous and oriented perpendicular to the axial loading direction.

Thesis Supervisor: John T. Germaine
Title: Senior Research Associate and Senior Lecturer of Civil and Environmental Engineering

ACKNOWLEDGEMENTS

I would like to thank my thesis supervisor and research advisor, Dr. John T. Germaine, for the countless hours of time and effort that he has dedicated to my success at MIT thus far. His extraordinary patience has been a delight throughout the last two years. He always manages to find time to help not only myself, but every other student who knocks on his overly beaten door. On paper, his responsibility is to act as a thesis and research advisor, but Dr. G's position is better described as a mentor, role model and trusted friend.

The MIT faculty are the best of the best, and I am grateful to have the opportunity to learn from them. Aside from Dr. G, Professor Andrew J. Whittle, Professor Herbert H. Einstein, and Dr. Lucy Jen in particular have instilled in me the academic skills and tools that I will use to further my career. Special thanks are extended to Dr. Lucy Jen for her ongoing mentorship.

The help and friendship of the all of the CEE staff is also appreciated, especially Stephen Rudolph, Sheila Fay and Carolyn Jundzilo-Comer.

I have been fortunate to make many friends over the past two years. I cannot possibly name everybody here; however, special mention goes to my lab group, Brendan Casey, Aiden Horan and Jana Marjanovic, as well as Stephen Morgan, Jay Miller, Nina Panagiotidou, Gonzalo Corral, Sherif Akl, MJ Qomi, and all the other residents of the third floor of building 1. It is a joy to see your smiling faces and share your enthusiasm for your work, day in and night out. I also have many friends from Tang Hall, my residence, with whom I play intramural sports and enjoy social outings. My 'Canadian partners in crime' and the Biology crew have helped me celebrate numerous Canadian holidays and hockey championships. I treasure the friendship of all of these amazing individuals.

I have thoroughly enjoyed playing with the MIT Women's Ice Hockey team since I arrived at MIT. The hard work, dedication and patience exemplified by the members, captains and coaches of this team are something I will strive to emulate in my life. The hockey skills that I am learning through playing with this team will help guide me through all facets of my life: I will bend my knees, keep my head up and keep my stick on the ice; in this way, I will be prepared for whatever comes my way.

To my roommates, Jingnan Lu and Ekaterina (Katya) Vinogradova, and previously Zhenqui (Kay) Wu: you are great friends to me and I will always remember the laughter and tears that we shared in 15A for years to come.

Finally, I would like to thank my family, especially my parents, Cameron and Dianne Adams, for their never ending support and encouragement throughout this seemingly never ending adventure. I would not be where I am today without you standing behind me, cheering me on.

My positive experiences over the last two years have encouraged me to continue my exploration of academia; equipped with the skills that I have acquired thus far, I eagerly await the challenges ahead.

To my father, Cameron R. Adams.

"It is our attitude, not our aptitude, which determines our ultimate altitude."

You taught me that true success requires hard work,

but also that all work and no play makes for a boring person.

I dedicate this thesis to you.

TABLE OF CONTENTS

List of Tables

List of Figures

1 INTRODUCTION

1.1 Background

The constant rate of strain (CRS) approach for soil testing was developed initially as a means of measuring the consolidation properties of a soil, however, it was quickly noted that the CRS method could be used to directly measure the hydraulic conductivity properties of fine grained soils. Because it is easy to automate, the CRS test method offers the advantage of continuous data collection during the loading process. This continuous data stream can be used to generate a void ratio vs. hydraulic conductivity relationship for a soil as opposed to making measurements at a single or a limited number of void ratios.

The original CRS theory was proposed by Smith and Wahls in 1969 by means of an approximate solution. This theory was more rigorously developed in 1970 when Wissa et al proposed both linear and non linear solutions assuming small strains and accounting for both transient and steady state behaviour. Wissa's solution has been further adapted to account for the large strains often induced in laboratory consolidation tests. Because of the many advantages of the CRS test method, it is now a very common test method used to measure both the consolidation and hydraulic conductivity properties of fine grained soils. The CRS method can only be used to measure the hydraulic conductivity of fine grained soils because the hydraulic conductivity must be low enough to induce sufficient excess pore generation at the base of the specimen during loading at a constant rate of strain.

Traditional permeameter methods are also widely used to measure the hydraulic conductivity of all types of materials and are not limited to find grained soils. More common permeameter methods include constant head and falling head tests as well as other less common constant flow tests. Permeameter methods measure the hydraulic conductivity of a soil specimen at a single void ratio; they are founded upon Darcy's law, are simpler to analyze and are not linked to ongoing consolidation behaviour of the soil specimen.

1.2 Research Objectives

The purpose of this research is to compare the results of hydraulic conductivity measurements using both the constant rate of strain (CRS) and constant head measurement techniques to

determine if the these two commonly used methods provide consistent results for a variety of naturally derived fine grained soils including both resedimented and intact materials ranging from low to high plasticity. Both techniques are commonly used in industry as well as in the MIT Geotechnical Laboratory.

The equipment used includes a standard Trautwein CRS device adapted for constant head testing by allowing control of the base pore pressure. The void ratio vs. log hydraulic conductivity relationship for a soil specimen was measured using the CRS test method during loading of a soil specimen, and then following unloading to an over consolidation ratio, the hydraulic conductivity was measured again using the constant head test method. In addition, for some specimens the measured hydraulic conductivity was verified using the constant head method in a flexible wall permeameter.

Initially, Resedimented Boston Blue Clay (RBBC) was tested, and the experimental program was later expanded to include Intact Boston Blue Clay, Intact Maine Clay, Intact San Francisco Bay Mud, Resedimented Kaolinite and Resedimented Ugnu Clay. These materials range from low plasticity clays (e.g. Maine Clay) to relatively high plasticity clays (e.g. San Francisco Bay Mud).

The results from the experimental program were used to analyze the agreement in the measured hydraulic conductivity between the CRS and constant head measurement techniques. The results are also used to analyze specimen swelling potential, which may lead to calculation errors in void ratio and hydraulic conductivity, the effects of non uniformities on the measured hydraulic conductivity, and the differences between resedimented and intact materials.

1.3 Organization

Chapter 2 provides a background summary and literature review covering methods of hydraulic conductivity measurement. A brief summary of permeameter techniques precedes an extensive treatment of the development of different methods of CRS analysis and their associated errors. Finally, a literature review details other relevant studies into the agreement between hydraulic conductivity measurement techniques.

Chapter 3 describes the materials used in this study including the material processing methods applied and the relevant index properties.

Chapter 4 details the equipment and procedures used in carrying out the sample fabrication and hydraulic conductivity testing. A detailed description of the resedimentation procedures, salinity test method, data acquisition system components, and computer automation setup is included in this chapter. Each hydraulic conductivity testing device, including the CRS and flexible wall permeameter, is individually detailed including the relevant drawings and step by step test set up methods.

Chapter 5 presents the data analysis methods used to evaluate the hydraulic conductivity and void ratio in each of the CRS and constant head test methods.

Chapter 6 reports and evaluates the results of two multi-stage and 10 single-stage CRS tests. The hydraulic conductivity of two specimens was additionally measured using the flexible wall permeameter device. This chapter also provides an extensive description of the effect of non uniformities, the effect of specimen swelling on the final specimen height measurements and measured void ratio errors, and finally the agreement of hydraulic conductivity measurement between the CRS and constant head measurement techniques.

Chapter 7 provides a summary of the thesis. The conclusions of the research are summarized and recommendations are made for future research.

2 BACKGROUND

2.1 Hydraulic Conductivity and Permeability

Hydraulic conductivity and permeability are often confused in soil mechanics literature. Hydraulic conductivity is a measure of the rate of flow of a particular fluid through a medium and its value varies as function of the fluid and the medium. Permeability, sometimes termed intrinsic permeability, is a property of the medium itself and is not related to the fluid flowing through the fabric. The hydraulic conductivity and permeability can be related by equation 2-1:

$$K = \frac{k\rho g}{\mu} \tag{2-1}$$

Where:

K is the hydraulic conductivity [L/T];
k is the [L^2], ρ is the density of the fluid [M/L^3];
g is the gravitational constant [L/T^2]; and
μ is the dynamic viscosity [M/LT].

Assuming constant fluid properties, the hydraulic conductivity and permeability are directly proportional. For the purposes of this paper, and to avoid confusion between geoscience and geoengineering conventions, the term hydraulic conductivity will be used when referring to flow specific data, and permeability will be used to refer to fabric specific properties.

2.2 Early History of Hydraulic Conductivity Testing

Henri Darcy, a civil engineer made famous for his discoveries relative to fluid flow, in particular the Darcy-Weisbach equation for pipe flow and Darcy's law for flow through porous media, was an engineer interested in quantifying the hydraulic conductivity of soils. He was the first to make systematic measurements of the flow through porous media investigating the flow of water through sand and filters for use in water filtration (Darcy, 1856). His definition of Darcy's law, describing the rate of saturated fluid flow through porous media, paved the way for modern hydraulic conductivity testing and is the basis for most any steady-state analysis used today. Darcy's law applies for saturated flow.

2.3 Types of Hydraulic Conductivity Tests

There are many different types of hydraulic conductivity tests that are suited to different types of soils, testing time scales, and laboratory or field setups. The most common methods include constant and falling head boundary conditions; these methods are described in detail herein. Other methods that have been developed include constant flow, constant volume variable head, and constant head constant volume tests (Germaine, 2009)

A permeameter is a laboratory device used to measure the hydraulic conductivity of a material; for each hydraulic conductivity test method there are different permeameter schematics that can be used. A given permeameter setup can often only test a limited range of hydraulic conductivities (i.e. a few orders of magnitude) due to physical constraints, mostly relating to the application of the hydraulic gradient and/or the flow volume required. Because natural hydraulic conductivity values are known to vary by up to 14 orders of magnitude (Germaine, 2009), different permeameters are typically required to test the hydraulic conductivity of different soils, for example a coarse sand and a clay.

2.3.1 Constant Head Tests

A constant head test is a simple, steady state hydraulic conductivity measurement method that is used to evaluate a specimen at a single and constant void ratio. A hydraulic gradient is applied and maintained across a specimen via a differential head at two points. Figure 2-1 shows a schematic constant head test setup (Germaine and Germaine, 2009).

The flow rate can be measured and the hydraulic conductivity computed according to Darcy's Law.

$$k = \frac{Q}{iA} \tag{2-1}$$

Where:

K is the hydraulic conductivity [L/T];
Q is the flow rate through the specimen in [L^3/T];
i is the dimensionless gradient; and
A is the area of flow [L^2/T].

Equation 2-1 applies only once flow has reached steady state; this can be verified by measuring the time variance of flow rate and ensuring that the inflow increment is equal to the outflow increment. Depending on the set up, the gradient i can be measured in different ways; Figure 2-1 measures the gradient using manometers to measure the change in hydraulic head between two points in the system, and the gradient is computed as this change in total head divided by distance between the manometer ports.

2.3.2 Falling Head Tests

The falling head method is another common hydraulic conductivity measurement method. Falling head tests do not require an input tank of constant head, and are applicable to materials over a wide range of hydraulic conductivity, especially those with medium and low hydraulic conductivity. Figure 2-2 shows a schematic drawing of a falling head test setup (Germaine and Germaine, 2009).

The hydraulic conductivity of a soil can be computed in a falling head test by equating the time varying flow rate in the inflow tube to that of the specimen:

$$a\frac{dh}{dt} = kA\frac{h}{L} \tag{2-2}$$

And solving for the hydraulic conductivity, k:

$$k = \frac{aL}{A(t_1 - t_0)} ln\left(\frac{h_o}{h_1}\right) \tag{2-3}$$

Where:

k is the hydraulic conductivity [L/T];
a is the area of the inflow tube [L^2];
A is the area of the specimen [L^2];
L is the length of the specimen [L];
h_0 is the initial height of water in the inflow column at t_o [L]; and
h_t is the height of water in the inflow column after some time t_1 [L}.

Some limitations of the falling head method include the physical height of the inflow tube (typically limited by the ceiling or availability of materials), as well as the effects of capillarity which can reduce the head applied to the specimen. For fine grained soils, in order to increase the gradient without increasing the volume of flow and hence the time duration of

the test, the engineer is tempted to reduce the area of the inflow tube, a. However capillarity effects become important as the area of the inflow column decreases (Germaine and Germaine, 2009) and this effect must be balanced to ensure the measured change in height reflects the change in head applied to the specimen. Unlike the constant head test, where manometers may be used to measure the head difference across a portion of the specimen, there is no method of measuring the actual hydraulic head applied to the specimen as a function of time in a falling head test.

2.3.3 General Comments Related to Permeameter Testing

Some general comments relative to running hydraulic conductivity tests include:

1) Flow through the specimen should be laminar such that Darcy's law remains valid. Head losses can occur in the specimen due to turbulent flow. To ensure laminar flow dominates, multiple gradients should be applied and tested in non-sequential order (neither constantly increasing nor decreasing) and the results plotted in terms of hydraulic conductivity vs. gradient. If significant turbulent head losses are occurring, the hydraulic conductivity will decrease with increasing gradient. Reducing the gradient will help avoid this problem.
2) The head loss throughout the measurement system may not be negligible, and as a result, effort should be made to measure the head loss across the specimen only.
3) The orientation of the specimen relative to gravity is important. Horizontal specimens may settle over the duration of a test, creating a gap between the top of the specimen and the boundary. This gap can act as a flow conduit and give incorrect hydraulic conductivity results; this is especially important for specimens with fixed boundary conditions and coarse grained specimens. Testing a specimen in an inclined or vertical direction can help mitigate this concern.
4) Soil saturation is important as often the saturated hydraulic conductivity is of interest. If backpressure is available, back pressuring the specimen is an optimal solution; if not, letting the permeant flow through the specimen for a period of time to equilibrate will help saturate the system. When initiating flow in an unsaturated specimen, apply the flow slowly. Application of a front of upward

flow helps remove air most efficiently. This allows the fluid front to progress slowly through the specimen, minimizing the chance that air bubbles will become trapped in the pore space.

2.4 Overview of Consolidation-based methods

2.4.1 Incremental Oedometer

Traditionally, incremental oedometer tests were used to obtain the compression characteristics, including the hydraulic conductivity, of cohesive soils. The hydraulic conductivity can be inferred from the computed coefficient of consolidation computed at each load increment.

The incremental oedometer test uses a procedure involving the application of loads using load increment ratios (LIR) of between 0.5 and 1, but more commonly closer to 1, to a specimen trimmed into a rigid ring, placed between two porous stones and submerged in a water bath allowing for double drainage. Figure 2-3 shows a typical incremental oedometer setup (Germaine and Germaine, 2009).

Incremental loads are left for a period of time during which the time deformation curve is measured. Each load increment requires separate analysis to determine the end of primary consolidation strain which is then used to create a compression curve (stress – strain relationship, typically e-log σ' space). Because most tests typically require at minimum 10 or more load increments to define a suitable compression curve, incremental oedometer tests are long in duration and intensive in data analysis.

There are two common analysis techniques used to reduce the time deformation curves for each load increment: root-time and log time methods. Figure 2-4 gives examples of these two methods (ASTM D2435). Each method can be used to compute the coefficient of consolidation for that increment, C_v. Typically however, there is a disagreement between the C_v values obtained from the two methods. Ladd (1996) estimates, based on numerous case histories, that

$$Cv_{root\ time} = 2 +/- 0.5\ Cv_{log\ time} \quad (2\text{-}4)$$

Typically the results from each of the two methods are averaged and the average coefficient of consolidation is reported. This discrepancy in coefficient of consolidation from the two methods is especially important, however, because the hydraulic conductivity computed using the incremental oedometer is based on the coefficient of consolidation:

$$C_v = \frac{k}{m_v \gamma_w} \tag{2-5}$$

Where:

C_v is the coefficient of consolidation [L^2/T];
k is the hydraulic conductivity [L/T];
γ_w is the unit weight of water [M/T^2L^2]; and
m_v is the coefficient of volume compressibility [LT^2/M];

Therefore a scatter in the coefficient of consolidation translates into a scatter in the hydraulic conductivity.

ASTM standard D2435 (Method A) prescribes that loads be left for 24 hours and that readings need only be taken at 0 and 24 hours time; this method, although reducing the amount of data analysis because it does not collect time deformation data, has the potential to incorporate significant secondary compression behaviour into the data set which can cloud the results, typically reducing both the maximum past pressure, σ'_p, and the slope of the virgin compression line in e-logσ' space, c_c. Also, because one does not have detailed time deformation curves at each load increment, the coefficient of consolidation, C_v, which is used to compute the hydraulic conductivity, k, cannot be computed using the two methods detailed in figure 2-4.

Further, only a limited number of stress strain data points are obtained at discrete loading intervals, and these points are spaced at wide, constant stress intervals. This wide spacing is because of the requirement of a relatively high LIR which is necessary to separate the primary consolidation and secondary compression components of each increment. As a result, the overall shape of the compression curve and the compression results are highly dependent on the interpretation of the engineer.

Finally, Incremental oedometer tests are hard to automate, and even if electronic data acquisition systems are installed, extensive data analysis and interpretation is still required to obtain representative compression and hydraulic conductivity characteristics from the data.

2.4.2 Constant Rate of Strain (CRS)

The constant rate of strain (CRS) method offers a rapid means of measuring the consolidation parameters of a soil that is replacing traditional oedometer methods. The CRS technique offers a direct method of computing the hydraulic conductivity of a soil and as such the CRS device can be classified as a permeameter.

Wissa worked at MIT and was one of the first to provide full analytic solutions to reduce CRS test data in 1971 (Wissa et al). Figure 2-5 shows Wissa's standard CRS apparatus. There are a number of different CRS device designs currently available, and custom designs are possible, however figure 2-5 shows a typical device including all required and relevant components.

Like an incremental oedometer, the test specimen is trimmed into a stainless steel ring and is placed between two porous stones. The specimen in the ring is installed within the device and the device filled with fluid. The base of the specimen is sealed from external leaks and the cell pressure via two O-rings. The CRS device offers the ability to backpressure the specimen and control the effective stress in the specimen, a significant advantage over the standard incremental oedometer test. Loading at a constant rate of strain is achieved by moving the piston using a gear driven load frame. The vertical applied load is measured by an external load cell, and the total stress is computed as the sum of the stress associated with the externally applied load, the mass of the piston, cell pressure influences and accounting for piston friction via calibration. Cell pressure causes an applied downward force on the specimen, but also an uplift force on the piston. A pressure transducer located as close as physically possible to the base stone is used to measure the excess pore pressure generated during loading. The excess pore pressure is a key measurement and is used to compute the hydraulic conductivity. One or two LVDT's are attached to the piston to measure the change in specimen height during loading.

Overall, CRS tests offer numerous benefits over incremental oedometer tests for a number of reasons:

1) The time and manpower requirements are significantly reduced in both the testing procedure and data analysis. The exception is for very low permeability soils which require very low strain rates increasing test time to equal or exceed that of the incremental oedometer;
2) The test procedure can be readily automated for computer control and measurement;
3) The engineer can obtain continuous compression data which improves data accuracy and resolution;
4) Secondary compression should not affect the results because the specimen is continuously strained at a constant rate;
5) Data analysis can be easily automated or programmed into a spreadsheet or standalone reduction program;
6) Back pressure saturation of the specimen is easily implemented; and
7) The device can be readily modified and for constant head hydraulic conductivity testing.

As with any testing method, the CRS device does have disadvantages, although it can be argued that the advantages far outweigh any disadvantage.

First, the CRS device does not incorporate periods of secondary compression and hence cannot offer insight into this process. Most notably, it cannot be used to determine the rate of secondary compression, c_α. This parameter is often necessary for projects where long term settlement is a concern, however in reference to hydraulic conductivity measurement this limitation is of little consequence.

Secondly, despite a constant rate of strain, transient conditions do develop upon initial loading until steady state is reached. Wissa et al (1971) offer solutions to deal with this transience (see section 2.3.2.1.2).

The numerous solutions are only applicable within a limited range of generated excess pore pressures which is a direct function of the strain rate. Consequently, low hydraulic conductivity soils must be tested a very low strain rates. ASTM D4186 specifies that the ratio of excess back pressure to the applied total stress ($\Delta u_b/\sigma_t$) should be between 3 and 15%.

Further, the solutions are applicable only to uniform specimens as they assume a uniform axial pore pressure distribution. Specimen non uniformities which alter the uniformity of the axial pore pressure distribution may cause errors with the interpretation of the measured data using the available solutions.

Finally, strain rate effects have been noted by many researchers. Leroueil et al (1983) noted significant changes in the preconsolidation stress as well as the stress strain curve of sensitive clays when tested in the CRS device at different strain rates varying from 0.24 %/hr to 30.6 %/hr (Figure 2-6, Leroueil et al, 1983).

2.4.2 CRS Hydraulic Conductivity Theory

CRS technology was first developed in the late 1960's and early 1970's. In 1959, Hamilton and Crawford proposed the concept of using a constant rate of strain loading to rapidly determine the stress strain relationship (e-logσ') as well as the preconsolidation stress (σ'_p), however they did not present a detailed method of analysis. In 1969 Smith and Wahls proposed an approximate linear solution for constant rate of strain consolidation loading, and in 1971 Wissa et al published a thorough linear solution that accounted for transient effects, in addition to developing a non linear solution. All solutions solve, in some form, for the hydraulic conductivity, the compressibility and the coefficient of consolidation. Other researchers have looked at solutions for different boundary conditions, in particular large strain, including Helm 1987, Lee 1981, Umehara and Zen 1979, Znidarcic et al, 1986 (Gonzalez, 2000).

Yoshikuni et al proposed a linear solution in 1995 that was not based on consolidation theory; this solution was very similar to Wissa's original linear solution, only it was not based on small strains. Gonzalez (2000) did work comparing the results of numerical modelling with no small strain assumption to the results of linear theory analysis assuming small strains and

found a divergence in the hydraulic conductivity results. However, by adjusting the specimen height to account for strain during the test, as was proposed by Yoshikuni et al, and is currently the ASTM standard, linear theory was found to predict the hydraulic conductivity well compared to the numerical simulations.

Since its first introduction, the CRS technique has been adopted in many countries including by the Norwegian Geotechnical Institute in 1980, the American Society for Testing Materials (ASTM) (Standard D4186) in 1982, the French Laboratories des Ponts et Chaussées in 1984 (Gonzalez, 2000).

2.4.2.1 Linear Theory

Linear theory assumes that the soil has a constant coefficient of volume compressibility (m_v) and it is currently the ASTM standard for analysis, although ASTM does not discount nor discourage use of non linear or other theories (ASTM D4186).

2.4.2.1.1 Smith and Wahls's Linear Theory

Smith and Wahls' linear theory applies only to steady state conditions and is modeled after Terzaghi's basic theory of consolidation. The following assumptions are adopted for linear theory:

1) The soil is homogenous and saturated;
2) Both the soil particles and pore fluid are incompressible relative to the soil skeleton;
3) Drainage occurs only in the vertical direction;
4) Darcy's law for flow through porous media applies; and
5) In a horizontal plane, both the total and effective stresses are uniform (i.e. differences in stress occur in the vertical direction only);

Assuming continuity of flow through a soil element, the basic consolidation equation is:

$$\frac{\partial}{\partial z}\left(\frac{k}{\gamma_w}\frac{\partial u}{\partial z}\right) = \frac{1}{1+e}\frac{\partial e}{\partial t} \qquad (2\text{-}6)$$

Where:

Z is the vertical coordinate of the soil element [L];
K is the hydraulic conductivity [L/T];
γ_w is the unit weight of water [M/T^2L^2];
u is the excess pore pressure [M/T^2L];
t is the time[T]; and
e is the void ratio.

The hydraulic conductivity is known to be a function of the void ratio, and by assuming it as such, K becomes a function only of time and is independent of the vertical position in the control volume. Following this, the assumption that the change in void ratio with time is small can be made; this is a small strain assumption. If the strain rate is constant, because specimens are confined and strain is 1D only, the rate of volume change is constant and therefore the rate of change in void ratio e, $\frac{\partial e}{\partial t}$, is also constant. Incorporating these assumptions, Smith and Wahls present the solution for the excess pore-water pressure at the base of the specimen as a function of the relationship between the hydraulic conductivity and the void ratio as:

$$\Delta u_b = \frac{\gamma_w s H^2}{k(1-e_{avg})}\left(\frac{1}{2} - \frac{b}{12s}\right) \tag{2-7}$$

Where:

Δu_b is the excess pore pressure measured at the base of the specimen [M/T^2L];
s is the rate of change of the average void ratio, $\frac{\partial e_{avg}}{\partial t}$ [1/T];
H is the height of the specimen at time t [L];
e_{avg} is the average void ratio at time t [];
k is the hydraulic conductivity [L/T];
b is a constant relating to the variation of void ratio with depth and time; and
b/s is a dimensionless ratio that relates to the change in void ratio with depth.

The above equation can be used to solve directly for the hydraulic conductivity knowing the s and b parameters, and the coefficient of consolidation can be computed according to equation 2-5. The s parameter can computed at any point during the test as the rate of change in the average void ratio, however b is a material specific constant. The ratio b/s can vary from 0 to 2, but this value must be known or assumed to compute the hydraulic conductivity of the specimen. As a result, equation 2-7 is considered a partial solution because it cannot be applied directly to device measurements to compute the hydraulic conductivity and consolidation parameters of a specimen.

2.4.2.1.2 Wissa's Linear Theory (Gonzalez, 2000)

Wissa et al developed a more through solution to Smith and Wahl's linear theory in 1971. The major difference between the solutions is that Wissa et al's solution is a complete solution whereas Smith and Wahls presented a partial solution.

Transient conditions occur when the piston begins loading. Wissa et al showed that transient conditions exist below a dimensionless time factor, Tv, of 0.5 and that steady state occurs when $Tv \geq 0.5$. Wissa proposed a method of calculating Tv as a function of F_3:

$$F_3 = \frac{(\sigma_v - \Delta u_b) - \sigma_{v,t=0}}{\sigma_v - \sigma_{v,t=0}} \tag{2-8}$$

Where:

σ_v is the vertical effective stress at a given time [M/T^2L];
Δu_b is the excess pore pressure at the base of the specimen at time t [M/T^2L]; and
$\sigma_{v,t=0}$ is the initial vertical effective stress, prior to loading [M/T^2L].

F_3 is a non linear function of Tv, and consequently Tv can be found either via iteration or graphically (Figure 2-7). In general, $F_3 < 0.4$ when $Tv < 0.5$ is the limit of transience. Gonzalez (2000) verified experimentally that this limit holds well for Resedimented Boston Blue Clay (RBBC) and Resedimented Vicksburg Buckshot Clay (RVBC).

In order to simplify Smith and Wahl's linear theory, and to include an initial transient portion followed by a steady state portion, Wissa et al (1971) refined the assumptions as follows:

1) Infinitesimal strains exist;
2) The coefficient of consolidation (Cv) is constant with a variation in hydraulic conductivity (k) and coefficient of volume compressibility (m_v) (this is consistent with Terzaghi's theory);
3) Flow and deformation occur in the vertical direction only;
4) Both the soil particles and pore fluid are incompressible relative to the soil skeleton; and
5) The soil is completely saturated.

The new governing equation for consolidation, similar to that of Terzaghi but formulated in terms of strain instead of pore pressures, becomes:

$$c_v \frac{\partial^2 \varepsilon}{\partial z^2} = \frac{\partial \varepsilon}{\partial t} \tag{2-9}$$

Where:

Cv is the coefficient of consolidation [L^2/T];
ε is the vertical strain [];
z is the vertical coordinate of a point[L]; and
t is the time[T].

The solution to equation 2-9 is in the form of strain as a function of the time factor, Tv, and X, a dimensionless spatial variable equal to z/H:

$$\varepsilon(X, T_v) = \dot{\varepsilon} t[1 + F(X, T_v)] \tag{2-10}$$

Where:

ε is the strain at a given location and time defined by X and Tv;
X is a dimensionless spatial variable equal to z/H;
z is the vertical coordinate (z=0 at top of the specimen, 0<z<H) [L];
H is the height of the specimen, also equal to the drainage distance [L];
$\dot{\varepsilon}$ is the strain rate, $\frac{\Delta \varepsilon}{\Delta t}$ [1/T];
Tv is the dimensionless time factor, equal to $\frac{c_v t}{H^2}$ [];
Cv is the coefficient of consolidation [L^2/T];
t is the actual time [T]; and

$$F(X, T_v) = \frac{1}{6T_v}(2 - 6X + 3X^2) - \frac{2}{\pi^2 T_v} \sum_{n=1}^{\infty} \left[\frac{\cos n\pi X}{n^2} \exp\left(-n^2 \pi^2 T_v\right) \right]. \tag{2-11}$$

Equation 2-11 is a complex relation that involves two components of strain, one related directly to the strain rate, and one related to the dimensionless factor F(X,Tv). F(X,Tv) in itself is a complex expression that both describes the steady state and transient portions of the strain distribution.

The effective stress in the specimen was defined by Wissa et al (1971) for steady state conditions as:

$$\sigma'_v = \sigma_v - \frac{2}{3} \Delta u_b \tag{2-12}$$

Where:

σ'_v is the effective vertical stress in the specimen [M/T^2L];
σ_v is the total vertical stress in the specimen[M/T^2L]; and
Δu_b is the measured excess pore pressure at the base of the specimen[M/T^2L].

Wissa et al noted that because the strain rate is constant through the specimen, the rate of change in both the vertical stress and the pore pressure distribution must also be constant. This can be combined to formulate a stress - strain relation for the soil in terms of the coefficient of volume compressibility, m_v:

$$m_v = \frac{\Delta\varepsilon_v}{\Delta\sigma_v} = \dot{\varepsilon}\frac{\Delta t}{\Delta\sigma_v} \tag{2-13}$$

The difference in stain at the top and bottom of the specimen at a given point in time can be computed using equations 2-10 and 2-11. The difference in stress between the top and bottom of the specimen is the excess pore pressure measured at the base of the specimen. Substituting these boundary conditions into equation 2-13, a relation for the hydraulic conductivity of the specimen may be obtained:

$$k_v = \frac{\dot{\varepsilon}H^2\gamma_w}{2\Delta u_b} \tag{2-14}$$

Where:

k_v is the vertical hydraulic conductivity [L/T];
$\dot{\varepsilon}$ is the strain rate, $\frac{\Delta\varepsilon}{\Delta t}$ [1/T];
H is the initial height of the specimen [L];
γ_w is the unit weight of water [M/T^2L^2]; and
Δu_b is the measured excess pore pressure at the base of the specimen[M/T^2L].

Because of the infinitesimal strain assumption, Wissa uses H, the initial height of the specimen and assumes that this remains constant throughout the test. Wissa's linear equation can be modified for large strains using equation 2-15:

$$k_v = \frac{\varepsilon\dot{H_o}H\gamma_w}{2\Delta u_b} \tag{2-15}$$

Where:

H_o is the initial height of the specimen [L];
H is the height of the specimen at any point in time [L]; and
All other variables are defined above for equation 2-14.

2.4.2.1.3 Yoshikuni et al's Linear Theory

Yoshikuni et al (1995) proposed a method of computing the hydraulic conductivity using the CRS device which does not utilize any consolidation theory. Consequently, they proposed that the CRS test be considered a multi-purpose hydraulic conductivity and consolidation test and that the hydraulic conductivity analysis be decoupled from consolidation analysis.

In order to decouple the hydraulic conductivity calculation from traditional consolidation theory, assuming steady state is reached in an 'engineering' sense rather than a mathematical sense, Yoshikuni et al (1995) described the strains in the specimen by:

$$\frac{\partial \varepsilon(z,t)}{\partial t} = \frac{d\dot{\varepsilon}(t)}{dt} = \frac{R}{H} \tag{2-16}$$

Where:

ε(z,t) is the strain at location z and time t;
$\dot{\varepsilon}(t)$ is the average strain at time t;
H is the thickness of the specimen [L]; and
R is the rate of displacement [L/T].

If Darcy's law is assumed to be valid and the hydraulic conductivity is assumed to be uniform across the specimen height (i.e. the void ratio is uniform), from the continuity equation for flow through a soil element can be written as:

$$\frac{\partial \varepsilon}{\partial t} = -\frac{k}{\gamma_w}\frac{\partial^2 u}{\partial z^2} \tag{2-17}$$

Where:

ε is the strain;
t is the time [T];
k is the hydraulic conductivity [L/T];
γ_w is the unit weight of water [M/T^2L^2];

u is the pore pressure [M/T^2L]; and
z is the vertical coordinate of a point in the specimen [L].

Solving this equation is achieved by applying the following boundary conditions

1) u =0 at z=0;
2) $\frac{\partial u}{\partial z}$=0 at z=H;

And setting u at z=H equal to u_b, the measured pore pressure at the base, the equation can be written to solve for the hydraulic conductivity:

$$k(t) = \frac{\gamma_w RH(t)}{2u_b(t)} \tag{2-18}$$

Which, when written in terms of the average strain rate, $\dot{\varepsilon}$, becomes

$$k_v = \frac{\dot{\varepsilon} H_1 H_2 \gamma_w}{2\Delta u_b} \tag{2-19}$$

Where:
H_1 is the initial specimen height (H_o), [L]; and
H_2 is the specimen height for a given time, corrected for apparatus compressibility [L].

Equation 2-19 above is the same as Wissa's equation modified for large strains (equation 2-15).

2.4.2.1.4 Comparison of Linear Theories and ASTM Standard

As mentioned, Gonzalez (2000) compared the hydraulic conductivity results of three different variations of Wissa's linear equation (equation 2-14, and modified version, 2-15) using different H values with numerical modelling results. He compared equations (figure 2-8) using the initial specimen height as per Wissa's original equation (Eqn 1-14 in figure 2-8) , the original specimen height corrected for apparatus compressibility (Eqn 1-30 in figure 2-8), as well as a function of the initial specimen height and the current specimen height corrected for apparatus compressibility, as per Wissa's equation modified for large strain and Yoshikuni et al's equation (Eqn 1-31 in figure 2-8), and found that the best results were given when the actual height of the specimen was incorporated into the relation, given in equation 2-15 and 2-19 (Eqn 1-31 in figure 2-8).

ASTM Standard D4186 has adopted this definition of the hydraulic conductivity, given in equation 2-19, for steady state conditions, i.e. where F > 0.4.

Therefore, the CRS device can be used to directly compute the hydraulic conductivity of the specimen, and this calculation can be thought of as based either on consolidation theory or on Darcy's Law and strain rate. The consolidation parameters can thus be computed from the hydraulic conductivity by substituting equation 2-5 into equation 2-19:

$$c_v = \frac{H_1 H_2}{2\Delta u_b} \frac{\Delta \sigma_v}{\Delta t} \tag{2-20}$$

Where all variables have been previously defined.

2.4.2.2 Other CRS Theories

Many other CRS theories exist, including Wissa's non linear theory, as well as the isochrone method proposed by Sheahan and Watters (1997).

Wissa's non linear theory assumes that the soil has a constant compression index, C_c (ASTM D4186). Gonzalez (2000) did much work investigating the differences between non linear and linear theory and found that there were not significant deviations when the excess pore pressure generated at the base was kept below 15% of the total applied stress (i.e. $\Delta u_b/\sigma_t$ <0.15). Table 2-1, modified from Gonzalez (2000) summarizes different researcher's recommendations of the value of $\Delta u_b/\sigma_t$. Figure 2-9 plots the difference in computed hydraulic conductivity measured for RVBC using linear and non linear theories as a function of the excess pore water pressure ratio at the base of the specimen (Gonzalez, 2000). For pore water pressure ratios below 15%, the linear theory predicts hydraulic conductivity 10% higher than the non linear theory, and the differences between the theories follows the theoretically computed difference. As such, non linear theory is not further discussed herein and the reader is referred to Gonzalez's 2000 SM thesis for further information.

Sheahan and Watters (1997) proposed an isochrone method, basically involving direct integration of the pore pressures measured throughout the specimen as opposed to that measured solely at the base of the specimen. They modified a CRS device to allow measurement of the pore pressure at three different locations within the specimen (Figure 2-

10) and ran tests on specimens of RBBC at three different strain rates: 0.1%, 1% and 3% per hour. They compare the results to Wissa's non-linear theory and find little deviation for strain rates generating excess pore water pressures at the base of the specimen up to 70% of the initial pore water pressure. However, it is important to note that their comparative measure is in reference to the original pore water pressure at the base of the specimen and not the total applied vertical stress, as are most researcher recommendations in Table 2-1, and that they base their analysis on comparison to conventional incremental oedometer results which are heavily based on data interpretation between measurement points. They also do not compare their results to the results of linear theory and, as Gonzalez has shown, there are significant deviations between the two theories for some clays as the excess pore pressure increases.

2.5 Other Research into Hydraulic Conductivity Theory Agreement

2.5.1 Moriwaki and Umehara - CRS, Constant flow, Oedometer Tests

Moriwaki and Umehara (2003) present a study where they compare the results of CRS permeability tests using the linear theory, oedometer consolidation tests using a closed cell, and constant flow hydraulic conductivity tests in the oedometer cell after each load increment. In order to run a constant flow hydraulic conductivity test in the oedometer cell they waited until the pore pressure had stabilized after each loading increment and then applied a constant flow via a flow pump which was installed in a load frame. Figure 2-11 shows a schematic drawing of their flow pump device and figure 2-12 shows their setup for running constant flow tests through the oedometer device.

Figure 2-13 shows the results of three methods of hydraulic conductivity testing for resedimented Hiroshima and Maizuru clay and natural Fukuyama and Nagasaki clay tested by Moriwaki and Umehara. Two different specimens are tested for each soil, one in the CRS cell, producing the CRS curve, and one in the oedometer apparatus, producing two data sets each of oedometer and constant flow permeabilities.

The constant flow tests were run at the end of each load increment during the oedometer test at two flow rates: 2.82 mm^3/min (K_{per1}) and 5.65 mm^3/min (K_{per2}). For the oedometer tests, the hydraulic conductivity was computed using two methods: Method 1 ($k_{OED,STD}$) is the

hydraulic conductivity computed according to equation 2-5. Method 2 ($k_{OED,MOD}$) modified the Cv in equation 2-5 value using the ratio end of primary to 24 hour strain:

$$C_v' = C_v \frac{\varepsilon_{EOP}}{\varepsilon_{24}} \tag{2-21}$$

Where:

C'_v is the modified coefficient of consolidation [L^2/T] computed using 24-hour strain;
C_v is the computed coefficient of consolidation [L^2/T] using the $\sqrt{t}$ method;
ε_{EOP} is the $\sqrt{t}$ method end of primary strain; and
ε_{24} is the strain after 24 hours.

This method of adjusting the coefficient of consolidation for the oedometer results by the ratio of the end of primary to 24 hour strain was originally proposed by Mikasa and Ohnishi in 1981 (Moriwaki and Umehara, 2003) to allow lab measured consolidation processes to be applied the field.

2.5.2 Dewhurst et al - CRS vs. Constant Flow Tests

Dewhurst et al (1996) present results from a single incremental consolidation test on a high plasticity silty clay (CH) on which constant flow tests were performed at each load interval. Loading between intervals was achieved via CRS loading techniques. Specimens were allowed to equalize for 24 hours following each CRS loading sequence prior to constant flow testing. Figure 2-14 presents the results plotted as hydraulic conductivity vs. vertical effective stress.

2.5.3 Tavenas et al - The Permeability of Natural Soft Clays

Tavenas et al (1983) performed extensive hydraulic conductivity testing on natural soft clays from Canada, USA and Sweden. They employed the constant head technique in the triaxial cell, as well as falling head technique in the oedometer apparatus.

2.5.3.1 Triaxial Constant Head Tests

In the triaxial device, Tavenas et al (1983) looked carefully at the sources of error associated with long duration hydraulic conductivity testing. They identified three key sources of error including external leakage, osmotic leakage through the membrane between the cell pressure

and specimen, and long term volume change error associated with application of the gradient and secondary compression. The first of these errors can be mitigated by limiting the number of connections and ensuring things are properly tightened and seated. The use of an immiscible cell fluid, such as silicone oil, prevents osmosis and diffusion through the membrane, and pre-saturation of the membrane with the permeant prevents losses to the membrane during the test. Finally, waiting for a period of 2 days to one week following the application of a constant head gradient prior to measurement of the hydraulic conductivity was found to help alleviate errors associated with specimen volume change.

In an attempt to prove the validity of Darcy's law in the face of supposition of threshold gradients, Tavenas et al tested different soils at different gradients and plotted the velocity - gradient relationship. If Darcy's law is valid, equation 2-21 should hold:

$$v = ki \tag{2-22}$$

Where:

v is the flow velocity [L/T];
k is the hydraulic conductivity [L/T]; and
i is the hydraulic gradient [].

Figure 2-15 (Tavenas et al, 1983) gives the results for three clays including Mattagami clay, Louiseville clay and Atchafalaya clay. A straight line drawn through the results for each clay intersects the plot at the origin suggesting that Darcy's law is valid for constant head testing in clays for a range of applied gradients of 0.1-50 within the accuracy of the test installation and interpretation. Therefore, if a threshold gradient does exist, it must be very small. Tavenas et al (1983) postulate that this result is of practical interest because it shows that hydraulic conductivity tests may be run at high gradients to maximize flow and minimize leakage and other detrimental effects such as those related to consolidation volume change.

2.5.3.2 Oedometer Falling Head Tests

Tavenas et al (1983) also performed falling head tests in the oedometer device. The errors associated with this test, resultant from swelling of the specimen due to gradient variation, were measured to be less than that associated with constant head tests in the triaxial device. As a result, the specimen was allowed to swell freely during the falling head tests. Figure 2-

16 compares the results of hydraulic conductivity measurements made in the oedometer cell using the falling head technique with those made in the triaxial cell on the same material but a different specimen using constant head techniques at the same void ratio. The 1:1 line is indicated.

Tavenas et al also performed CRS tests and compared them to results of falling head tests. They cite one example, given in Figure 2-17, for Louiseville clay where the hydraulic conductivity measured using the CRS device is much higher than that measured using falling head tests in the oedometer device when the stress is in excess of the preconsolidation stress, σ'_p. Tavenas et al hypothesize that this deviation is due to an increase in the exit gradient at the base of the specimen beyond the preconsolidation stress related to non uniform stress and pore pressure distributions that develop in the soil as the yield surface is approached. This results in a non uniform void ratio distribution in the soil, with the void ratio near the base of the specimen where the excess pore pressure is measured and the hydraulic conductivity calculation is made not being representative of the average void ratio in the specimen. The calculated hydraulic conductivity is overestimated in the region of the preconsolidation stress. This combination of phenomena contribute to a computed void ratio vs. hydraulic conductivity relationship that is different than the actual relationship measured using falling head tests, as is show in on figure 2-17

Table 2-1: Recommended values of ratio of excess pore water pressure at the base of the specimen and applied total stress, Δub/σt (adapted from Gonzalez, 2000)

$\Delta u_b/\sigma_{vt}$	Soil Tested	Reference
0.50	Kaolinite, Ca Montmorillonite, Messena Clay	Smith and Wahls, 1969
0.02-0.05	Boston Blue Clay (BBC)	Wissa et al, 1971
0.1-0.15	Bakebol Clay	Sallfors, 1975
0.3-0.5	Kentucky Soils	Gorman et al, 1978
0.15	Singapore Marine Clay	Lee et al, 1993
0.70[1]	Resedimented Boston Blue Clay (RBBC)	Sheahan and Watters, 1997
<0.15	RBBC and Resedimented Vicksburg Buckshot Clay (RVBC)	Gonzalez, 2000
0.03-0.15	N/A	ASTM Standard D4186-06

(1) Value reported is the ratio of $\Delta u_b/u_b$, equal to the ratio of the maximum excess pore water pressure at the base to the original base pore water pressure prior to loading.

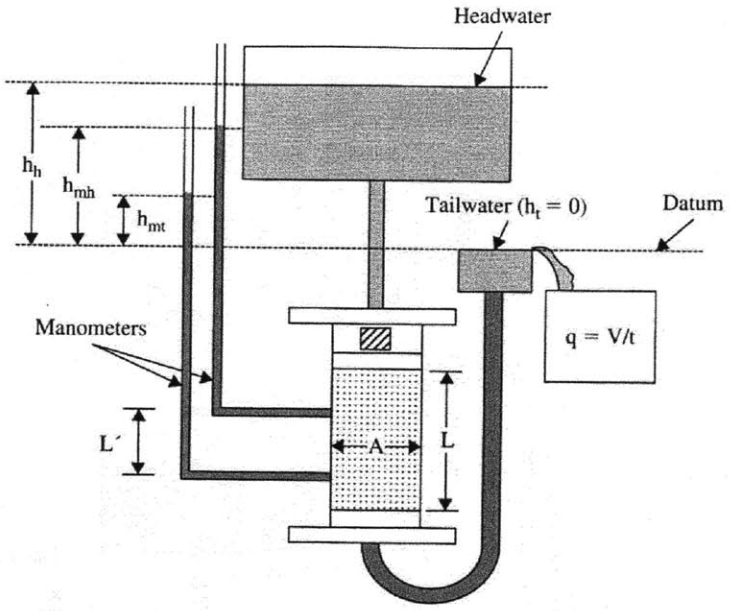

Figure 2-1: Schematic diagram showing a constant head test with downward flow through the system. (Germaine and Germaine, 2009) Sideport manometers are included to measure the head loss through the specimen and disclude system head losses

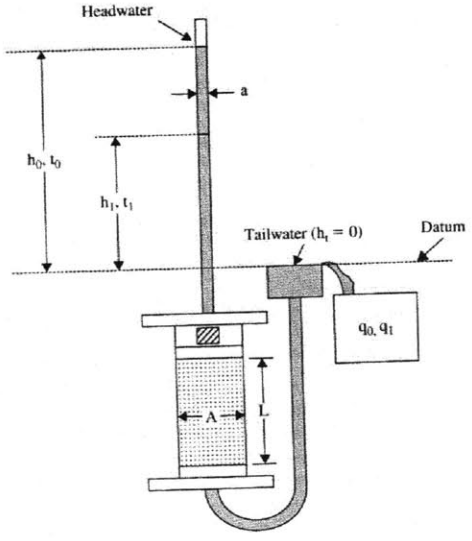

Figure 2-2: Schematic diagram showing a falling head test (Germaine and Germaine,2009)

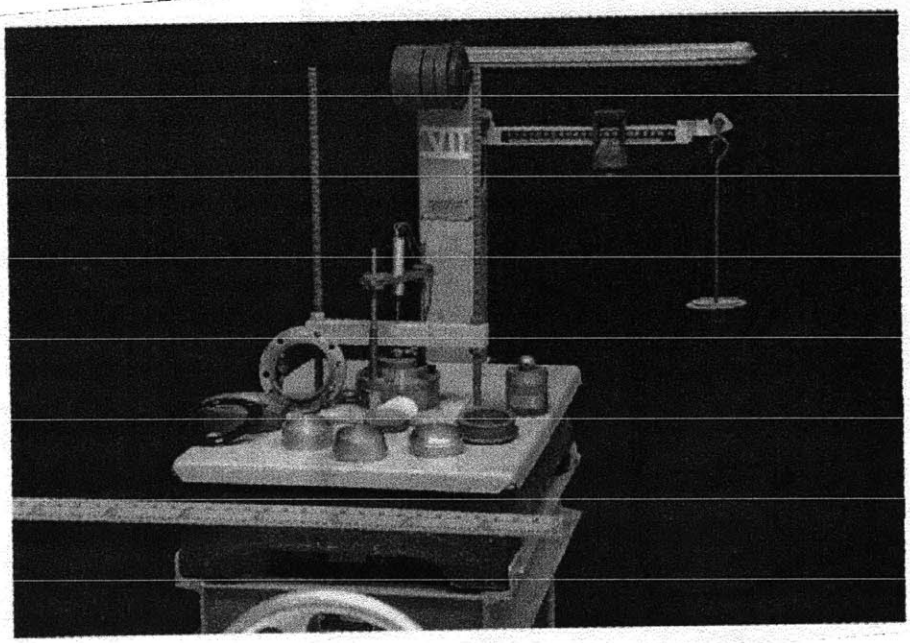

(a) Typical Setup with loading frame and all components

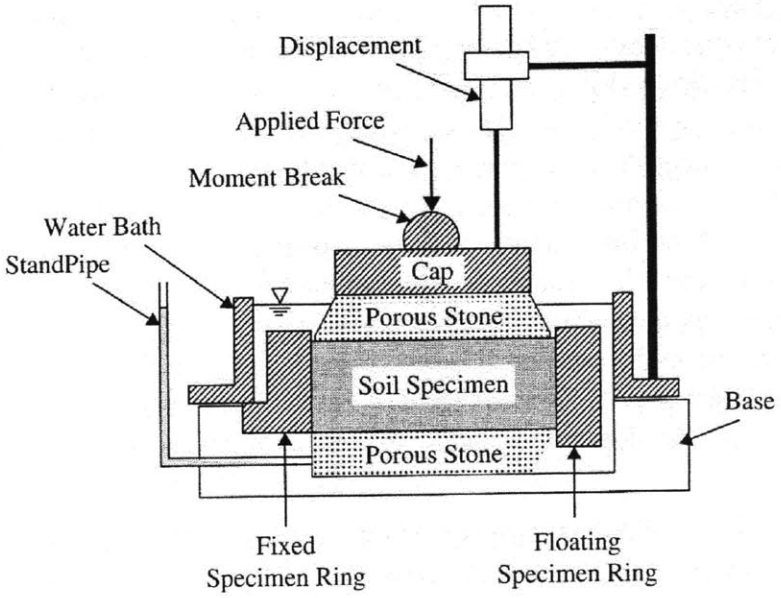

(b) Close up of soil specimen with boundary conditions and applied forces

Figure 2-3: Typical incremental oedometer setup (Germaine and Germaine, 2009)

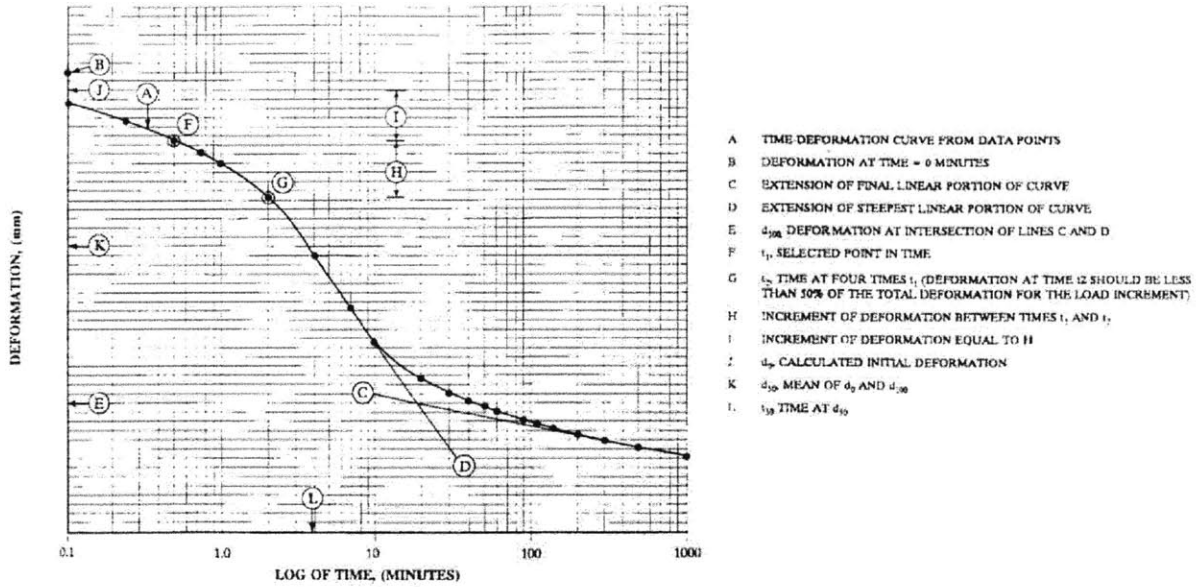

(a) Log Time Method

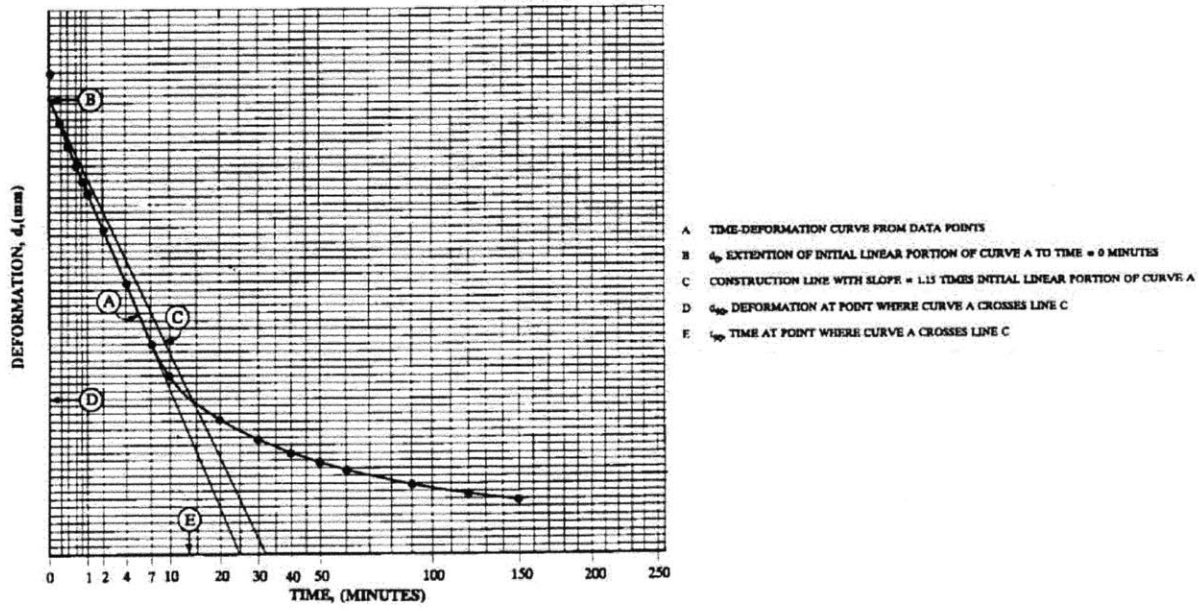

(b) Root Time Method

Figure 2-4: Example of Log of time and Square Root of time methods for time-deformation curve analysis in the incremental oedometer method (ASTM D2435).

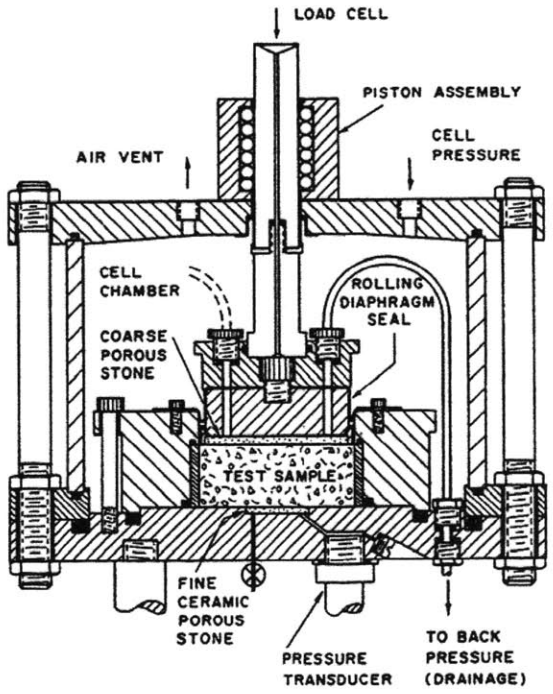

Figure 2-5: Wissa's Constant Rate of Strain cell (Wissa et al, 1971)

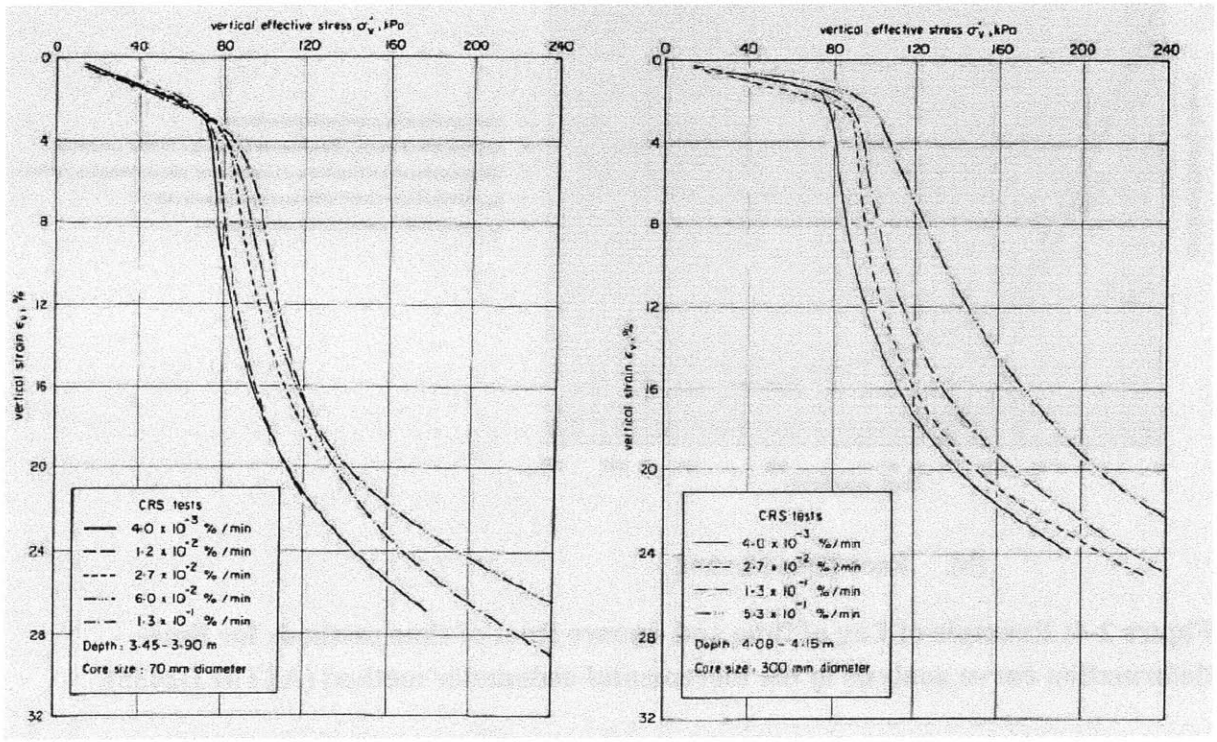

Figure 2-6: Strain rate effects for a natural sensitive clay from Gloucester (south of Ottawa, Canada) (Leroueil et al, 1983)

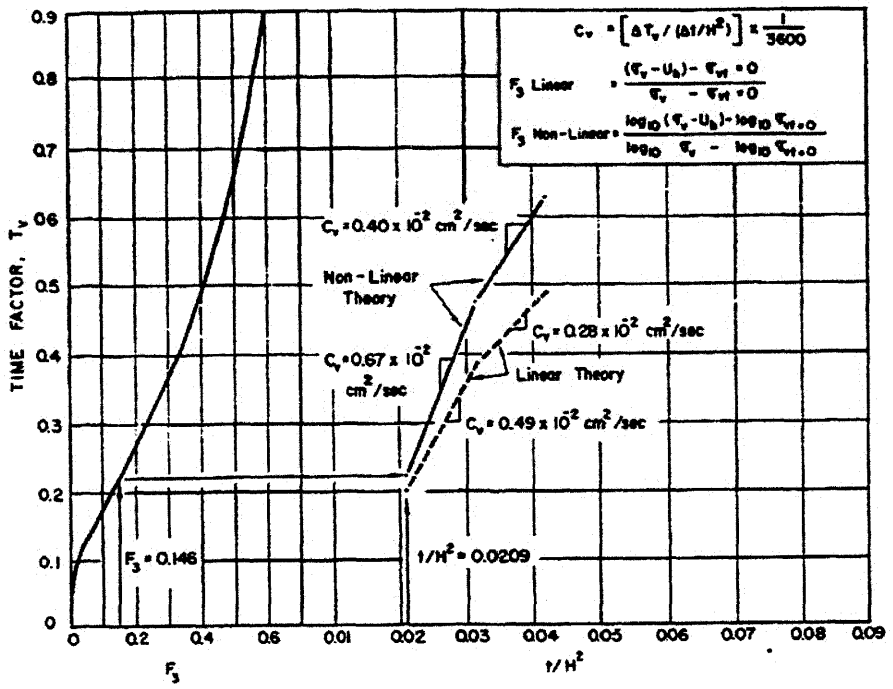

Figure 2-7: Graph relating dimensionless time factor, Tv, to F3 for use in determining if steady state conditions have been reached (Wissa et al, 1971)

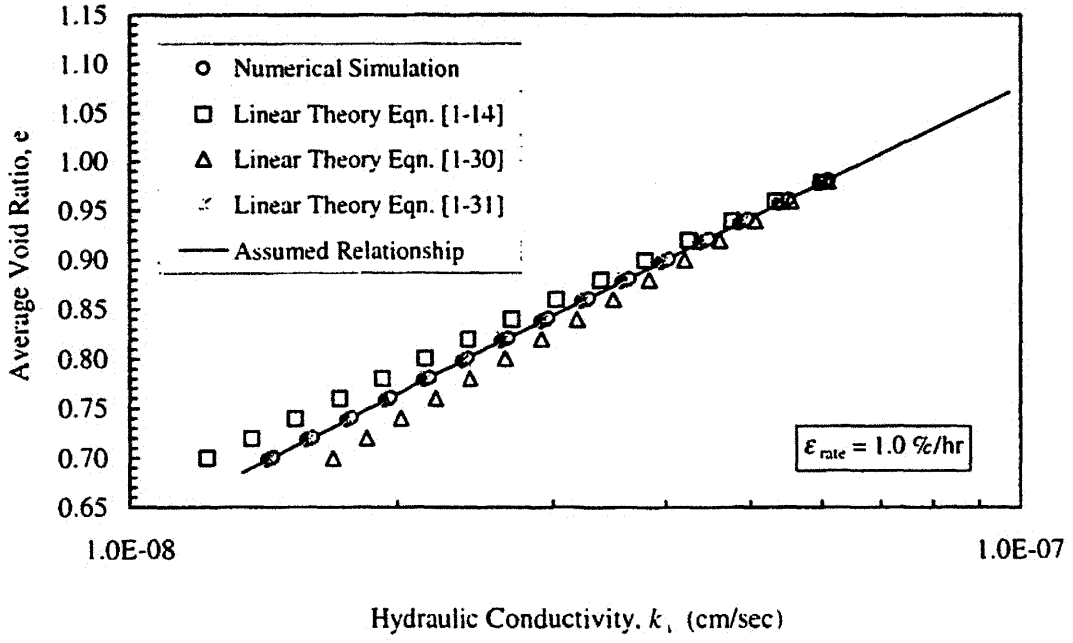

Figure 2-8: Comparison of three variations of Linear CRS Theory (Gonzalez, 2000)

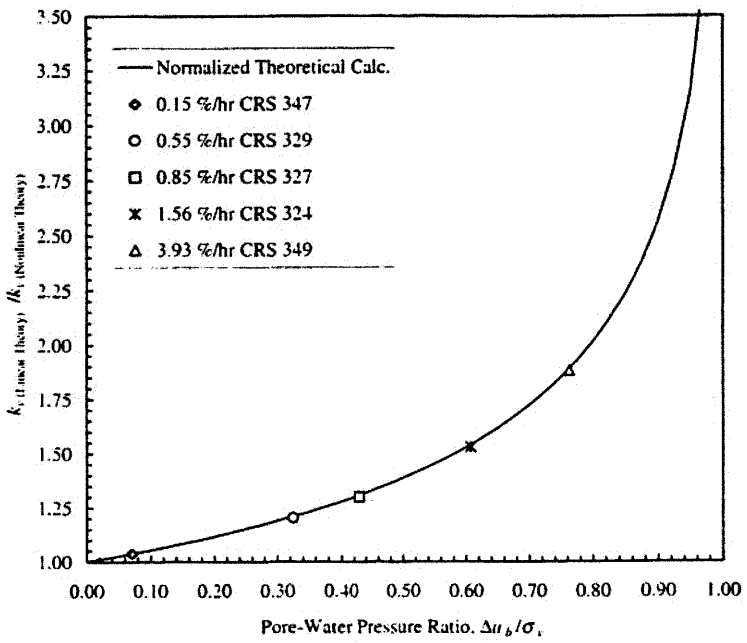

Figure 2-9: Comparison of the hydraulic conductivity from Linear and Non Linear theory for Resedimented Vicksburg Buckshot Clay (RVBC) CRS consolidation (Gonzalez, 2000)

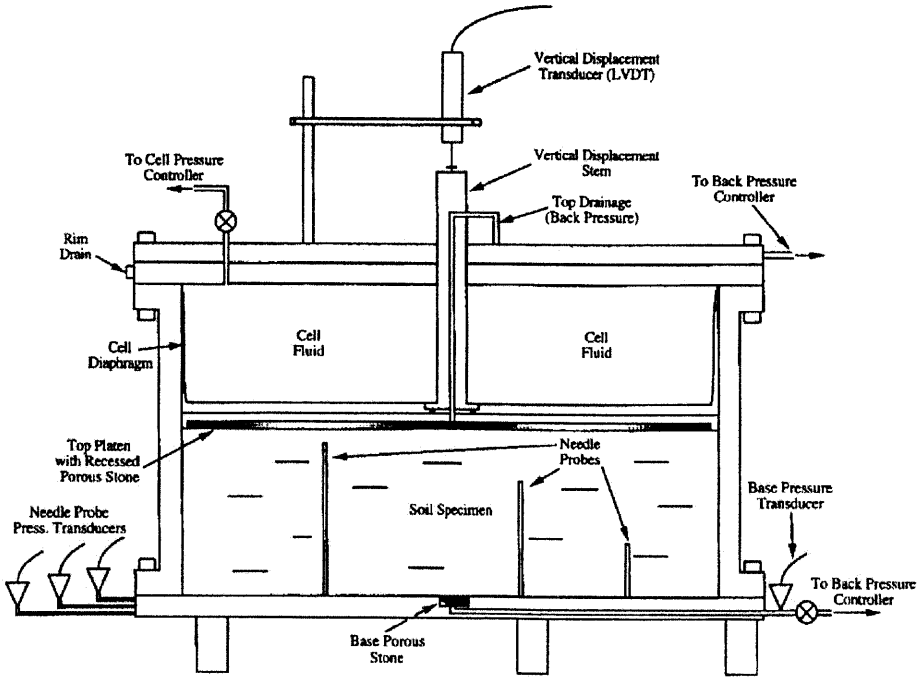

Figure 2-10: Cross section of an instrumented CRS (Rowe) cell to measure pore pressure at 5 points in the specimen including top, bottom and 3 mid-depth points (Sheahan and Watters, 1997)

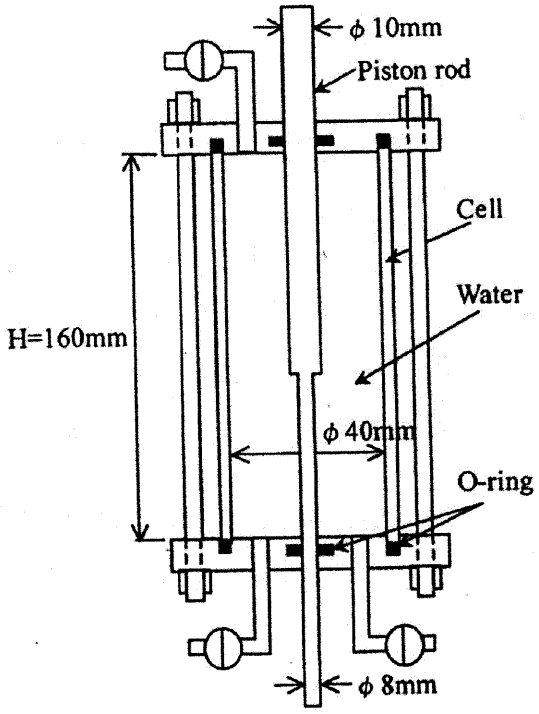

Figure 2-11: Schematic of flow pump device used to run constant flow tests in closed oedometer cell (Moriwaki and Umehara, 2003)

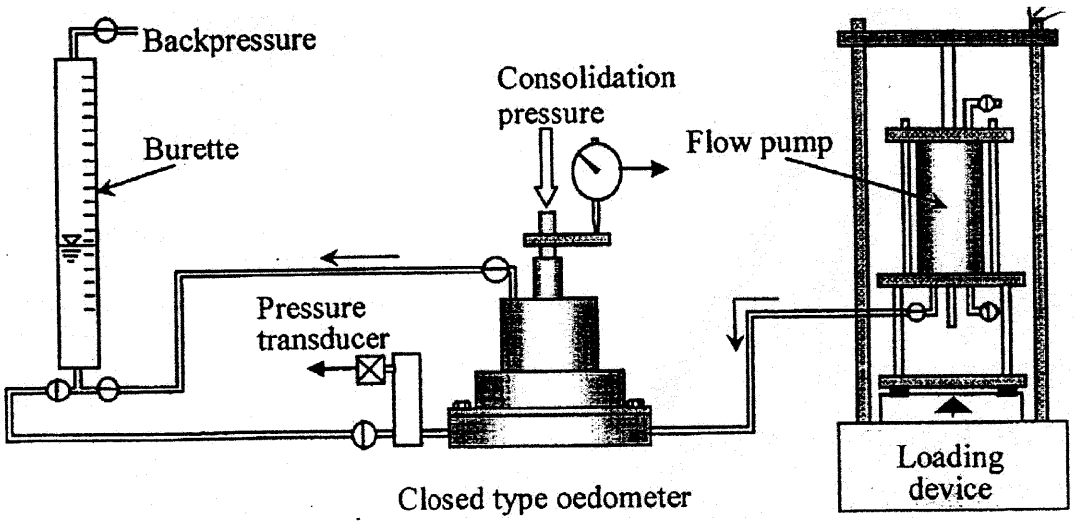

Figure 2-12: Closed oedometer set up to allow constant flow tests between load increments (Moriwaki and Umehara, 2003)

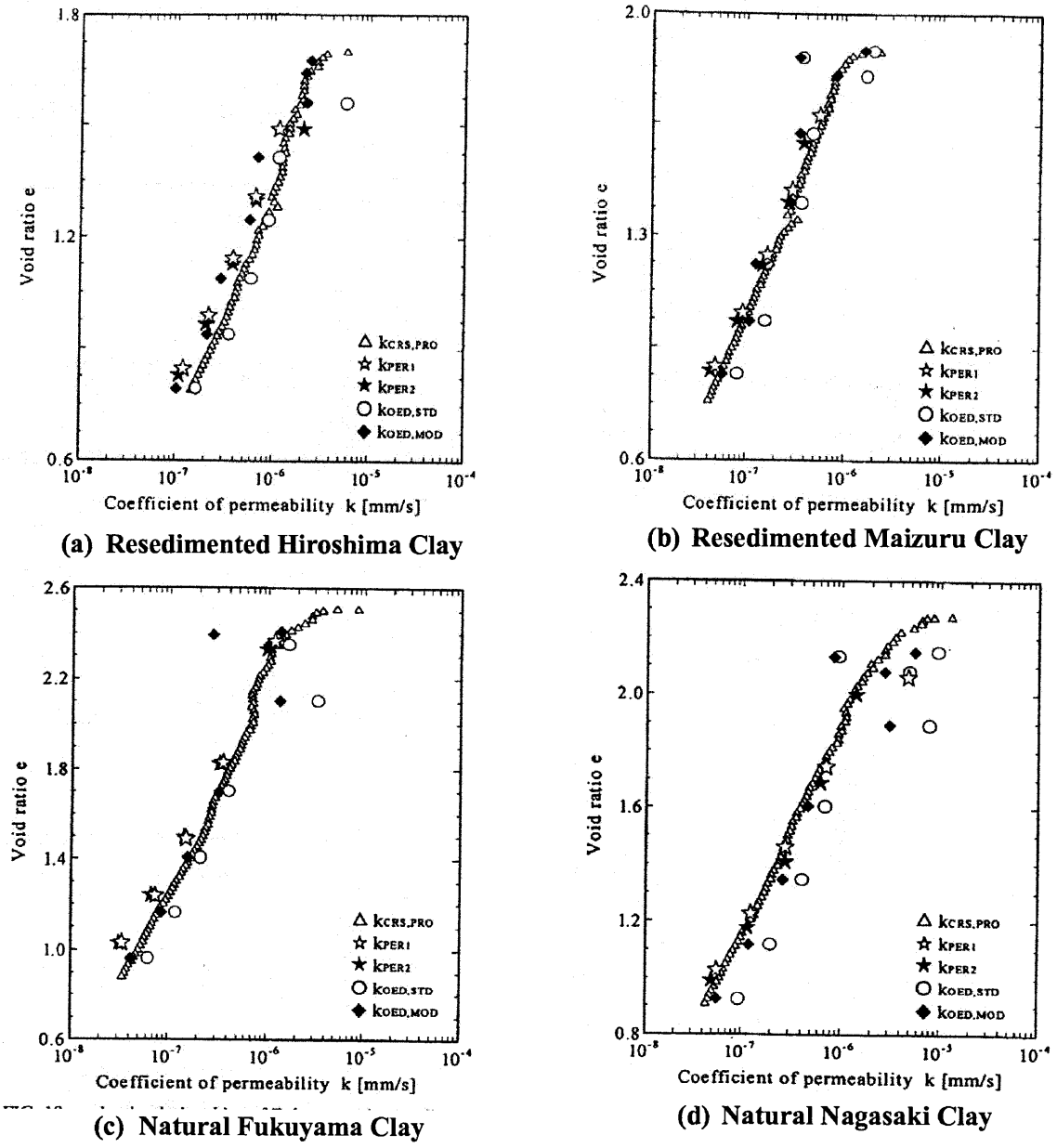

Figure 2-13: Comparison of constant flow, CRS and oedometer permeability calculations (Moriwaki and Umehara, 2003)

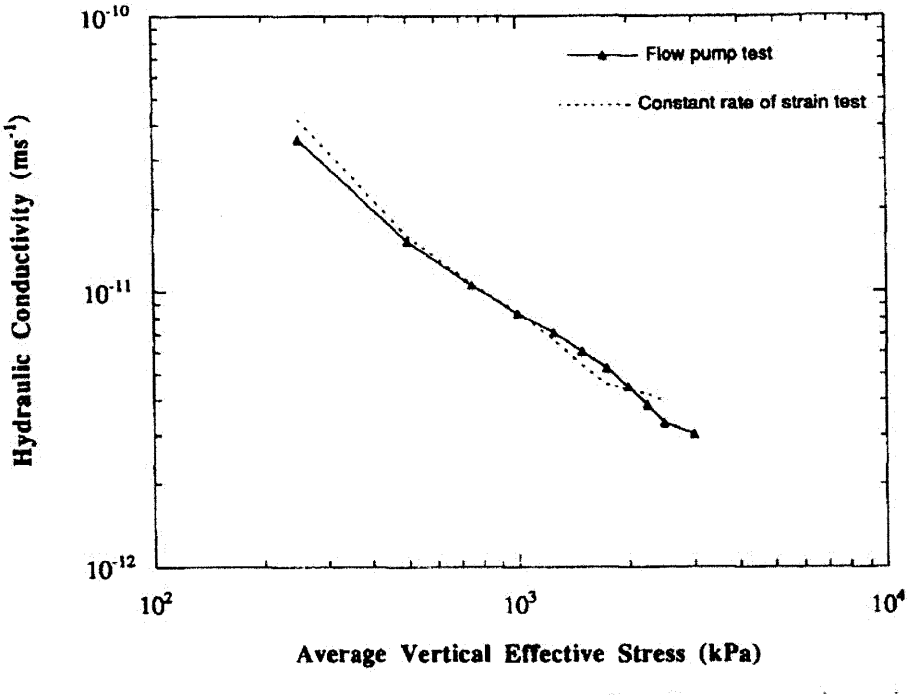

Figure 2-14: Comparison of Constant Flow and CRS measured hydraulic conductivities (Dewhurst et al, 1996)

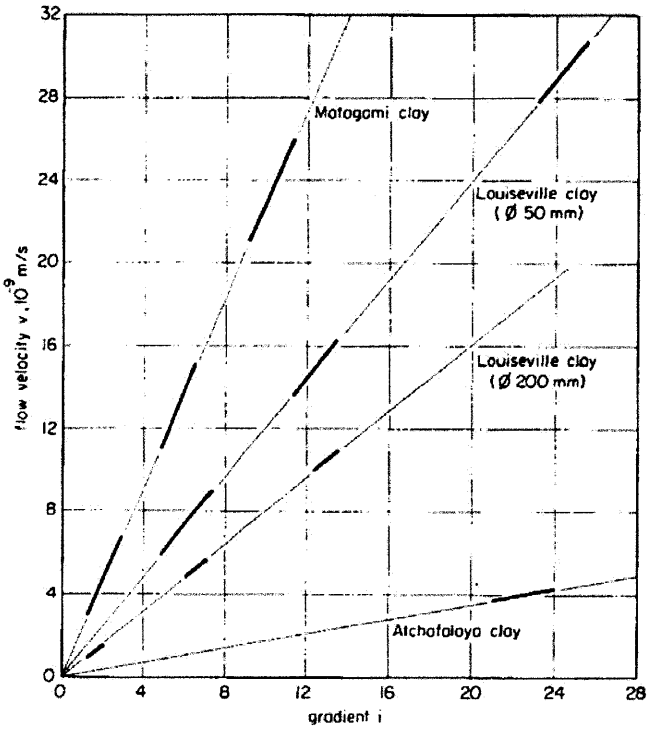

Figure 2-15: Flow velocity vs. gradient for different soils (Tavenas et al, 1983)

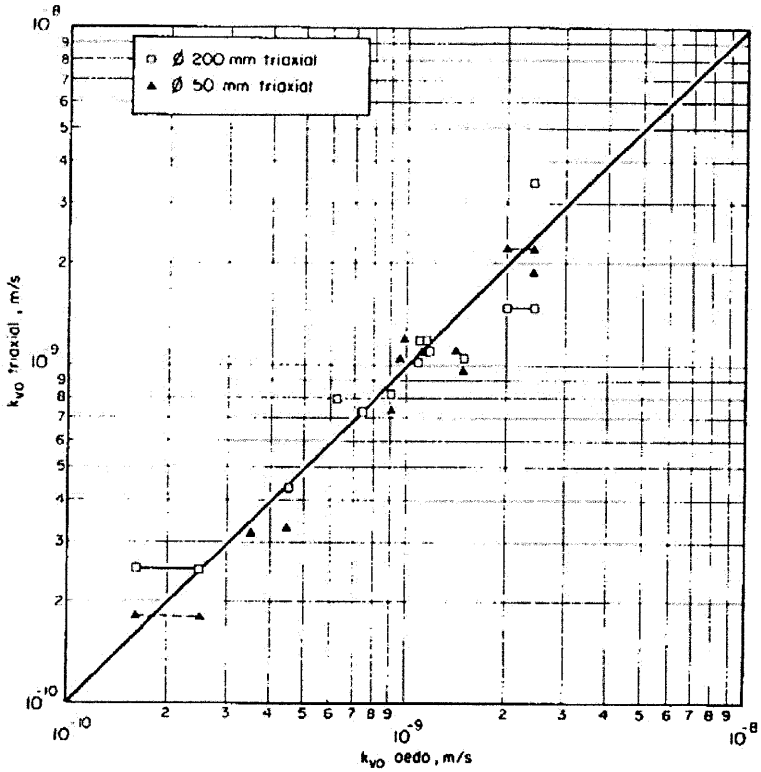

Figure 2-16: Relationship between hydraulic conductivity measured using constant head test in the triaxial cell and falling head test in the oedometer apparatus (Tavenas et al, 1983).

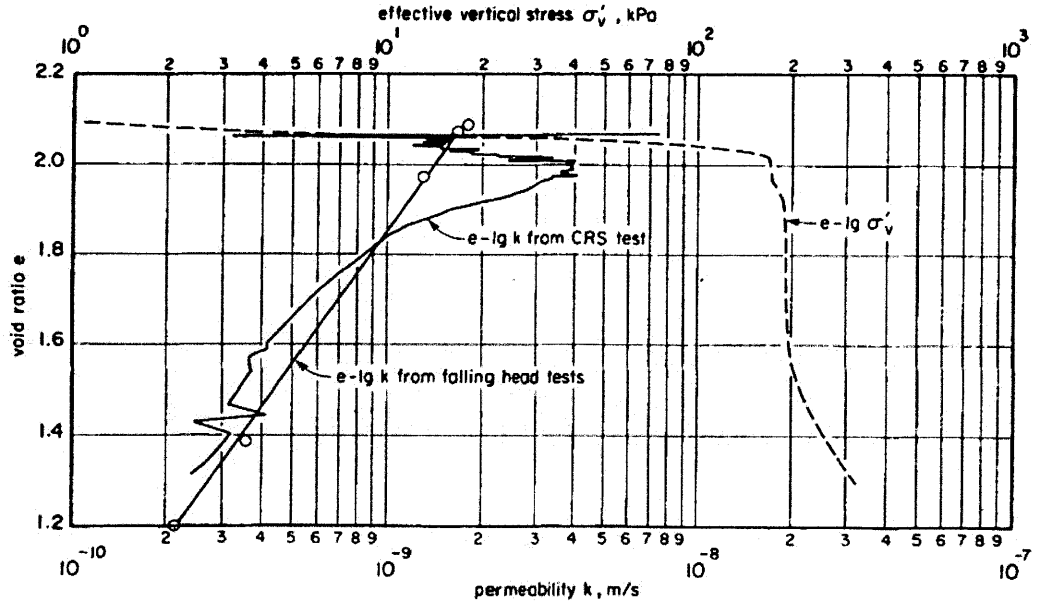

Figure 2-17: Void ratio vs. hydraulic conductivity relationships for Louiseville Clay (Tavenas et al, 1983)

3 MATERIALS

3.1 Introduction

The purpose of this chapter is to describe the materials used for testing in this investigation and to detail the material processing procedure. Two categories of materials are examined: laboratory resedimented clays and intact clays. Laboratory resedimented clays are fabricated in the laboratory setting using 1D consolidation techniques in settling tubes and use processed source materials. The resedimentation procedure employed to fabricate these materials is detailed in Chapter 4. Intact materials comprise tube samples of soils left over from a variety of projects associated with the MIT Geotechnical Laboratory.

3.2 Material Processing

3.2.1 Resedimented Soils

3.2.1.1 Resedimented Boston Blue Clay

Series IV Boston Blue Clay powder is produced from block samples of Boston Blue Clay that were obtained from under the Biology building (#62) on the MIT campus in Cambridge, MA in 1992. Approximately 2500 kg of soil was obtained from a depth of 12 m (Abdulhadi, 2009). Cauble (1996) describes the material processing procedure. The material was softened with tap water and mixed into a thick slurry which was then passed through a #10 US Standard sieve to remove all large particles including gravels, shell fragments and non-natural particles. The soil passing the #10 sieve was then oven dried at a temperature of 60^0C and ground by the Stuartevant Company to 95% passing the #100 standard US sieve using a roller mill process. The material was not processed as one unit, and hence two blending operations were employed to mix and manually randomize the powder before storing in sealed 40 gallon drums.

3.2.1.2 Resedimented Ugnu Clay

Jones (2010) describes the method employed to process core samples of Ugnu clay for resedimentation. Boring AK 36771 C6, samples T-2 and T-3 were used. Material was removed from the tubes using a chisel and hammer and initially hand processed using a

mortar and pestle until the material passed the #200 (0.75 mm) sieve. This process was very time and energy intensive, and as a result a ball mill grinder was devised using steel shot as a grinding material. This system is well described by Jones in his 2010 SM dissertation. The material was ground using the ball mill grinder until all material passed the #200 sieve; SEM analysis indicated that the largest particles in the final material were approximately 10 microns.

3.2.1.3 Resedimented Kaolinite

Kaolinite powder is a commercially available material marketed as Speswhite China Clay. It is produced from deposits in the southwest of England. The material used in this study was sourced from EEC International.

3.2.2 Intact Materials

Intact materials are obtained from standard push tube samples. Tubes are 2.8" diameter galvanized steel or brass and are capped and sealed at each end (Figure 3-1). The tubes are x-rayed and the radiographs (Figure 3-2) are used to determine locations of poor sample quality which are not used for testing. Once a suitable specimen is located within the tube, the section is cut from the tube with a band saw. All cut edges of the sample tube are smoothed and processed to remove metal burs for safety reasons. The soil adjacent to the cut portions of all pieces of sample tube is disturbed from the cutting process and often contains metal fragments; this is removed via scraping. The portions of the sample tube not containing the specimen to be tested are sealed with wax to retain moisture and taped back together for later use. A log sheet records to location of the cut section and the testing performed.

The specimen is extruded from the tube section first by cutting along the inner circumference of the sample tube with a piece of piano wire. The specimen is then pushed out of the tube by placing it against a raised object of equal diameter (Figure 3-3) and pushing the specimen tube down.

3.3 Index and Material Properties

This section presents the index properties of the materials tested where available. All index properties have been tested as per the ASTM standard method unless otherwise stated. Table 3-1 summarizes the Atterberg limits, clay fractions, specific gravities and Unified Soil Classification System (USCS) classifications of all materials, where available. Figure 3-4 plots all clays on the standard plasticity chart. The source of information for each measurement is given in Table 3-1, and is also described in the following sections.

3.3.1 Resedimented Boston Blue Clay

Resedimented Boston Blue clay has been extensively tested at MIT and hence the index properties are well established from previous tests. Boston Blue Clay was deposited in the Boston, MA region about 13,000 years ago and is a marine clay. Series IV BBC power is used in this study. Table 3-2 presents the index properties of Series I - III BBC powder (after Cauble, 1996) and Table 3-3 presents the index properties of Series IV BBC Powder (after Abdulhadi, 2009). Figure 3-5 presents the particle size analysis of RBBC powder performed by Julia Schneider of the University of Texas at Austin. In general, the plastic limit is 23%, the liquid limit 46% and the plasticity index 23%. The clay fraction is 56%, and the soil is classified as a low plasticity clay (CL) according to the Unified Soil Classification System (USCS). The specific gravity value used in this study is 2.78.

3.3.2 Resedimented Ugnu Clay

Jones (2010) describes the index testing undertaken for Ugnu clay powder in accordance with ASTM standards. The plastic limit is 26%, the liquid limit 58%, and the plasticity index 32%. Figure 3-6 (Jones, 2010) gives the particle size analysis results; the clay fraction is 44%. The soil is classified as a high plasticity clay as per the USCS. The specific gravity was measured to be 2.70.

3.3.3 Resedimented Kaolinite

The index properties of the Kaolinite powder were not tested for this study. Because this is a commercially available product, approximate properties are available. Richard Baker Harrison Ltd. provided detailed properties and chemical analysis for Speswhite China Clay

from southwest England. The specific gravity is 2.6, and the material has a clay fraction varying between 76 and 83%. The Atterberg limits are unknown.

3.3.4 Intact Boston Blue Clay

The Intact BBC Sample tested was sample S3 from boring BIO TP2A, depth 51'-53'. The index properties of Intact Boston Blue clay were not tested. Boston Blue clay properties are known to vary spatially as well as by depth (Johnson, 1989). For this study, the properties of the intact BBC tested, in particular the specific gravity, are assumed to be equivalent to those of RBBC.

3.3.5 Intact San Francisco Bay Mud (SFBM)

The Intact SFBM sample tested was sample S-23 from boring TTB-11, depth 95' - 97.5'. The Atterberg Limits and specific gravity of the San Francisco Bay Mud were tested on the specific sample used for hydraulic conductivity testing in this investigation.. The plastic limit was 29%, the liquid limit 73%, and the plasticity index 44%. The USCS classification is a high plasticity clay, CH. The specific gravity is 2.72. The clay fraction or particle size analysis was not tested.

3.3.6 Intact Maine Clay

The Intact Maine Clay samples that were tested were sample U2 from boring SSAF2 and sample U2 from boring SAAF3. The material properties were not tested for this study though the mineralogy is known to be similar to BBC. The specific gravity value used is 2.78. The clay fraction is approximately 30% though this may vary spatially and by depth. Reynolds (1991) gives typical Atterberg limits of Maine clays as liquid limit 30%, plastic limit 20%, and plasticity index 10%. The USCS classification is a low plasticity clay, CL.

Table 3-1: Summary of material Atterberg Limits, clay fraction and USCS classification

Material	Liquid Limit (%)	Plastic Limit (%)	Plasticity Index (%)	Clay Fraction (%)	USCS Class.	Specific Gravity	Reference
RBBC	46	23	23	56	CL	2.78	Abdulhadi, 2009
RUgnu	58	26	32	44	CH	2.70	Jones, 2010
RKaolinite	N/A	N/A	N/A	76-83	N/A	2.60	Richard Baker Harrison Ltd.
Maine Clay	30	20	10	30	CL	2.78	Reynolds, 1991
SFBM	73	29	44	N/A	CH	2.72	Tested here
BBC	46	23	23	56	CL	2.78	Abdulhadi, 2009

Table 3-2: Index properties of RBBC Series I to III (after Cauble, 1996)

Year	Researcher	Series	Source Batch	G_s	w_l	w_p	I_p	Clay Frac. <2μm (%)	Salt (g/l)
1961	Bailey	Ia	MIT	2.77	30.0	17.5	12.5	40	2-3
			1139		34.7	17.7	17.0		35
1963	Jackson				36.2	19.5	16.7		16.7
1964	Varallyay		S4		32.6	19.5	13.1		
			S5		33.3	20.4	12.9	35	16.8
			S6		32.8	20.3	12.5		16.0
1965	Ladd, R.S.	Ib		2.77	45	22	23		16
1965	Preston		S1	2.77	45.6	23.4	22.2	35	24
1966	Braathen		S2	2.77	45.4	23.1	22.3		22
1967	Dickey				34.5	23.9	19.6		
1970	Kinner		100	2.78	43.5	19.6	23.9	50	
			150		43.5	19.6	23.9		
			200		38.1	17.8	20.3	52	8
			300		39.7	21.6	18.1		10
			400		39.4	21.3	18.1	52	10
			800		41.5	19.5	22.0	48	16
			900		41.2	18.7	22.5	54	16
			1000		41.1	19.5	22.6	58	16
			1100		42.0	20.6	21.4		16
			1200		40.2	18.6	21.6	48	16
			M101		40.7	19.6	21.1	52	
			M104		40.3	19.6	20.7		
			M107		41.3	19.6	21.7		
			M200		42.3	18.5	23.8	52	
			M400		39.8	18.9	20.9	47	
1971	Ladd et al.		160	2.78	38.1	17.8	20.3		8
			1300		42.1	22.1	20.0		16
			1500		43.8	20.6	23.2		16
1984	Bensari	II	105	2.75	47.6	23.3	24.3		16
			111	2.75	47.1	24.9	22.2		16
1985	O'Neill		105-112	2.78	41.3	22.1	19.2	52	16
1989	Seah	III	200-207	2.78	45.2	21.7	23.5	58	16
1991	Sheahan		210,214, 216		45.6	21.4	24.2		
1993	Cauble		217-218	2.78	37.0	21.3	15.7		
1994	Santagata		219-220		40.4	20.9	19.5		

Table 3-3: Index properties of RBBC Series IV (after Abdulhadi, 2009)

Year	Researcher	Batch	w_l (%)	w_p (%)	I_p (%)	G_s	Clay fraction (%)	Salt g/L
1994	Zriek	powder	46.4	22.5	23.9	2.78	60.1	
1994	Sinfield	powder	47.0	23.8	23.2	2.79		
		402	46.8	22.4	24.4			
		403	47.2	23.3	23.9			
1996	Cauble	powder				2.81		
		401	46.7	21.8	24.9			
		404	47.4	21.9	25.5			10.4
		405	45.2	22.1	23.1			10.0
		406	45.0	22.6	22.4		57.6	12.5
		407	44.6	23.0	21.6		57.8	13.1
		408	44.7	23.9	20.8		58.7	10.1
		409	45.4	24.0	21.4		56.8	13.0
		410	46.6	25.0	21.6			13.4
		411	46.7	24.5	22.2		56.9	10.2
		413	45.5	24.3	21.2			9.7
		414	46.3	24.3	22.0			12.0
		415	46.1	24.7	21.4			10.5
		416	46.7	24.0	22.7			12.9
		417	47.2	24.5	22.7			13.2
1998	Santagata	418						
		419	47.8	23.3	24.5			
1998	Force	420	45.2	22.6	22.6			
2009	Abdulhadi	powder	46.5	23.5	23.0	2.81	56.0	11.1

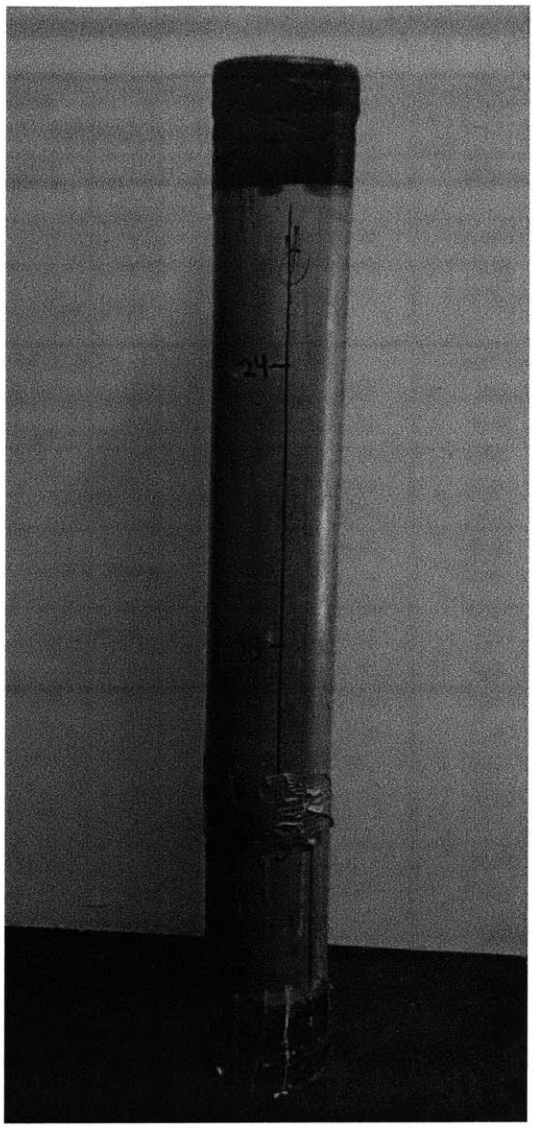

Figure 3-1: Sample tube used to obtain a specimen for testing. Tube has been cut and resealed below 18" where a specimen has been removed for testing.

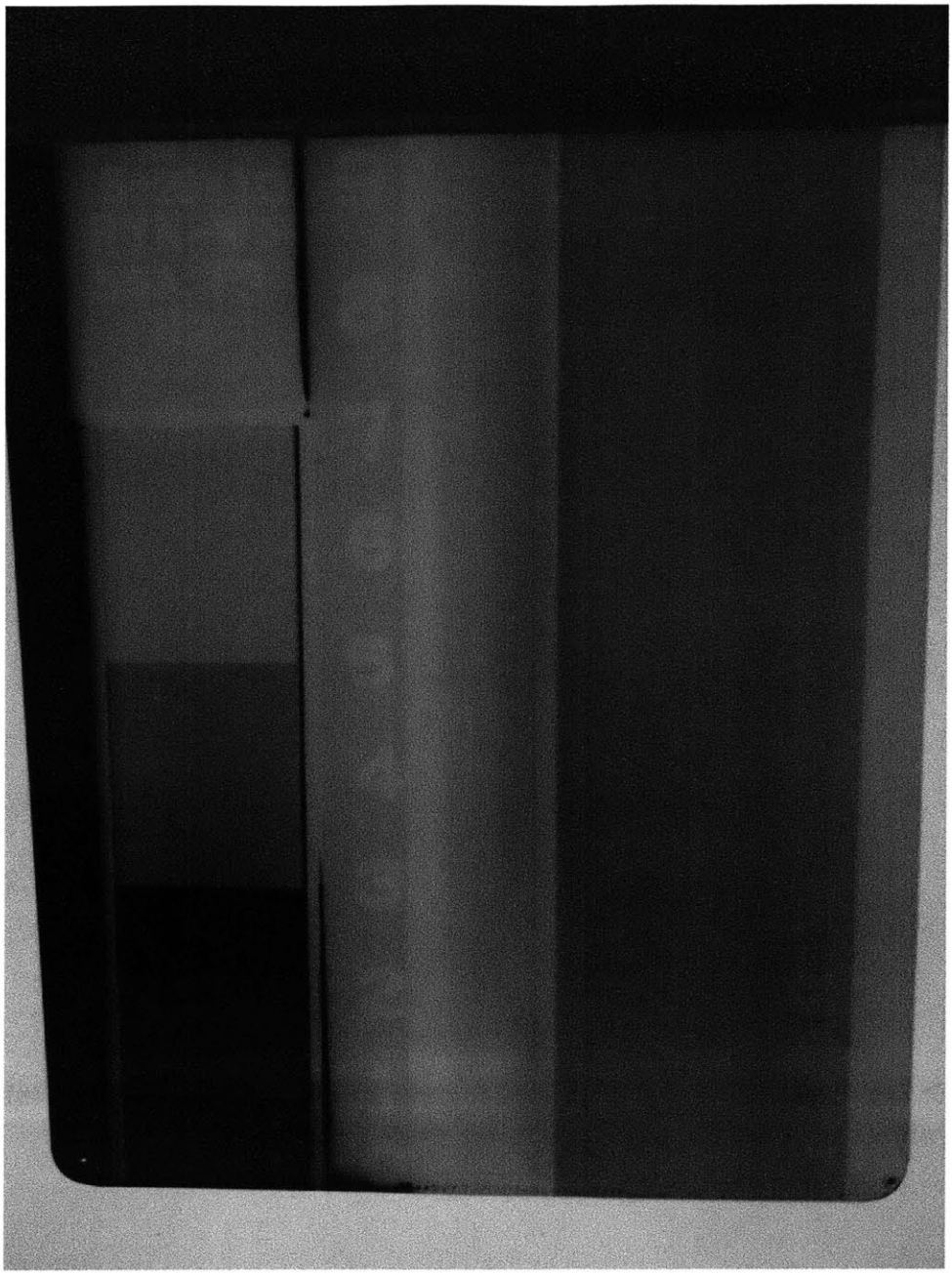

Figure 3-2: Radiograph of a section of a sample tube showing relatively uniform sample.

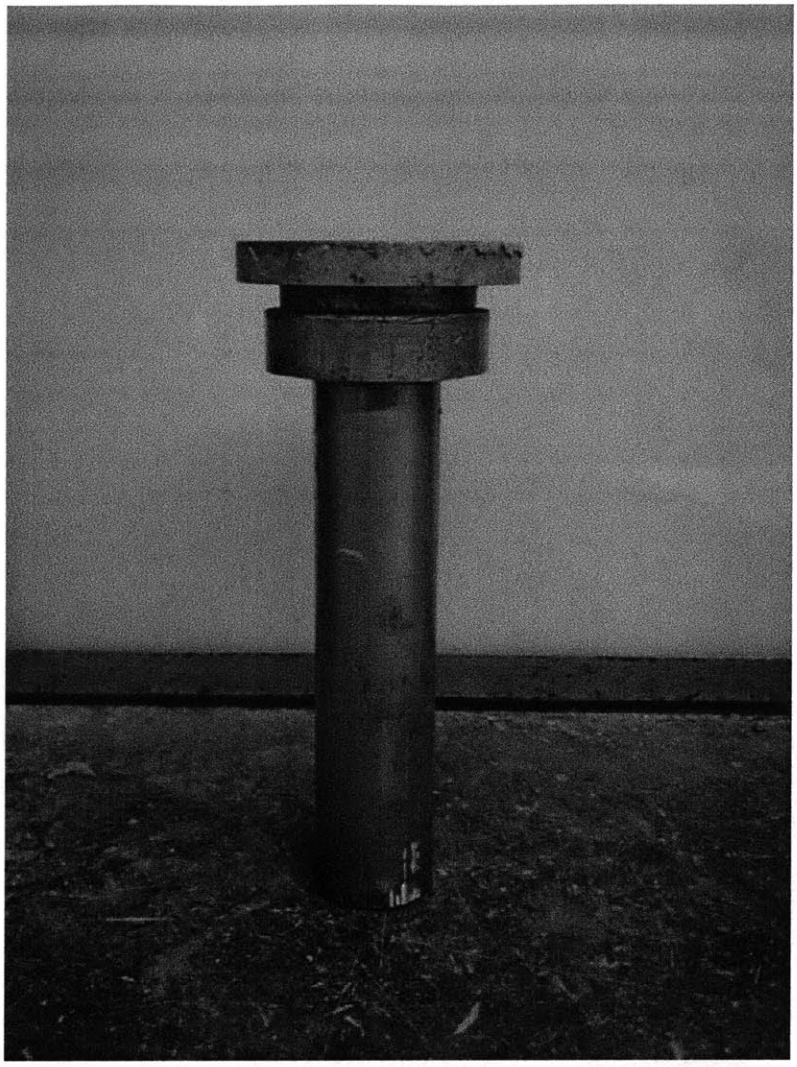

Figure 3-3: Jacking object that can be used to push specimen out of a sample tube. The top of the object is approximately equal to the specimen diameter.

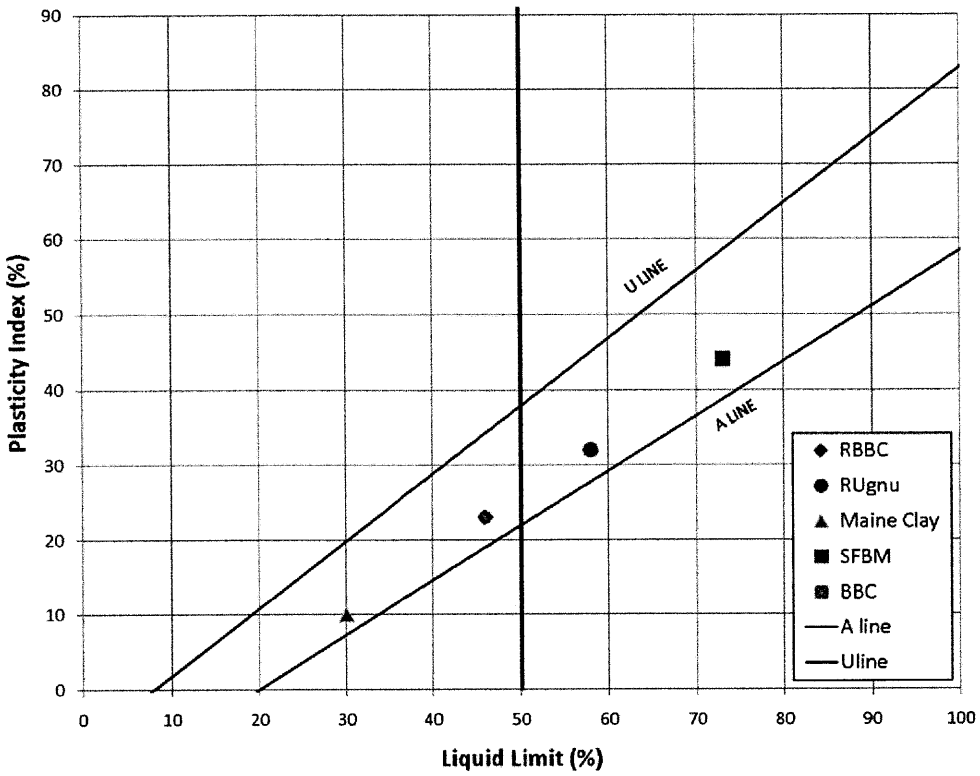

Figure 3-4: Plasticity Chart showing all materials tested.

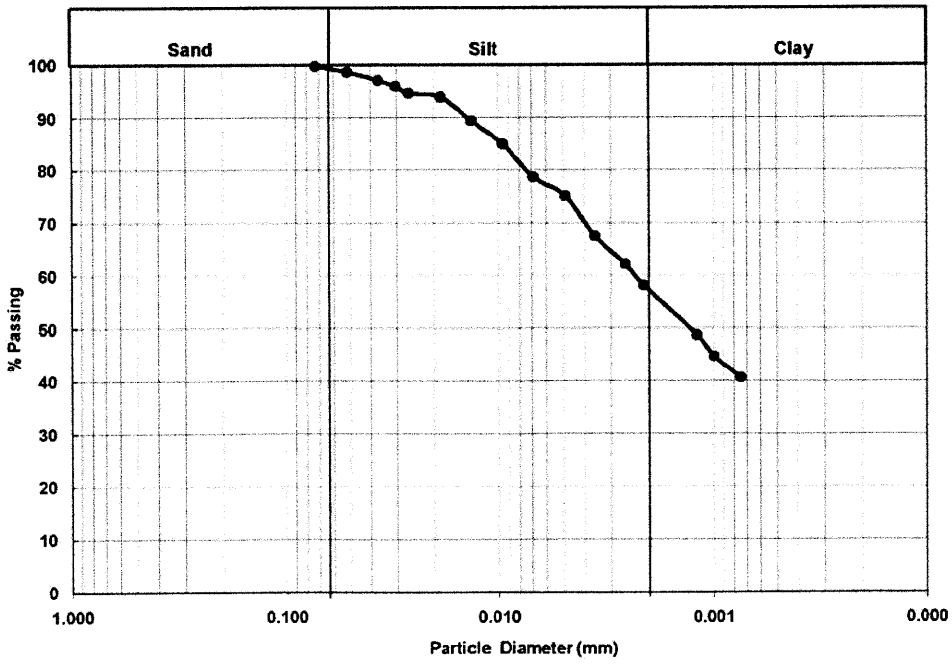

Figure 3-5: Particle Size Analysis of RBBC Series IV (performed by Juila Schneider, University of Texas at Austin)

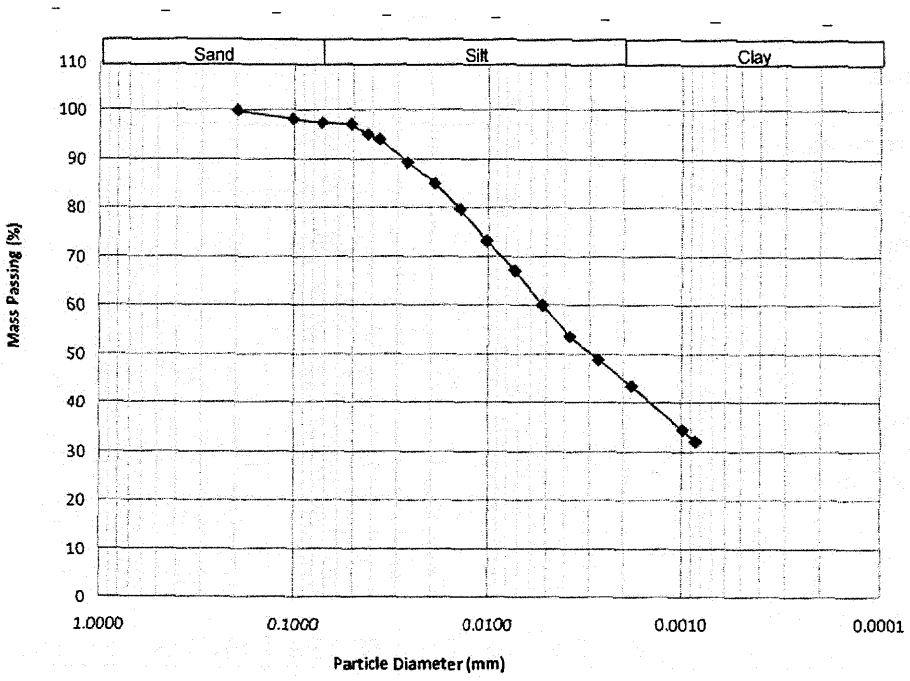

Figure 3-6: Particle Size Analysis of Ugnu Clay (after Jones, 2010)

4 EQUIPMENT AND PROCEDURES

4.1 Introduction

The purpose of this chapter is to describe the equipment and procedures used in this study. Section 4.2 describes the resedimentation method used to fabricate the Resedimented Boston Blue Clay (RBBC), Resedimented Ugnu and Resedimented Kaolinite samples in detail. Section 4.3 outlines a salinity test procedure; salinity tests are conducted for all hydraulic conductivity test specimens to ensure that the permeant fluid is at approximately the same salinity as the pore water fluid of the specimen being tested so as not to induce any salt induced related effects into the results.

Section 4.4 provides an overview of the data acquisition and automation systems used in the MIT Geotechnical Laboratory. This section provides all relevant transducer information for all of the testing devices used in this study. Finally, section 4.5 describes each of the two hydraulic conductivity measurement devices used in this study: the Constant Rate of Strain (CRS) and Flexible Wall Permeameter Devices. For each device, the general characteristics, specimen dimensions, and a brief outline of the set up procedure are presented and relevant problems encountered during the testing program are addressed.

4.2 Resedimentation

4.2.1 Introduction

Resedimentation involves consolidating a uniform, homogeneous workable slurry one dimensionally in a rigid walled sedimentation column called a consolidometer. With incremental loading over time, resedimentation produces a soil sample that can be cut into one or more specimens and trimmed to the desired size and shape for testing.

Resedimentation of BBC was first undertaken at MIT in 1961 by Bailey (Abdulhadi, 2009). Series IV BBC is currently being used, and has been in use since the early 1990's. Germaine refined the process of resedimentation in 1982 to produce fully saturated and uniform samples using RBBC with a salt concentration of 16 g/L, and resedimentation techniques at MIT have been evolving ever since (e.g. Seah 1990, Abdulhadi 2009).

4.2.2 Method

4.2.2.1 Resedimented Boston Blue Clay

BBC powder is mixed with distilled water at 100% water content and 16g/L salt content. The water content represents approximately 2 times the liquid limit. This is slightly higher than Burland's 1990 recommendation of 1.0 to 1.5 times the liquid limit; other researchers have suggested other values ranging from 0.75 to 2.0 times the liquid limit (Sheeran and Kirzek, 1977, Allman and Atkinson, 1992, Cotecchia and Chandler, 1997, and Skempton, 1944). Abdulhadi (2009) found that mixing BBC powder at 100% water content results in a workable slurry that has no lumps, is stable, does not exhibit particle segregation during consolidation and does not produce free water without the addition of applied forces on a slurry column.

Pure sea salt is used, and it is mixed with the water prior to mixing with the soil powder. A salt concentration of 16g/L was originally used in the 1960's; samples are batched at this salt concentration and consolidated with free access to water at this salt concentration, and this produces samples with a pore water fluid salt concentration in this range. Adding salt produces a flocculated soil structure and helps reduce particle segregation during sedimentation (Abdulhadi, 2009) in addition to mimicking a natural brackish marine depositional environment.

4.2.2.2 Resedimented Ugnu Clay

Ugnu clay power was mixed at 110% water content equivalent to just under twice the liquid limit. A sea salt concentration of 16 g/L was used.

4.2.2.3 Resedimented Kaolinite

The liquid limit of the kaolinite is unknown; therefore salt water at a salt concentration of 16 g/L sea salt was gradually mixed with the kaolinite powder until a workable slurry was formed with approximately the same consistency as the RBBC slurry. The mass of water added was measured, and the resultant water content of the slurry was 142%.

4.2.3 Procedure

The clay powder is gradually added to the salt water mixture in a standard kitchen electric mixer fitted with a flat beater attachment for mixing (Figure 4-1) and mixed on low speed for approximately 20 minutes, wiping the sides of the bowl at intervals to ensure full and complete mixing. Once a smooth, uniform slurry is generated, the slurry is transferred under vacuum into a vacuum cylinder (Figure 4-2) and de-aired under approximately 15 to 25 inches of Mercury (in Hg) vacuum pressure for 1 to 2 hours to remove any air bubbles. If higher vacuum pressure is available the de-airing time may be reduced. The slurry is shaken regularly during the de-airing process. The slurry is then poured into 3" inside diameter settling columns of varying heights (12" to 18") using a funnel to minimize air inclusion during the pouring process (Figure 4-3). Two people are required to pour the slurry; one person holds the funnel ensuring that the base of the funnel is kept just at the top of the rising column of slurry. The second person pours the slurry into the funnel gradually ensuring that pressure flow does not develop (i.e. the funnel does not ever flow full).

The settling columns are PVC plastic tubes with 3 inch internal diameter and 1/4 or 1/2 inch wall thickness. The rigid walled settling column is cleaned with silicone oil prior to slurry placement to help minimize friction during consolidation. The base of the column is plugged by a porous stone and an oversized filter screen (figure 4-4) made of 05/15 nylon mesh by Sefar Nitrex. The filter screen is placed adjacent the soil slurry. Sometimes, as in figure 4-4, the stone is propped up on a 4" PVC spacer in order to change the location of the slurry column in the settling tube so that they may be placed in deep settling tanks with other samples that are resedimented for other projects, however this has no effect or relevance to the resedimentation procedure for this project. The settling column is set up in a reservoir that can be filled with water later, however the reservoir is drained during pouring of the slurry to prevent leakage around the base porous stone.

Once the slurry is placed, a filter screen and porous stone are placed on top with the filter screen adjacent to the slurry. Often placement requires the use of a shop vacuum to suspend and lower the stone onto the slurry, removing the vacuum as the stone approaches the slurry (i.e. within about 1 cm of the top of the slurry). The reservoir is then filled with saline water

at 16g/L sea salt to a level above the base of the slurry column, and the same solution is poured into the top of the slurry column. The water level in the reservoir is marked so it can be maintained via filling with distilled water on a daily basis to account for evaporation losses, maintaining a constant salt content.

A resedimentation log is filled out (Figure 4-5) and the sample is incrementally loaded over time using load increments of approximately 1. PVC Spacers measuring 2.9" diameter are used initially to fill the sedimentation column. Spacer heights of 2,4,6,8 and 12 inches are used. Once sufficient spacers are added that there is some stick up out of the sedimentation column, the sample is loaded either by carefully stacking weights on top of the spacers or hanging weights on a hanger system suspended off the PVC spacers (Figure 4-6). Samples are incrementally loaded to 100 kPa and unloaded to an over consolidation ratio (OCR) of 4, requiring a maximum applied mass of 45.6 kg.

4.2.4 Effect of OCR 4

For BBC, Ladd (1965) showed that an OCR of 4, the lateral stress ratio, Ko is equal to 1 providing hydrostatic effective stress conditions (Figure 4-7). As a result, the shear strains during sample extrusion and trimming should be minimal and the sample should be close to a perfect sampling condition.

The OCR 4 requirement for a hydrostatic effective stress condition is well known for BBC, however this condition is not well known for other soils resedimented in this study. A general relation for the lateral stress ratio Ko as a function of OCR was proposed by Ladd (1998) in equation 4-1:

$$K_o = K_{oNC}(OCR)^N \tag{4-1a}$$

$$N \sim 1 - K_{oNC} \tag{4-1b}$$

Where for clays, Ladd (1998) gives K_{oNC} as varying between 0.45 and 0.7. Therefore, given the potential variance in the normally consolidated Ko, the OCR which produces a Ko of 1 can vary from 3.28 for $K_{oNC} = 0.7$ to 4.27 for $K_{oNC} = 0.45$. For the purposes of this study, all samples were unloaded to an OCR of 4 during resedimentation prior to trimming.

Once the loading and unloading process was completed in the sedimentation columns, samples were extruded for trimming as described in Chapter 3.

4.3 Salinity Testing

4.3.1 Introduction

The salt concentration of the pore fluid is known to affect the hydraulic conductivity of fine grained soils. It is hypothesized that changes in pore fluid salinity can affect fabric which in turn directly influences the hydraulic conductivity of a soil specimen.

Resedimented soil samples tested in this investigation were batched at 16g/L salt content and allowed to sediment with free access to water at 16g/L salt content. This does not, however, mean that the pore fluid of the samples will be 16g/L. The salt content of the natural tube samples tested was unknown, however most soils are marine in origin and thus are likely to have sedimented in some degree of brackish or saline water. As a result, the pore fluid salt content of every sample analyzed in this study was tested. For resedimented samples, salinity testing provides an effective means of evaluating the resedimentation process in terms of repeatability. Using the results of salinity testing, the salinity of the permeant used during hydraulic conductivity testing of intact specimens was adjusted so as not to introduce any salt related effects into the hydraulic conductivity results. The salt used for all specimens tested, as well as for all salinity testing was pure sea salt with no additives sourced from a local grocery store.

4.3.2 Salinity Test Method

A trace portable conductivity meter, model 23226-505 from VWR International was used for salinity measurements. The salinity meter was calibrated against a 1 g/L solution to obtain the relationship between measured conductivity and salinity. This calibration was performed by John Grennan (Grennan, 2010) by testing various concentrations of sea salt and measuring the electrical conductivity. Figure 4-8 gives the calibration curve.

There is currently no standard test method for salinity analysis. The following protocol is used at MIT (Martin 1982, Grennan 2010, Germaine and Germaine, 2009)

1. Tare the centrifuge tube
2. Add moist, not oven dried soil to the tube to equivalent of 15 g dry mass;
3. Record the mass of moist soil added to the tube;
4. Add distilled water to the tube to approximately 45 g total mass (200% water content);
5. Record the mass of distilled water added;
6. Fill a total of 4 tubes with soil for testing;
7. Fill an additional 4 tubes with a reference salt solution. 1 g/L sea salt solution was used;
8. Cap tube, shake soil tubes vigorously, let sit over night;
9. Shake soil tubes in wrist action shaker for 20 minutes;
10. Place all tubes in centrifuge and run at approximately 5000 RPM for 20-30 minutes. A Damon/IEC Division, IEC HT Centrifuge was used in this study;
11. Decant the supernatant liquid from each tube into a clean 10 mL glass beaker;
12. Pair each soil tube with a reference salt solution tube (4 pairs);
13. Clean probe with distilled water and dry;
14. Measure the conductance of the reference salt solution;
15. Clean the probe with distilled water and dry;
16. Measure the conductance of the soil supernatant liquid;
17. Repeat from step 13 until at least 2 consistent readings of each the soil supernatant and reference salt solution have been obtained;
18. Clean all equipment, repeat from step 13 with each other the other 3 soil reference salt solution pairs;
19. Clean and store the probe and all equipment.

Using the calibration relationship in figure 4-8 the salinity of the supernatant liquid can be found when compared to the salinity of the reference salt solution. The use of the reference salt solution helps eliminate temperature effects. The salinity of the specimen can then be computed by multiplying the salinity measurement computed by the testing water content and dividing it by the natural water content (equation 4-2):

$$RSS = SS\,x\,\frac{w_c}{w_n} \tag{4-2}$$

Where:

RSS is the salinity of the test specimen (g/L);
SS is the salinity of the supernatant liquid (g/L);
w_c is the water content of the soil specimen (%); and
w_n is the natural water content of the soil specimen (%);

The water content of the soil during salinity testing is approximately 200% given the testing methodology. For this research, the natural water content of the soil is obtained prior to hydraulic conductivity testing on a specimen derived from the same sample as the salinity test material. It is well documented in the MIT Geotechnical Laboratory that there is a variation in water content between specimen trimmings and the actual tested specimen, sometimes by up to 2%, with the actual specimen always having the higher water content. Therefore, neither the specimen trimmings nor the material used for the salinity test are used to measure the natural water content of the soil specimen.

4.4 Data Acquisition Equipment

4.4.1 Introduction

The MIT Geotechnical Laboratory employs many devices to run laboratory tests, most of which are automated. This section describes the elements common to many devices including measurement instrumentation devices, data acquisition and computer control programs.

4.4.2 Measurement Instrumentation

Geotechnical tests such as constant rate of strain and constant head tests analyzed in this study require careful measurement of the time rate of deformation, force and volume change. These measurements are possible using non automated methods, including stop watches for time, burettes for volumes, dial gauges for deformation, and proving rings for force measurements. However, automation simplifies the measurement process, extends measurement capabilities and allows for a higher frequency of measurements with a reduced labour load. Transducers can be used to measure physical quantities that change during a test. At MIT a central data acquisition system (described in section 4.4.3) is used to record transducer readings all over the lab based on tasks that are set by the user. The transducers that are used for this study can be subdivided into four categories: load cells, axial displacement transducers, pressure

transducers, and volume change transducers. All transducers used in the MIT geotechnical laboratory require a common input voltage of 5.5 volts of Direct Current (DC) and output a DC current. Each transducer is calibrated to obtain a calibration factor, and has a characteristic resolution and stability. Table 4-1 and Table 4-2 describe the transducer characteristics used for each of the CRS device and Flexible Wall Permeameter, respectively. The following sections briefly describe each of the four categories of transducer type.

4.4.2.1 Load Cells

The load cell used in the CRS device is a Data Instruments Model JP 2000 load cell with a capacity of 2000 lb (8.9 kN). The load cell uses a shear beam geometry to concentrate stains in an instrumented section. Strains are measured with strain gauges whose output voltage can be related to the applied load using the calibration relationship.

4.4.2.2 Axial Displacement Transducers

The axial deformation of the specimen during CRS loading is measured using one or two Linear Variable Differential Transformers (LVDT) manufactured by Trans-Tek Inc. The linear range is approximately 2.5 cm. An LVDT is comprised of three coils including one primary coil in the centre and two secondary coils on either side. A current in the primary coil creates a magnetic field which induces a voltage in each of the secondary coils, and this voltage is proportional to the mutual inductance with the primary coil. As a ferrous core moves through the centre of the coils, the mutual inductance is altered, changing the voltage response. A slight movement of the core produces a nearly linear change in the differential voltage output between the two secondary coils. This differential voltage can be related to the displacement using the calibration factor.

4.4.2.3 Pressure Transducers

Pressure transducers are used on both the CRS and Flexible Wall Permeameter devices. They are used to accurately measure applied cell pressures and specimen pore pressures at different locations. All pressure transducers used are manufactured by Data Instruments and are of type AB/HP or AB and measure the gauge pressure by means of deflection of a steel diaphragm instrumented with strain gauges. The pressure transducers are of the sealed type (PSIS). The

CRS device uses two 200 psi (1400 kPa) pressure transducers to measure the cell and pore pressure, and the Flexible Wall Permeameter uses one 2000 psi (14000 kPa) pressure transducer to measure the cell pressure and two 100 psi (700 kPa) pressure transducers to measure the top and base pore pressures.

4.4.2.4 Volume Change Transducers

Volume change of the specimen is measured for multiple reasons. First, in hydraulic conductivity measurement, the time rate of volume change is used to compute the flow rate of permeant through the specimen and then the hydraulic conductivity. For the Flexible Wall Permeameter, the volume change during back pressure and consolidation is measured to compute the change in specimen dimensions. Volume change is computed by measuring the displacement of a piston in a Pressure Volume Actuator (PVA) by means of a string pot. The area of the piston is known and remains constant; therefore the volume change is a function of displacement only. String pots are similar to LVDT's in that they measure displacements; however they use a spring loaded spool and a sensor that detects rotation which can be linked to the cable's linear extension or velocity using a time measurement. Unlike an LVDT, which can be enabled to work using gravity alone, a string pot requires tension to be maintained on the end of the string. The string pot is favoured over the LVDT because it has a much larger range (30 cm vs. 2.5 cm), has a very high output, has a very linear output with little system backlash and has little to no A/C noise associated with the readings (Grennan, 2010). The string pots used for all volume measurements on both the CRS and Flexible Wall Permeameter devices are manufactured by Celesco and are type SP1. They have a range of 30 cm but are installed on PVA's with a maximum piston stroke length of approximately 17 cm giving a volume range of 48 cm^3 with a piston diameter of 3/4 inch (1.905 cm).

4.4.3 Data Acquisition System

A centralized computer based data acquisition system is used in the MIT Geotechnical laboratory to provide a single location for collection and storage of all transducer measurements; Grennan (2010) describes this system. The computerized system is flexible allowing users to specify customized and sometimes complicated transducer recording schedules based on experimental needs; multiple schedules can be run simultaneously. A

centralized data acquisition system is a cost effective and efficient means of recording digital data in large laboratories and is heavily relied upon at MIT.

Figure 4-9 is a schematic drawing of the central data acquisition system (Germaine and Germaine, 2009). The components of the system can be sub divided into 4 categories:

1) The laboratory testing device, such as the CRS device, which includes the transducers, power supply, junction box, voltmeter and ground;
2) A switching mechanism which allows the data acquisition mechanism to connect to a particular transducer to make a measurement;
3) An Analogue to Digital (A/D) converter that converts the voltage output from each transducer and the power supply to a digital word which can be read by a computer; this device is critical to the precision of the final measurement; and
4) A computer which controls the process and components and performs all administrative and computational tasks associated with collecting and archiving the measurements associated with all programmed tasks.

The MIT Geotechnical data acquisition system uses a PC equipped with an Intel 486 microprocessor and driven by Microsoft's Windows XP operating system. This computer is interfaced with an expanded channel Hewlett Packard HP3497A data acquisition unit equipped with a very low noise 5.5 digit integrating analogue to digital converter with auto-ranging amplification capabilities to four voltage scales (0.1, 1, 10 and 100V). The system is currently configured to simultaneously monitor 140 channels distributed throughout the laboratory while providing analogue to digital conversion and data storage capabilities at speeds of up to 1 Hertz.

4.4.4 Computer Control System

Many standard testing devices in the MIT Geotechnical Laboratory, including the CRS and Flexible Wall Permeameter devices used in this study, are automated and computer controlled. Grennan (2010) summarizes the automation history of the MIT Geotechnical laboratory. Modification of existing manual system components was initiated in the early 1990's. Sheahan (1991) first developed an automated stress path triaxial cell for testing; this

was followed by automation of the high pressure triaxial cell (Anderson, 1991), the direct simple shear device (Ortega, 1992), and a special Caisson Element test cell (Cauble, 1996).

Sheahan and Germaine developed a series of BASIC control programs beginning in the early 1990's that have been updated and modified since, and continued automation as well as development of the automation system(s) has been ongoing to improve flexibility and quality control as well as to bring automation to new devices. The advantages of automation include a significant reduction in labour requirements with respect to making the actual measurements, as well as a reduction in the potential for incorporating human error into the test progression. Further, computer control increases the flexibility of the test sequence.

Automation is controlled by drive systems using closed loop feedback control. This is employed using the following steps:

1) The transducers make measurements of the actual stress-strain state of the specimen;
2) The voltage output of the transducer is sent to the computer via an A/D converter and converted to engineering units using a calibration factor and zero value;
3) The software compares the engineering units with a prescheduled time history of the specimen state that is set by the user upon initiation of the test or test stage;
4) A control algorithm makes a calculation based on step 3 to decide what action needs to be taken by the motors to maintain the prescribed stress-strain state schedule;
5) The signal is sent to the motors which then carry out the computed action.

Sheahan et al (1990) describe the closed loop feedback control system as direct measurements being taken as a part of an iterative system in order to maintain specific time histories of each parameter being measured.

Figure 4-10 (Grennan, 2010) presents the basic hardware components required to undertake this process. An A/D converter converts the analogue voltage output of the transducers to a digital word readable by the computer. Multichannel AD 1170 converters, manufactured by Analog Devices, are used in the MIT Geotechnical Laboratory as they provide high precision

with a minimum of 18 bit resolution. A computer processes the signals converted by the A/D converter, and computes a new command signal to be sent to the testing device according to the programmed and calibrated algorithm. This signal is sent out through a digital to analogue (D/A) converter located in the computer to be converted into a voltage signal readable by the control motors. Strawberry Tree Inc. D/A converters with 12 bit resolution and ± 5 volt range are used. A motor driver turns the DC servo motor at a rate that is proportional to the command voltage. A variety of different motors are used in the MIT Geotechnical Laboratory. The CRS apparatus uses Electro Craft model G362T-AZF Rev E, part #0372-18-013 motors for both the cell and pore volume PVA's. The Flexible Wall Permeameter Apparatus used Electro Craft Model E352, Part #0352-10-501 motors for the cell and both pore pressure PVA's.

Automated control is carried out using a control program written in QBASIC. The program allows the user to set up the system for testing as well as to control the different components of a test. The program is really two separate modular programs which call each other. The first program is a setup program where the user enters the test specific data including specimen dimensions, transducer calibration factors, transducer zero values, transducer channel numbers relating to the computer control, and other test specific parameters. This program then calls the second program, the control program, and stores the user specified information in memory for use by the control program. The program was originally developed for triaxial testing, but with continuous updating and expansion of automation through the laboratory, many different control programs have been developed allowing for task-specific applications. General functions are organized into component modules, including initial pressure up, back pressure saturation, consolidation and shear phases are basic components of this program. For this work, the Triaxial control program has been modified to create two different versions, one for use with each of the CRS and the Flexible Wall Permeameter devices.

For the CRS apparatus, the shear phase control module has been modified for 1D uniaxial loading of the specimen at a constant rate of strain. More extensive modifications were required to adapt the control program for use with the Flexible Wall Permeameter apparatus.

Modifications included the addition of a third volume measurement and control system, and the ability to control a second pore pressure. Shear modes were removed as no piston is used in this test method. The output display was also significantly modified to display meaningful data pertaining to a hydraulic conductivity test.

Despite local computer control, the central data acquisition system is used to record all data for all tests conducted in the laboratory.

4.5 Testing Procedures

4.5.1 Introduction

This section describes the test procedures for the Constant Rate of Strain (CRS) and Flexible Wall hydraulic conductivity tests conducted for this research. This section does not describe the limited index testing that was undertaken on select materials to determine the material properties; index testing was previously described in Chapter 3.

4.5.2 Constant Rate of Strain (CRS) Tests

4.5.2.1 Introduction

The history and development of the CRS test and associated analysis was discussed extensively in Chapter 2. For this research, CRS tests were performed in a standard Trautwein CRS apparatus, shown schematically in Figure 4-11 (ASTM D4186). A specimen is encased between two filter screen – porous stone pairs in a rigid ring. Fixed boundary conditions force one dimensional deformation. Filter screens of type Sefar Nitrex, 05/15 are used. The specimen is incrementally back pressured over a period of 72 minutes and loaded at a constant rate of strain via a piston while the excess pore pressure generated at the base of the specimen resultant from loading is measured.

Two types of tests were performed in the CRS apparatus: standard one dimensional constant rate of strain (CRS) loading tests, and constant head tests using a fixed piston at a constant strain. For standard CRS tests only one means of pressure control is necessary to control the cell pressure; however a second means of pressure control was added to the standard CRS setup used for this research to allow control of the base pore pressure of the specimen as

required for constant head testing in the CRS device. Pressure control is achieved using pressure volume actuators (PVA's) that are equipped with motors connected to a computer allowing for algorithmic computer control. Figure 4-12 is a photograph of two pressure volume actuators with fluid reservoirs on top to allow for refilling. The PVA is plumbed to the base of the specimen via plastic or copper tubing, Swagelok connections and a valve. Figure 4-13 shows a photograph of the CRS device with the additional plumbing and valve allowing connection of the base pore pressure to the external PVA.

Strain was measured using an LVDT holding plate fitted onto the piston, as seen in figure 4-13. Initially one LVDT was used, but then a second LVDT was added, as shown in figure 4-13, to measure piston rotation. The measurements from both LVDT's are averaged to give the average specimen deformation.

The applied load was measured using an external load cell and the adjustments due to the weight and area of the piston and frictional losses were accounted for during calibration.

4.5.2.2 Procedure

1. Obtain a natural or resedimented specimen. Clean and oil the inside of the CRS ring with silicone lubricant. Record the mass of the CRS ring and a filter screen. Record the mass of the recess tool. Trim and level the ends of the soil specimen, taking one moisture content from each end's trimmings. Carefully and slowly trim the specimen into the rigid CRS ring (Figure 4-14) using the trimming device, and taking and additional two moisture content measurements using the trimmings. The final specimen dimensions are 0.926 inches (2.3516 cm) high and 1.247 inches (3.169 cm) in diameter. When the ring is full of soil, carefully remove the ring from the trimming device and trim and level the excess soil at both ends of the ring. Levelling can be accomplished using a knife edge. Apply a filter screen to the cutter end of the trimming ring and create a recess at this end of the trimming ring using the recess tool. Cut and level the extruded soil at the other end of the trimming ring. Record the mass of the trimming ring including the soil, filter screen and recess tool. Place another filter screen at the other end of the specimen.

2. Set up the apparatus by flushing all lines to ensure they are free of air. Put a base porous stone in the base of the device. Load the specimen ring into the device with the recessed end up. Place the top porous stone into the recess. Apply two O rings around the outer base of the rigid ring, first a larger O ring 0.134" (3.37 mm) thick and then a smaller diameter O ring 0.066" (1.65 mm) thick. These O rings seal the base of the specimen from the cell fluid as well as prevent leaks of the cell fluid out of the device. Replace the top half of the CRS device and screw it tightly. Drop the piston gently until it cleanly contacts the top porous stone.
3. The following is a deviation from standard practice which is further discussed in section 4.5.3.3. Record the load cell zero value and load the device into the load frame. Open the bottom pore pressure valve connecting the base porous stone to the cell volume. Do not fill the cell with fluid yet. Ensure that the cell plug is open, allowing air to flow freely into and out of the cell. Align the piston, and manually increase the load, monitoring it using a voltmeter. Increasing the load forces the specimen to seat on the base porous stone in the case where there is a gap between the top of the porous stone and the base of the trimming ring. Monitor the dissipation of load with time as well as the change in LVDT voltage with time. Once the load and LVDT voltages stabilize following a period of change, the specimen should be seated. Maintain a small seating load (1 to 2 kg) on the specimen.
4. Keeping the valve connecting the base porous stone to the cell reservoir open, fill the cell reservoir with fluid. Back pressure saturate the specimen in increments of 50 kPa to 200 kPa, and then in increments of 100 kPa to 400 kPa with 12 minutes of equalization time between increments, maintaining at least 5 kPa of axial effective stress on the specimen. Once fully back pressured, re-zero the base pore pressure transducer to the cell pressure transducer, and then close the valve connecting the base porous stone to the cell reservoir.
5. Initiate the constant rate of strain loading sequence at the desired strain rate. Using the computer control system, this requires specification of the desired strain rate, the maximum allowable total stress and the maximum allowable strain. The load cell used in this research has a maximum capacity of 2000 lbs (8.9 kN). Given the specimen

dimensions, this represents a maximum total axial stress of 2800 kPa. Tests conducted for this research were run to a maximum axial force of 2400 kPa or less. The specified strain rate varied with the soil type; generally a strain rate that will result in an excess pore pressure not exceeding 15% of the axial effective stress is desired. In general, for all soils tested in this investigation, the required strain rate was well known from previous CRS studies completed at MIT.

6. Following completion of the loading sequence let the specimen pore pressures equalize for at least 24 hours. Higher plasticity specimens may require longer equalization periods. Unload the specimen to an over consolidation ratio (OCR) of 4. Again, allow the specimen to equalize for a period of 24 hours or more dependent on the plasticity.
7. Initiate constant head testing. First close the valve connecting the pore pressure transducer to the specimen pore pressure and then open the valve connecting the same transducer to the pore pressure PVA. The pressure transducer and pore pressure PVA are now hydraulically disconnected from the specimen. Pressurize the pore pressure PVA and associated lines. Once pressurized, open the valve connecting the base porous stone to the cell pressure and then open the valve connecting the base porous stone to the pore pressure transducer. Performing this sequence of operations hydraulically connects the cell pressure and pore pressure PVA's and connects the system, allowing it to equalize to the cell pressure without subjecting the specimen to any large pore pressure jumps. Further, the system is hydraulically connected via valves and lines and does not need to equalize through the specimen.
8. Initiate a constant head gradient by closing the valve connecting the base porous stone to the cell pressure. Maintain the cell pressure as constant and reduce the pore pressure by the desired pressure differential (typically 5 kPa to 15 kPa). Maintain the constant head gradient for 8 to 24 hours or as required until flow equilibrium is reached between the inflow and outflow volume increments and an accurate measurement of the specimen hydraulic conductivity can be made.

9. Repeat for at least 3 gradients. Make sure to neither consistently increase nor decrease the applied gradient. Test additional gradients as required if significant variability in the measured hydraulic conductivity is noted.
10. Re-equalize the system by opening the valve connecting the base porous stone to the cell pressure. Allow the specimen to re-equilibrate. This process may be quick for low plasticity specimens (20 minutes to 1 hour) or may take up to 24 hours for high plasticity specimens. The amount of time required for equalization should be judged based on the amount of time required for the specimen to equalize to application of a constant head gradient.
11. Quickly remove the specimen from the CRS device by removing the cell pressure and the load and then disassembling the device. Carefully push the specimen out of the ring and remove the porous stones and filter screens. Measure the height at a minimum of 8 points along the circumference using a pair of digital callipers. If no further testing is to be completed, mass the specimen and put in an oven to dry. Record the dry mass after 2-3 days.

The apparatus compressibility was measured using a stainless steel dummy specimen with the same physical arrangement of filter screens and porous stones as is used with soils testing; this process is described in detail in Chapter 5. The compressibility of the stainless steel is assumed negligible compared to that of the apparatus. The load deformation curve of the apparatus was measured and an average function derived to allow subtraction of the apparatus deformation from the measured deformation to give the true specimen deformation for a given applied load.

4.5.2.3 Important Details

4.5.2.3.1 Bottom Seating Errors

The CRS testing program identified an important design flaw in the CRS device. Analysis of several tests identified a disagreement in the final specimen dimensions between calculations based on the LVDT deformation measurements and physical deformation of the specimen. The final specimen volume can be computed using the initial specimen height minus the specimen deformation measured using the LVDT and corrected for apparatus compressibility.

Combined with the dry mass of the specimen, the final void ratio may be calculated. The final void ratio can also be computed by using phase relations, either using a mass based, volume-based or mixed approach. A mass based approach requires knowledge of the specific gravity of the solids, the density and salt concentration of the fluid, and the saturation of the specimen. A volume based approach requires knowledge of the total specimen volume, the volume of water removed on oven drying, and the salinity of the pore water. Equation 4-3a gives the phase relations for a mass based void ratio calculation, and equation 4-3b for a volume based calculation.

$$e = \frac{V_v}{V_s} = \frac{V_w + V_{salt}}{V_s} = \frac{\frac{M_w + M_{salt}}{\rho_{saltaq}}}{\frac{M_s}{G_s \rho_{H20}}} \tag{4-3a}$$

$$e = \frac{V_v}{V_s} = \frac{V_T - V_s}{V_s} = \frac{V_T - \frac{M_s}{G_s \rho_{H20}}}{\frac{M_s}{G_s \rho_{H20}}} \tag{4-3a}$$

Where:

e is the void ratio;
V_v is the volume of the voids [L^3];
V_s is the volume of the solids[L^3];
V_{salt} is the volume of the salt[L^3];
V_w is the volume of the water[L^3];
M_w is the mass of the water [M];
M_{salt} is the mass of the salt equal to $\frac{M_w[salt]}{\rho_{H20}}$ [M];
[salt] is the pore fluid salt concentration [M/L^3];
M_s is the mass of solids, equal to the dry mass minus the mass of the salt [M];
G_s is the specific gravity of the solids [];
ρ_{H20} is the mass density of the water; and
ρ_{saltaq} is the mass density of the salt water at the pore fluid salt concentration.

In general, the final specimen void ratio computed at the end of the test using either equation 4-4a or 4-4b agreed very well, indicating full saturation of the specimens. It was found, however, that the void ratio computed using the corrected specimen deformation measured with the LVDT was always lower than that measured using the specimen mass and specimen dimensions. This error was sometimes in excess of a void ratio of 0.05.

As a result, the apparatus compressibility was checked, as was the method of analysis, further discussed in chapter 5, and some significant deviations were found in the apparatus compressibility measurements. This is further discussed in chapter 5. It was then discovered that the base porous stone was not flush with the base of the CRS apparatus, meaning that when the specimen in the rigid ring was placed into the apparatus, a gap existed between the top of the base porous stone and the bottom of the specimen. During back pressure this gap would fill with water and during CRS loading this volume of water would move through the specimen as the specimen was seated on the base porous stone. This process is recorded by the LVDT as specimen deformation or thinning. The gap was measured to be approximately 0.010 inches (0.254 mm) with the stones that were in use at the time. For an initial specimen height of 2.3516 cm, this results in an error in the measured strain of 1%. For a specimen with an initial void ratio of 1.0 loaded to a measured void ratio of 0.6, the error in the final void ratio is 0.02. Figure 4-15 shows the location of this gap in the CRS schematic.

The gap results from errors associated with manufacturers tolerances in the porous stone manufacturing process. To help avoid this in future tests, the stones were replaced with slightly thicker stones, reducing the size of the gap, and a step was added (section 4.5.2.2) during the set up procedure to pre-seat the specimen on the stone by displacing it downwards within the rigid ring with the base drainage valves open prior to filling the cell with fluid. Chapter 6 discusses the effects of the push through error on the results and the effectiveness of this technique on reducing this error in subsequent tests.

4.5.2.3.2 Other problems

Aside from the base seating errors already discussed, only minor problems were encountered. The San Francisco Bay Mud (SFBM) specimens proved very difficult to test for unknown reasons. During the CRS loading mode of the test, the control program always seemed to lose its target value of strain and stop allowing the stress to reduce as the pore pressure dissipated, basically unloading the specimen. This may potentially be caused by a missed electrical signal at some point during the test. The loading sequences for the SFBM specimens took about 3 days to complete, significantly longer than for any other specimen. Curiously, however, this

issue occurred only for SFBM specimens, it occurred numerous times, and it always occurred just after the test progress had been checked late at night.

4.5.3 Flexible Wall Hydraulic Conductivity Tests

4.5.3.1 Introduction

Two Flexible Wall Permeameter tests have been conducted for this research due to high demand for this device for another project. This section briefly describes the flexible wall hydraulic conductivity apparatus as well as the test procedure for specimens previously trimmed and tested using the CRS method.

The flexible wall hydraulic permeameter is a modified triaxial cell with a fixed piston that is plumbed to allow control of one cell pressure and two pore pressures. A specimen is encased in a rubber membrane and sits between a base platen and a top cap with a porous stone and filter screen on each end. For these measurements, 5 cm square end cap adapters were used as they were available from another experimental setup and provided a sufficiently large surface for the circular porous stones from the CRS device to sit on while at the same time being smaller than the stone. Further, their use would not require any device modifications associated with testing the thinner CRS specimens. Figure 4-16 gives a solid view of the complete apparatus including the plumbed manifold and figure 4-17 gives a dimensioned section view of the cell and specimen only. Both drawings show the apparatus with a cubic shaped specimen; this research used the same setup only with a shorter, round 'hockey puck' shaped CRS specimen.

The specimen is placed in a pressurized cell fluid that simulates a hydrostatic stress field and holds the membrane onto the specimen. The pore pressure at the top and bottom of the specimen may be independently controlled, or can be hydraulically connected as in a conventional triaxial apparatus to allow double specimen drainage, for example during back pressure and consolidation stages of a test. Independent control of two pore pressures allows for the application of a differential pressure and a constant head gradient, initiating flow for a constant head hydraulic conductivity test. Pressure control is achieved as in the CRS device

by pressure volume actuators (PVA's) with pistons that are driven by computer controlled motors (Figure 4-12).

The Flexible Wall Permeameter gains its name because the rubber membrane provides a flexible boundary condition and allows deformation all three dimensions. Volume change is computed by measuring the inflow or outflow from the pore pressure PVA's using the stringpot measurements. In this set up it is not possible to determine the deformation or strain along a particular axis of the specimen; only the volumetric deformation may be measured. This measurement can be affected by leaks, thus it is important to reduce leakage as much as possible. For the Flexible Wall Permeameter, leakage can be gauged by the time rate of volume change during back pressure once the desired back pressure has been achieved or by testing for pressure dissipation in the pore pressure system under fixed volume and constant cell pressure. Typically, the time rate of volume change at the end of back pressure is minimal, and sometimes it is less than the resolution of the stringpot measurement system over a period of many hours. This phenomenon is described and shown in chapter 5.

Tavenas et al (1983) found that a minimum of 25 kPa of cell pressure was required to prevent flow along the specimen boundary between the specimen and the membrane; cell pressures many times this minimum are applied in this work. A viscous cell fluid, silicone oil, is used to apply cell pressure to the system. Silicone oil is used for many reasons, most notably because it aids in preventing leaks. It was originally introduced into the MIT lab for use with frozen soils and has been used in many different applications since. Oil does not penetrate the rubber membranes used to seal the specimens in the cell, and it is immiscible with water-based permeants, therefore the use of oil as a cell fluid prevents the initiation of flow through the intact membrane. This setup does not prevent large leaks such as tears in the membrane where volumes of cell fluid are introduced into the pore fluid system. Thus far, system leakage has been minor.

4.5.3.2 Procedure

The following is the procedure used to test specimens in the Flexible Wall Permeameter that have previously been tested in the CRS apparatus.

1. Clean and grease the base platen, and the base and top cap adapters using general purpose vacuum grease. Record zero values for all pressure transducers and string pots. Snap the square end base adapter onto the base platen.
2. Carefully remove the specimen from the CRS apparatus following step 11 of section 4.5.2.2. Replace the filter screens and porous stones and center the specimen on the square end base adapter. Put the square top cap on top of the specimen.
3. Expand a 2.5 inch (6.35 cm) diameter rubber membrane onto a membrane stretcher and place over the specimen. Stretch four greased O rings onto an O ring stretcher and apply two each to the O ring surfaces of the base and top caps, leaving a space equal to the width of one O ring between them. Apply another rubber membrane over the specimen using the membrane stretcher and then two more O rings, one each on the top and bottom caps, filling in the gap left between the two existing O rings. This doubly sealed O ring method has been used at MIT for many years and is found to create an excellent seal. Connect the top cap drainage line to the apparatus drainage line extending from the base. Figure 4-18 shows the specimen set up at this point for a cubic specimen; the only difference the only difference between this figure and the set up described here is the specimen shape and dimensions.
4. Apply a vacuum to the pore pressure lines to perform a leak check. First remove the base pore pressure transducer and then disconnect the pore pressure lines from the PVA's by closing off the required valves. Make sure the specimen is hydraulically connected to the pore pressure lines (i.e. all relevant valves are open). Apply the vacuum through a specially made vacuum cylinder, shown in figure 4-19. The cylinder is partially filled with water and plugged with a rubber stopper through which one or more pieces of tubing passes, connecting to the pore pressure lines of the apparatus through the pressure transducer housings. One end of these tubing sections is submerged in water of the appropriate salt concentration (equal to that of the permeant). As the vacuum is applied, air is removed from the pore pressure lines and can be seen as bubbles exiting through the water from the

tubing sections. This provides a good means of performing an initial leak check of the pore pressure system prior to complete set up.

5. If no leaks are found, assemble the apparatus. Put the cell wall and top caps on and screw everything tightly together. While applying the vacuum to the specimen, fill the cell with silicone oil and pressurize it to equal the axial effective stress that the specimen last experienced in the CRS device. Release the vacuum once the desired cell pressure is reached. This causes saturation of the pore pressure lines and porous stones when water is drawn into the tubing connected to the pore pressure transducer housings.
6. Connect and zero the base pore pressure transducer. Initiate computer control the maintain the cell pressure for pressure up and adjust the valves so that the base pore pressure transducer measures only the specimen pore pressure. Start a new task on the data acquisition system to monitor all channels at 4 minute intervals.
7. Allow the system to pressure up until the pore pressure has stabilized. This takes approximately 3-4 days for CRS specimens which reached a sampling effective stress of 100% of the last applied stress in the CRS device.
8. Backpressure the specimen using the same increments as step 4 of section 4.5.2.2. Make sure the top and base pore pressures are hydraulically connected to allow for double drainage.
9. Recompress the specimen to the same isotropic stress state as was applied at the end of the CRS test. This step was not necessary for either of the two specimens tested as the sampling effective stress was 100% of that at the end of the CRS test and no further increases in stress were necessary.
10. Apply a constant head gradient by hydraulically disconnecting the base and top pore pressure PVA's and then increasing the base pore pressure by $\Delta u/2$ and decreasing the top pore pressure by $\Delta u/2$ where Δu is the desired differential pore pressure. The differential pore pressure ranged from 10 to 30 kPa for this research. Maintain the gradient for 8 to 24 hours as required until flow equilibrium is reached between the inflow and outflow increments and an accurate measurement of the specimen hydraulic conductivity is made.

11. Repeat for at least 3 gradients. Make sure to neither consistently increase nor decrease the applied gradient. Test additional gradients as required if significant variability in the measured hydraulic conductivity is noted.
12. Hydraulically connect the base and top pore pressure PVA's and set the pressures equal. Allow the specimen to equalize for a period of time. This process may be quick for low plasticity specimens (20 minutes to 1 hour) or may take up to 24 hours for high plasticity specimens. The amount of time required for equalization should be judged based on the amount of time required for the specimen to equalize to application of a constant head gradient.
13. Remove the specimen from the apparatus by reducing the cell pressure, draining the cell, and disassembling the apparatus. The membranes must be removed by vacuuming onto the membrane stretcher. Measure the specimen height and diameter at a minimum of 8 points around the circumference using a pair of digital callipers. Mass the specimen and place in an oven to dry for 2-3 days. Record the dry mass.

4.5.3.3 Problems

The main problem noted with the Flexible Wall Permeameter tests was that the specimen void ratio did not match that computed in the CRS tests. This problem is discussed in section 4.5.2.3. There were no other significant problems with this test.

Table 4-1: Characteristics of instrumentation used in CRS apparatus

Measurement	Device	Calibration Factor	Range	Resolution	Stability
Axial Deformation	External LVDT	2.110 cm V/V	2.5 cm	±0.0015% (0.1 mV)	±0.0045% (0.3 mV)
Axial Deformation	External LVDT	-2.043 cm V/V	2.5 cm	±0.0015% (0.1 mV)	±0.0045% (0.3 mV)
Axial Force	External Load Cell	-272.683 kN V/V	8.9 kN	0.05 N (0.001 mV)	0.1 N (0.002 mV)
Cell Pressure	External Pressure Transducer	-68940 kPa V/V	1400 kPa	0.01 kPa (0.001 mV)	0.03 kPa (0.003 mV)
Pore Pressure	External Pressure Transducer	-68740 kPa V/V	1400 kPa	0.01 kPa (0.001 mV)	0.05 kPa (0.005 mV)
Cell Volume	External Stringpot	96.320 cm3 V/V	48 cm^3	±0.004% (0.1 mV)	±0.004% (0.1 mV)
Pore Volume	External Stringpot	96.415 cm3 V/V	48 cm^3	±0.004% (0.1 mV)	±0.004% (0.1 mV)

Note: Resolution and Stability based on central data acquisition system, calculations based on specific dimensions.

Table 4-2: Characteristics of instrumentation used in Flexible Wall Permeameter apparatus

Measurement	Device	Calibration Factor	Range	Resolution	Stability
Cell Pressure	External Pressure Transducer	-693352 kPa V/V	14000 kPa	0.13 kPa (0.001 mV)	0.26 kPa (0.002 mV)
Base Pore Pressure	External Pressure Transducer	-34399 kPa V/V	700 kPa	0.006 kPa (0.001 mV)	0.024 kPa (0.004 mV)
Top Pore Pressure	External Pressure Transducer	-34283 kPa V/V	700 kPa	0.006 kPa (0.001 mV)	0.018 kPa (0.003 mV)
Base Pore Volume	External Stringpot	96.128 cm3 V/V	48 cm^3	± 0.004% (0.1 mV)	± 0.004% (0.1 mV)
Top Pore Volume	External Stringpot	96.350 cm^3 V/V	48 cm^3	± 0.004% (0.1 mV)	± 0.004% (0.1 mV)

Note: Resolution and Stability based on central data acquisition system, calculations based on specific dimensions.

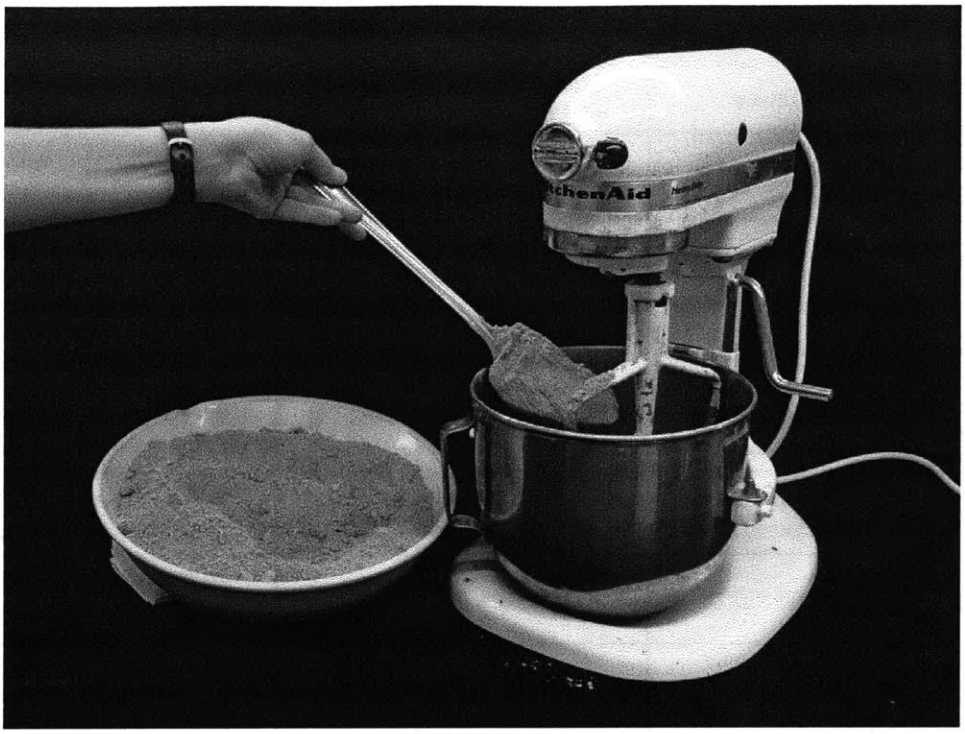

Figure 4-1: Mixing RBBC powder with 16 g/L sea salt at 100% water content in an electric mixer with beater attachment

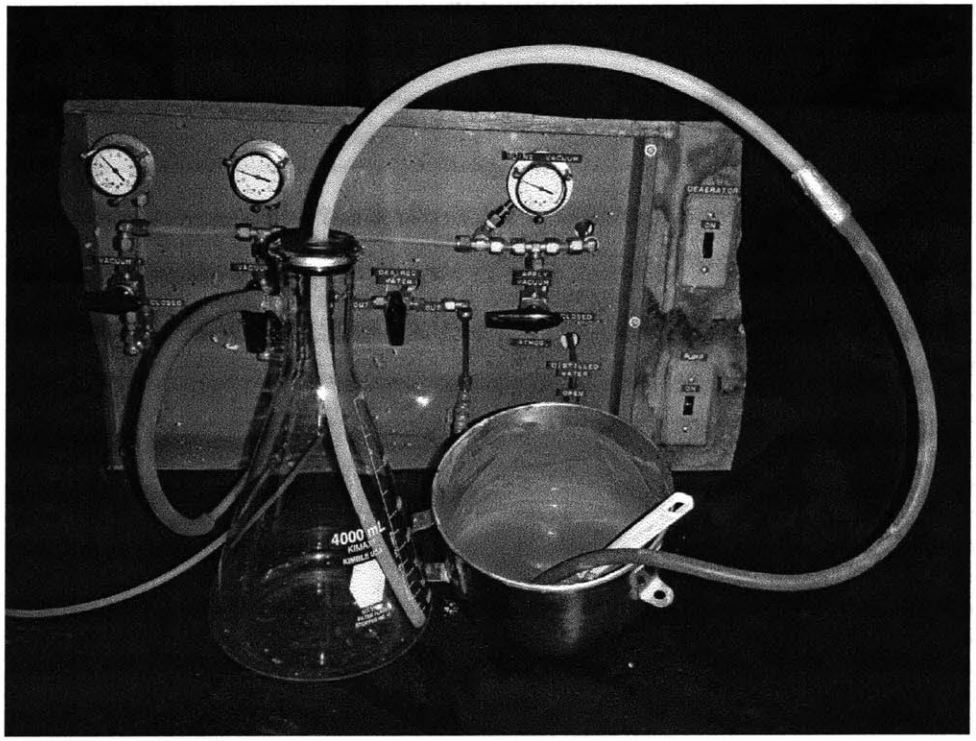

Figure 4-2: Transferring the RBBC slurry to a vacuum cylinder for de-airing

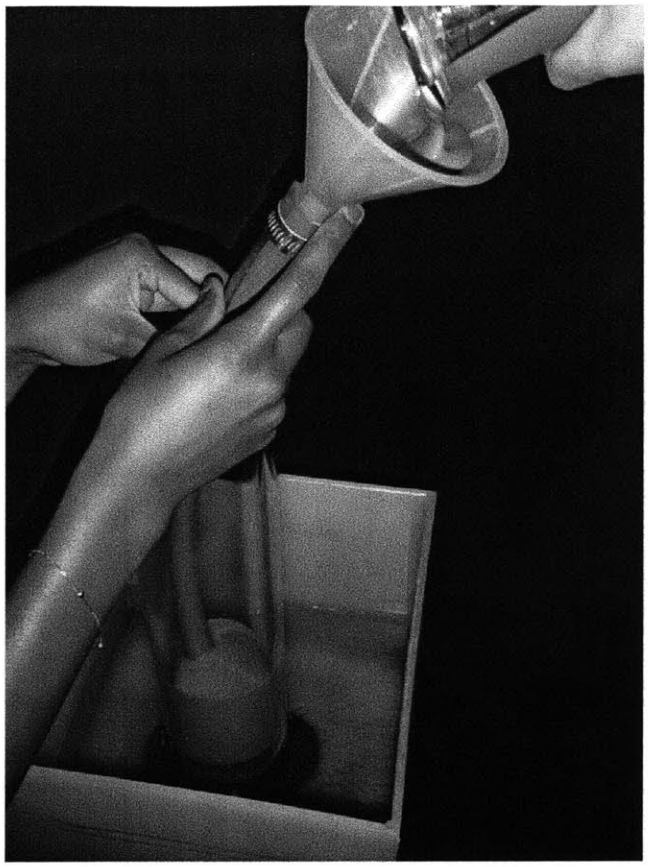

Figure 4-3: Pouring the RBBC slurry into 3" ID settling columns using a funnel method.

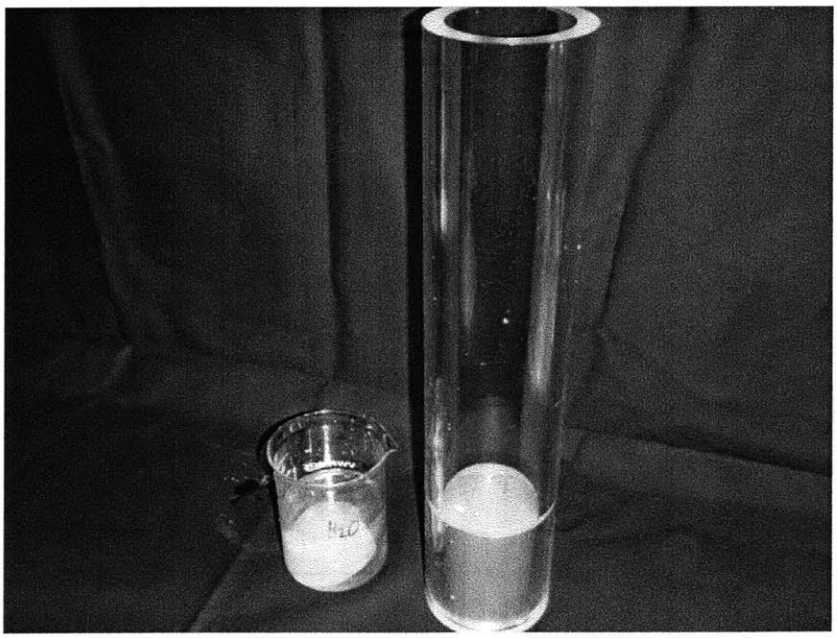

Figure 4-4: Configuration of base porous stone and filter paper in settling column

850g kaolinite 1225 g salt soln.
16 g/L salt 1206 g H2O + 19 g salt

MIT GEOTECHNICAL LABORATORY

Resedimentation Sample Data Sheet

Project: ALA Thesis
Sample No.: RS166
Source Material: Kaolinite
Water Content: 144 %
Salt Conc.: 16 g/L

LVDT Cal Factor (cm/(v/v)): N/A
Data Acq Channels: LVDT: N/A Vin: N/A

Tested By: ALA
Start Date: Dec 27 '10
Consolidometer: Pot
Area (cm²): 3"
Reference Height (mm): 8g + 0.65cm top 0.6cm

INC No.	Mass Added (g or kg)	Mass Type	Total Mass (g or kg)	Starting Date	Starting Time	Starting Input (volts)	Starting LVDT (volts)	Starting Height (mm)	Ending Input (volts)	Ending LVDT (volts)	Data Acq. File Name	Remarks
s			stone	Dec 27/10	11:00	—	—	28cm	—	—	—	Porous stone
1	304 g	2" spacer	304 g	Jan 1/11	13:35	—	—	24.4cm	b4	add	spacer	ref top + 5cm
2	304 g	2" spacer	608 g	Jan 7/11	11:45	—	—	28.9cm	b4	add	spacer	ref top + 5cm
3	-608g + 1241g	8" spacer	1241 g	Jan 11/11	16:42	—	—	32.7cm	b4	add	spacer	ref top - 10cm + 20.4cm
4	1 kg	weight	2241 g	Jan 14/11	18:05	—	—	42.65cm	—	—	—	
5	2 kg	weight	4.2 kg	Jan 19/11	11:00	—	—	41.6cm	—	—	—	
6	4 kg	weight	8.2 kg	Jan 26/11	17:00	—	—	40.3cm	—	—	—	
7	tot = 14 kg	weight	15.2 kg	Jan 31/11	10:20	—	—	39.0cm	—	—	—	
8	tot = 30 kg	weight	31.2 kg	Feb 2/11	12:00	—	—	37.6cm	—	—	—	
9	tot = 45 kg	weight	46.2 kg	Feb 5/11	10:55	—	—	—	—	—	—	
10	tot = 21.5 kg	weight	22.7 kg	Feb 8/11	11:50	—	—	—	—	—	—	
11	tot = 10 kg	weight	11.2 kg	Feb 11/11	10:30	—	—	—	—	—	—	
12												
13												
14												
15												

Comments:

Final Extruded Height (mm): _____

Figure 4-5: Sample resedimentation log

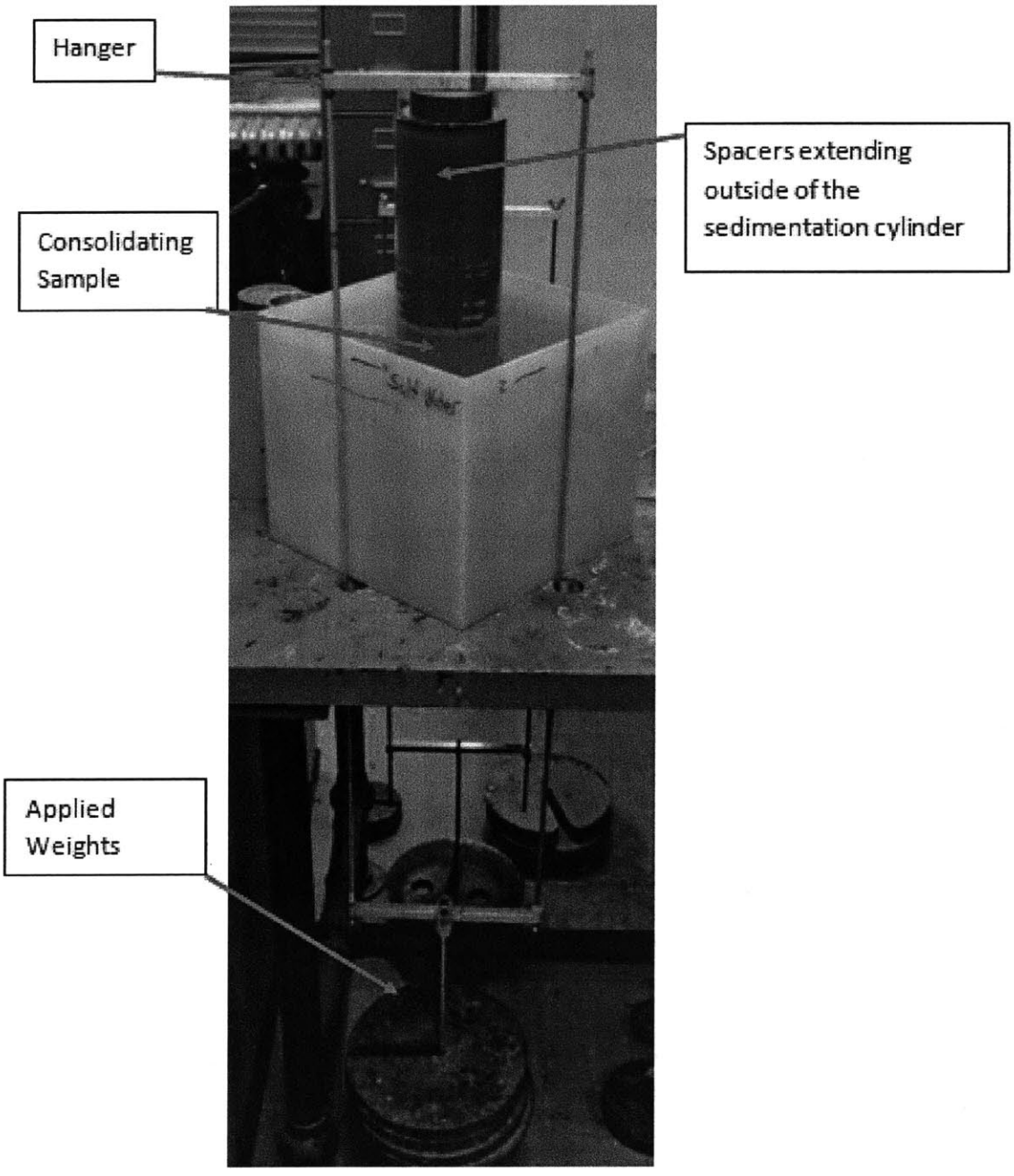

Figure 4-6: Hanger set up for sample loading

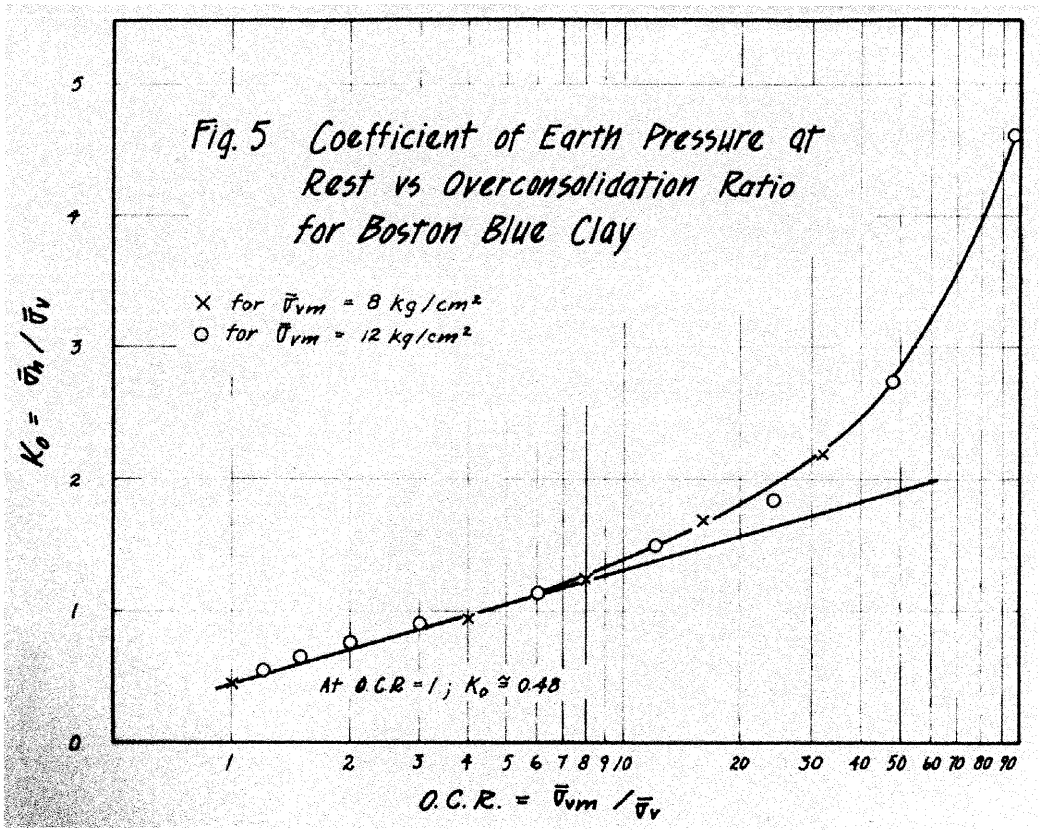

Figure 4-7: Lateral stress ratio, Ko vs. OCR for Boston Blue Clay (Ladd, 1965)

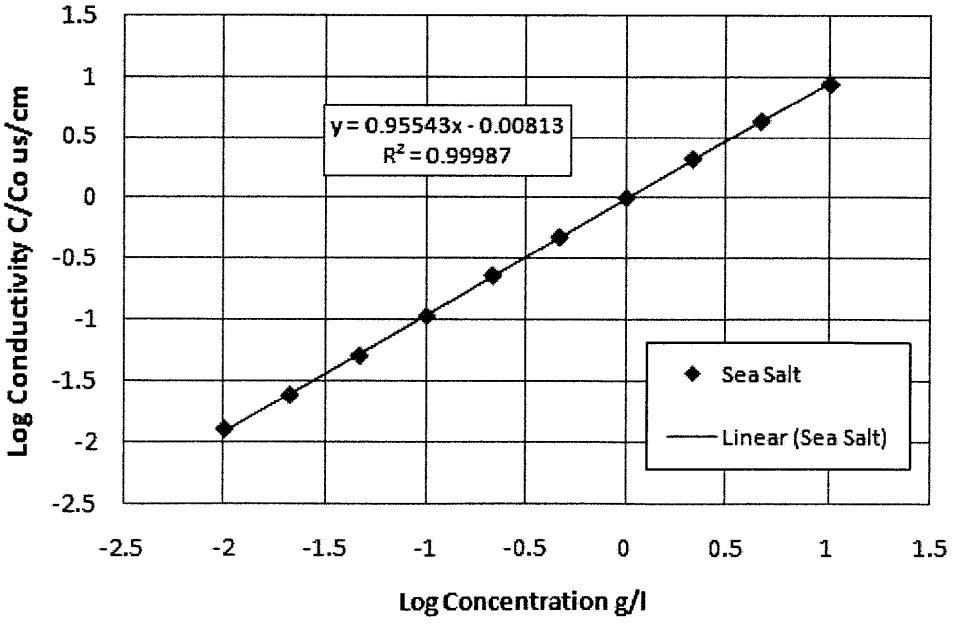

Figure 4-8: Salinity conductivity calibration curve for conductivity meter model 23226-505 VWR International

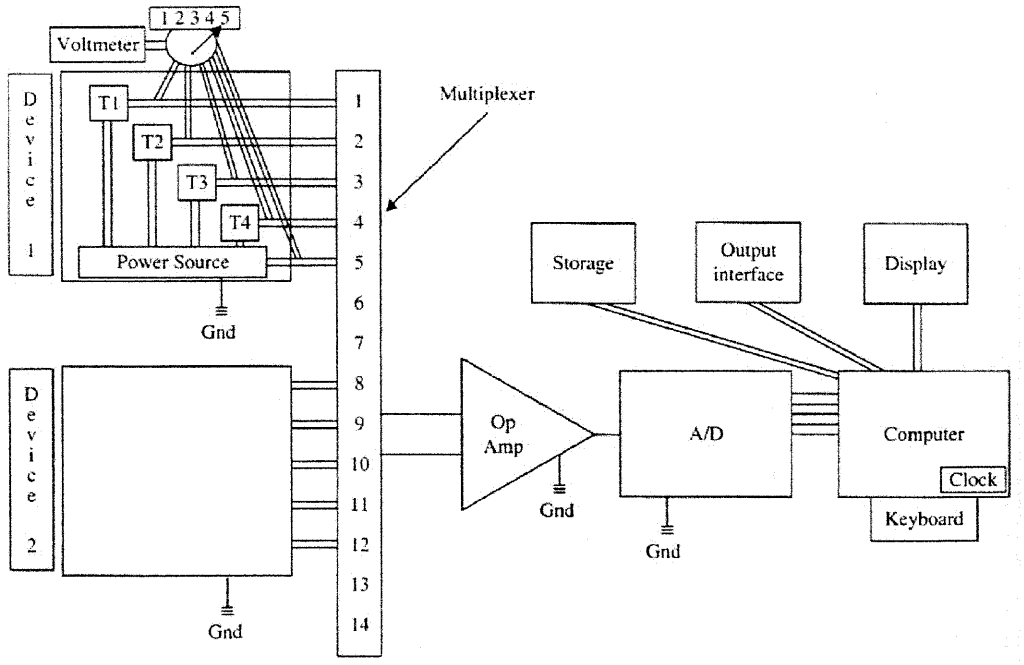

Figure 4-9: Schematic drawing of a centralized data acquisition system (Germaine and Germaine, 2009)

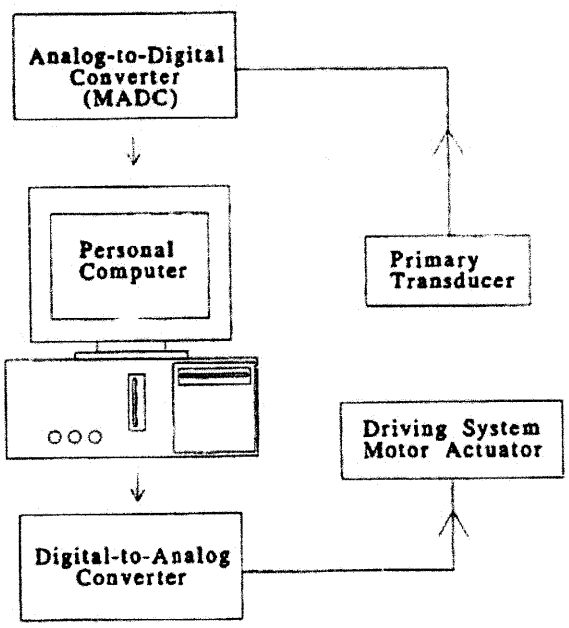

Figure 4-10: Schematic diagram of control system hardware components (Grennan, 2010)

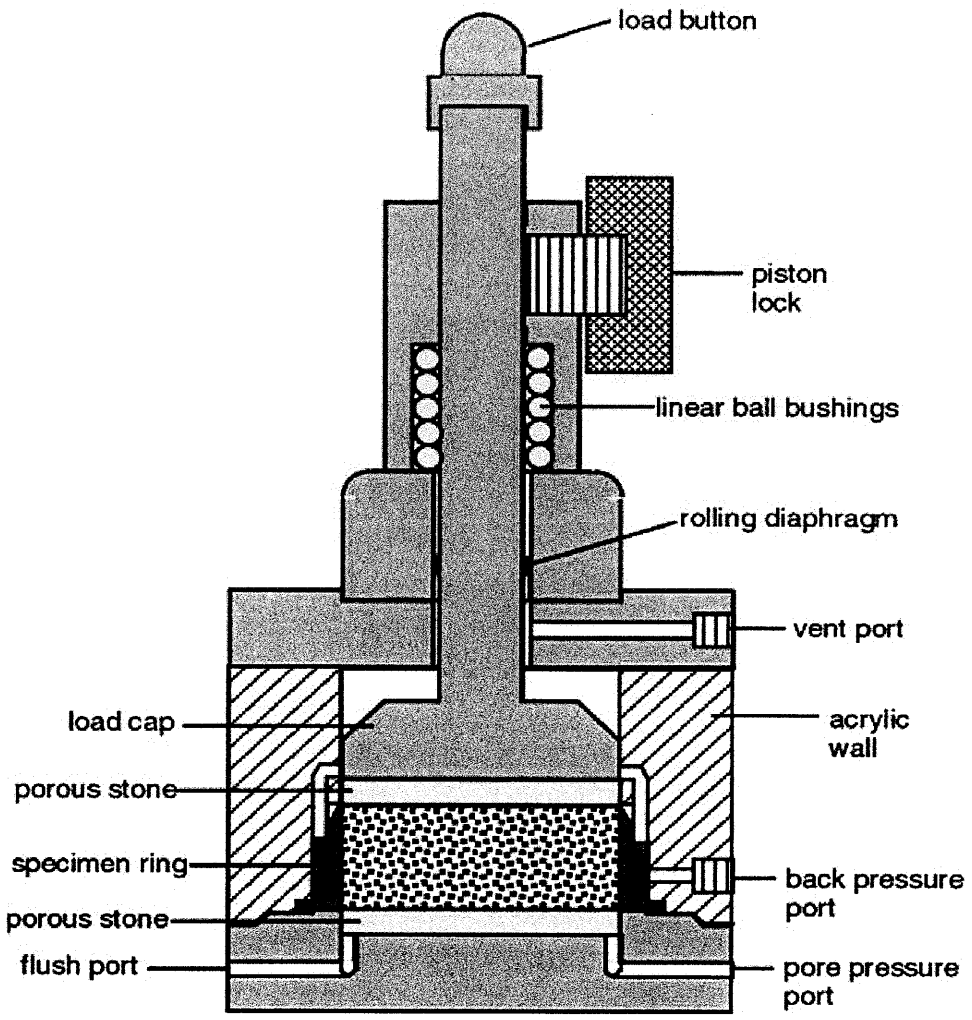

Figure 4-11: Schematic of a standard Trautwein CRS apparatus (ASTM D4186)

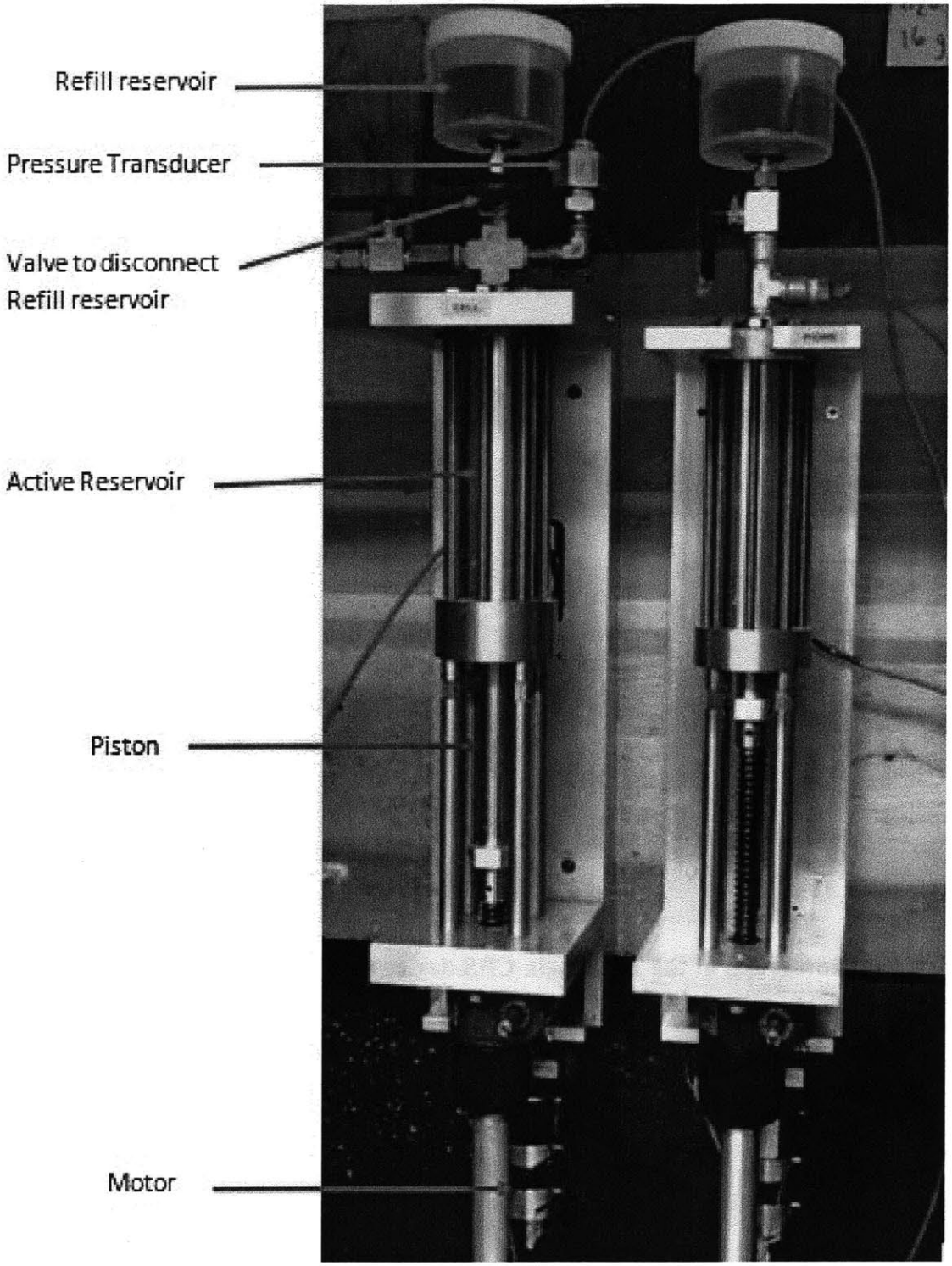

Figure 4-12: Photograph of the Pressure Volume Actuators used for pressure control and volume measurement in the CRS and Flexible Wall Permeameter devices.

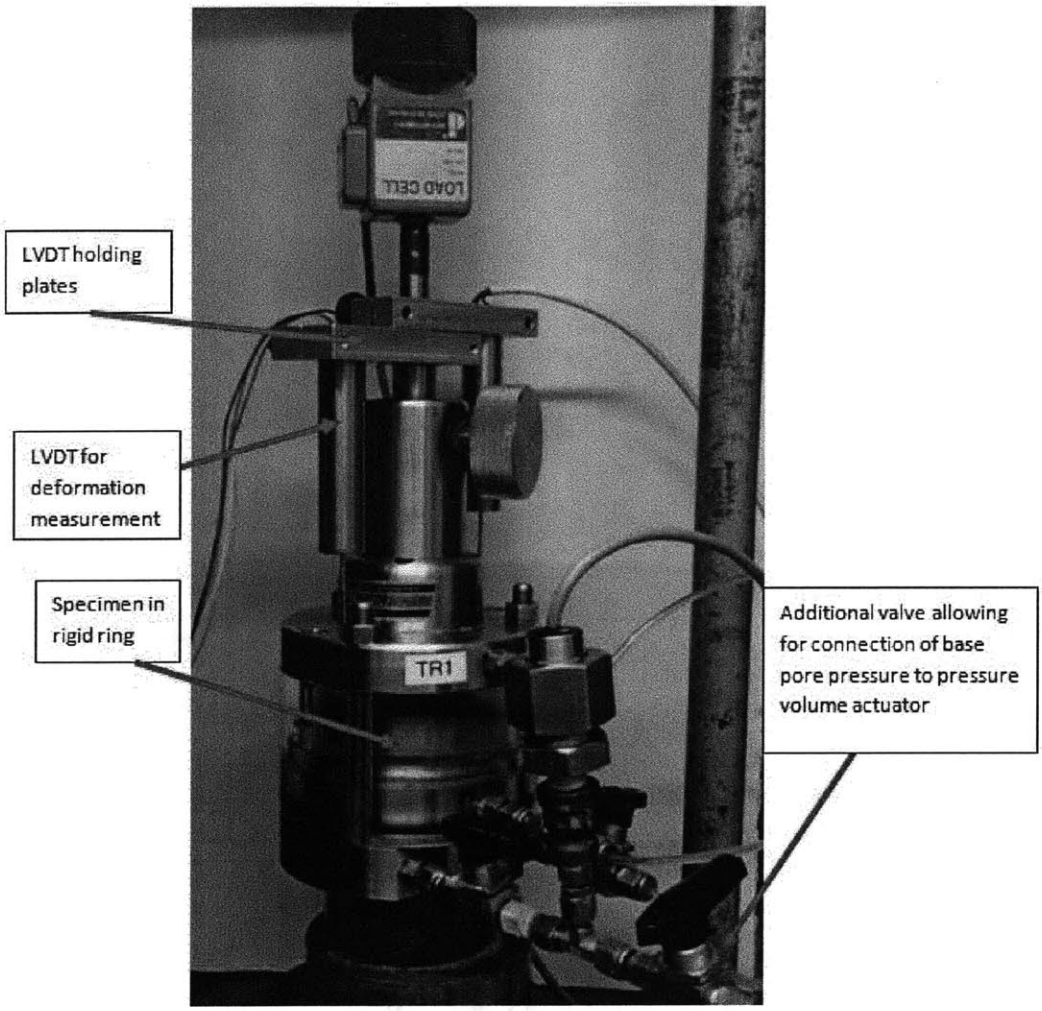

Figure 4-13: Photograph of the Trautwein CRS device used for this research

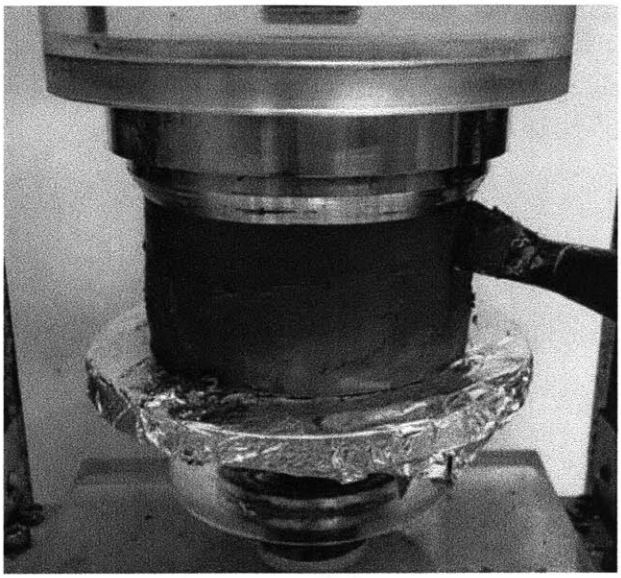

Figure 4-14: Trimming a CRS specimen into the rigid CRS Ring

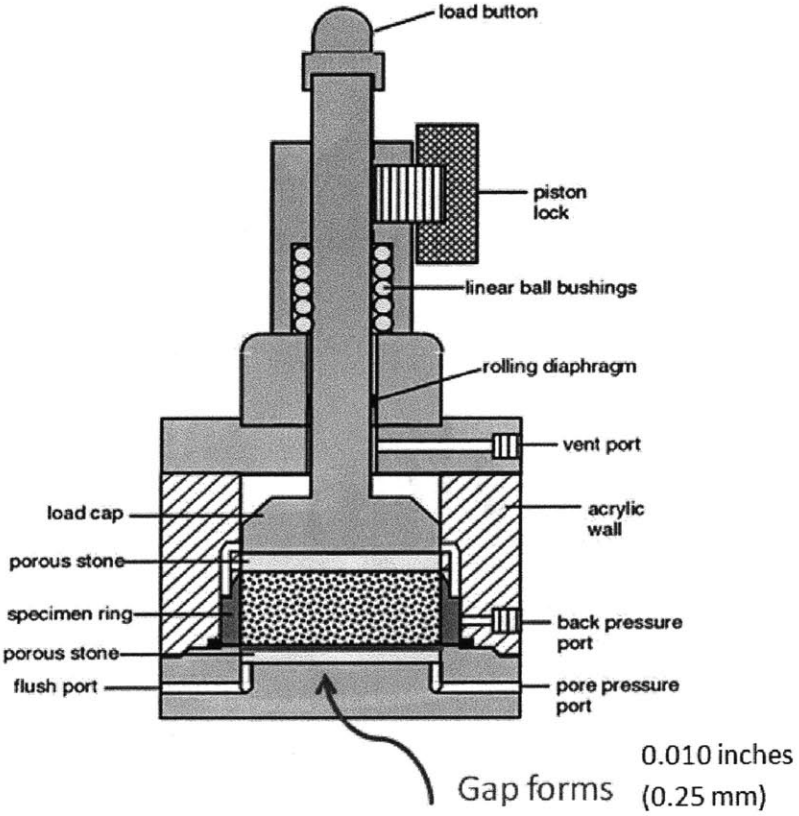

Figure 4-15: Illustration of formation of gap between specimen and porous stone in CRS apparatus

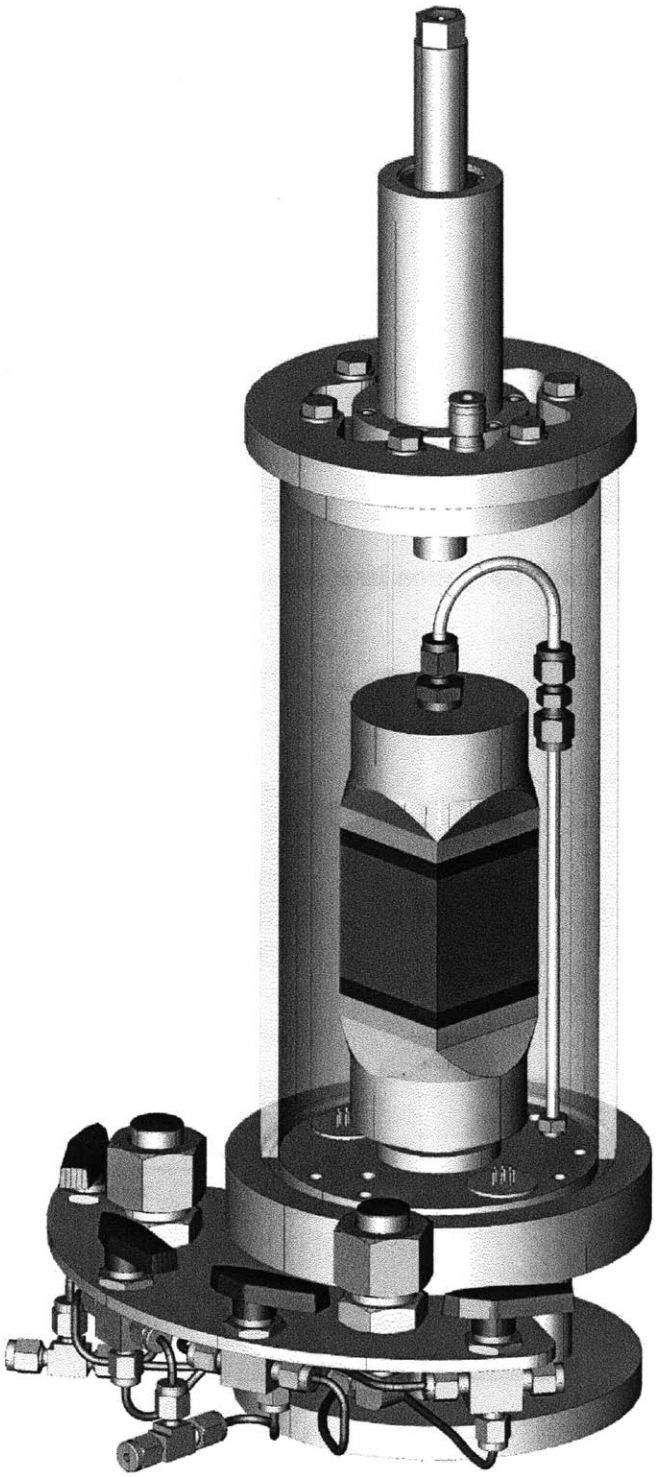

Figure 4-16: Solid view of the Flexible Wall Permeameter showing manifold and cubic shaped specimen

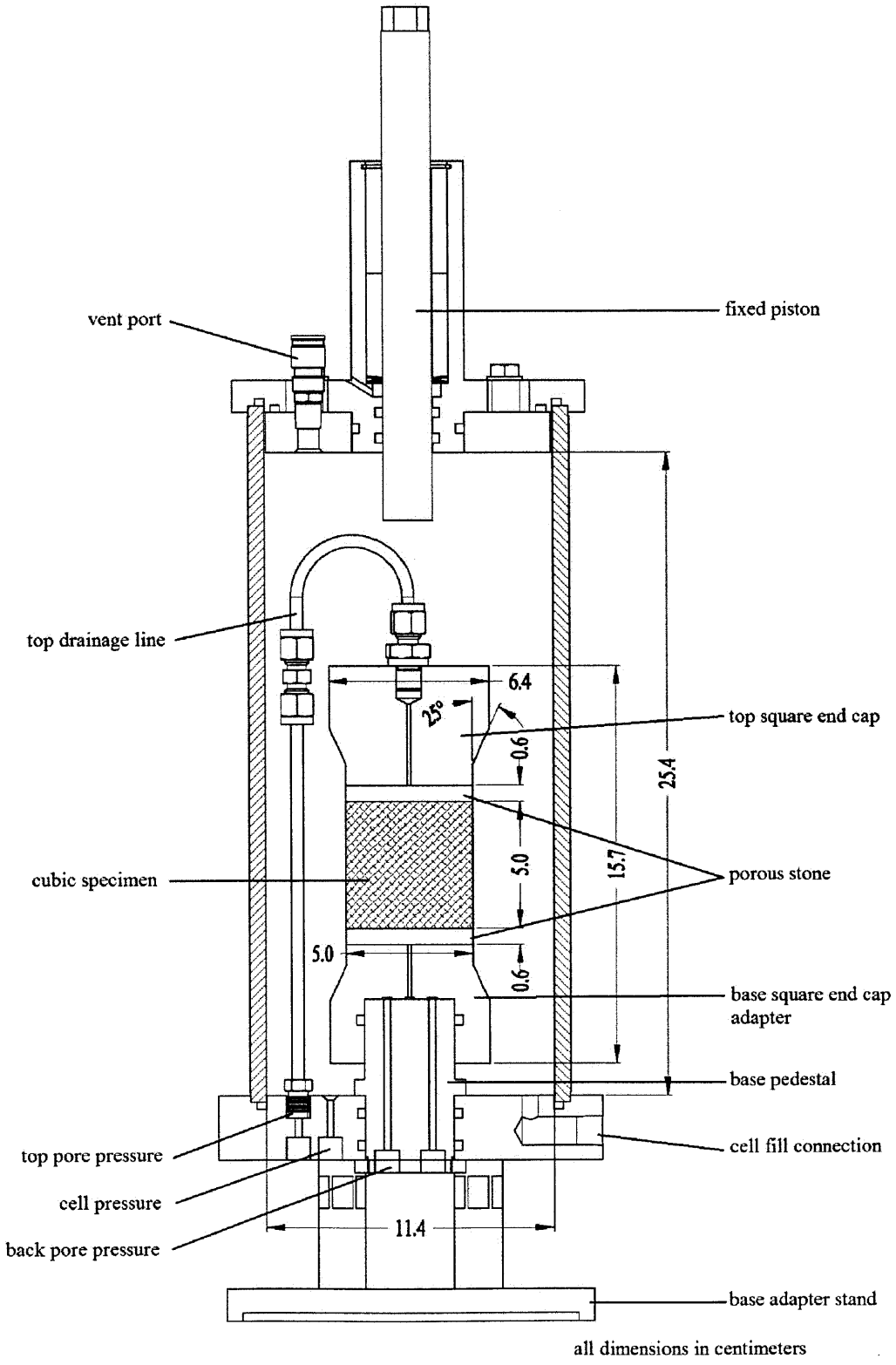

Figure 4-17: Dimensioned section of the Flexible Wall Permeameter with cubic specimen

Figure 4-18: Photograph of partial setup of specimen for Flexible Wall Permeameter (cubic specimen)

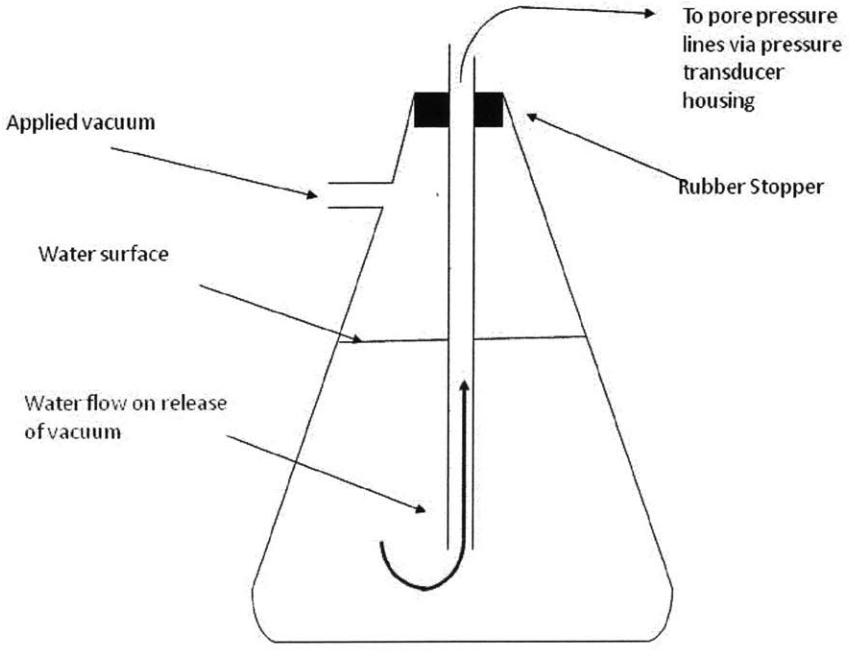

Figure 4-19: Schematic drawing of vacuum cylinder used to drain and saturate pore pressure lines of flexible wall permeameter

5 DATA ANALYSIS METHODS

5.1 Introduction

This chapter presents the different methods of analysis used in this investigation. This discussion includes analysis of the CRS loading measurements to determine the compression and hydraulic conductivity characteristics using Linear theory, and analysis of the constant head test measurements to determine the hydraulic conductivity. A brief discussion of leakage analysis in the flexible wall permeameter is presented. All results are summarized, analysed and discussed in Chapter 6.

5.2 One Dimensional Loading Data Analysis

5.2.1 CRS Reduction Program

The CRS loading data were analyzed using a QBasic analysis program written by Dr. John T. Germaine for use in the MIT Geotechnical Laboratory. Appendix 1 contains a printout of the program code. The program takes as input a data file from the central data acquisition system and requires user input of the transducer calibration factors, zero values, initial specimen height and height of solids. The program performs a linear steady state analysis using Wissa's equation modified for large strain described in Chapter 2. It computes the strain, void ratio, axial effective stress, pore and cell pressures, hydraulic conductivity, excess pore pressure, compressibility, coefficient of consolidation, work and excess pore pressure as a percentage of the applied load at each increment. In addition to performing the raw calculations, it offers the advantage of applying linear regression over a specified increment to compute the strain rate and computing the moving average pore pressure over the same increment. The average pore pressure and the strain rate computed using regression are then used to compute values of the coefficient of consolidation and the hydraulic conductivity that are not affected by the high frequency of data acquisition measurements. With respect to this research, the regression and averaging method helps smooth the void ratio vs. log hydraulic conductivity curve considerably.

Two regression parameters are required as inputs by the user, including the strain increment to be used and the moving window to smooth the pore pressure data. For these analyses, data

points are taken at 2 minute intervals during loading increments and strain increment of 0.5% and a moving window of 3 readings were found to produce relatively smooth curves.

5.2.2 Determination of Steady State

The CRS reduction program described in section 5.2.1 computes a hydraulic conductivity for each measurement point during the entire test including periods of back pressure saturation, hold stress, loading and unloading; it cannot distinguish between the different phases of the test. Figure 5-1 plots the complete computed void ratio vs. log hydraulic conductivity results for a test conducted on RBBC. Hydraulic conductivity measurements are only representative when the strain rate is sufficiently large so as to induce an excess pore pressure at the base of the specimen. As a result, the true hydraulic conductivity results have to be extracted from the computed results.

All data pertaining to periods of back pressure saturation, hold stress and unloading periods were removed from the computed results by manual inspection of the dataset. . Unloading typically occurred so rapidly that insufficient data was collected to permit computation of the hydraulic conductivity vs. void ratio curve. At the start of loading a period of transience develops; this is described in detail in Chapter 2. The reduction program assumes steady state conditions only and thus this initial must also be removed. Transience occurs initially as the specimen equilibrates to the onset of loading; this transience lasted in general only for the first few data points that were recorded for most specimens tested in this research. At the end of loading, the hydraulic conductivity curve is affected by the regression analysis's averaging method; this method extends the regression line to those strain measurements taken after the completion of steady state loading, incorporating data recorded during the hold stress routine initiated at the end of the loading sequence in to the results. This portion of the computed hydraulic conductivity results was also removed.

The true transient portions of the data set are removed according to the F_3 criteria; steady state occurs when Tv> 0.5, or F_3 >0.5 as described in chapter 2, section 2.4.2.1.2. F_3 is computed using the excess pore pressure and the applied total axial stress, and figure 2-7 is used to determine Tv as a function of F_3. This analysis resulted in removal of only the first few data points during the loading sequence of each data set.

Following removal of true transient portions of the data, the void ratio vs. log hydraulic conductivity curve was plotted and often erratic or unusual behaviour was observed in the initial portions of the curve (figure 5-2). Sometimes, as in figure 5-2, the computed hydraulic conductivity actually increased with a decrease in void ratio. However, a steady, linear trend was always evident in the middle portion of the curve. The erratic initial portions of the curve are thought to be a result of flow occurring through the bottom boundary of the specimen to equilibrate the pressure in the base measurement system. In the theoretical derivation of the hydraulic conductivity using the CRS technique the bottom of the specimen is a no flow boundary. The pore pressure measurement system, including the porous stone and drainage lines, has a relatively small volume and the transducer is located as close to the lower boundary as physically possible; however, in order to measure the pore pressure at this boundary, some flow must occur across this 'no flow boundary'. This is an experimental deviation from the CRS theory, and results in a scattered curve for the initial portion of the test. From experience at MIT, it is thought that the effect of this deviation from the theoretical ideal boundary condition varies with the stiffness of the soil, with stiffer soils being affected more than softer soils.

The scattered initial portions of the void ratio vs. log hydraulic conductivity curve were removed; this should not affect results as the deviation from ideal boundary conditions affects measurements at high void ratios representing the start of the test, and this study focuses on the results obtained at lower void ratios measured near the maximum applied stress. Finally, a linear void ratio vs. log hydraulic conductivity trend resulted for most soils (Figure 5-3).

5.2.3 Apparatus Compressibility

The reduction program (section 5.2.1) uses two apparatus compressibility curves, one accounting for the deformation due to loading by the piston and one for the deformation due to pressurization of the cell. These apparatus compressibility curves were previously measured and are included in the program code (Appendix 1). However, because of problems encountered related to non agreement in the measured void ratio, discussed in Chapter 4 as bottom seating error, the apparatus compressibility due to loading by the piston was re-measured in this investigation.

The apparatus compressibility was measured by performing two separate tests on a stainless steel dummy specimen. Each test included two complete load –unload sequences to the maximum axial effective stress tested (2000 kPa) and used the same cell pressure used for specimen testing (400 kPa). The specimen deformation was assumed negligible and all measured deformation assumed to be apparatus deformation. The results were combined and plotted in terms of deformation vs. load (Figure 5-4). The load measurement is presented in kilograms force and not SI units because this is how it is applied in the CRS reduction program code. An average power law trend line was determined and this relationship was used in the CRS reduction program (section 5.2.1) to correct the measured deformation as a function of the measured applied load.

Figure 5-5 plots the newly measured apparatus compressibility curve specific to the MIT08 Trautwein CRS device and compares it with the relationship that was previously being used for all Trautwein CRS devices in the MIT Geotechnical Laboratory. There is a significant difference between the two curves, ranging from 0.023 to 0.025 cm, which accumulates rapidly over the low stress range.

The measured bottom seating error, discussed in Chapter 4 section 4.5.2.3.1, was also measured to be 0.025 cm. Thus, apparatus compressibility errors and bottom seating errors may have equally contributed to the discrepancies in void ratio that were noted during the CRS testing program. This result was encouraging because the measured potential for bottom seating error did not account fully for the void ratio errors that were measured in the specimens tested.

5.3 Constant Head Test Analysis

5.3.1 Hydraulic Conductivity Calculation

This section describes the method of analysis used to compute the hydraulic conductivity from data collected when a differential constant head gradient is applied to the specimen. In the CRS device, this gradient is applied by maintaining the cell pressure at the back pressure value, typically 400 kPa, and reducing the base pore pressure by the applied differential pressure, as described in chapter 4. Flow is from top to bottom. For the flexible wall

permeameter, both the top and base pore pressures are adjusted by one half the applied differential pressure. Flow is from bottom to top.

The data are recorded at 4 minute intervals using the central data acquisition system and at minimum the pore pressures applied to the specimen and the associated volume changes are measured. In the CRS device, the height of the specimen is also measured by tracking the LVDT and correcting this for apparatus compressibility, as discussed in section 5.2.3.

The inflow and outflow volumes are plotted vs. time. These should form straight lines that are superimposed; any offset indicates an inequality in the inflow and outflow increments at some point during the test. In fact, some offset is often the case as some degree of swelling and/or consolidation occurs upon application of the differential pressure. If the pore pressure is reduced, the effective stress increases and the specimen is reconsolidated. Conversely, if the pore pressure is increased, the effective stress decreases and the specimen swells. Figure 5-6 shows this phenomenon schematically for the case of a specimen tested in the constant head permeameter where each of the top and base pore pressures is adjusted. Figure 5-7 shows a typical flow volume vs. time curve for a constant head gradient. When a differential head is applied to the specimen, initially there is potential for inequality in the inflow and outflow measurements as the specimen volume adjusts to the newly applied stress regime, as demonstrated in figure 5-6. For the specimen shown in figure 5-7 this adjustment period is hardly noticeable as the cumulative inflow and outflow volumes are not only equal but follow the same trends with time (i.e. have the same slope) for the entire period of measurement. Figure 5-8 plots the moving average flow rate computed over a 40 minute interval. This plot is quite unsteady plotted at this scale; the PID control algorithm controls the pressures, not the flow rate which is dependent on the pressures. The flow into the specimen is better controlled than that out of the specimen; on average both the inflow and out flow are steady with time in the sense that neither experience a net increase nor decrease in flow rate with time. Finally, figure 5-9 presents the same results in terms of the differential flow rate, Qin – Qout, vs. time. This differential flows rates are in the order of 10^{-6} cm^3/s whereas the flow rates through this specimen, two orders of magnitude higher than the average flow rates from figure 5-8. Although initially variable, after a short time, the differential flow rates level off, on average,

but maintain a time dependant oscillation again stemming from the periodicity in the flow rates seen in figure 5-8 and likely affected by the control system.

The pressure vs. time measurements for each of the base and top pore pressures are plotted vs. time in figure 5-10. For this example, the top pore pressure, equal to the cell pressure in the CRS is much better controlled using the algorithmic computer control than the base pore pressure, however the small variance is actually quite good. The computer control uses a Proportional Integral Derivative (PID) algorithm using 4 coefficients and these coefficients are adjusted when necessary to provide as consistent and accurate of control as possible, producing the relatively smooth pressure vs. time trends seen in figure 5-10.

Finally, the gradient vs. time trend can be computed using the pressure vs. time trend for each of the two pore pressures, knowing the salinity and corresponding density of the permeant and knowing the height of the specimen measured by the LVDT in the case of the CRS, or by measuring the actual specimen dimensions after testing for the flexible wall permeameter. The gradient is equal to the change in head of the specimen over the change in length, and is computed by converting the measured pore pressures to hydraulic heads according to equation 5-1:

$$i = \frac{dh}{dl} = \frac{\frac{\Delta P}{\rho_p}}{dl} \tag{5-1}$$

Where:

i is the applied gradient [];
dh is the change in total head across the specimen [L];
dl is the length of the specimen [L];
ΔP is the pore pressure differential across the specimen [M/L^2]; and
ρ_p is the unit weight of the permeant [M/L^3].

The unit weight of the permeant was assumed equal 1.0 g/cm^3 for all specimens; this value corresponds to that used in the CRS reduction program for computation of the CRS hydraulic conductivity results. Figure 5-11 gives a typical gradient vs. time plot. This plot is quite steady because each of the pore pressure measurements used to compute the gradient are also relatively steady with time owing to the calibrated PID control algorithm.

In order to determine the onset of steady state given the apparent periodicity in the inflow and outflow measurements, as a rule of thumb, hydraulic conductivity calculations excluded at least the first 5000 seconds, or 1 hr 23 minutes of a test. This was done for all tests. For tests where the flow volume vs. time curve (figure 5-7) showed a significant difference between the inflow and outflows, and/or there were evident deviations from a steady state in any of the pressure vs. time, gradient vs. time or incremental volume vs. time curves, this window was extended, sometimes up to 10000 seconds (2 hr 45 minutes). Generally the hydraulic conductivity computational period extended to the end of data collection for a test.

Once three different gradients were tested, the computed hydraulic conductivity was often very close for each gradient. A few tests experienced a slightly higher than average standard deviation in the computed hydraulic conductivity; in these cases the steady state window for computation of the hydraulic conductivity for an individual gradient was adjusted to see if there was any affect on the results. It was consistently found that adjusting the computational data window beyond the bounds of the rule of thumb guidelines resulted in no change in the computed hydraulic conductivity.

The hydraulic conductivity was computed according to equation 5-2, based on Darcy's law, discussed in Chapter 2:

$$K = \frac{Vin+Vout}{2\Delta tiA} \tag{5-2}$$

Where:

K is the hydraulic conductivity [L/T];
Vin is the inflow volume over the defined computational period [L^3];
Vout is the outflow volume over the defined computational period [L^3];
Δt is the defined computation period [T];
i is the computed hydraulic gradient (equation 5-1) []; and
A is the area of flow [L^2].

For the CRS constant head tests, the area of flow is fixed and is equal to the area of the CRS ring. For the flexible wall permeameter, the area of flow is variable however for the two tests performed in this investigation the area of flow was measured to be the same as that in the CRS device.

5.3.2 Void Ratio Determination

There was much emphasis placed on evaluating the precision of the void ratio calculation for each specimen during this investigation, especially with the identification of the bottom seating error, discussed in Chapter 4.

Two void ratios are computed for each constant head test performed in the CRS device, and by comparing these two void ratios a quantitative estimate of the potential error incorporated into the test may be derived. This is further discussed in Chapter 6.

The first void ratio computation method uses the initial specimen height, constrained by the height of the CRS ring and depth of recess tool during trimming, and the deformation that occurs as a result of axial loading as measured by the LVDT measurement system and corrected for apparatus compressibility. The measured specimen height and area, as well as the dry mass of the specimen are used to compute the void ratio. This void ratio computation method is the same that the CRS reduction program uses to compute the void ratio at any point during the test.

The second void ratio computation is obtained after all testing is complete. The specimen is removed from the CRS apparatus as quickly and carefully as possible. The cell pressure and axial load are released simultaneously and the piston is locked in place. The apparatus is disassembled and the specimen removed from the rigid specimen ring and all excess water removed. The specimen height is measured at a minimum of 8 points around the circumference and the wet mass is recorded. This process takes a maximum of 5-6 minutes, minimizing the potential for swelling before a height measurement can be made. The specimen is then oven dried for a minimum of 2 days in an oven at 110°C and the dry mass is recorded. Using these data, the void ratio can be computed using both a volume based or mass based approach as discussed in section 4.5.2.3.1 (equation 4-3).

5.3.3 Leak Test - Flexible Wall Permeameter

Leakage was assessed during the back pressure phases of the flexible wall permeameter test and turned out to be an important consideration for the constant head hydraulic conductivity measurements.

In the flexible wall permeameter, each specimen was allowed to equilibrate with no volume change until the pore pressure stabilizing, allowing measurement of the sampling effective stress, equal to the applied cell pressure minus the measured pore pressure. The specimen is back pressured at this sampling effective stress. It was assumed that any measured volume change during back pressure is associated with pressurization of the pore pressure measurement and control system and the specimen void space, and not with volume change of the specimen itself. Theoretically, based on this assumption, the measured volume change vs. time during back pressure should become constant once the system and specimen are fully saturated. Any deviation from constant volume, especially a linear volume change vs. time trend, could indicate either a leak in the system or pressure driven dissolution of air into water, if air was trapped in the system.

Both of the two specimens tested in the flexible wall permeameter reached a sampling effective stress equal to the target hydrostatic effective stress state for hydraulic conductivity testing (i.e. the same effective stress state as they were last exposed to in the CRS device). This allowed for back pressuring at the testing effective stress, meaning that no reconsolidation phase was required. As such, where a leak was detected, it was readily evident and measurable in the volume change vs. time plot measured during the back pressure phase of the test sequence. For the specimens tested, one specimen experienced a leak and one did not. Figure 5-12 shows the back pressure volume vs. time plot for the case of no leak and figure 5-13 gives the same plot for the case where a leak was measured.

In both of these figures, the back pressure volume change is measured starting a 0.0 cm^3 volume at zero time. The volume axis of the plots is scaled to show the difference between a detectable leak and a non detectable leak; in figure 5-12 the volume change with time after 20,000 seconds is smaller than the resolution of the string pot measurement system, however figure 5-13 shows a linear increase in volume with time after 20,000 seconds with the leak rate indicated.

The linear increase in volume with time seen in figure 5-13 was identified as a leak and not due to trapped air in the system because a physical leak was located in the plumbing

connecting the top pressure PVA to the flexible wall permeameter apparatus. The leak was both visible and detectable by touch.

The leak rate measured was an order of magnitude lower than the estimated flow rate through the specimen. Therefore, given an accurate measure of the leak rate, constant head testing was allowed to continue with flow measurements adjusted according to the measured leak rate.

It is important to note the different measured volumes for the back pressure phase for the two different tests; ignoring the leak, figure 5-12 shows a back pressure volume change in the order of 0.3 cm^3, and figure 5-13 reports a volume five times this amount, approximately 1.5 cm^3. The reasons for this difference is unknown, but could be attributed to ineffective or differential vacuuming of the pore pressure lines when the cell was filled, leading to differences in the volume of trapped air in the system.

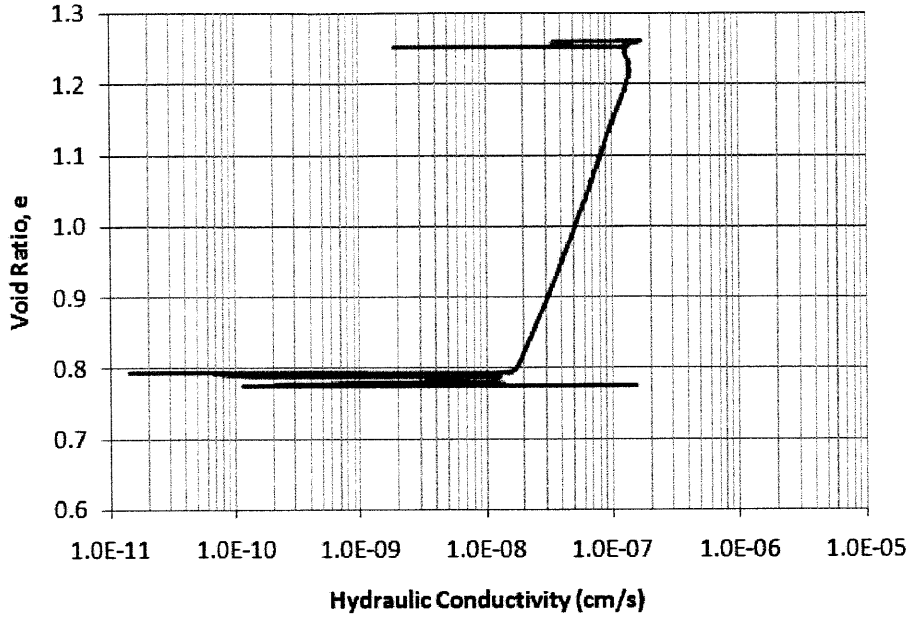

Figure 5-1: Typical void ratio vs. log hydraulic conductivity curve for entire test duration (CRS 1190)

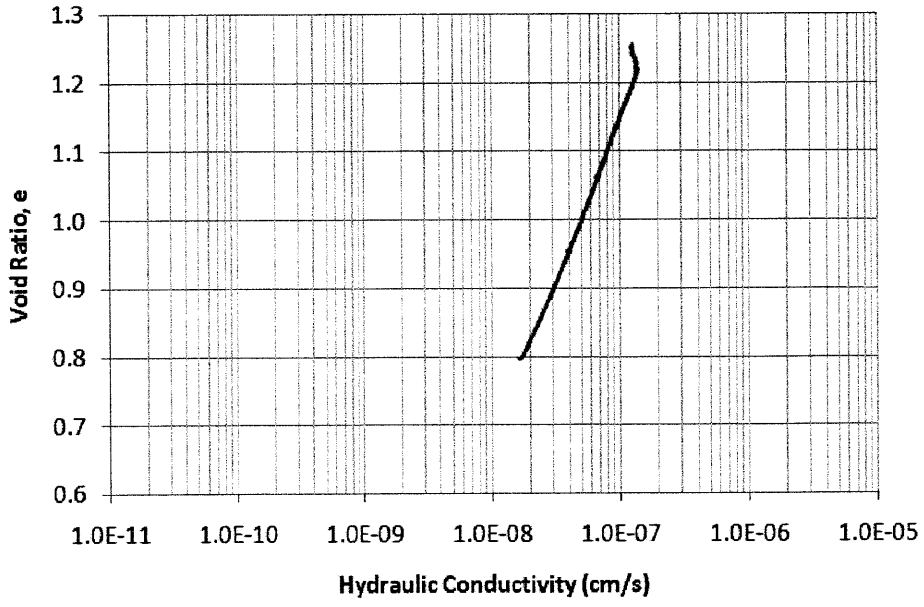

Figure 5-2: Typical void ratio vs. log hydraulic conductivity curve for loading portion of test with saturation, hold stress and unloading portions removed (CRS 1190)

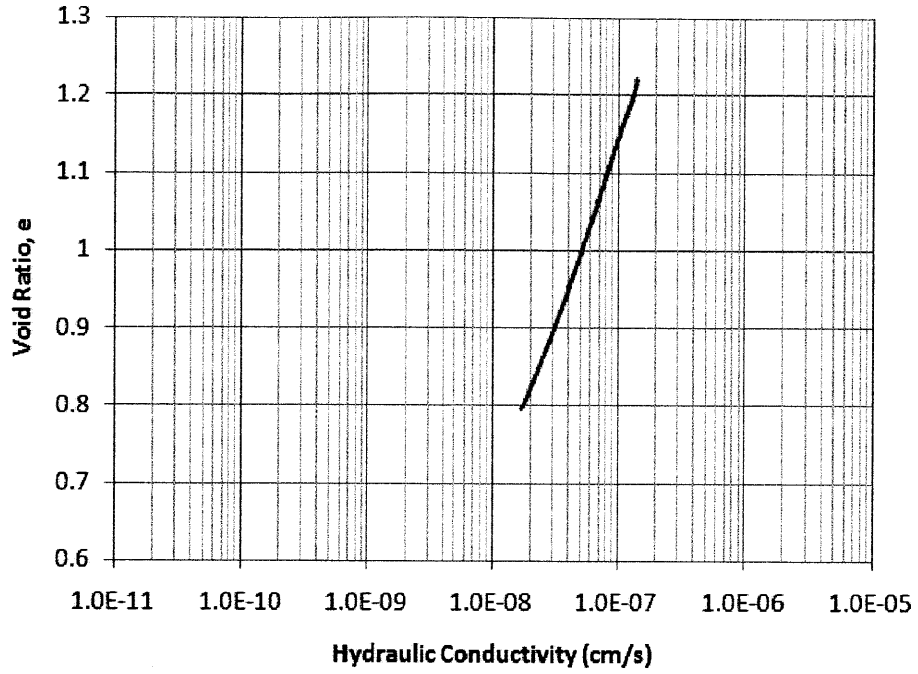

Figure 5-3: Typical final linear void ratio vs. log hydraulic conductivity curve (CRS 1190)

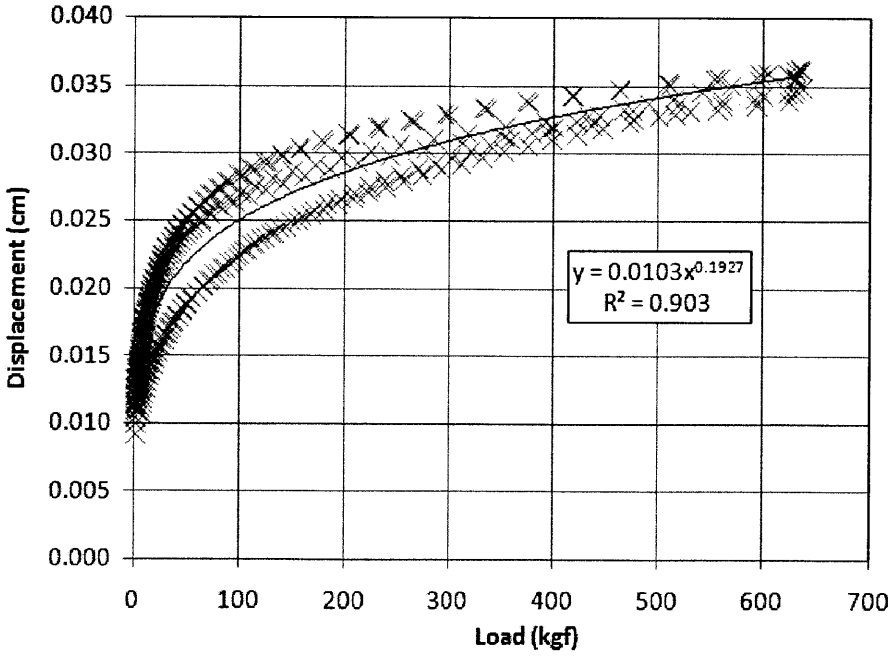

Figure 5-4: Apparatus compressibility measurements on CRS MIT08 (CRS 1169 and CRS 1167)

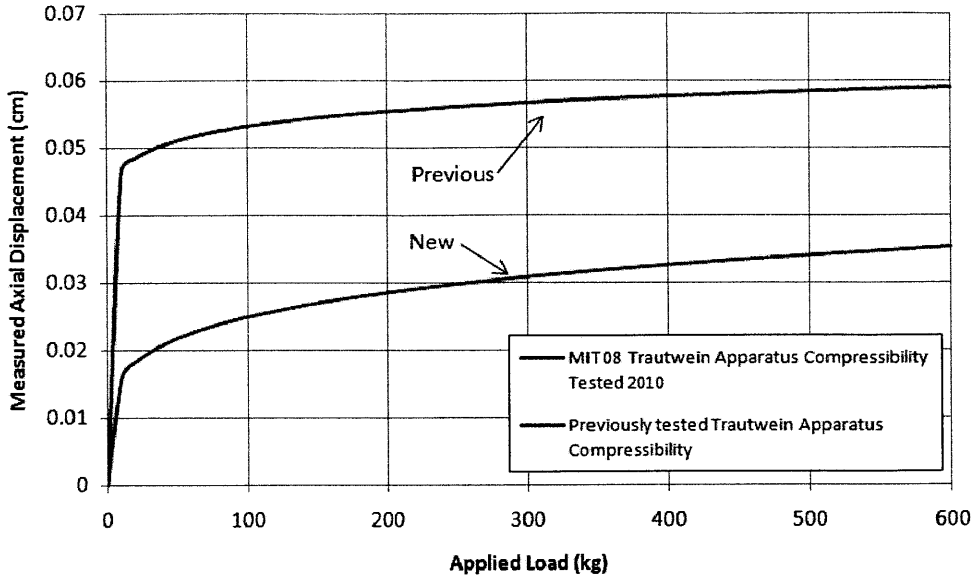

Figure 5-5: Comparison of new and old apparatus compressibility measurements

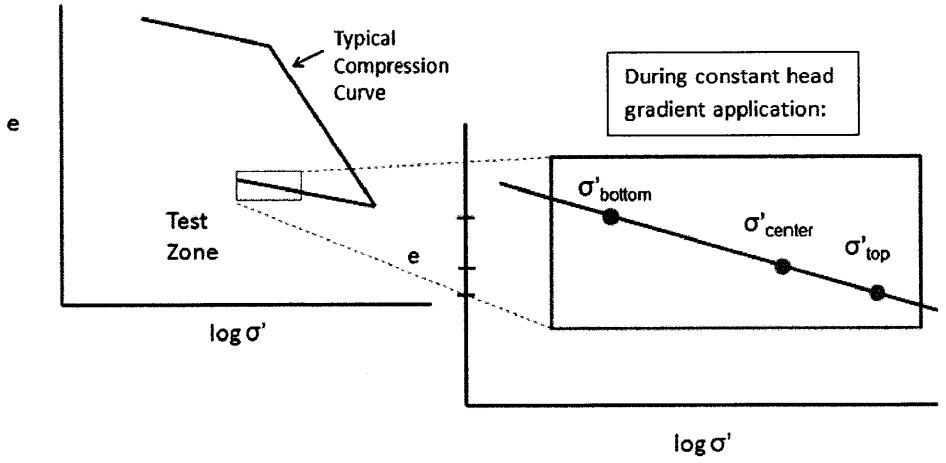

Figure 5-6: Typical consolidation behaviour during application of a constant head gradient

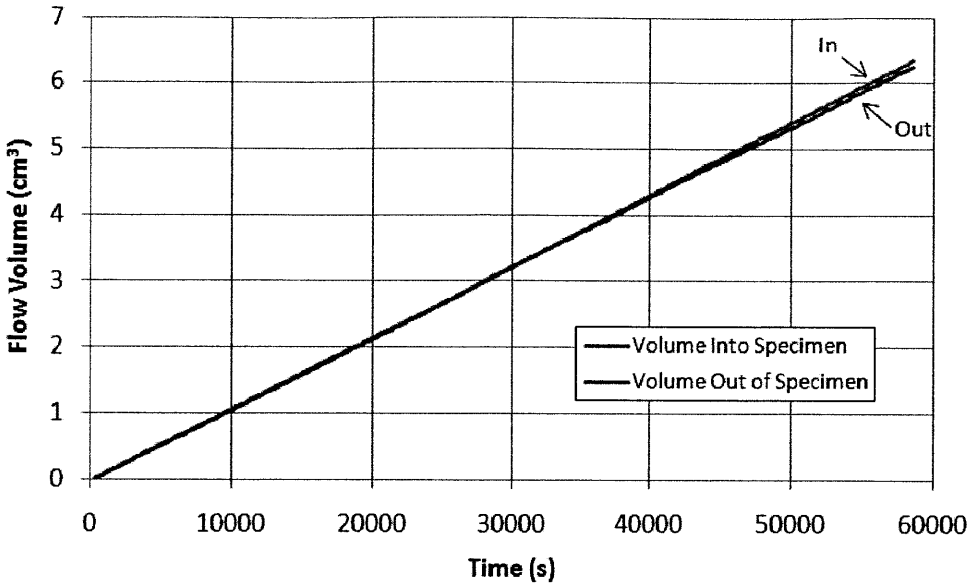

Figure 5-7: Typical flow volume vs. time plot during a constant head gradient (CRS 1210, Gradient 2)

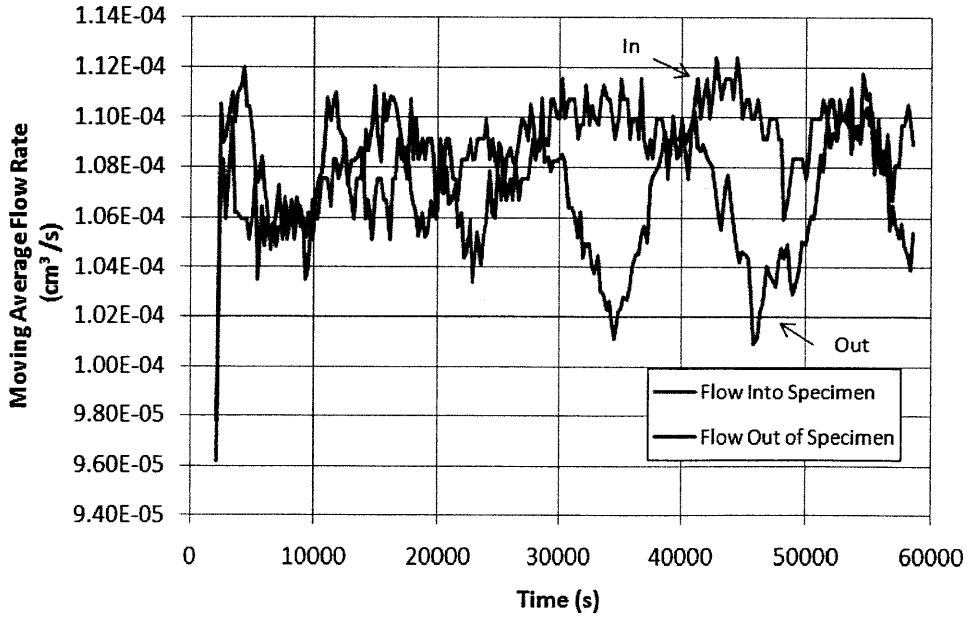

Figure 5-8: Typical moving average flow rate vs. time curve. Moving Average flow computed over a 40 minute time period (CRS 1210, Gradient 2)

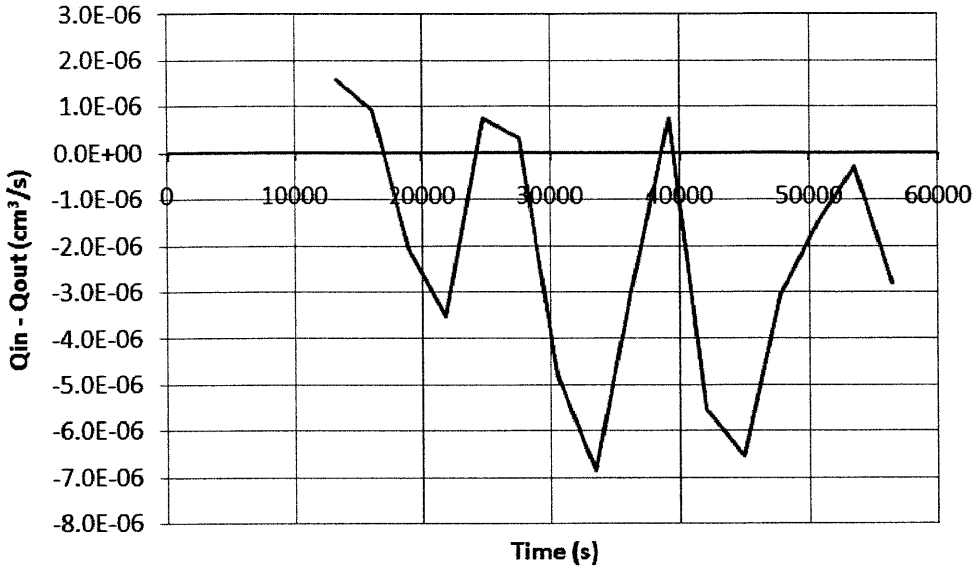

Figure 5-9: Typical differential flow vs. time plot during a constant head gradient (CRS 1210, Gradient 2)

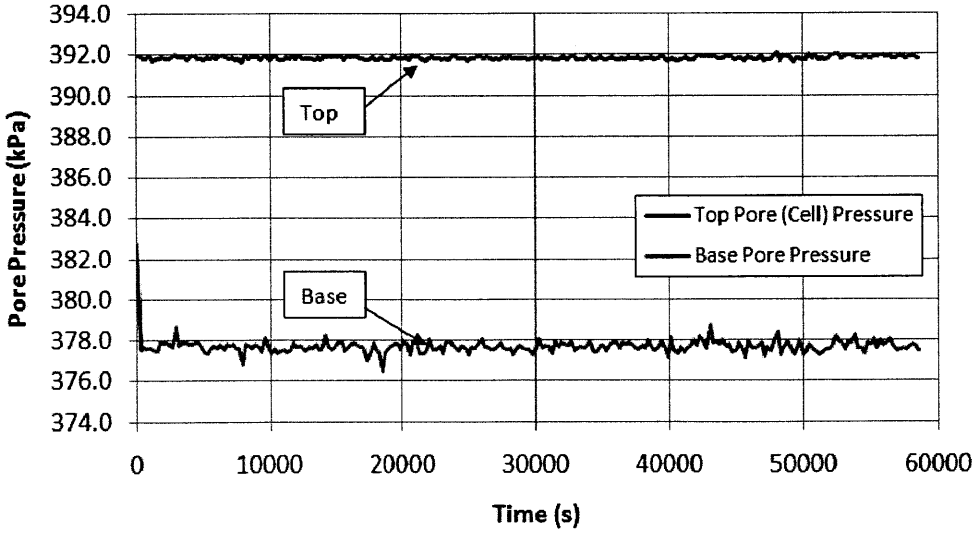

Figure 5-10: Typical pressure vs. time for top and base pore pressures during a constant head gradient (CRS 1210, Gradient 2)

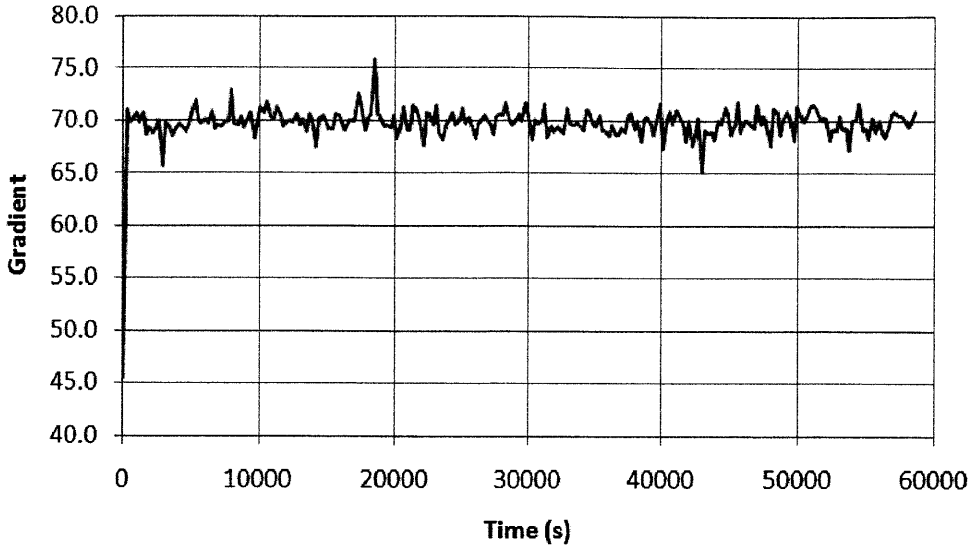

Figure 5-11: Typical gradient vs. time plot during for a constant head gradient (CRS 1210, Gradient 2)

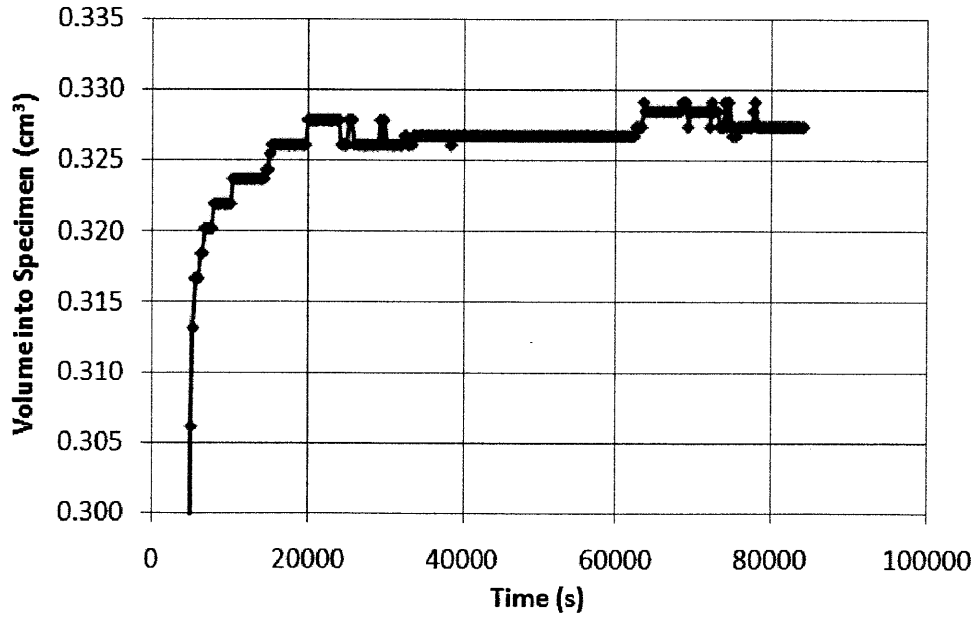

Figure 5-12: Backpressure volume vs. time plot showing no leakage. Zero volume change corresponds to the start of the back pressure phase (HC012 - CRS 1161 specimen).

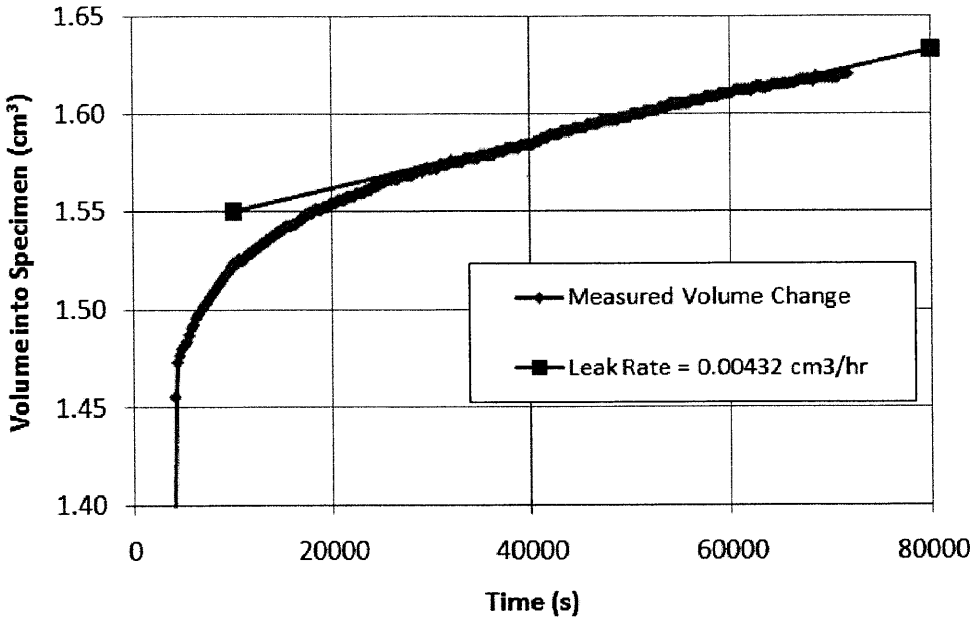

Figure 5-13: Backpressure volume vs. time plot showing detectable leakage. Zero volume change corresponds to the start of the back pressure phase (HC015 - CRS 1175 specimen).

6 RESULTS AND DISCUSSION

6.1 Introduction

This chapter presents the results of the CRS and constant head hydraulic conductivity testing program.

First, section 6.2 presents results from two multi-stage CRS tests. Section 6.3 presents the results from two specimens whose hydraulic conductivity was measured in both the CRS and flexible wall permeameter device. This comparison led to the discovery of the bottom seating error.

Section 6.4 presents the results of all hydraulic conductivity tests performed in this study. In addition to the two specimens analysed using multi-stage CRS tests, a total of ten different specimens including six resedimented and four intact specimens were analysed using a single staged CRS test. The measured hydraulic conductivity and compression behaviour is presented for each specimen in the form of three plots, including the void ratio vs. log effective stress, the excess pore pressure ratio (du/σ) vs. log axial effective stress, and the void ratio vs. log hydraulic conductivity. A table summarizes the pore fluid salinity measurements, used to achieve salt balanced flow during permeation, for each specimen. A brief discussion reviews the hydraulic conductivity results on a specimen by specimen basis, and describes any problems encountered during CRS or constant head test program. An in-depth discussion treats two noticeable errors in the data set: the error in specimen height between two different measurement methods, and the error in measured hydraulic conductivity between the CRS and constant head techniques. The effect of noted non uniformities on the measured hydraulic conductivity is also included in this discussion.

Finally, a conclusion is drawn as to the difference between hydraulic conductivity measurements made by CRS and constant head measurement techniques. This conclusion is based on comparison with the results of an interlaboratory study conducted by Benson et al (2010) investigating the reproducibility of the saturated hydraulic conductivity measured in a flexible wall permeameter.

6.2 Multi-Stage CRS Tests

Two multi-stage CRS tests measured the hydraulic conductivity of RBBC specimens. A multi-stage CRS test loads, unloads and then reloads a specimen multiple times. They hydraulic conductivity is measured during loading sequences using the CRS method of measurement and after unloading using the constant head method of measurement. Figures 6-1 and 6-2 give the measured compression curves and excess pore pressure curves for CRS 1147. Figures 6-3 and 6-4 give the same for CRS 1158. Figures 6-5 and 6-6 plot the void ratio vs. log hydraulic conductivity trend computed from CRS loading measurements and super impose the three constant head test measurements for each of CRS 1147 and CRS 1158.

The compression curve for each multi-stage CRS test (figures 6-1 and 6-3) show the locations of the constant head hydraulic conductivity tests and divides the test sequence into 7 steps which are indicated on the plot. The excess pore pressure plots (figure 6-2 and 6-4) present only those pore pressure measurements made during the loading stages of the CRS test. They include measurements from the onset to the termination of loading, and thus include measurements made during both periods of transience and instability in the base pore pressure measurement. Both transient and instable data points were removed from the data set prior to the hydraulic conductivity analysis. The regions of the pore pressure data set that were used in calculation of the hydraulic conductivity are delineated in axial effective stress space at the top of the excess pore pressure plots. The corresponding regions are also delineated on the compression plots (figures 6-1 and 6-3) on the left hand side in void ratio space. Finally, the excess pore pressure curves for multi-stage CRS tests show multiple stages of loading which overlap. These stages are identified in the legend as loading increments 1, 2, and 3; the start, peak and end of each stage's pore pressure curve, along with the related region of hydraulic conductivity measurement, is labelled with the corresponding increment number for clarity.

The specimen height for these tests was computed using the initial specimen height, accounting for the specimen deformation measured by the LVDT, and corrected for apparatus compressibility. From these results we can see that, throughout the progression of a CRS test on RBBC, the constant head and CRS void ratio - hydraulic conductivity trend is in very good

agreement within the stress range tested to a maximum of approximately 1600 kPa axial effective stress.

It is interesting to note that the scatter in the void ratio vs. log hydraulic conductivity curve from the CRS measurements increases as the specimen is reloaded. This is likely a combined result of two factors: the smoothing function of the CRS reduction program and instabilities in the base pore pressure measurement.

First, the CRS reduction program averages the pore pressures and performs linear regression to obtain strain rates. As a result, errors and instabilities at one point in the data set can be carried further into the data set. Secondly, as described in Chapter 5, when loading is initiated, transient strain conditions occur throughout the specimen. This is easily identified and removed from the data set using the F_3 criteria from figure 2-7 (chapter 2). However, even after steady state is reached, flow must occur through the base of the specimen to pressurize the pore pressure measurement system. This incorporates instability in to the base pore pressure measurement, which is seen as scatter in the computed hydraulic conductivity. This flow requirement is a deviation from the assumed boundary conditions used to derive the linear steady state CRS equation. The effect of the base pore pressure instability is thought to increase with increasing stiffness, as is evidenced with the increased scatter with each subsequent stage in the multi-stage CRS tests. Further, because each stage tested in this research was run for a shorter period of time, the base pore pressure was not given sufficient time or stress range to stabilize at higher stress and soil stiffness. This meant that the instable data could not be removed without removing the entire data set.

Therefore, CRS loading tests that are conducted using a single loading stage to a relatively high target effective stress incorporate less uncertainty into the measured void ratio vs. log hydraulic conductivity relationship computed using steady state linear theory than would a multi-stage CRS test conducted to the same target effective stress.

6.3 Comparison of CRS and Flexible Wall Permeameter Hydraulic Conductivity Measurements

The next step in the testing process was to compare the constant head hydraulic conductivity and void ratio measurements made in the CRS device to those made in the flexible wall permeameter. These devices are described in chapter 4. Two tests were undertaken whereby the specimen hydraulic conductivity was first measured in the CRS device using both CRS loading and constant head measurement techniques, and then measured in the flexible wall permeameter using the constant head technique. Figure 6-7 plots the CRS compression results for CRS 1161, performed on RBBC, and figure 6-8 plots the excess pore pressure measurements during CRS loading. Both plots indicate the respective regions where the hydraulic conductivity was computed (i.e. once transience and instabilities in the data set were removed). Figure 6-9 plots the hydraulic conductivity results from both the CRS and flexible wall permeameter tests. Figures 6-10 through 6-12 plot the same for CRS 1175, also performed on RBBC. Table 6-1 presents the computed void ratio and hydraulic conductivity results from the constant head tests in the CRS and flexible wall permeameter devices.

From the plots, the measured hydraulic conductivity between the CRS and constant head methods and the CRS and flexible wall permeameter devices with very close. However there is a definite shift in the constant head hydraulic conductivity, with that measured in the flexible wall permeameter being higher than that measured in the CRS device. This would indicate that some swelling, however small, has occurred.

On the other hand, CRS 1161 and CRS 1175 both show a disagreement in the void ratio measurement between the CRS constant head measurement and the flexible wall permeameter constant head measurement. The CRS constant head void ratio is computed using the initial specimen dimensions and specimen deformation measured using the LVDT. The flexible wall permeameter constant head void ratio is computed by measuring the specimen dimensions immediately following removal of the specimen from the flexible wall permeameter device. It may also be computed using the initial dimensions upon installation in the flexible wall permeameter and correcting for any measured volume change due to recompression and secondary compression during the flexible wall constant head test. The specimen is assumed

to maintain constant volume during back pressure, with the measured back pressure volume change accounting for pressurization of the pore pressure lines and control system, as well as the specimen void space at constant volume. For for both specimens tested, no consolidation volume change was measured throughout the week long duration of the test and the specimen dimensions measured upon removal from the CRS device matched those following removal from the flexible wall permeameter to within the accuracy of a pair of standard callipers (0.01 mm).

The specimen height computed using the deformation measurement from the LVDT during the CRS test was found to be lower than that measured using callipers. Because the hydraulic conductivity is computed using the specimen height as the length of the flow path in calculation of the hydraulic gradient, errors in the specimen height can lead to calculation errors in the computed hydraulic conductivity. Therefore, errors in specimen height affect both void ratio and hydraulic conductivity calculations.

The difference in void ratio measurements could be affected by swelling of the specimen upon removal of the load; however, RBBC has a generally low swelling potential and should not swell much. The difference in the specimen height between that measured after the specimen was removed from the device and the height predicted using the LVDT deformation measurements was back calculated to be between 0.015" and 0.020" (0.38mm and 0.51 mm).

This error was confirmed by checking void ratio calculations using both volume-based and mass-based approaches: if the specimen is fully saturated, the correct specimen void ratio can be confirmed by verifying the agreement between the void ratio computed using the specimen volume measured using callipers and the void ratio computed using the specimen mass knowing the salinity of the pore fluid and the mass density of the soil grains (section 4.5.2.3.1). If these two void ratios agree, then this void ratio is the true specimen void ratio. Therefore, if the void ratio computed using the measured LVDT deformation does not agree with the mass based and volume based void ratio calculation, there is a measurement error somewhere associated with the LVDT measurement system.

Many routes were investigated to determine the source of this error, including verifying the apparatus compressibility equations (chapter 5). Piston rotation was considered; the installation of a second LVDT to measure piston rotation proved that this potential source of error was minimal. The LVDT itself was recalibrated 3 separate times and no error was found in the calibration factor.

Finally, it was discovered that there was a gap between the bottom surface of the specimen ring and the top of the base porous stone causing a bottom seating error. This would allow a plug of water to form under the specimen upon back pressure of the CRS device. This plug of water would slowly move through the specimen during CRS loading. The LVDT would measure this complex motion as pure deformation, resulting in lower void ratios throughout the test.

The bottom seating gap is caused by deviations in the height of the porous stone used in the base of the CRS apparatus that are within the manufacturer's tolerances. For the porous stones used for CRS 1161 and 1175, the gap between the specimen and the porous stone on start up was measured to be approximately 0.010" (0.25 mm). This equates to 1% strain for the specimen geometry tested.

A new procedure was developed to pre-seat the specimen on the porous stone and minimize the potential for bottom seating errors in the deformation measurement (chapter 4, section 4.5.2.2). The RBBC specimen tested in CRS 1175 came from a sample that was large enough to produce two specimens; the second specimen from this sample was tested in the CRS device using the new setup method (CRS 1188). Figures 6-13 and 6-14 give the compression and excess pore pressure plots for CRS 1188, and figure 6-15 plots the permeability results for CRS 1188 in comparison with CRS 1175.

Figure 6-15 illustrates the effect of bottom seating error on the measured void ratio vs. log hydraulic conductivity trend for a CRS test. CRS 1188 loaded a specimen from the same sample as CRS 1175. The curve is essentially shifted up in void ratio and shows that the procedural change leads to very good agreement with the flexible wall permeameter constant head measurement in terms of the void ratio vs. hydraulic conductivity trend.

Figure 6-16 compares the compression curves for tests CRS 1175 and CRS 1188, illustrating the effect of bottom seating error on the measured compression behaviour of a fine grained soil. The compression curve from the improved procedure, CRS 1188, reaches a higher axial effective stress at a given void ratio. The slope of the virgin compression line can be computed; for CRS 1175 Cc = 0.352 and for CRS 1188 Cc = 0.372, both computed over an axial effective stress range of 200 to 1000 kPa. Further, there is a significant shift in the preconsolidation stress, σ'_p.

Improper specimen seating during set up of a CRS test can create a bottom seating error; even a small bottom seating error can incorporate significant error into the measured compression and hydraulic conductivity characteristics of a fine grained soil. This error can be minimized by pre-seating the specimen on the porous stone during set up prior to loading.

6.4 Presentation and Discussion of Results

Following the discovery and correction of the bottom seating error described in section 6.3, the experimental program was extended to include more RBBC specimens as well as different intact and resedimented materials. Tests were completed on 2 more specimens of RBBC (CRS 1190 and CRS 1191), one specimen of intact BBC (CRS 1197), 2 specimens of intact Maine Clay (CRS 1206 and CRS 1210), one specimen of resedimented Kaolinite (CRS 1207), one specimen of intact San Francisco Bay Mud (CRS 1212) and one specimen of resedimented Ugnu Clay (CRS 1215). All materials are described in Chapter 3.

6.4.1 Salinity Results

Table 6-2 presents salinity results for each specimen tested, as well as the salinity of the permeant that was used for the CRS and constant head tests. The salinity of resedimented specimens was measured after the specimens were tested in the CRS device so as not to destroy the sample; intact materials were tested prior to CRS testing to identify the pore water salinity and adjust the permeant salinity accordingly.

Permeant salinity control was accomplished with mixed results; the salinity of the resedimented specimens was always measured to be lower than the batching salinity of 16 g/L, with an average salinity of 11.7 g/L. This was likely due to the batching set up; excessive

crystallization of salt along the edges of the batching reservoir was noted which reduced the salinity of the reservoir fluid over time. The specimen had free access to this fluid throughout the resedimentation process, and a reduction in salinity of this fluid likely reduced the salinity of the resedimented specimens. Because this phenomenon was not noticed until later in the experimental program, all resedimented specimens were tested with a permeant salinity of 16 g/L. For the intact specimens, the salinity of the permeant used in CRS and constant head testing more closely matched the salinity of the pore fluid because salinity testing could be undertaken prior to CRS testing. However, for some specimens the pore fluid salinity was not tested and a default permeant salinity of 16 g/L was used in CRS and constant head testing. For other specimens incorrect permeant salinities were applied even when the pore fluid salinity measurement was available. This was due to operator error.

6.4.2 Individual Test Results Discussion

Figures 6-17 through 6-40 present the compression, excess pore pressure and hydraulic conductivity results for each test performed in numerical order according to the test ID. The excess pore pressure curves present measurements for loading stages only, and include measurements made during identified periods of transience and instability in the base pore pressure measurement. Transient and instable data points were removed for the hydraulic conductivity analysis, as described in chapter 5. The regions of the pore pressure data set that were used in calculation of the hydraulic conductivity are delineated in axial effective stress space at the top of the excess pore pressure plots. The corresponding regions are also delineated on the compression plots (figures 6-1 and 6-3) on the left hand side in void ratio space.

The hydraulic conductivity plots present three different results. The first is the void ratio vs. log hydraulic conductivity relationship computed from measurements made during CRS loading in the CRS device. Periods of transience and base pore pressure instability have been removed from the data set, and results are only reported when the excess pore pressure divided by the total axial stress was less than 15%, which is shown by Gonzalez (2000) to give less than 10% error in the hydraulic conductivity (Chapter 2). The second result is the constant head hydraulic conductivity measurement made in the CRS device and using the

specimen height computed using the LVDT deformation measurement. This result best relates to the CRS measured hydraulic conductivity curve because it uses the same specimen height measurement method and is not affected by potential specimen swelling. The third result is the constant head hydraulic conductivity measurement made in the CRS device but with the void ratio and hydraulic conductivity computed using the specimen height measured using callipers immediately following removal from the CRS apparatus upon completion of all testing. This measurement may be affected by specimen swelling following removal from the CRS device. Therefore, the difference between the two constant head measurement points is that they represent the same constant head test but different specimen height measurements and therefore result in different computed void ratio and hydraulic conductivity values. The exception is for CRS 1161 and CRS 1175, which have already been discussed, where the third result is a hydraulic conductivity measurement made using the constant head method in the flexible wall permeameter.

Overall, even when there is a large, noticeable difference in void ratio between the two constant head calculation methods, for example CRS 1207, CRS 1197, and previously presented CRS 1175 and CRS 1161 with bottom seating errors, the effect on the computed hydraulic conductivity is minimal. Errors in void ratio can be caused by specimen swelling upon load removal, which is not measured and varies based on material, time and stress level, as well as the success of the specimen pre-seating method to reduce bottom seating error. This is further discussed in section 6.4.3.

The following is a brief discussion of the results of each individual test. Table 6-3 summarizes the details of each test completed in the CRS device, including the back pressure, the maximum effective stress, the effective stress prior to constant head testing, and the three hydraulic gradients applied to the specimen during constant head testing. Table 6-4 provides the relevant information for the two flexible wall hydraulic conductivity tests.

6.4.2.1 CRS 1161, CRS 1175 and CRS 1188

CRS 1161 and CRS 1175 have a known base seating error, and CRS 1188 was set up with the new procedure in an attempt to remove this error. Section 6.3 discussed these results extensively.

These specimens are all made from RBBC. Table 6-2 gives their corresponding batch sample numbers and batch salinities. The void ratio vs. log hydraulic conductivity trend for these specimens is very linear; the oven dried specimens appeared uniform.

The normalized excess pore pressure vs. effective axial consolidation stress plot for CRS 1161 starts at a very high normalized excess pore pressure at a low effective stress; this was because the specimen started the CRS loading stage at essentially zero deviator stress after back pressure and therefore the rapid rise in pore pressure is not shown on the log scale.

6.4.2.2 CRS 1190 and CRS 1191 and CRS 1188

CRS 1190 and CRS 1191 came from the same sample of RBBC; the sample ID and measured salinity is given in table 6-2. The agreement between the CRS and constant head hydraulic conductivity and void ratio, shown in figures 6-19 and 6-22, is very good.

There is a slight difference in the measured void ratio vs. log hydraulic conductivity trend between these specimens; Figure 6-41 superimposes the CRS void ratio vs. log hydraulic conductivity curves for CRS 1190, CRS 1191 and CRS 1188, all RBBC specimens, for comparison. This figure highlights the natural variability within the same specimen, as well as the variance associated with the CRS test method. Specimen 1191 and specimen 1190 are from the same sample, so there should not be significant variability between the results of CRS 1191 and CRS 1190.

The void ratio vs. log hydraulic conductivity trends for these three specimens is very linear. The oven dried specimens appeared uniform and no non uniformities were noted during specimen trimming.

The normalized excess pore pressure vs. effective axial consolidation stress plot for CRS 1188 is lacking information at the start of the test, with only 3 points forming the initial increase and then decrease in normalize excess pore pressure. This was due to a sudden increase in effective stress. It is unknown why there was a sudden increase in effective stress, however, it could be related to a number of factors, for example the load frame motor not being turned to computer control, leading to a build up of control signal from the PID algorithm.

6.4.2.3 CRS 1197

CRS 1197 was performed on intact BBC. The constant head hydraulic conductivity measurement is offset from the CRS hydraulic conductivity curve (Figure 6-25). Further, there was a significant disagreement between the void ratio computed using the LVDT measured deformation and the final measured specimen dimensions. This may be due to improper base seating; however, it is most likely due to specimen swelling following load removal.

During trimming a coarser layer approximately 3 mm thick was noted in the middle of the specimen. This axial non uniformity is not evident in the oven dried specimen, nor was it evident on the radiograph. This axial non uniformity may affect the pore pressure distribution that is developed in both the constant head and CRS hydraulic conductivity tests. CRS theory assumes a constant coefficient of consolidation, Cv, in the axial direction which may not be the case. In this case, the constant head hydraulic conductivity was measured to be higher than the CRS hydraulic conductivity at a given void ratio. Assuming the two hydraulic conductivity measurements should otherwise be equal, this would indicate that the axial non uniformity had the effect of increasing the base pore pressure during the CRS loading measurement. The void ratio error may be due to swelling as mentioned; the presence of the coarser layer could provide freer access to water upon load removal making swelling easier and more likely to occur as compared to a uniform specimen.

6.4.2.4 CRS 1206

CRS 1206 was performed on intact Maine Clay. The constant head hydraulic conductivity measurement is offset from the CRS hydraulic conductivity curve (Figure 6-28). There is not a significant void ratio error in the constant head measurement.

During trimming a coarse layer approximately 2 mm thick was noted in the upper 1/3 of the specimen. This axial non uniformity is evident in the oven dried specimen, which formed a defined crack, shown in figure 6-42. As described in section 6.4.2.3, the axial non uniformity may affect the pore pressure distributions that develop and therefore the measured hydraulic conductivities using the CRS and constant head methods. The constant head test resulted in a

lower measured hydraulic conductivity than the CRS measured hydraulic conductivity; assuming that the CRS and constant head hydraulic conductivity measurements should otherwise be equal, this indicates that the axial non uniformity had the effect of lowering the base pore pressure during the CRS loading measurement.

6.4.2.5 CRS 1207

CRS 1207 was performed on resedimented Kaolinite. The constant head hydraulic conductivity measurement is slightly offset from the CRS hydraulic conductivity curve (Figure 6-31). Further, there was a significant disagreement between the void ratio computed using the LVDT measured deformation and the specimen dimensions.

There were no observed specimen non uniformities; further, because this specimen was resedimented, it should be as uniform as possible.

Kaolinite is known not to hold its preconsolidation pressure very well, and the compression curve (Figure 6-29) shows a very steep recompression slope (Cr = 0.066, Cc = 0.399), especially compared to BBC (average values in this study of Cr = 0.028, Cc = 0.351), so it is possible that swelling occurred between removal of the applied load and measurement of the specimen dimensions. It has a very rounded compression curve, with a very poorly defined preconsolidation pressure.

6.4.2.6 CRS1210

CRS 1210 was performed on intact Maine clay. There was a slight disagreement between the void ratio measured using the LVDT and that measuring the specimen dimensions, curiously, with the LVDT measurement being higher. This indicates that bottom seating error should not be a cause, nor should swelling. The specimen did not slump following removal from the rigid specimen ring, and retained shape and diameter very well.

One possible explanation for why the specimen height measured with callipers is lower than that measured with the LVDT in this case is that the specimen got shorter and fatter during CRS loading. Maine clay trims into the rigid trimming ring very loosely and hence there is some potential for lateral expansion during the CRS test. An initial void ratio error is caused

by assuming the specimen diameter equal to the inner ring diameter, and this error would over predict the initial void ratio, shifting the void ratio vs. log hydraulic conductivity curve up.

The hydraulic conductivity measured using the constant head method is higher than that measured during CRS loading. There were not any noted specimen non uniformities, either during trimming or after oven drying of the specimen, however a slight non uniformity may have existed that was not visually evident.

6.4.2.7 CRS 1212

CRS 1212 was performed on intact San Francisco Bay Mud. The specimen had several rusty planar discoloured zones aligned at angles to the axial loading direction, as shown in figure 6-43. These discoloured zones did not appear to have any fractures or differing grain size during trimming. After the specimen was oven dried, a large crack appeared perpendicular to the axial loading direction, shown in figure 6-44. This shows evidence of an axial non uniformity. This crack did not propagate along a single rusty discoloured zone, rather it propagated along another plane in the specimen, intersecting multiple discoloured zones, as is discernible in figure 6-44.

The constant head test measurement in the CRS device matched very well with the CRS measured void ratio vs. hydraulic conductivity curve, however there was a significant difference in the specimen height as measured with callipers upon removal from the device compared with that computed using the LVDT measured deformation.

From an earlier test which failed, it was known that San Francisco Bay Mud specimens are extremely difficult to remove from the specimen ring after completion of a CRS test. As a result, the final specimen height was first measured in the ring along with the height of the porous stone and a filter paper prior to removal from the ring. This proved to be an interesting experiment because once removed, the specimen height was re-measured to gain an idea of the combined effect of swelling and removal from the ring on the measured specimen height. Prior to removal from the ring the average specimen height was measured to be 21.33 mm once the average height of the porous stone and filter paper were removed from the measurement. It took approximately 5 minutes to forcefully remove the specimen from the

rigid ring. Following removal, the specimen height was re-measured to be 21.38 mm. The specimen swelled 0.05 mm during this time. This corresponds to an almost negligible void ratio error of just less than 0.01 at the final specimen void ratio. However, prior to the initial measurement the load had already been removed for approximately 5 minutes. Given that specimen swelling is a logarithmic process with respect to time, this shows that specimen swelling is a real phenomenon that can affect the final specimen measurements, even when the time between load removal and specimen dimensioning is minimized.

With respect to the CRS test, difficulty was experienced with loading the specimen. For an unknown reason, an electronic signal to the motor was lost and this caused the loading process to stop and the excess pore pressure in the specimen was allowed to decay until the problem was noticed. Once noticed, loading was reinitiated at the same strain rate and the CRS hydraulic conductivity measurement continued. The hydraulic conductivity curve was generated by stitching together the data collected from each of the two loading segments. This stitching process is evident from a slight disconnect in the curve around void ratio 0.95 where the transient portion and those measurements associated with flow necessary to re-pressurize the base pore pressure measurement system were removed.

6.4.2.8 CRS 1215

CRS 1215 was performed on Resedimented Ugnu clay. The hydraulic conductivity measured in the constant head test is lower than that measured in the CRS test. There were no specimen non uniformities noted.

As with CRS 1212, the final specimen height was measured twice, once in the rigid specimen ring with the stones and filter paper included, and once after removal from the specimen ring. The final specimen height with the specimen still in the ring was measured to be 17.32mm. Once removed from the ring, the final specimen measured 17.45 mm high, giving a difference in height of 0.13 mm. This corresponds to a void ratio error of 0.012.

6.4.3 Void Ratio Results and Swelling Potential

Table 6-5 presents the final void ratio results for each specimen. The final specimen void ratio was computed in two ways; first using the final specimen height computed using the initial

specimen height, the LVDT measured deformation, computed apparatus compressibility and the dry mass, and secondly using the measured final specimen dimensions. The compression indices, Cc and Cs, representing the slope of the virgin compression line and the swelling line in void ratio vs. log effective stress space, respectively, are also presented in this table.

The initial specimen void ratio and degree of saturation is provided as a reference for each specimen. This initial void ratio is computed using both a mass based and volume based approach. A comparison of these two methods of calculation at the initial condition shows that the two methods are well constrained for saturated specimens. The difference varies from 0.004 to 0.025 in void ratio. This means that any deviation in the void ratio computed using these two methods at any point during the test must be related to an error in a measurement used in the calculation. The most likely measurement error is the specimen height used in the volume based void ratio calculation. The closer the volume based void ratio calculation gets to the mass based void ratio calculation, the less error in the measured specimen dimensions.

The final void ratio computed using the actual specimen dimensions is taken as the average of the mass and volume based calculations. This accounts for errors incorporated into the mass based void ratio calculation due to specimen swelling between removal of the load and measurement of the wet mass of the specimen, as well as other potential effects on the specimen resulting from removal from the device and rigid specimen ring. Therefore, this average value incorporates some error, however compared to the differences between void ratios computed based on the LVDT measured heights and the actual final specimen heights, which varies from 0.0 to -0.10 in void ratio, this error is small.

At the end of the test some swelling can occur, as was measured in CRS 1212 and CRS 1215 (Section 6.4.2.7 and 6.4.2.8). This may account for some of the differences in between the final specimen heights computed using the LVDT measured deformations and those measured using callipers. Bottom seating errors may still be a problem in some specimens despite the procedural change after discovery of this error in CRS 1175.

These two tests in which swelling was measured provided interesting results. The measured swell for the RUgnu clay in CRS 1215 was much more significant than for the SFBM in CRS

1212. RUgnu clay has a lower plasticity than SFBM (figure 3-4), however the SFBM tested in CRS 1212 was loaded to a higher stress than the RUgnu clay in CRS 1215 (1960 kPa vs. 1570 kPa, respectively). The two specimens underwent constant head testing at the same effective stress (560 kPa) and were allowed to fully equilibrate to this stress level. Therefore, the swelling experienced should be a function of both time, in terms of the rate of swelling since neither specimen was allowed to equilibrate prior to measurement of the final specimen height, and the slope of the swelling line, Cs. CRS 1215 actually had a lower Cs value than CRS 1212 (0.036 vs. 0.065). The time required to remove the RUgnu CRS 1215 specimen from the ring is estimated to be significantly less, almost half that of the SFBM CRS 1212 specimen. The actual time, from removal of the load, to measurement of the specimen height was not measured. Because the RUgnu clay is less plastic than the SFBM, it should equilibrate to the load removal faster, as a function of the relative values of unloading coefficient of consolidation, Cv. Because unloading occurred so quickly, constant rate of strain unloading was not reached and a good measure of the unloading Cv was not obtained. More testing and data is required to compute the expected swelling between load removal and specimen dimensioning to verify that the errors seen are accountable from specimen swelling.

To gain an idea of the potential effect of swelling on the full data set, figure 6-45 plots the void ratio error vs. the slope of the swelling line, Cs. Here, a distinct trend of increasing void ratio error with increasing Cs is evident. A linear regression line has been fit with an R^2 value of 0.7438 indicating that there is a relationship between the two parameters, though it is arguable if a linear relationship is most representative.

6.4.4 Hydraulic Conductivity Results

Table 6-6 presents the hydraulic conductivity results for each test. The constant head hydraulic conductivity computed using the LVDT measured deformation is compared against the hydraulic conductivity at the equivalent void ratio interpolated or extrapolated from the CRS void ratio vs. log hydraulic conductivity curve. Thus, the difference in hydraulic conductivity in table 6-6 is representative of the difference in measurement between the CRS loading and constant head techniques at the same void ratio.

6.4.4.1 Effect of Non Uniformity

As discussed in section 6.4.2, non uniformities were noted in some specimens during trimming and/or in the oven dried specimen following the completion of CRS and constant head testing. These non uniformities are noted in table 6-6 in the comments column. Non uniformities may affect the results of CRS and constant head test hydraulic conductivity results in a number of ways.

Relative to CRS testing, CRS theory is based on the assumption of a constant coefficient of consolidation in the axial direction. A non uniformity may affect this assumption, which would affect pore pressure and stress distributions that are derived based on this assumption. The type, degree and location of distortion would logically be dependent on the type, size, location and continuity of the non uniformity. Constant head tests, on the other hand, ideally form linear pore pressure distributions throughout the specimen. Non uniformities could distort the constant head pore pressure distribution as well, however in the constant head test given that the distribution is linear the distortion is somewhat more intuitive. A potential scenario could be a high permeability layer in a low permeability specimen where the pore pressure distribution across the high permeability is essentially constant, and the flow length is reduced; assuming the flow length as the specimen height would lead to computed hydraulic conductivity that is too high. The relationship between the constant head and CRS hydraulic conductivities is not intuitive given this analogy.

Three specimens tested in this study had a non uniformity: CRS 1197 (section 6.4.2.3), CRS 1206 (section 6.4.2.4) and CRS 1212 (section 6.4.2.7). Of these three tests, two had a coarse layer present: CRS 1197 and CRS 1206. In CRS 1197, the ratio of the hydraulic conductivity measured using the CRS method to that measured using the constant head method was 0.85 (table 6-6) meaning the constant head hydraulic conductivity was higher; CRS 1206 showed the opposite trend with a ratio of 1.09. CRS 1212 had another type of non uniformity, marked by discolouration in the moist specimen and then by a distinct crack in the oven dried specimen that intersected discoloured planes. The constant head hydraulic conductivity of this test more closely matched that measured using the CRS technique, with a ratio of 0.96. Seven

other tests were performed, detailed in table 6-6, with measured ratios of the CRS to constant head hydraulic conductivity ranging from 1.2 to 0.87.

Therefore, it is determined that the range of variability between the constant head and CRS hydraulic conductivity results for the three specimens with a demonstrated non uniformity is within the range of that measured for the global test data. The CRS and constant head test methods measure the same average hydraulic conductivity for non uniform specimens provided the non uniformity itself is uniform, continuous and oriented perpendicular to the loading and flow direction.

All non uniformities were noted in intact specimens. Resedimented specimens have been shown to be uniform (section 4.2) and therefore represent the agreement between the two methods given uniform conditions.

6.4.4.2 Effect of Sample Type: Intact vs. Resedimented Specimens

The average ratio of the measured CRS to constant head hydraulic conductivity for the 6 resedimented specimens tested is 1.00, with a maximum value of 1.20 and a minimum value of 0.87. The corresponding average ratio for the 4 intact specimens tested is 0.94 with a maximum value of 1.09 and a minimum value of 0.85. Given the small sample size, neither resedimented nor intact specimens have statistically different hydraulic conductivity measurements using the CRS and constant head techniques. Overall for all 10 specimens tested the ratio of the CRS to constant head hydraulic conductivity is was 0.98, with the average minus one standard deviation equalling 1.0 for the range of hydraulic conductivities tested varying from 1 e-9 to 6 e-8 cm/s.

From this the conclusion is drawn that the CRS technique predicts the same hydraulic conductivity as the constant head method. In the range of hydraulic conductivities tested, the difference between the two methods often lies in the third and sometimes the second significant digit. For field applications where the hydraulic conductivity is highly variable, this difference is negligible. However, for laboratory testing this difference can mean the difference between a material passing or failing a specification.

6.4.4.3 Comparison with Interlaboratory Study Using a Flexible Wall Permeameter

The results of this study are compared with the results of a round robin study performed by Benson et al (2010) using ASTM/ISR reference soils that tested the reproducibility of the saturated hydraulic conductivity measured in a flexible wall permeameter. The comparison study issued three different soils to 12 laboratories for hydraulic conductivity testing. Specimens of each soil were mixed and compacted by Benson and distributed as intact specimens pre-trimmed for flexible wall hydraulic conductivity testing. The three soils are classified as a low plasticity silt, a low plasticity clay and a high plasticity clay. Table 6-7 gives the soil name, classification, Atterberg limits and grain size characteristics of the soils in terms of percent fines and percent clay content. Figure 6-46 plots these soils on the standard plasticity chart for comparison with the soils tested in this study.

Each laboratory was sent three specimens of each soil and asked to perform a flexible wall hydraulic conductivity test following specified guidelines to measure the saturated hydraulic conductivity of the specimen. The hydraulic conductivities were in the range of 10^{-7} to 10^{-9} cm/s, comparable to those measured in this study, and were reported to only 2 significant digits.

Table 6-8 summarizes the individual laboratory statistics for each soil. Each laboratory tested three specimens of each soil type. The maximum and minimum measured hydraulic conductivities as well as the ratio of the maximum to minimum hydraulic conductivity and the coefficient of variation of the measurements on the three specimens is tabulated.

For the ML soil, average ratio of the maximum to minimum hydraulic conductivity for a single laboratory is 1.49; for a CL soil this ratio is 1.21, and for a CH soil this ratio is 1.75. The coefficient of variation was 0.21, 0.10 and 0.26 for the ML, CL and CH soils, respectively. There was no trend in coefficient of variation with increasing plasticity; the lowest coefficient of variation was for the CL soil which corresponds to the soil type that the participating laboratories are likely to have the most experience in testing using the flexible wall hydraulic conductivity method.

Table 6-9 summarizes the hydraulic conductivity results from the CRS and constant head testing, presented in table 6-6, in terms of the maximum and minimum hydraulic conductivity and makes no differentiation between which measurement is higher; this allows for comparison with the interlaboratory study results. The average ratio of the maximum to minimum measurement comparing the CRS to the constant head technique is 1.11. The range is 1.02 to 1.20.

Table 6-10 tabulates the constant head hydraulic conductivity measurements made in the CRS device for each hydraulic gradient applied to each specimen tested. The ratio of the maximum to minimum hydraulic conductivity measurement for each specimen is computed to determine the variability in the constant head test method for measurements made on the same specimen. The average ratio is 1.04, with a maximum ratio of 1.09 and a minimum of 1.02.

From these results, the difference between the hydraulic conductivity measurement between the CRS and constant head techniques (1.11) is less than that expected from a single laboratory testing a given soil independent of plasticity using the flexible wall permeameter method (1.21 for a CL soil). The difference between the two techniques is slightly higher, 1.11 as compared to 1.04, than the average variability within the constant head technique alone, and it is close to the range of variability of the constant head technique, which varies up to 1.09 in table 6-10.

Therefore, it is concluded that the CRS and constant head techniques produce the same hydraulic conductivity measurement:

1. Within the range of variability that would normally be expected, on average, from a single laboratory testing the same soil multiple times using the same measurement method; and
2. Within the range of variability of the constant head test method for the same specimen using different applied hydraulic gradients.

This conclusion is drawn on a sample size of 10 tests including 6 resedimented specimens, 4 intact specimens, of which 3 specimens had a demonstrated non uniformity and 2 specimens

have a known bottom seating error. There is potential for other unknown non uniformities and bottom seating errors in the data set.

It is important to remember that the ratio of the maximum to the minimum measured hydraulic conductivity in table 6-8 compares measurements made using one measurement technique on three different specimens of the same soil type. Thus, the variability seen in the ratios of the maximum to the minimum measured hydraulic conductivity values in table 6-8 is representative of natural variability of the soil and the laboratory's ability to apply a consistent measurement technique. Those ratios reported in table 6-9 compare measurements made using two different techniques on the same specimen, and in table 6-10 compare measurements made using a single technique on the same specimen. Thus, the results in tables 6-9 and 6-10 represent the variability between two different measurement techniques. Nevertheless, comparing the relative ratios gives insight into the relative difference in measurements between the CRS and constant head hydraulic conductivity measurement techniques.

Table 6-1: Comparison of CRS and Flexible Wall Permeameter constant head hydraulic conductivity measurements

CRS Test ID	Flexible Wall Permeameter Test ID	CRS Constant Head Measurements		Flexible Wall Permeameter Constant Head Measurements	
		Void Ratio (LVDT Measurement)	Hydraulic Conductivity	Void Ratio (Specimen Dimensions)	Hydraulic Conductivity
CRS1161	HC012	0.74	1.59E-08	0.80	1.62E-08
CRS1175	HC015	0.74	1.55E-08	0.80	1.61E-08

Table 6-2: Salinity results

Test ID	Material	Batch Number / Sample	Measured Salinity	Salinity of permeant
			g/L	g/L
CRS1161	RBBC	B11	14.4	16.0
CRS1175	RBBC	B13	10.3	16.0
CRS1188	RBBC	B13	10.3	16.0
CRS1190	RBBC	B15/ RS 158	11.2	16.0
CRS1191	RBBC	B15/ RS 158	11.2	16.0
CRS1197	Intact BBC	BIO TP2A S3	N/A	16.0
CRS1206	Intact Maine Clay	SAA F2 U2	0.4	16.0
CRS1207	RKaolinite	RS166	11.7	16.0
CRS1210	Intact Maine Clay	SAA F3 U2	0.4	4.3
CRS1212	Intact San Francisco Bay Mud	TTB-11 S23	0.4	0.4
CRS1215	RUgnu	RS167	12.6	16.0

Table 6-3: CRS hydraulic conductivity test summary

Test ID	Material	Back Pressure	Target Strain Rate	Max Effective Stress	Effective Stress prior to Constant Head Test	Constant Head Gradients Tested		
						1	2	3
		(kPa)	%/hr	kPa	kPa			
CRS1161	RBBC	392	1.00	1798	1484	28.2	84.3	56.1
CRS1175	RBBC	392	1.00	1901	1851	31.4	86.9	59.4
CRS1188	RBBC	392	1.00	1907	N/A	N/A	N/A	N/A
CRS1190	RBBC	392	1.00	1514	1527	52.9	78.7	26.3
CRS1191	RBBC	392	1.00	1339	1185	53.4	26.5	80.9
CRS1197	Intact BBC	392	1.00	1926	1820	47.6	71.3	23.6
CRS1206	Intact Maine Clay	392	0.7	1488	1422	47.1	23.2	70.7
CRS1207	RKaolinite	392	2.50	1923	1585	53.3	81.4	64.7
CRS1210	Intact Maine Clay	392	0.80	1522	1503	45.7	69.5	22.5
CRS1212	Intact San Francisco Bay Mud	392	0.18	1959	1781	94.3	70.5	118.0
CRS1215	RUgnu Clay	392	1.00	1566	1476	58.6	117.0	87.9

Table 6-4: Flexible Wall Permeameter hydraulic conductivity test summary

Test ID	Material	CRS Test ID	Back Pressure	Effective Stress	Gradients Tested		
					1	2	3
			kPa	kPa			
HC012	RBBC	CRS1161	392	490	164.8	54.7	109.3
HC015	RBBC	CRS 1175	392	587	53.1	106.4	85.7

Table 6-5: Void ratio results

Test ID	Material	Cc	Cs	Specimen Initial Void Ratio Measurements e_o				Initial Sat (%)	Specimen Final Void Ratio Measurements				
				Volume calc	Mass calc	Difference			OCR	Void Ratio			
										LVDT Meas.	Calliper Meas.	Difference	
				e_{vol}	e_{mass}	(e_{mass}/e_{vol})	$(e_{vol}-e_{mass})$			e1	e2	e1-e2	e1/e2
CRS1161	RBBC	N/A	N/A	1.34	1.36	1.02	-0.025	101.9	3.0	0.74	0.80	-0.06	0.92
CRS1175	RBBC	N/A	N/A	1.28	1.28	1.00	-0.001	100.1	3.5	0.74	0.80	-0.06	0.93
CRS1188	RBBC	0.372	0.023	1.27	1.29	1.01	-0.018	101.4	N/A	N/A	N/A	N/A	N/A
CRS1190	RBBC	0.361	0.030	1.24	1.25	1.00	-0.006	100.5	3.2	0.79	0.81	-0.02	0.97
CRS1191	RBBC	0.364	0.032	1.29	1.31	1.01	-0.013	101.0	3.5	0.80	0.82	-0.02	0.98
CRS1197	Intact Natural BBC	0.308	0.027	0.98	0.99	1.01	-0.008	100.8	3.4	0.73	0.78	-0.04	0.94
CRS1206	Intact Maine Clay	0.144	0.007	0.83	0.82	0.99	0.004	99.5	3.1	0.60	0.60	0.00	1.00
CRS1207	RKaolinite	0.400	0.066	1.61	1.62	1.01	-0.014	100.9	3.2	0.93	1.03	-0.10	0.90
CRS1210	Intact Maine Clay	0.188	0.011	0.91	0.92	1.01	-0.005	100.6	3.2	0.69	0.68	0.00	1.00
CRS1212	Intact San Francisco Bay Mud	0.468	0.065	1.06	1.04	0.98	0.019	98.2	3.5	0.82	0.87	-0.05	0.95
CRS1215	RUgnu	0.461	0.036	1.24	1.23	1.00	0.004	99.7	2.8	0.62	0.65	-0.03	0.96

Table 6-6: Hydraulic conductivity results

Test ID	Material	CRS Hydraulic Conductivity Measurements		Constant Head Hydraulic Conductivity in CRS				Difference $K_{CRS}/K_{constant\ head}$			Comment
					LVDT Measurements						
		Hydraulic Conductivity	Void Ratio	OCR	Hydraulic Conductivity		Void Ratio	Avg.	+1 St. Dev	-1 St. Dev	
					Average	Standard Deviation					
		cm/s			cm/s	cm/s					
CRS1161	RBBC	1.72E-08	0.74	3.0	1.59E-08	4.75E-10	0.74	1.08	1.05	1.12	bottom seating error
CRS1175	RBBC	1.53E-08	0.74	3.5	1.55E-08	1.77E-10	0.74	0.98	0.97	0.99	bottom seating error
CRS1190	RBBC	1.61E-08	0.79	3.2	1.75E-08	4.12E-10	0.79	0.92	0.90	0.95	
CRS1191	RBBC	2.14E-08	0.80	3.5	2.23E-08	8.23E-10	0.80	0.96	0.93	1.00	
CRS1197	Intact BBC	9.23E-09	0.73	3.4	1.08E-08	5.03E-10	0.73	0.85	0.82	0.90	non uniformity
CRS1206	Intact Maine Clay	4.86E-08	0.60	3.1	4.45E-08	6.92E-10	0.60	1.09	1.08	1.11	non uniformity
CRS1207	RKaolinite	5.52E-08	0.93	3.2	6.32E-08	6.41E-10	0.93	0.87	0.86	0.88	
CRS1210	Intact Maine Clay	4.20E-08	0.69	3.2	4.95E-08	7.86E-10	0.69	0.85	0.83	0.86	
CRS1212	Intact San Francisco Bay Mud	1.10E-09	0.82	3.5	1.15E-09	2.34E-11	0.82	0.96	0.94	0.98	non uniformity
CRS1215	RUgnu Clay	2.79E-09	0.62	2.8	2.33E-09	3.79E-11	0.62	1.20	1.18	1.22	
							Avg.	**0.98**	0.96	1.00	
							St. Dev.	**0.12**	0.12	0.12	

Table 6-7: Index properties of ASTM/ISR reference soils used in the Interlaboratory Study (Benson et al, 2010)

Material	Soil	Atterberg Limits		% Fines (< 75 μm)	% Clay (< 2 μm)
		Liquid Limit	Plasticity Index		
Buckshot Silt	ML	27	4	99	14
Annapolis Silty Clay	CL	33	13	89	34
Buckshot Clay	CH	60	39	99	55

Table 6-8: Individual laboratory results for measured flexible wall hydraulic conductivity from the Interlaboratory Study (Benson et al, 2010)

Lab	Measured Hydraulic Conductivity (cm/s)											
	ML Specimen				CL Specimen				CH Specimen			
	Max	Min	Max/ Min	Coeff. Of Variation	Max	Min	Max/ Min	Coeff. Of Variation	Max	Min	Max/ Min	Coeff. Of Variation
A	8.8E-07	7.4E-07	1.19	0.10	3.8E-08	3.4E-08	1.12	0.06	1.4E-09	1.2E-09	1.17	0.08
B	1.4E-06	9.9E-07	1.41	0.21	5.6E-08	4.5E-08	1.24	0.12	3.9E-09	2.9E-09	1.34	0.16
C	1.6E-06	9.8E-07	1.63	0.34	4.3E-08	3.4E-08	1.26	0.12	3.4E-09	1.6E-09	2.13	0.39
D	1.5E-06	8.7E-07	1.72	0.26	3.6E-08	3.0E-08	1.20	0.10	1.5E-09	1.3E-09	1.15	0.07
E	1.4E-06	7.8E-07	1.79	0.31	3.6E-08	3.4E-08	1.06	0.03	3.6E-09	2.8E-09	1.29	0.13
F	1.4E-06	1.2E-06	1.17	0.09	3.7E-08	2.7E-08	1.37	0.16	6.7E-09	2.5E-09	2.68	0.48
H	1.1E-06	8.4E-07	1.31	0.14	3.7E-08	3.6E-08	1.03	0.02	2.7E-08	8.9E-09	3.03	0.61
I	1.1E-06	9.1E-07	1.21	0.09	3.6E-08	3.1E-08	1.16	0.08	2.4E-09	1.6E-09	1.50	0.20
K	1.2E-06	1.0E-06	1.20	0.09	3.8E-08	3.4E-08	1.12	0.06	2.2E-09	1.7E-09	1.29	0.14
L	1.1E-06	8.6E-07	1.28	0.13	4.6E-08	4.0E-08	1.15	0.07	2.8E-09	1.7E-09	1.65	0.26
M	2.0E-06	9.1E-07	2.20	0.49	4.6E-08	3.5E-08	1.31	0.14	4.3E-09	1.9E-09	2.26	0.38
N	2.6E-06	1.5E-06	1.73	0.27	5.2E-08	3.4E-08	1.53	0.21	1.6E-09	1.1E-09	1.45	0.19
Avg.			1.49	0.21			1.21	0.10			1.75	0.26

Table 6-9: CRS and constant head hydraulic conductivity results in terms of maximum and minimum

Test ID	Material	Void Ratio	Measured Hydraulic Conductivity (cm/s)				
			CRS	Constant Head	Max	Min	Max / Min
CRS1161	RBBC	0.75	1.72E-08	1.59E-08	1.72E-08	1.59E-08	1.08
CRS1175	RBBC	0.74	1.53E-08	1.55E-08	1.55E-08	1.53E-08	1.02
CRS1190	RBBC	0.79	1.61E-08	1.75E-08	1.75E-08	1.61E-08	1.08
CRS1191	RBBC	0.81	2.14E-08	2.23E-08	2.23E-08	2.14E-08	1.04
CRS1197	Intact BBC	0.74	9.23E-09	1.08E-08	1.08E-08	9.23E-09	1.17
CRS1206	Intact Maine Clay	0.61	4.86E-08	4.45E-08	4.86E-08	4.45E-08	1.09
CRS1207	RKaolinite	0.94	5.52E-08	6.32E-08	6.32E-08	5.52E-08	1.15
CRS1210	Intact Maine Clay	0.69	4.20E-08	4.95E-08	4.95E-08	4.20E-08	1.18
CRS1212	Intact San Francisco Bay Mud	0.83	1.10E-09	1.15E-09	1.15E-09	1.10E-09	1.05
CRS1215	RUgnu Clay	0.63	2.79E-09	2.33E-09	2.79E-09	2.33E-09	1.20
						Average	1.11

Table 6-10: Summary of measured hydraulic conductivity for CRS constant head tests

Test ID	Material	Measured CRS Constant Head Hydraulic Conductivity (cm/s)				Max	Min	Max/Min
		Gradient 1	Gradient 2	Gradient 3	Gradient 4			
CRS1161	RBBC	N/A	N/A	N/A		N/A	N/A	N/A
CRS1175	RBBC	1.53E-08	1.57E-08	1.56E-08		1.57E-08	1.53E-08	1.02
CRS1188	RBBC	N/A	N/A	N/A		N/A	N/A	N/A
CRS1190	RBBC	1.71E-08	1.76E-08	1.79E-08		1.79E-08	1.71E-08	1.05
CRS1191	RBBC	2.20E-08	2.32E-08	2.16E-08		2.32E-08	2.16E-08	1.07
CRS1197	Intact BBC	1.05E-08	1.07E-08	1.14E-08		1.14E-08	1.05E-08	1.09
CRS1206	Intact Maine Clay	4.51E-08	4.38E-08	4.49E-08		4.51E-08	4.38E-08	1.03
CRS1207	RKaolinite	6.28E-08	6.36E-08	6.41E-08		6.41E-08	6.28E-08	1.02
CRS1210	Intact Maine Clay	4.91E-08	4.93E-08	5.05E-08		5.05E-08	4.91E-08	1.03
CRS1212	Intact San Francisco Bay Mud	1.18E-09	1.15E-09	1.14E-09		1.18E-09	1.14E-09	1.04
CRS1215	RUgnu Clay	2.29E-09	2.37E-09	2.33E-09	2.35E-09	2.37E-09	2.29E-09	1.04
							Avg.	**1.04**

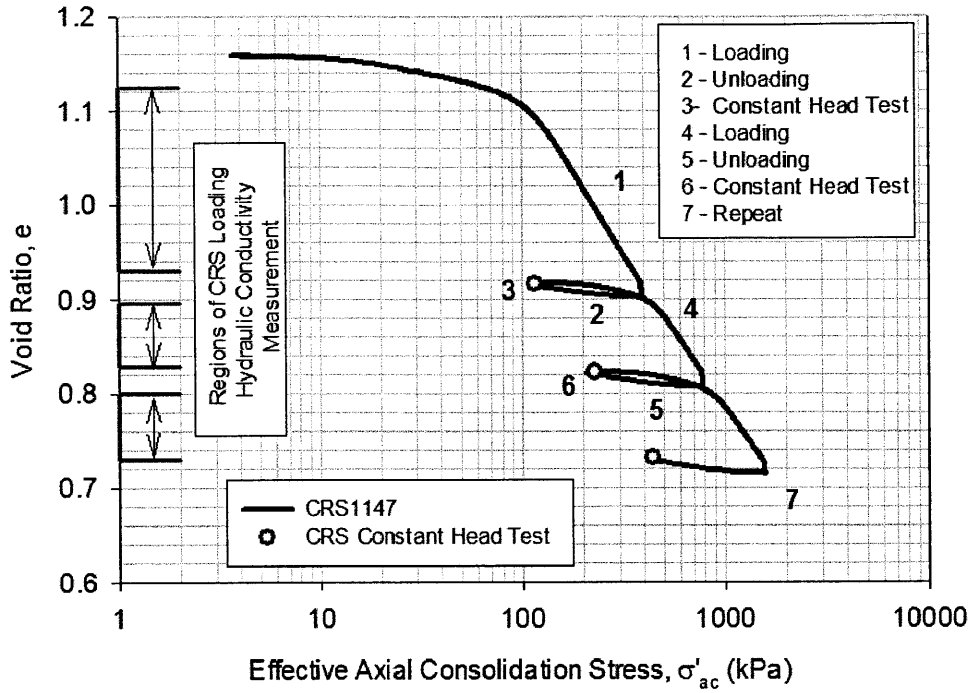

Figure 6-1: CRS 1147 compression curve showing location of constant head and CRS hydraulic conductivity tests

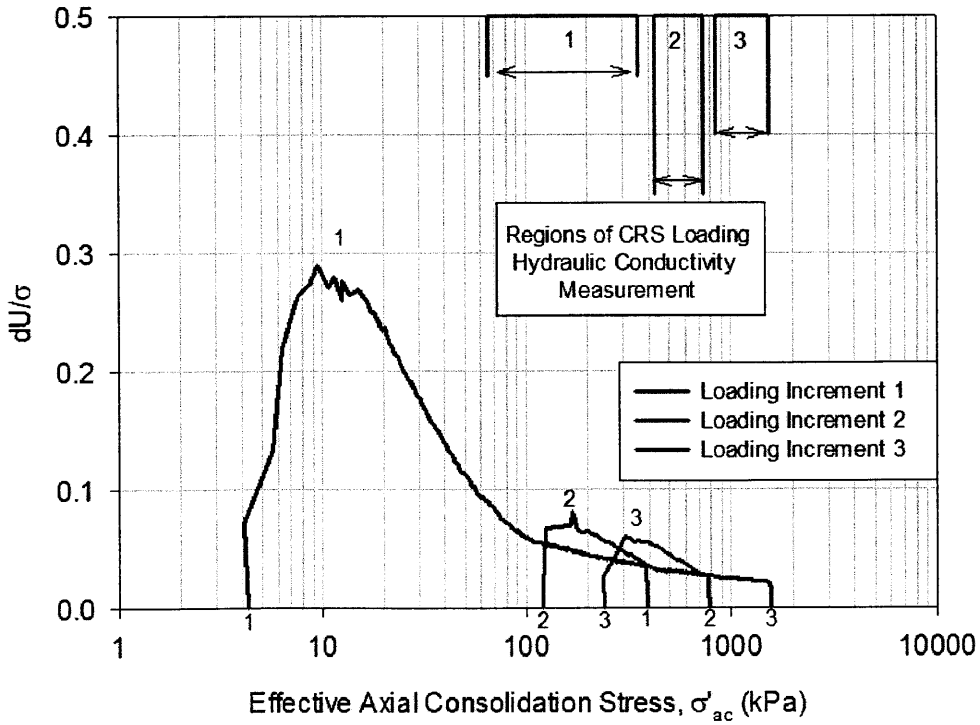

Figure 6-2: CRS 1147 excess pore pressure ratio vs. stress

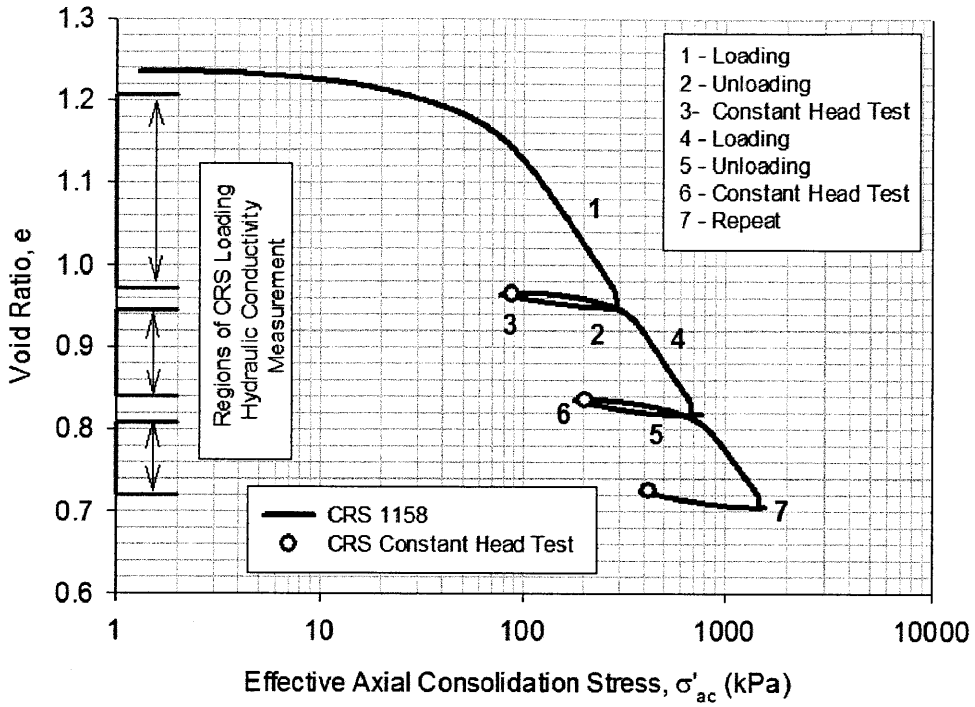

Figure 6-3: CRS 1158 compression curve showing location of constant head and CRS hydraulic conductivity tests

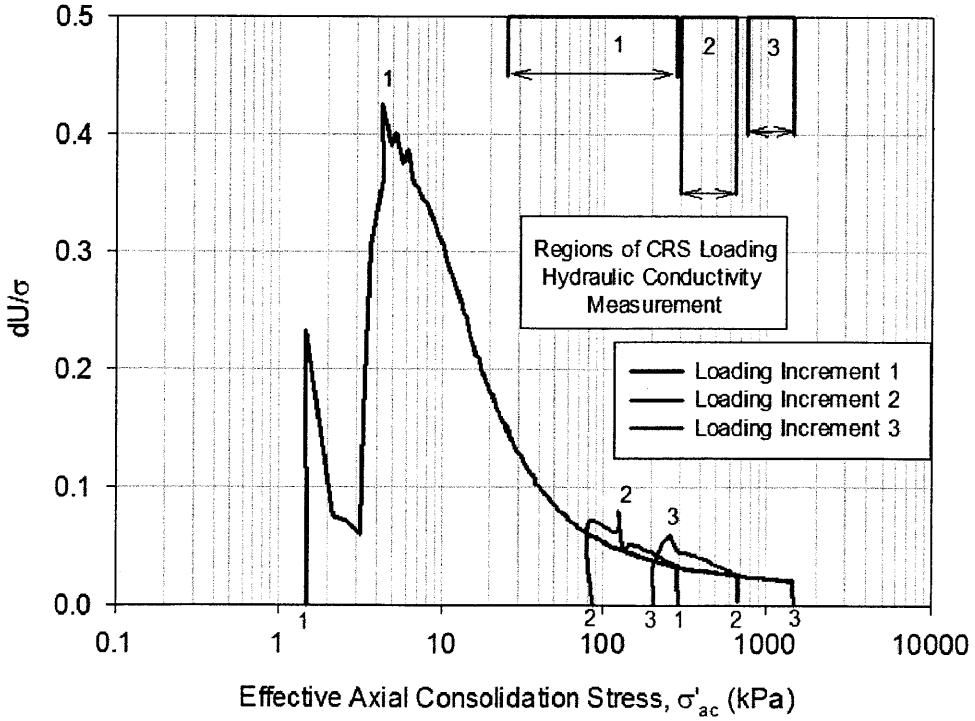

Figure 6-4: CRS 1158 excess pore pressure ratio vs. stress

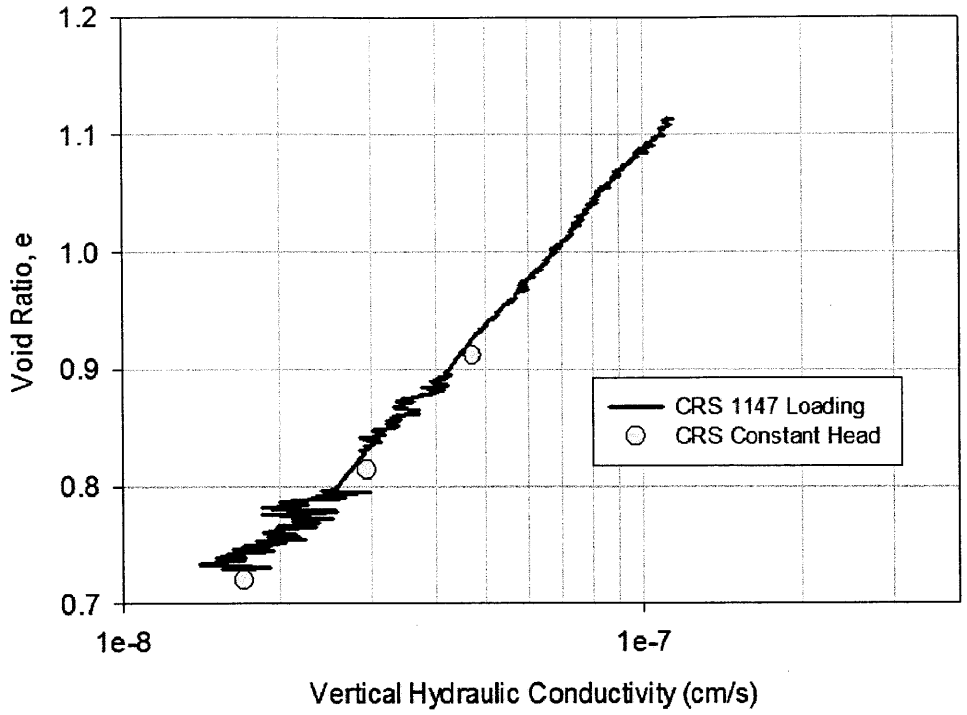

Figure 6-5: CRS 1147 void ratio vs. log hydraulic conductivity measurements

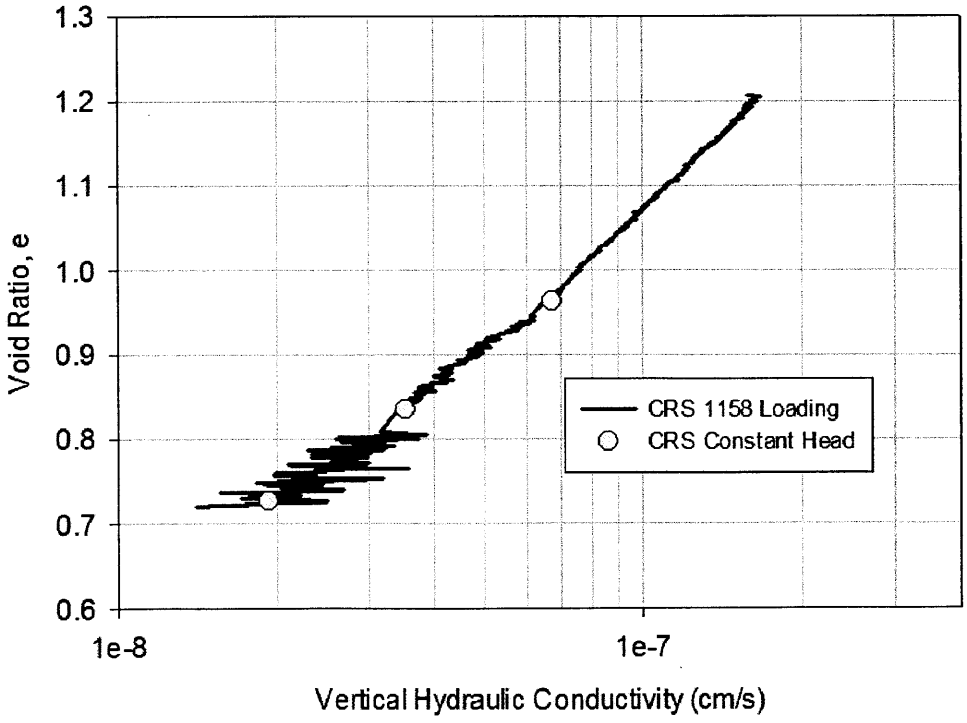

Figure 6-6: CRS 1158 void ratio vs. log hydraulic conductivity measurements

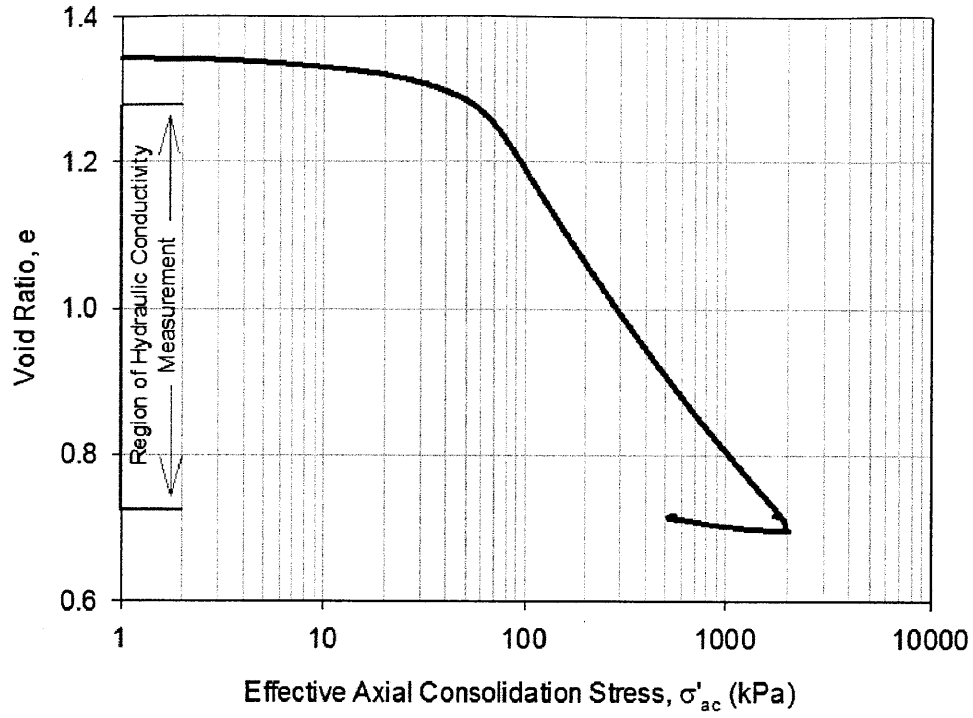

Figure 6-7: CRS 1161 compression curve

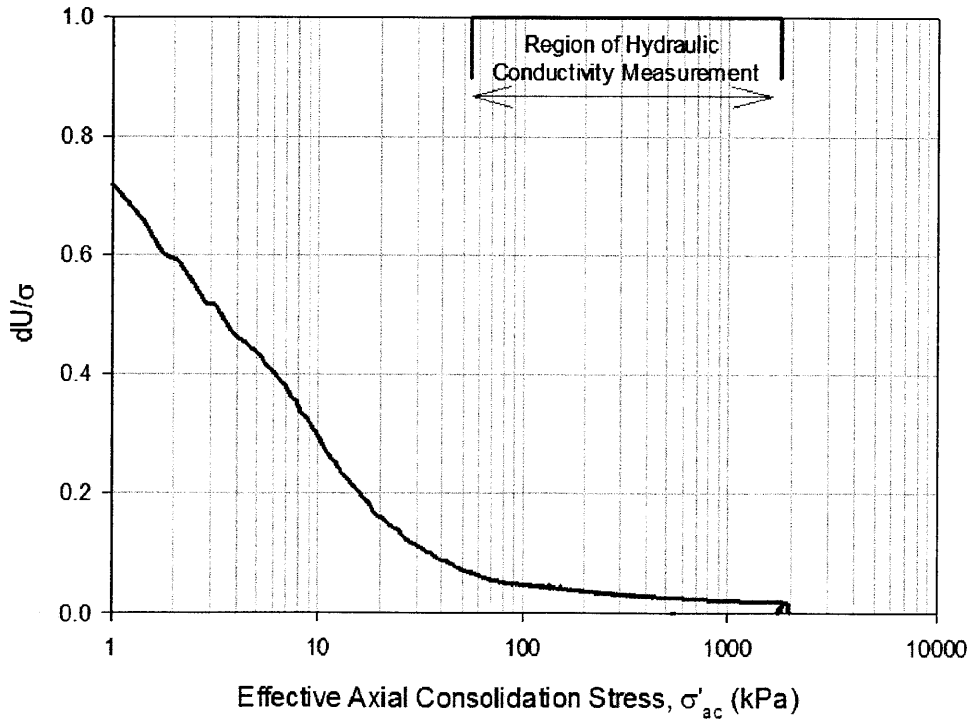

Figure 6-8: CRS 1161 excess pore pressure ratio vs. stress

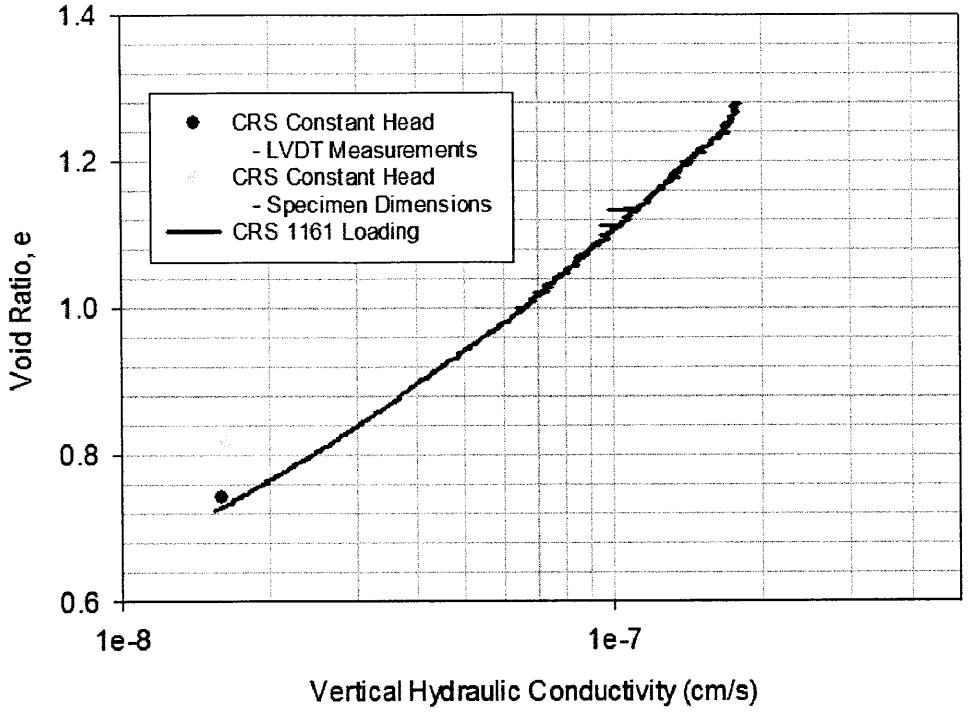

Figure 6-9: CRS 1161 void ratio vs. log hydraulic conductivity measurements

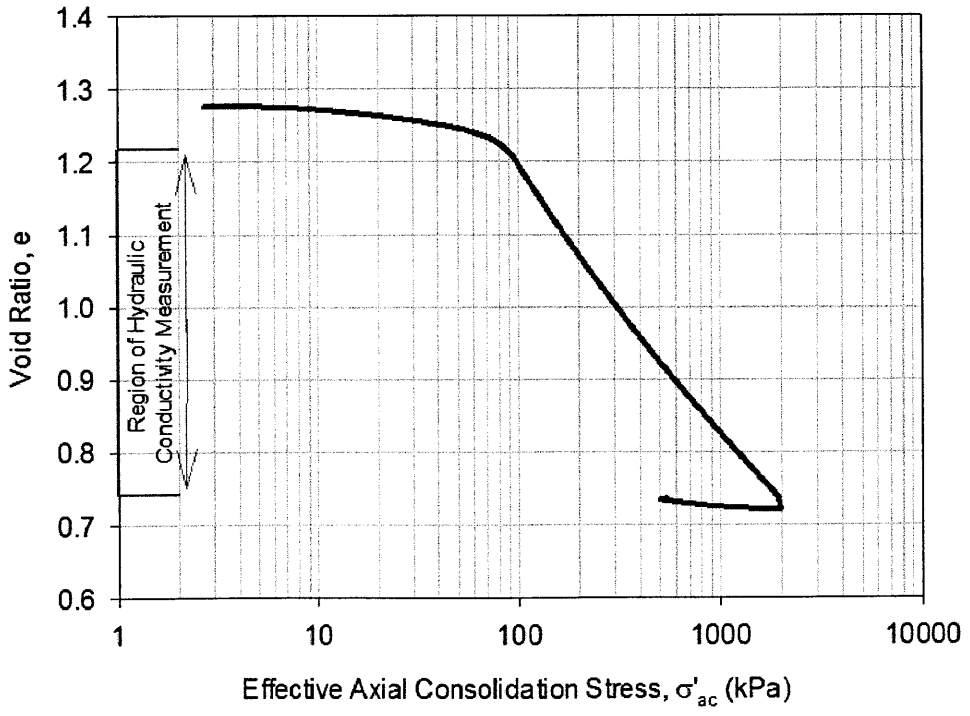

Figure 6-10: CRS 1175 compression curve

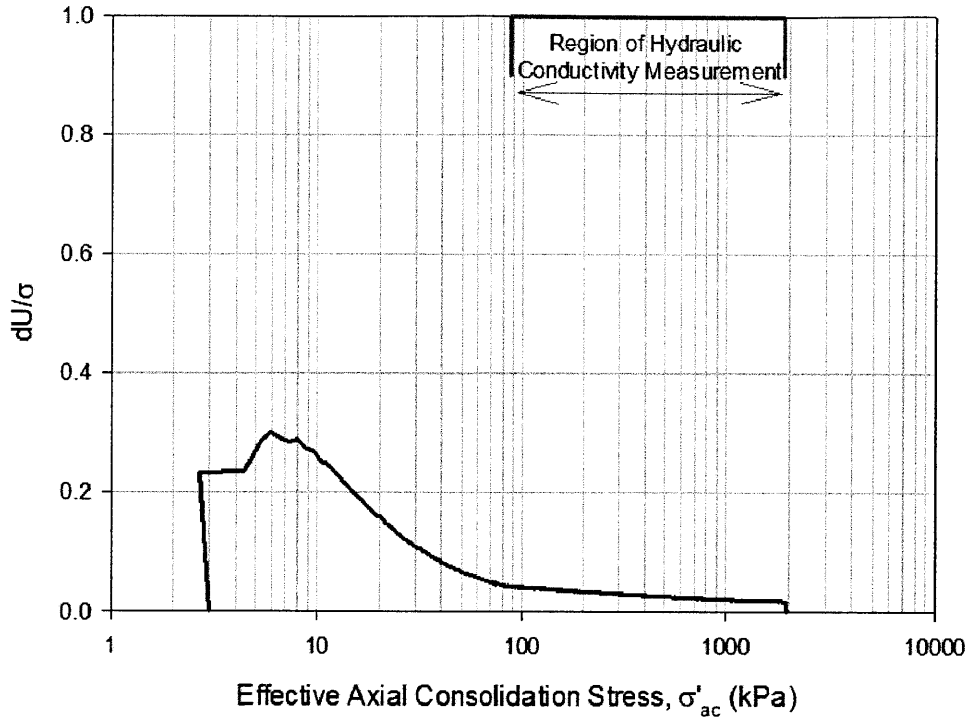

Figure 6-11: CRS 1175 excess pore pressure ratio vs. stress

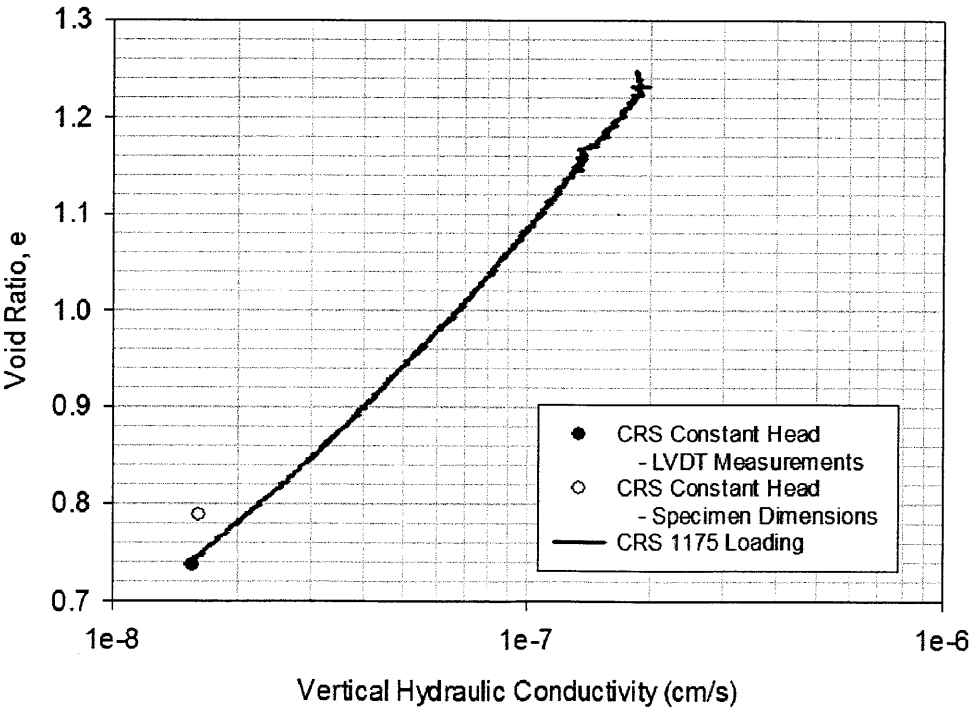

Figure 6-12: CRS 1175 void ratio vs. log hydraulic conductivity measurements

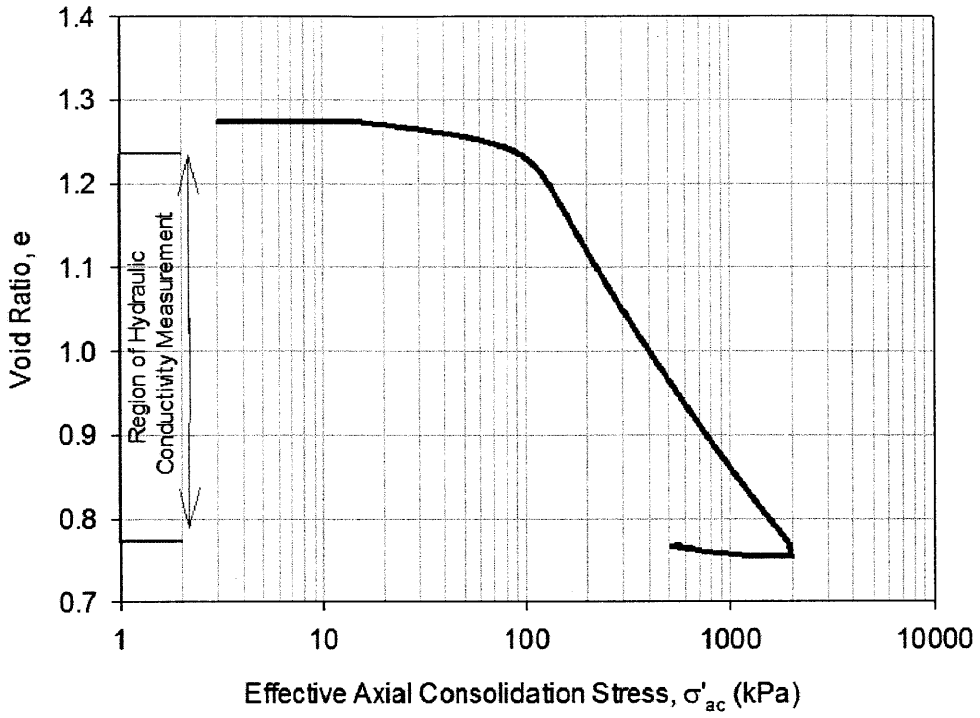

Figure 6-13: CRS 1188 compression curve

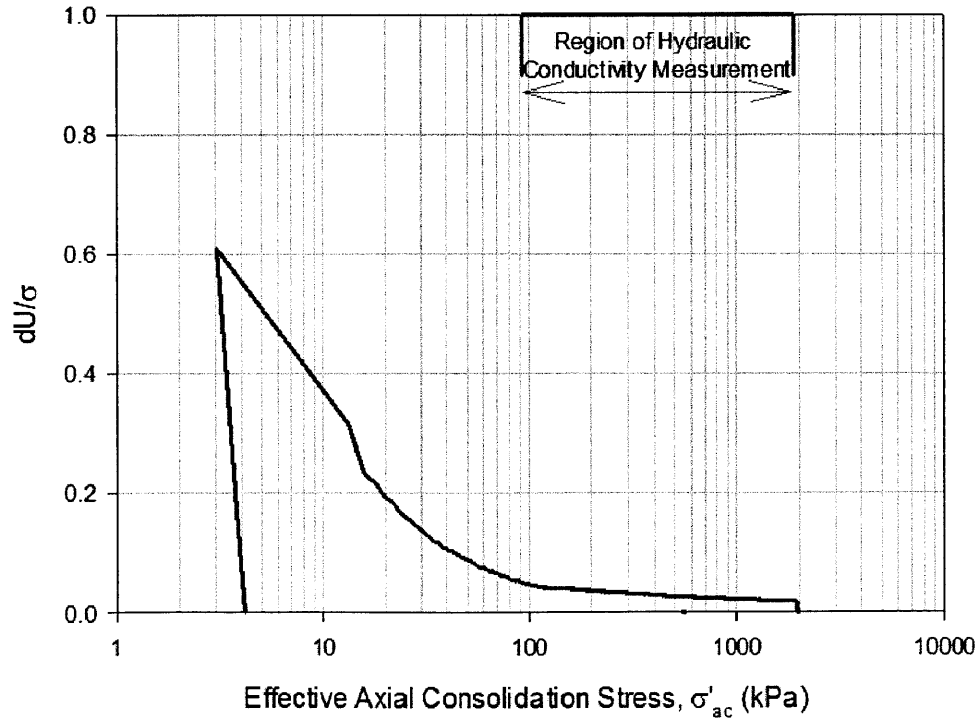

Figure 6-14: CRS 1188 excess pore pressure ratio vs. stress

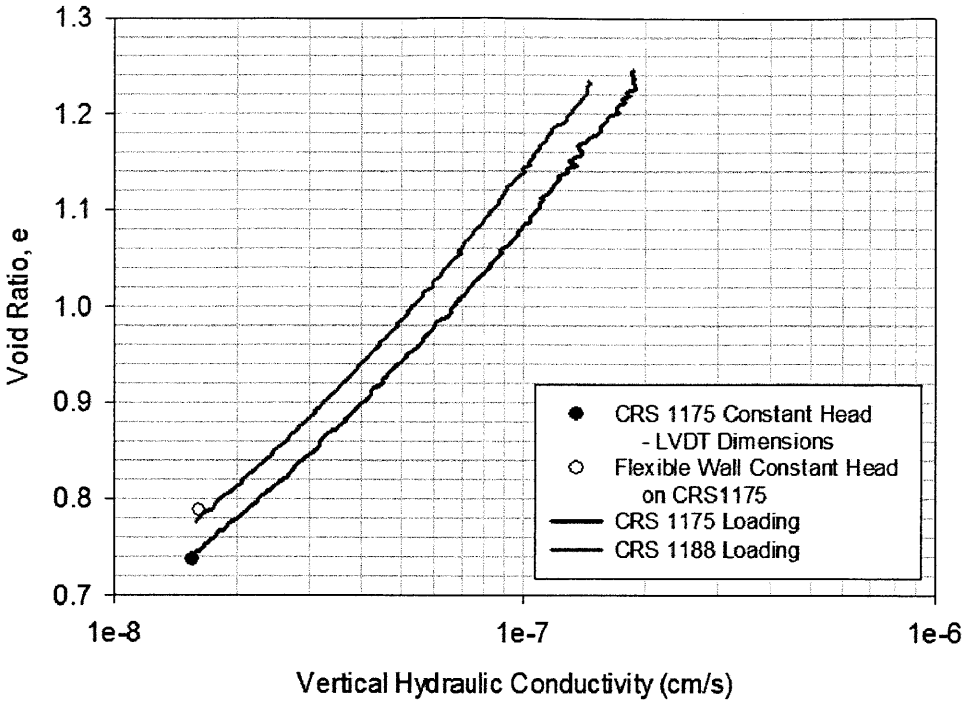

Figure 6-15: CRS 1175 void ratio vs. log hydraulic conductivity measurement showing comparison with CRS 1188

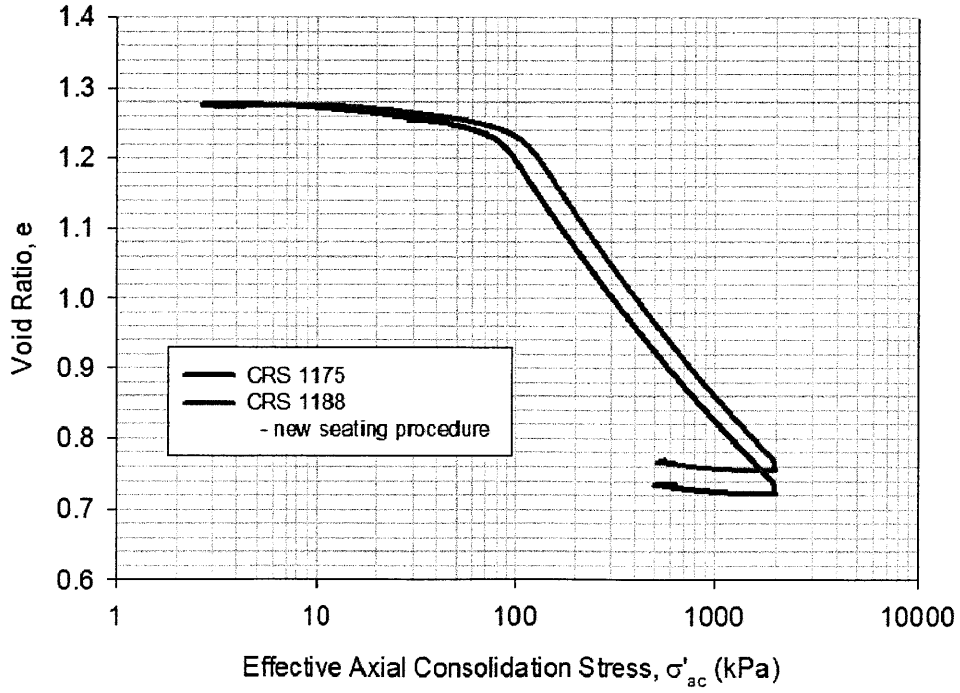

Figure 6-16: CRS 1175 and CRS 1188 compression curves illustrating effect of bottom seating error

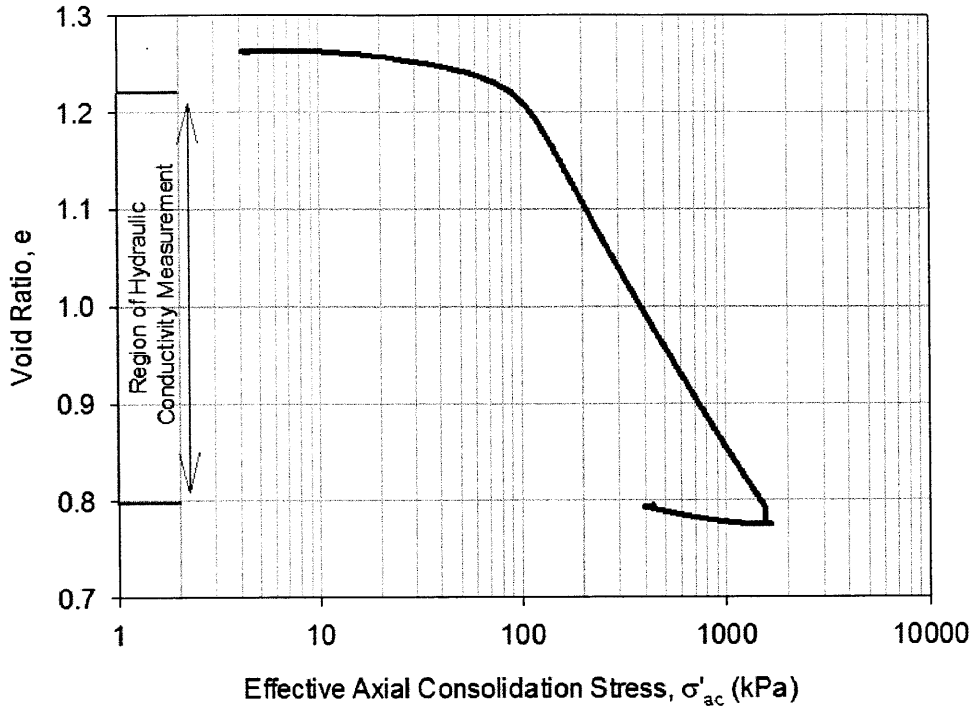

Figure 6-17: CRS 1190 compression curve

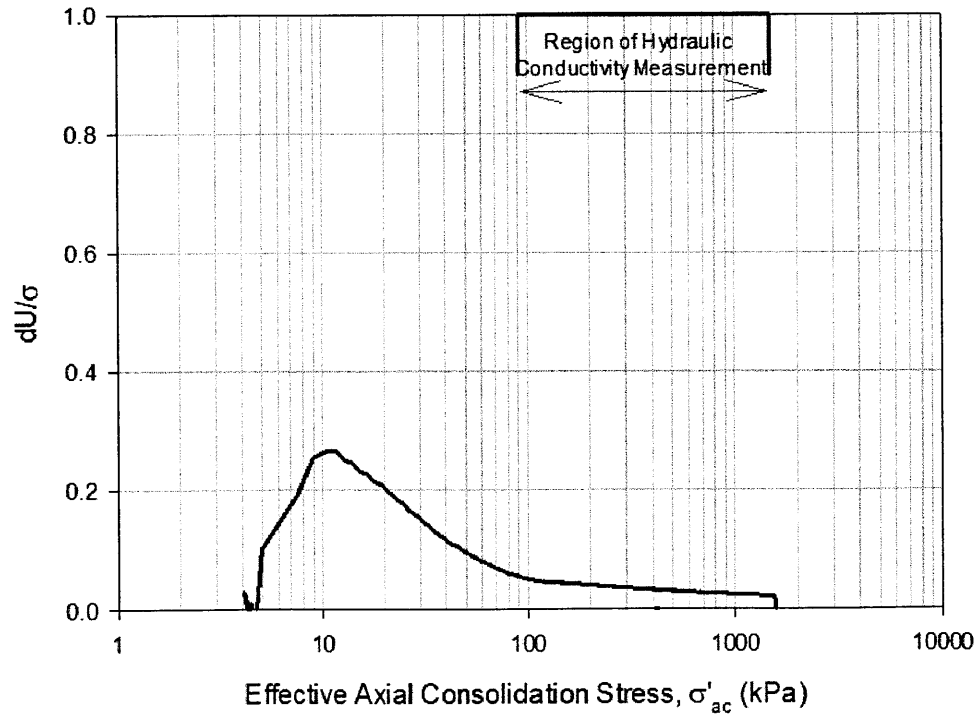

Figure 6-18: CRS 1190 excess pore pressure ratio vs. stress

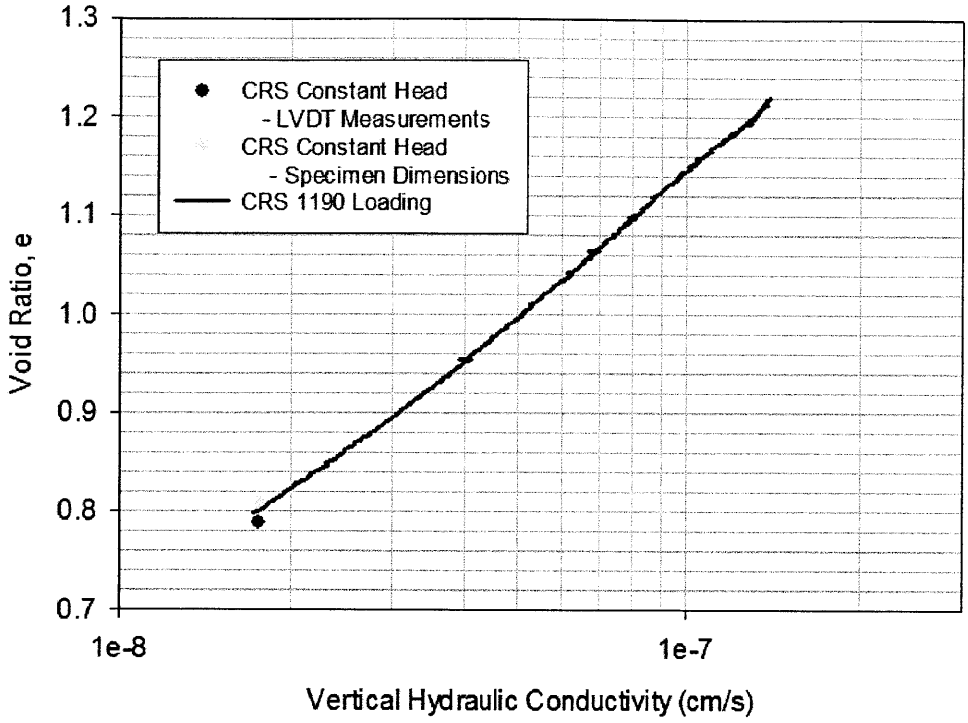

Figure 6-19: CRS 1190 void ratio vs. log hydraulic conductivity measurements

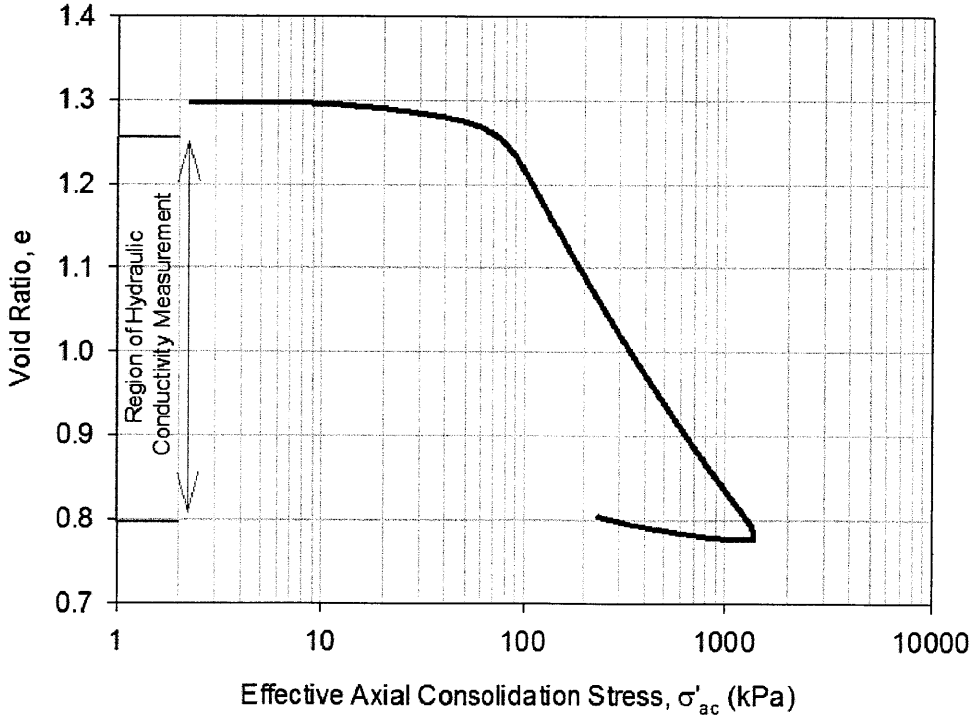

Figure 6-20: CRS 1191 compression curve

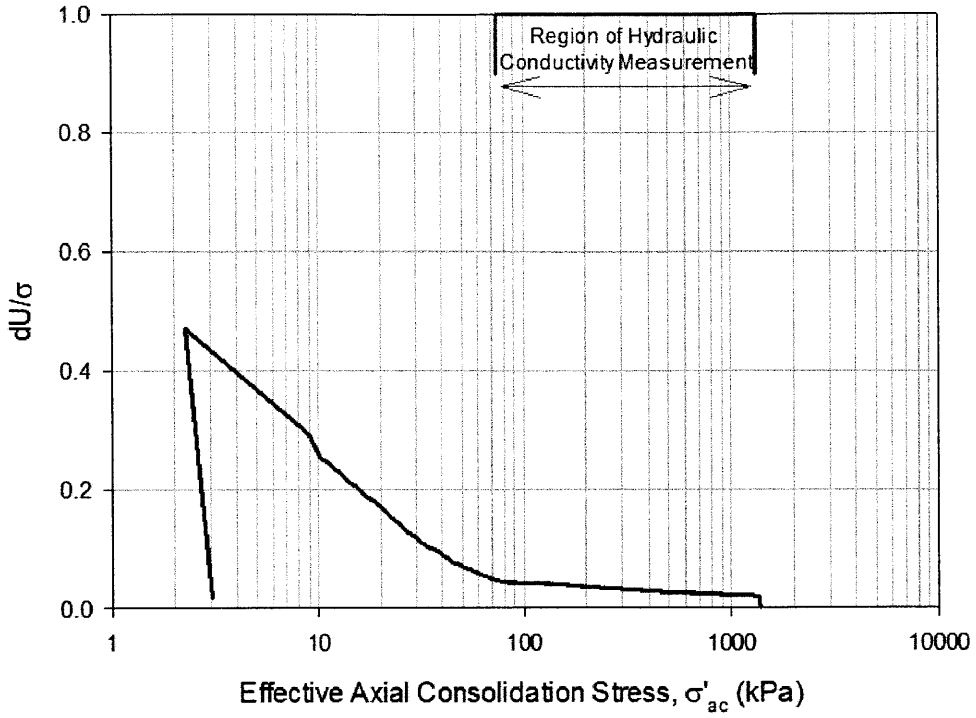

Figure 6-21: CRS 1191 excess pore pressure ratio vs. stress

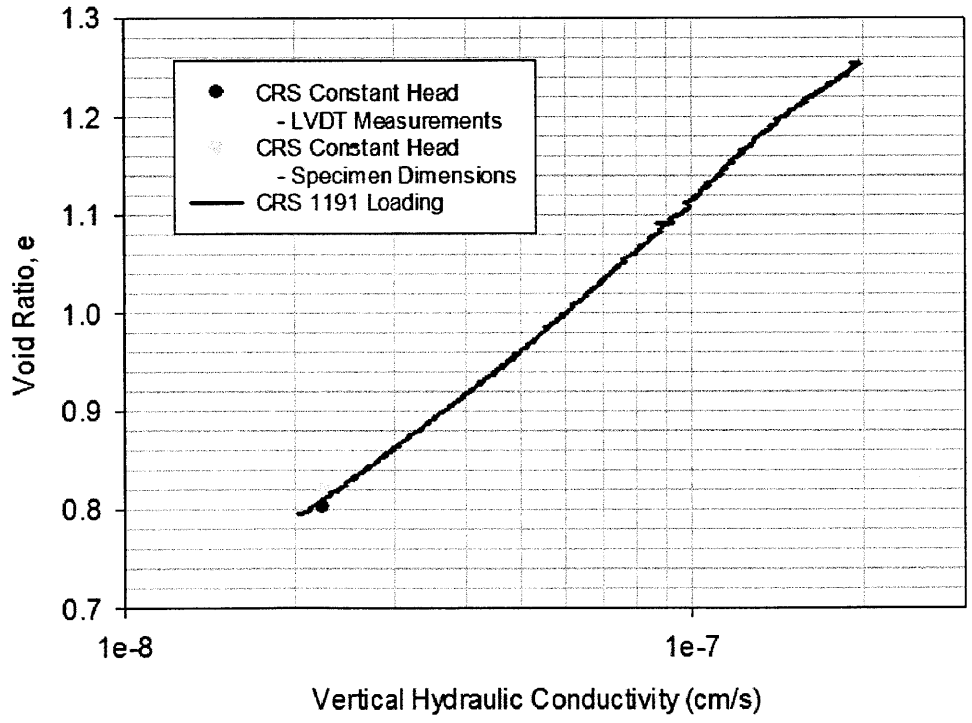

Figure 6-22: CRS 1191 void ratio vs. log hydraulic conductivity measurements

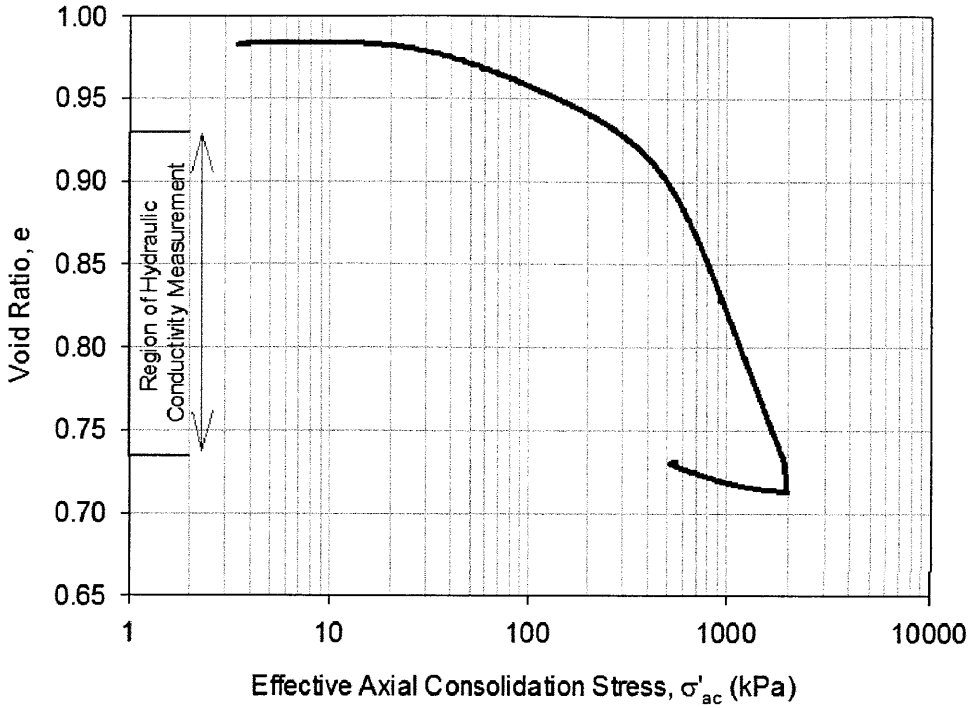

Figure 6-23: CRS 1197 compression curve

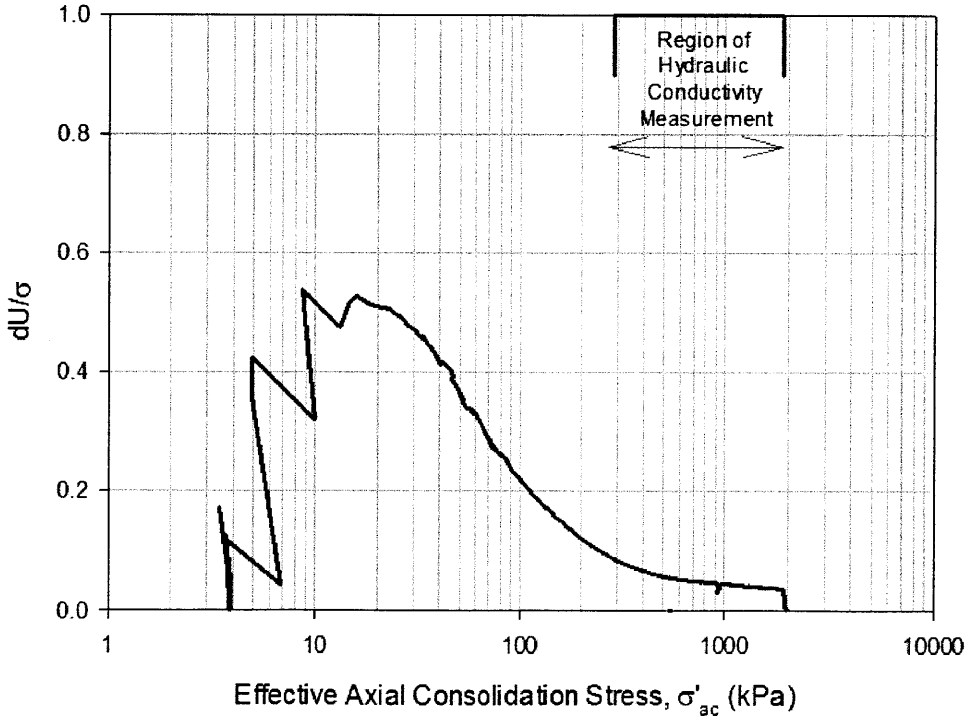

Figure 6-24: CRS 1197 excess pore pressure ratio vs. stress

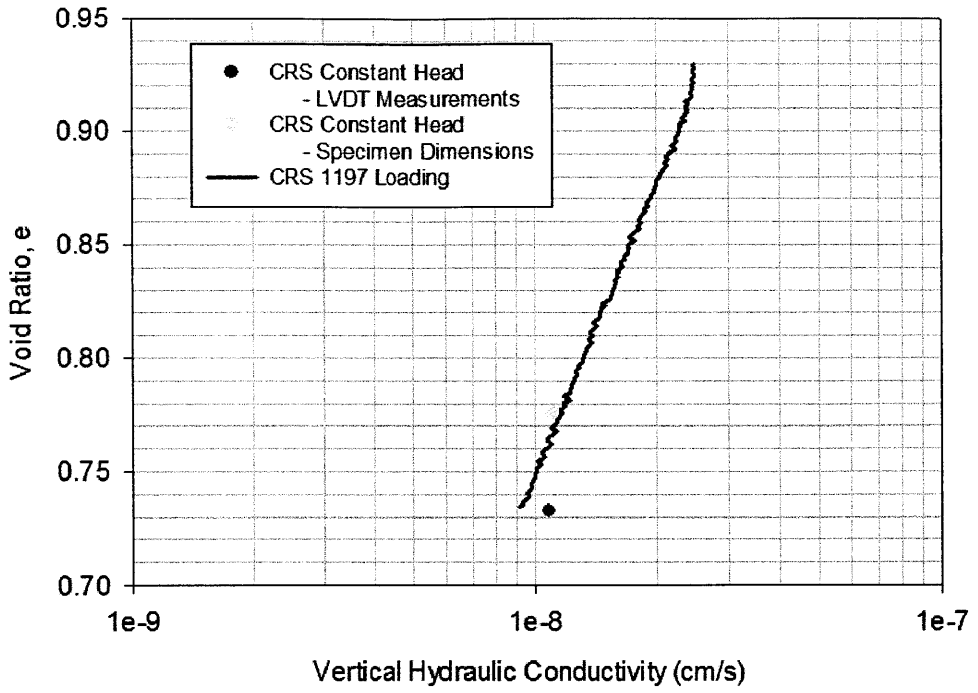

Figure 6-25: CRS 1197 void ratio vs. log hydraulic conductivity measurements

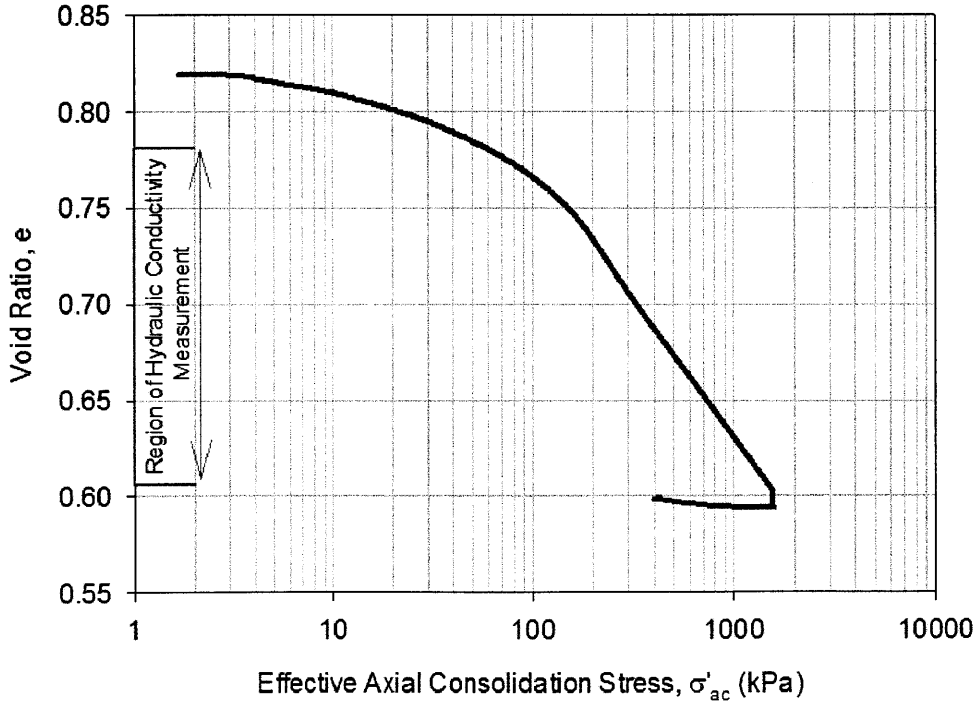

Figure 6-26: CRS 1206 compression curve

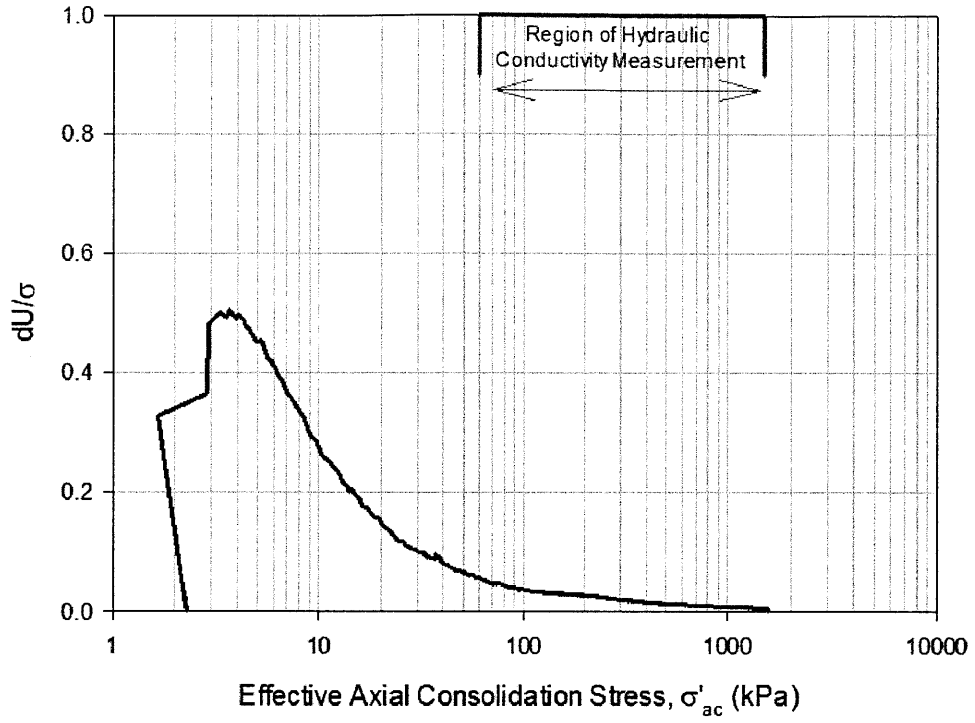

Figure 6-27: CRS 1206 excess pore pressure ratio vs. stress

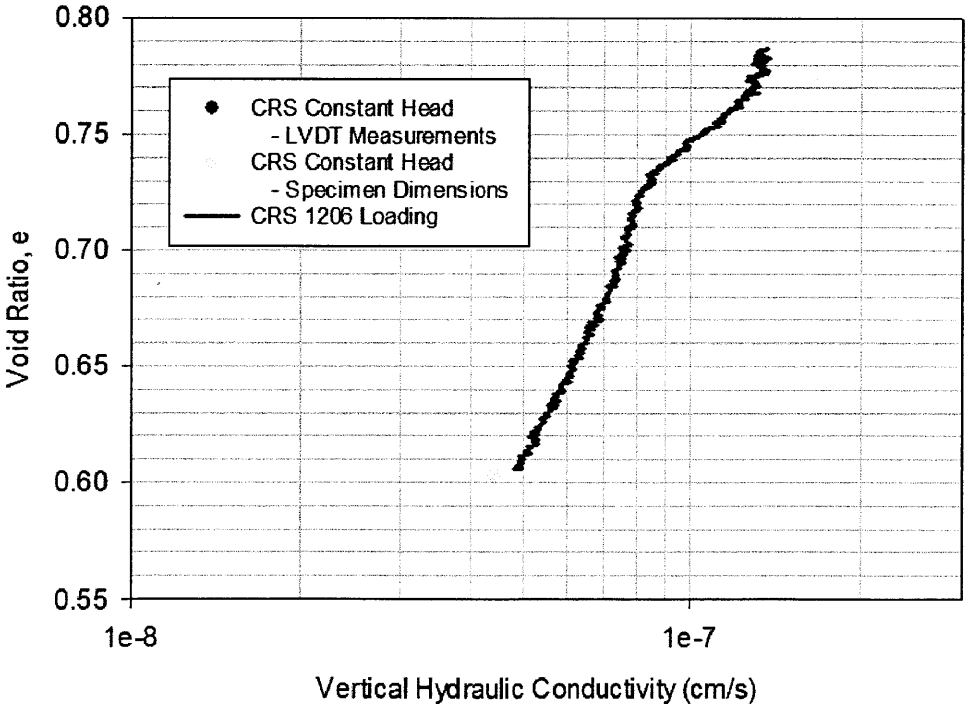

Figure 6-28: CRS 1206 void ratio vs. log hydraulic conductivity measurements

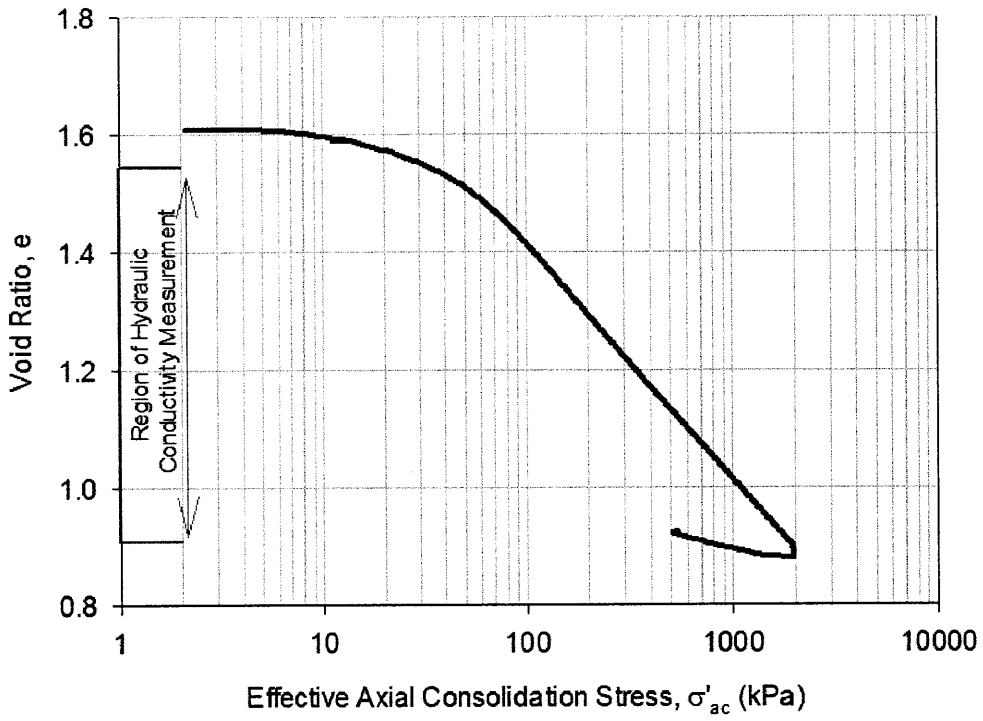

Figure 6-29: CRS 1207 compression curve

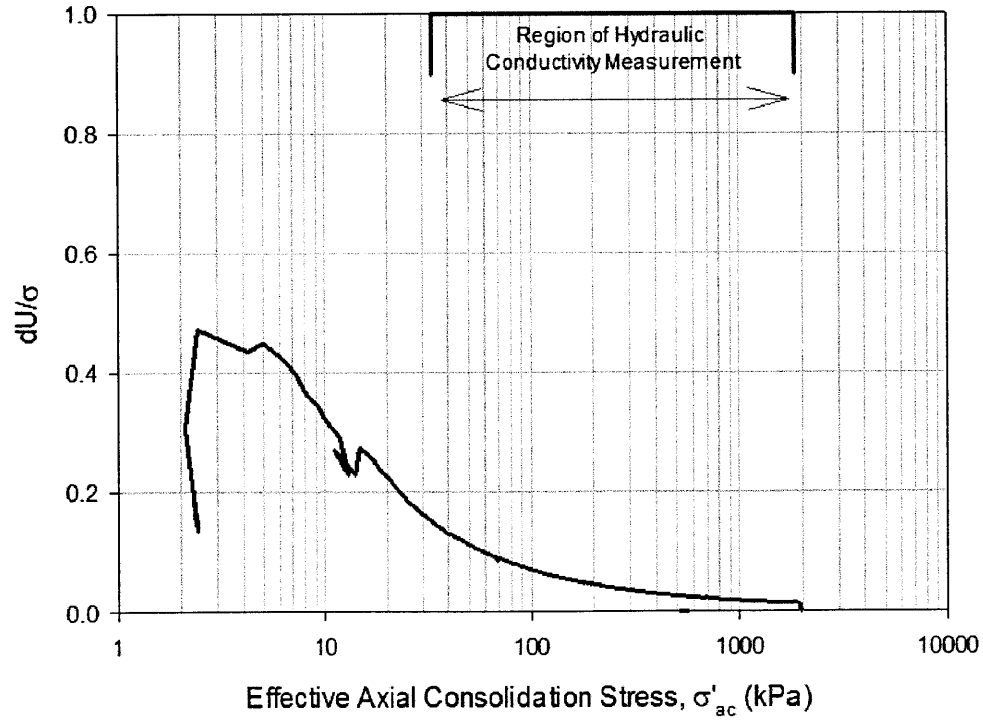

Figure 6-30: CRS 1207 excess pore pressure ratio vs. stress

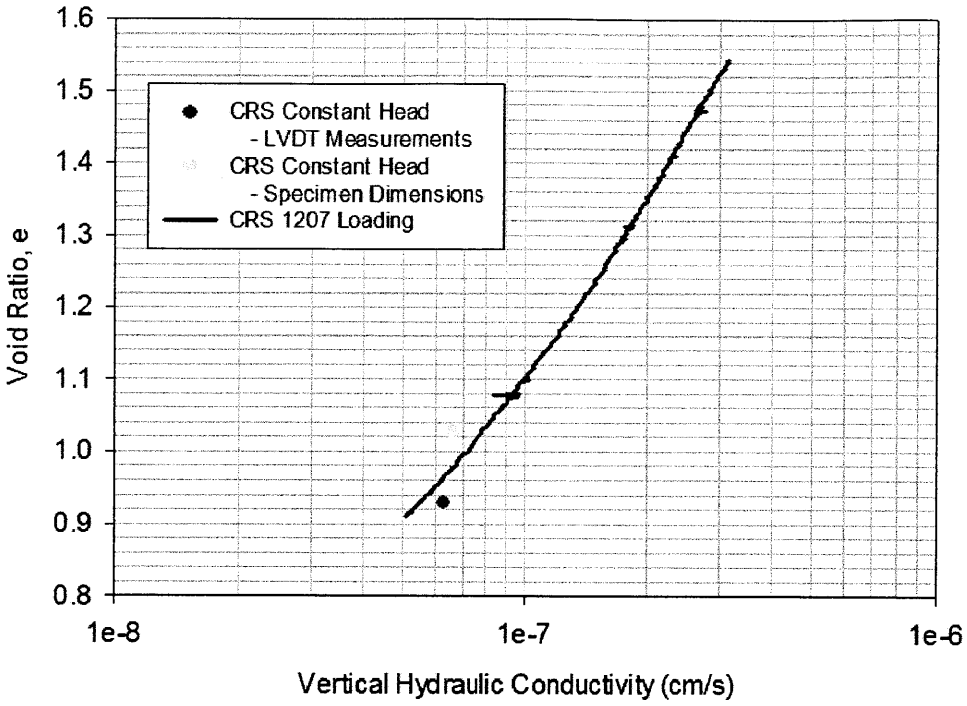

Figure 6-31: CRS 1207 void ratio vs. log hydraulic conductivity measurements

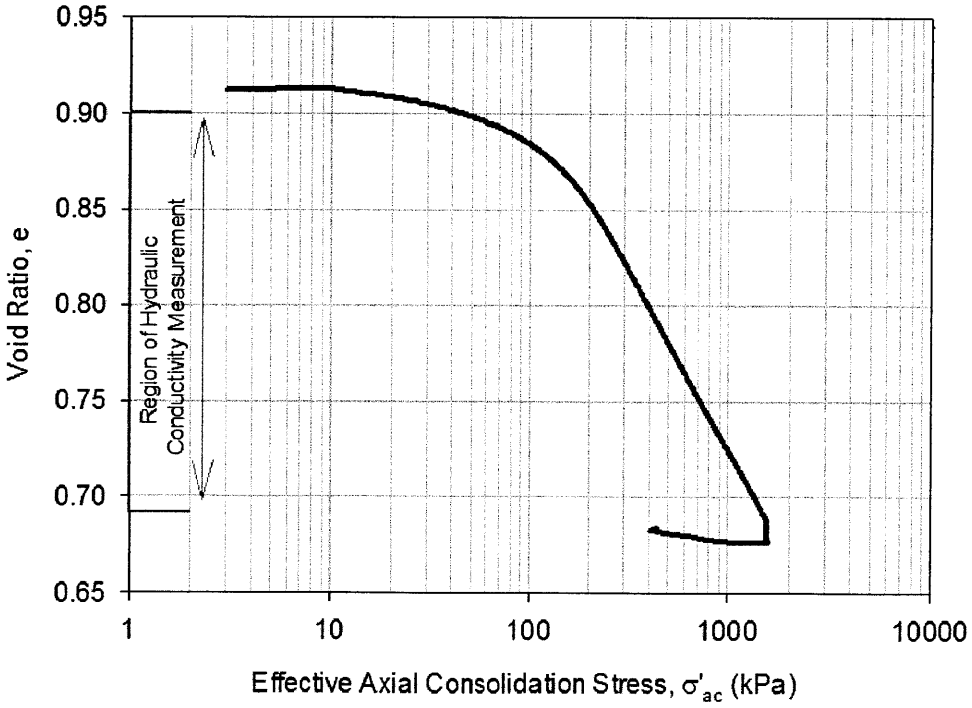

Figure 6-32: CRS 1210 compression curve

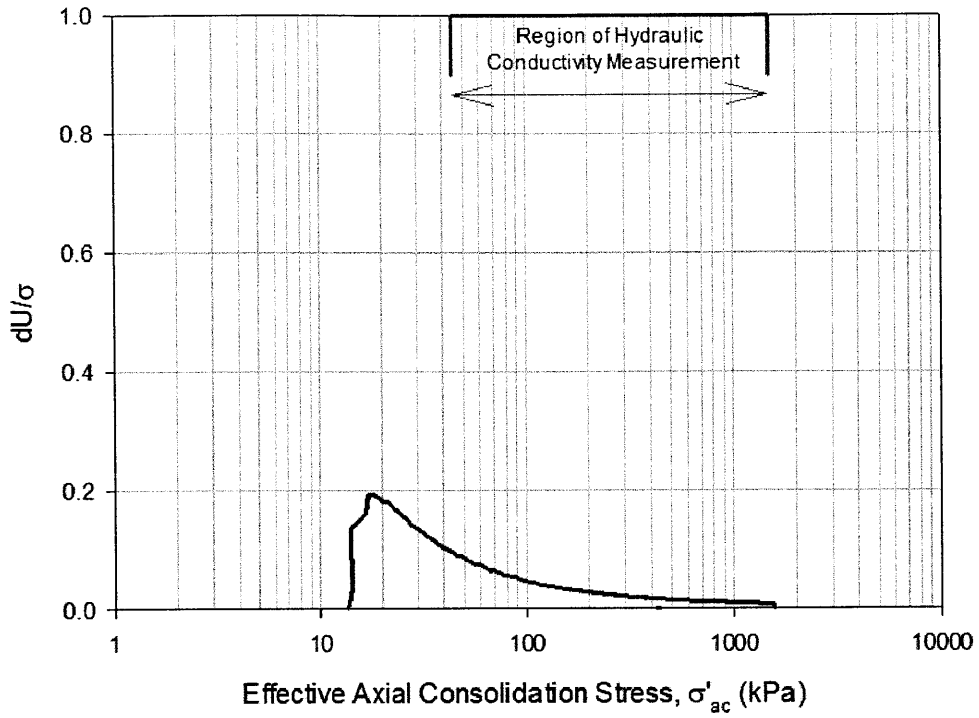

Figure 6-33: CRS 1210 excess pore pressure ratio vs. stress

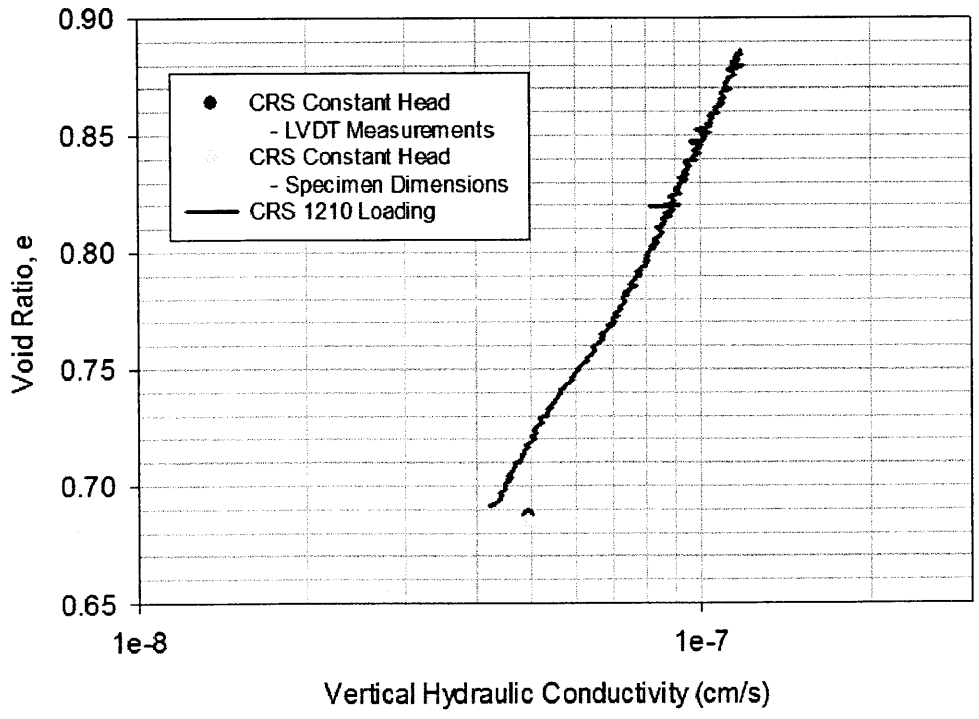

Figure 6-34: CRS 1210 void ratio vs. log hydraulic conductivity measurements

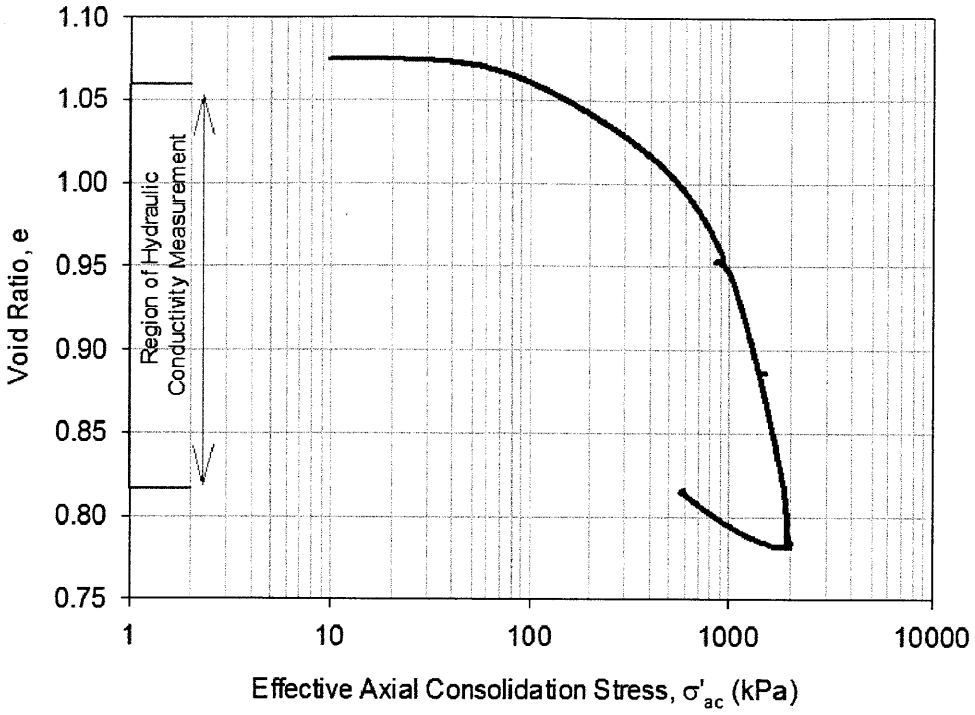

Figure 6-35: CRS 1212 compression curve

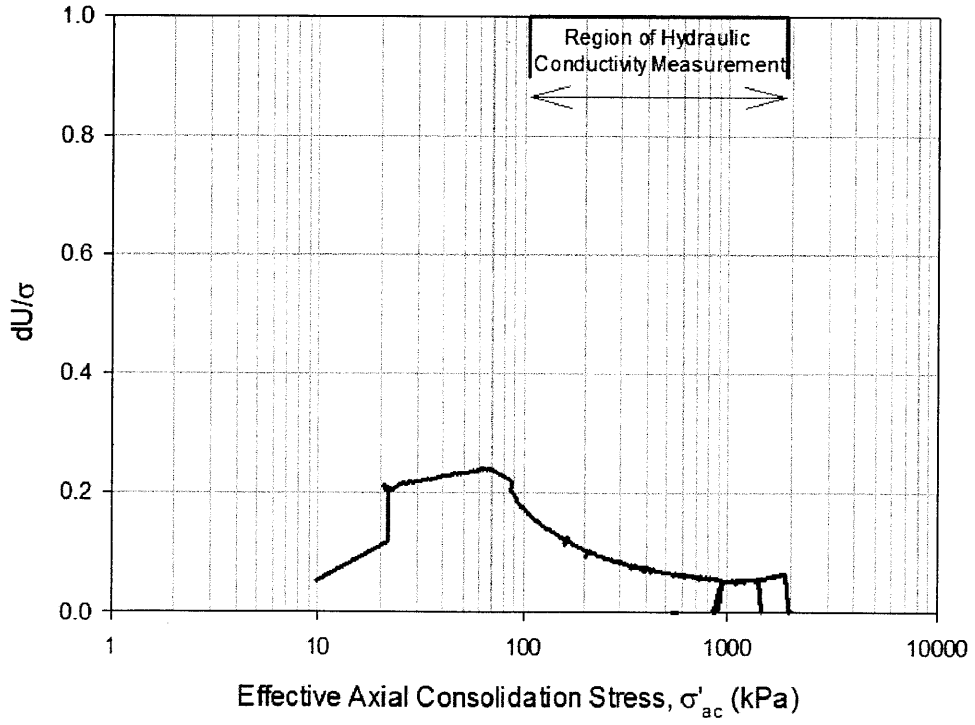

Figure 6-36: CRS 1212 excess pore pressure ratio vs. stress

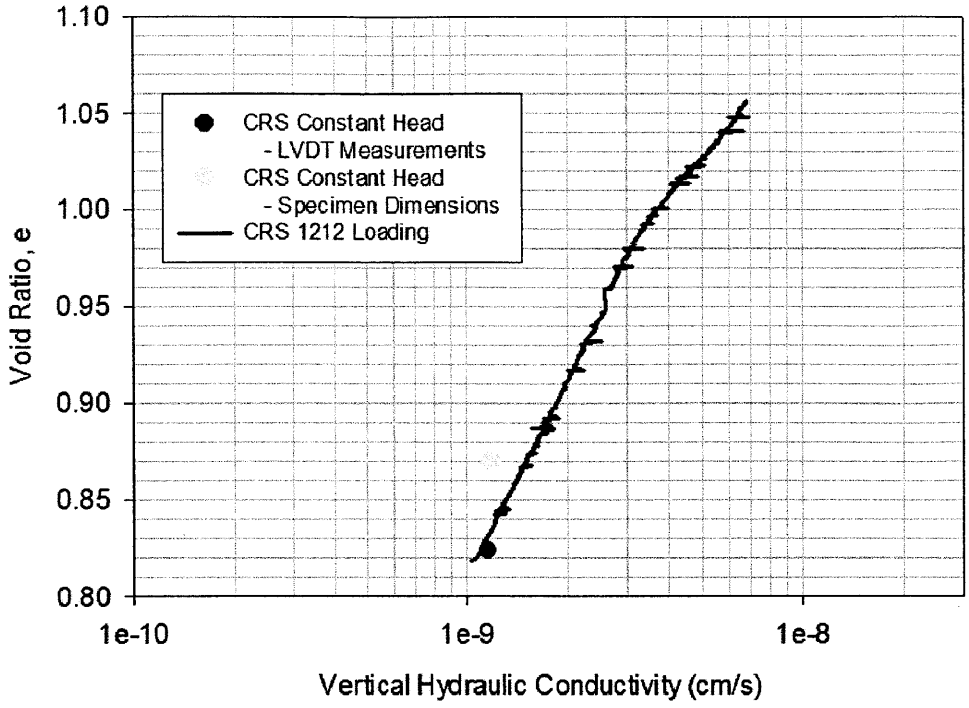

Figure 6-37: CRS 1212 void ratio vs. log hydraulic conductivity measurements

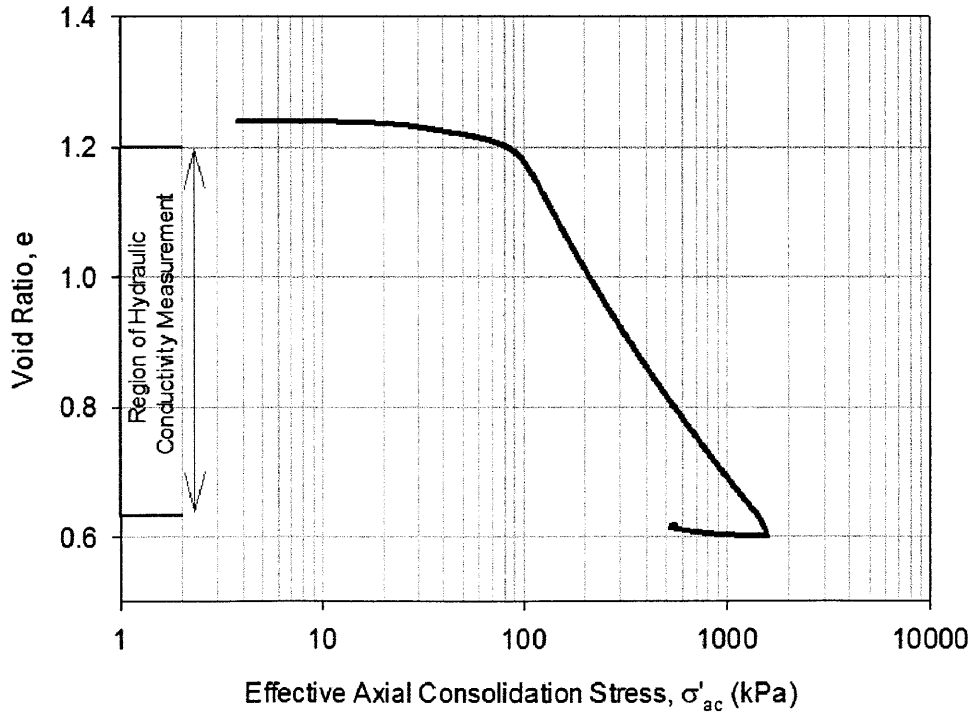

Figure 6-38: CRS 1215 compression curve

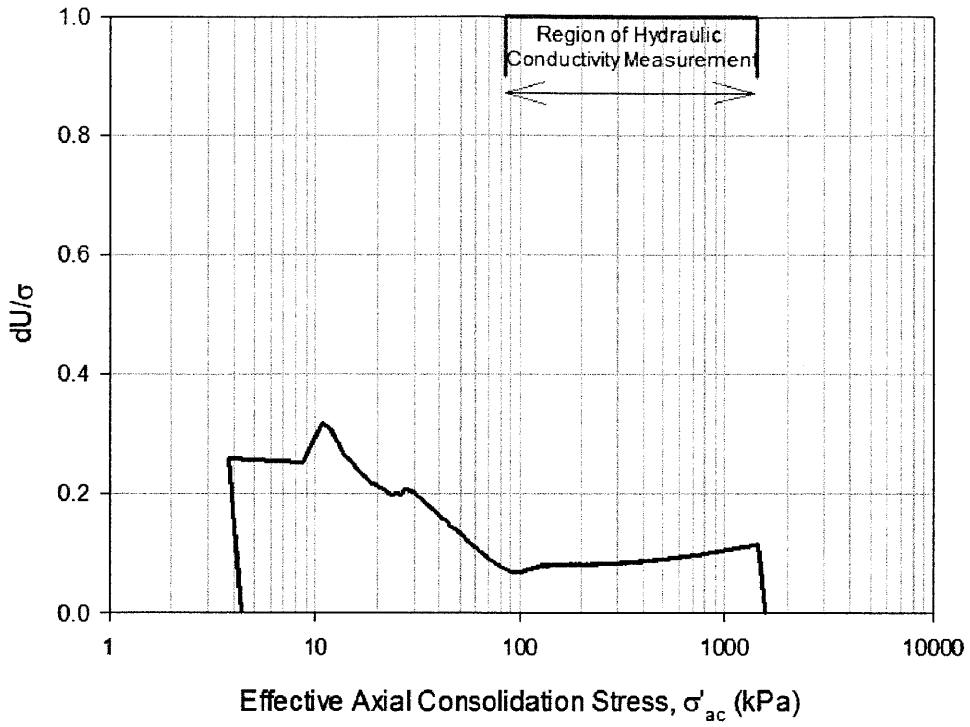

Figure 6-39: CRS 1215 excess pore pressure ratio vs. stress

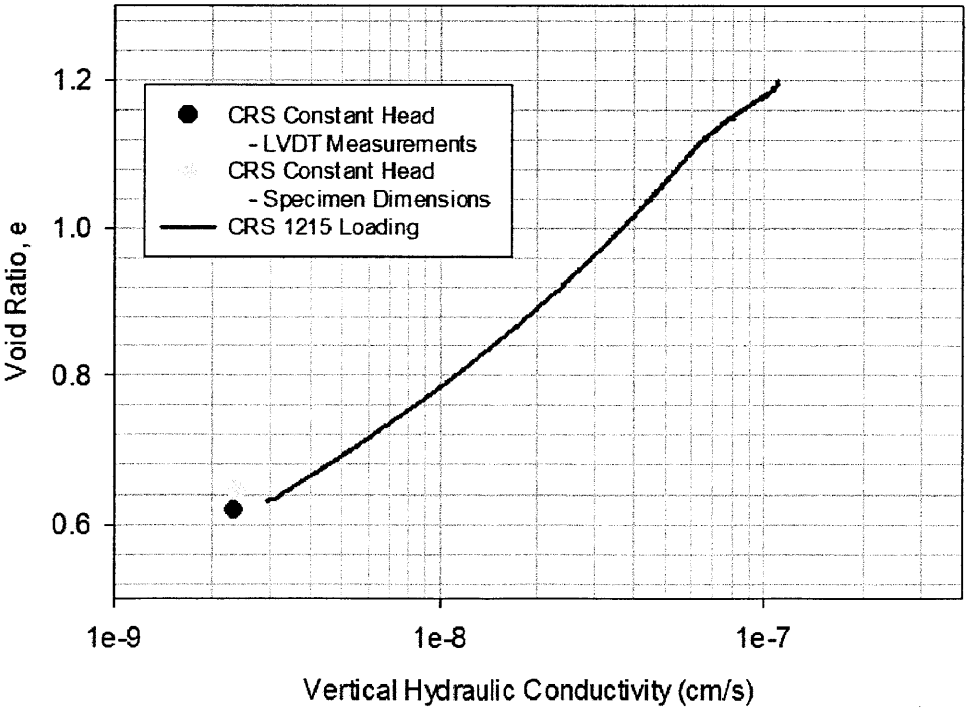

Figure 6-40: CRS 1215 void ratio vs. log hydraulic conductivity measurements

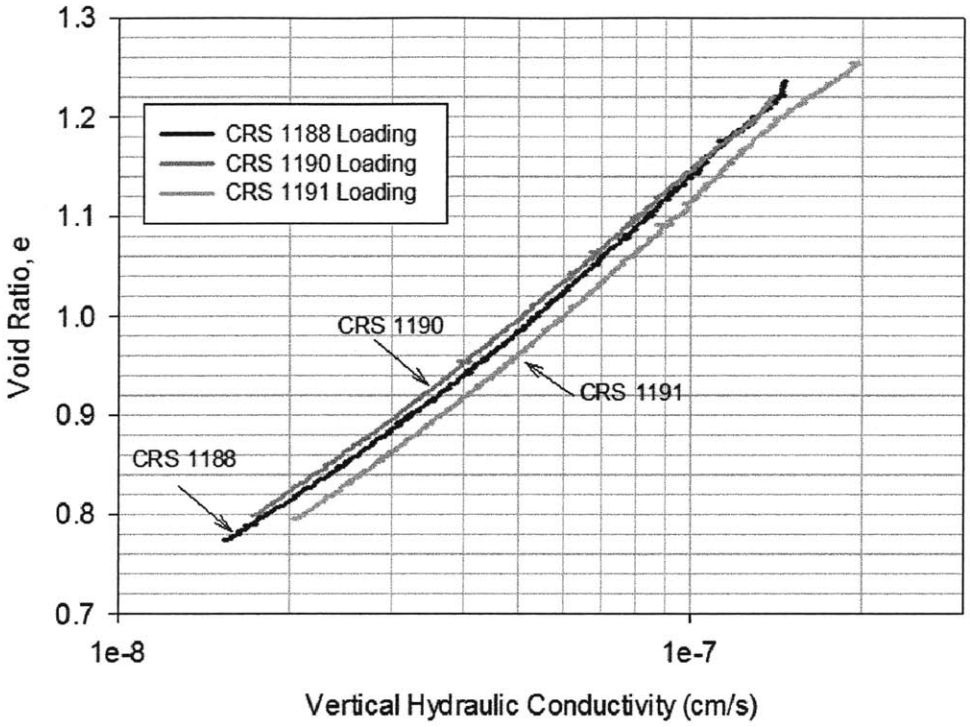

Figure 6-41: CRS 1188, CRS 1190 and CRS 1191 void ratio vs. log hydraulic conductivity measurements

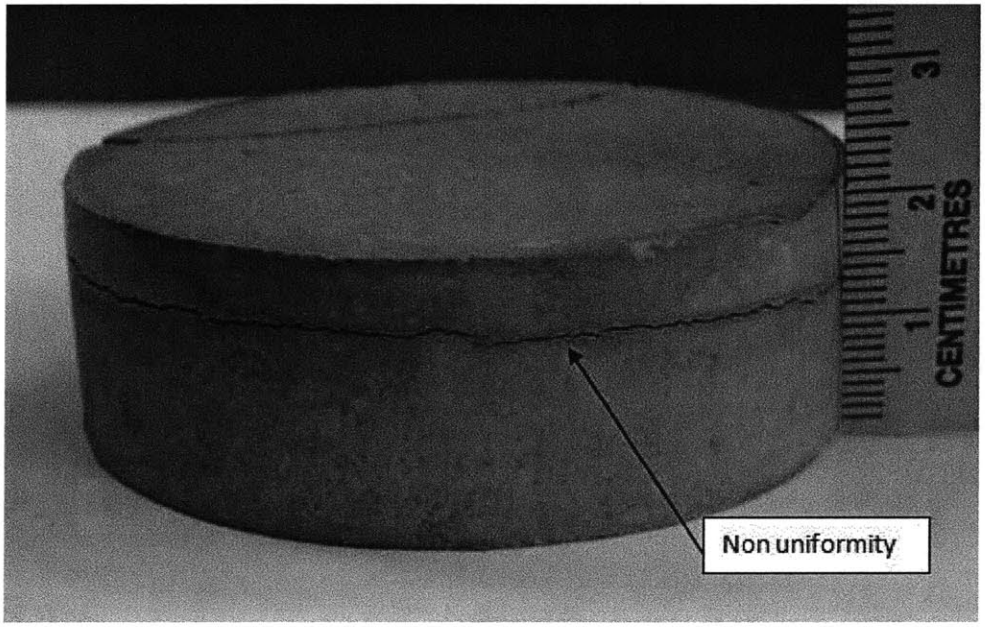

Figure 6-42: Axial non uniformity in oven dried CRS 1206 specimen

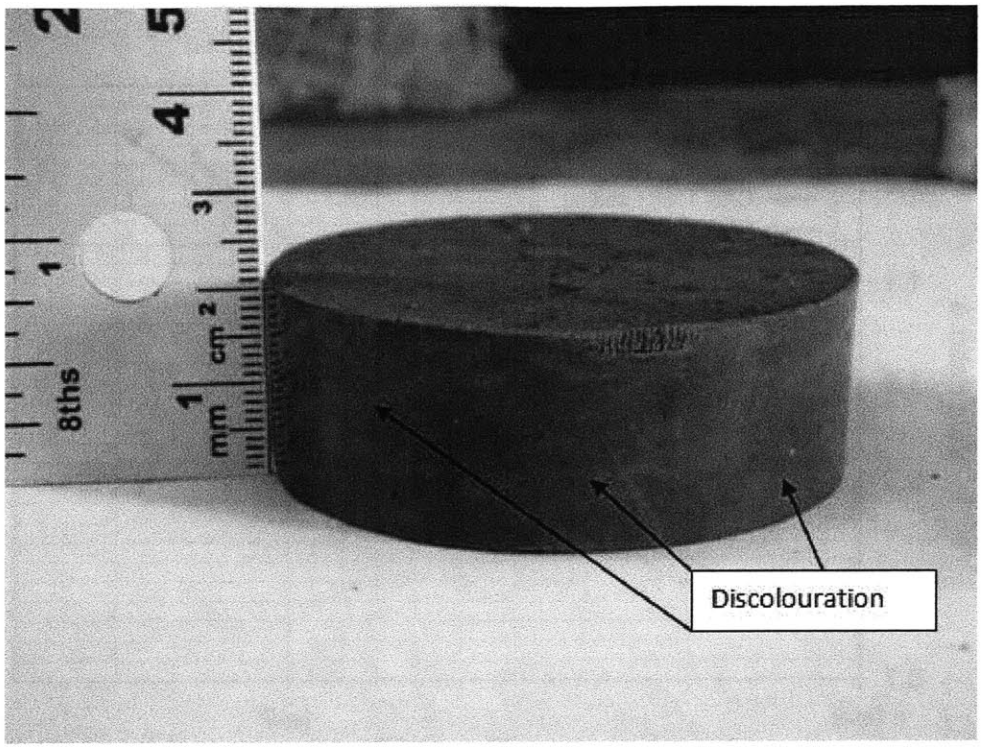

Figure 6-43: Discolouration in moist CRS 1212 specimen

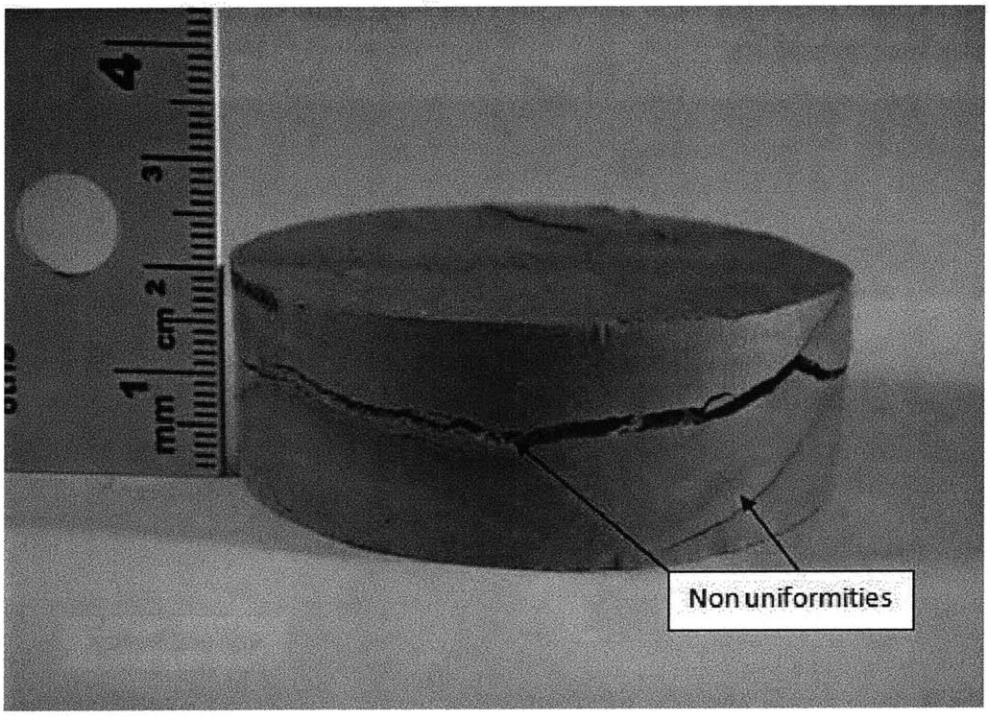

Figure 6-44: Axial non uniformities in oven dried CRS 1212 specimen

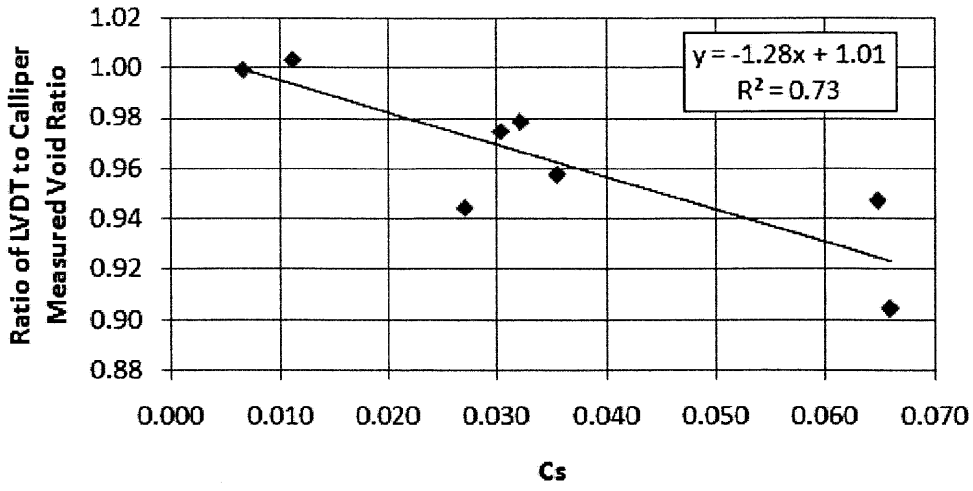

Figure 6-45: Ratio of LVDT to calliper measured void ratio vs. swelling index, Cs

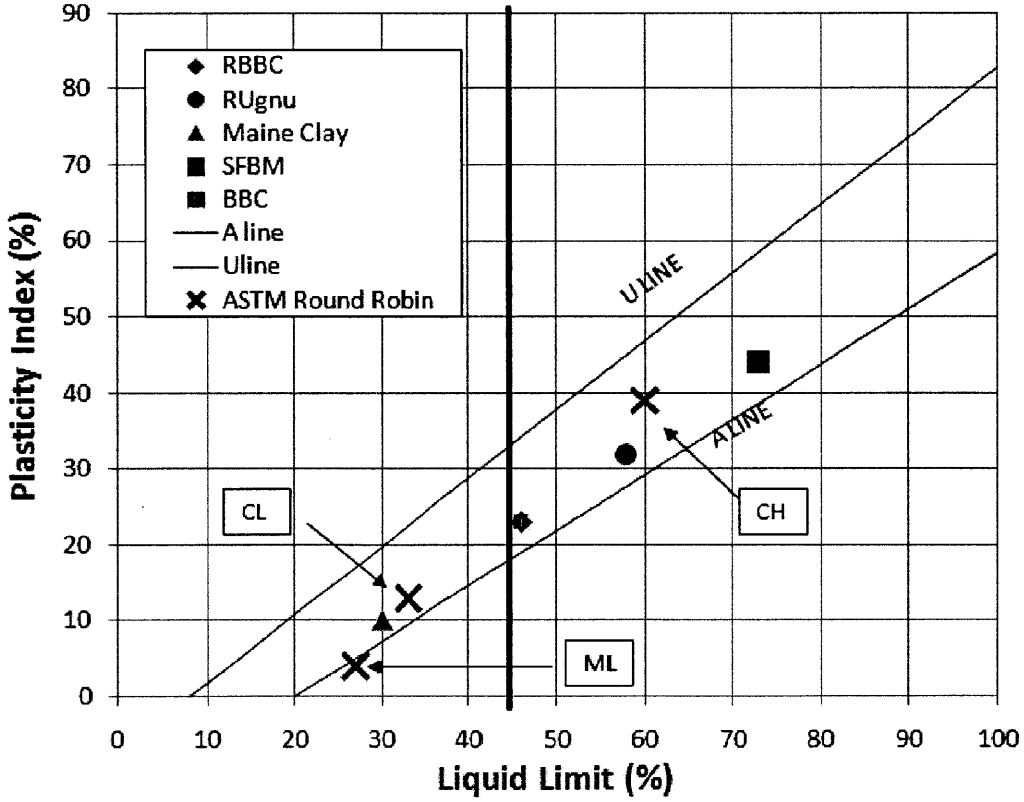

Figure 6-46: Plasticity chart with Interlaboratory study soils plotted with materials tested in this study (Benson, 2010)

7 SUMMARY, CONCLUSIONS AND RECOMMENDATIONS

7.1 Summary of Work Undertaken at MIT

The purpose of this research is to compare the results of hydraulic conductivity measurements made using both the constant rate of strain (CRS) and constant head measurement techniques to determine if the these two commonly used measurement methods provide consistent results for a variety of naturally derived fine grained soils including both resedimented and intact materials ranging from low to high plasticity. Both techniques are commonly used in industry as well as in the MIT Geotechnical Laboratory.

A literature review briefly described various permeameter methods available for measuring the hydraulic conductivity of a material at a given void ratio and then focused on the development of constant rate of strain method which can measure the hydraulic conductivity as a function of void ratio. Linear methods of CRS data reduction were adopted for use in this study. Linear methods were first derived by Wissa (1971) for small strains and later modified for large strains, and they are applicable after an initial period of transience which can be defined as a function of the excess pore pressure and applied stress, also defined by Wissa (1971).

Hydraulic conductivity measurements were made on a number of resedimented and intact materials in both the CRS and flexible wall permeameter device. The CRS and constant head techniques for hydraulic conductivity measurement were both applied using the CRS device, and the constant head technique was also applied using the flexible wall permeameter device. The index properties of the materials tested including the Atterberg limits, clay fraction, grain size distribution, specific gravity and salt concentration were either tested in-house according to the relevant ASTM standard, or gathered from databases in the MIT Geotechnical Laboratory or the available Literature. Permeant salt concentration was adjusted based on pore fluid salt concentration measurements to provide salt balanced flow.

First, two multi-stage loading tests measured the hydraulic conductivity of Resedimented Boston Blue Clay (RBBC) through three complete load-unload cycles using the CRS

technique during loading and the constant head technique following equilibration after unloading.

The hydraulic conductivity of two more specimens of RBBC was measured in both the CRS and Flexible Wall Permeameter devices. For each of these sequential tests the specimen was first loaded at a constant rate of strain, measuring the hydraulic conductivity using the CRS technique, and then unloaded to perform a constant head test in the CRS device. The specimen was then removed from the CRS device and installed in the Flexible Wall Permeameter where the hydraulic conductivity was measured using the constant head technique. These tests lead to identification of bottom seating errors in the CRS device.

Finally, the hydraulic conductivity of eight more specimens of different materials covering a range of plasticity and including both resedimented and intact (tube sample) materials was measured in the CRS device using both the CRS and constant head techniques. The results were analyzed to determine if there was a difference between the CRS and constant head hydraulic conductivity measurements at the same void ratio.

7.2 Results and Conclusions

This section summarizes the key results and conclusions drawn from the individual tests. In total, the hydraulic conductivity of two specimens was measured using the multi-stage CRS approach and that of ten specimens was measured using single stage CRS techniques followed by constant head measurements in either the CRS device and/or the flexible wall permeameter. This included six resedimented specimens and four intact specimens, three of which had a noted axial non uniformity. Specimens ranged from low to high plasticity clays. The range of hydraulic conductivities measured was from 1e-9 to 6e-8 cm/s. Hydraulic conductivity measurements computed using the CRS technique were only recorded after transient and instable data points had been removed and when the measured excess pore pressure ratio, $\Delta u/d\sigma$ was less than 15%; this criteria was shown to result in less than 10% error in the measured hydraulic conductivity by Gonzalez (2000).

7.2.1 Multi-stage CRS Tests

The constant head hydraulic conductivity measurements agreed well with the CRS hydraulic conductivity measurements. However, the CRS void ratio vs. log hydraulic conductivity relationship gained an increasing degree of scatter with each subsequent loading cycle. This is likely due to two factors: the effect of curve smoothing, which can carry errors through the data set, and the instability of the base pore pressure. Initially when specimens are loaded transient strains develop throughout the specimen; transient data points are removed for a steady state analysis, however the scatter noted was not due to transient conditions. Every time loading is initiated, flow must occur through the base of the specimen to pressurize the pore pressure measurement system, leading to a period of instability in the measured excess pore pressure used to compute the hydraulic conductivity. This instability is likely a function of soil stiffness because the degree of scatter increases with each subsequent loading cycle, as the specimen gets stiffer.

As a result, it is most accurate to measure the hydraulic conductivity of a fine grained soil specimen using the CRS technique during a single loading increment or over long loading periods so that the base pore pressure can stabilize. This allows for instable measurements to be removed from the dataset while still retaining sufficient data to compute a void ratio vs. log hydraulic conductivity relationship for the specimen.

7.2.2 Bottom Seating Errors

Bottom seating errors were identified in the CRS device. These errors can occur when the top of the base porous stone is not flush with the base of the specimen ring, creating a gap between the base of the trimmed specimen and the top of the base porous stone. This error is the result of variance within the manufacturer's tolerance in the porous stone height and therefore has the potential to be a common error associated with the CRS test method.

Bottom seating errors lead to errors in the measured strain and the shape of the compression curve, which in turn results in errors in the computed void ratio, hydraulic conductivity and measured compression behaviour of the soil. A bottom seating error causes the void ratio vs. log effective stress compression curve to shift towards lower void ratio and lower effective

stress, and the void ratio vs. log hydraulic conductivity curve to shift towards lower void ratio and higher hydraulic conductivity. It also causes errors in the preconsolidation pressure, σ'_p, shifting it towards lower effective stress. The average strain error measured in this study was in the range of 1% for a measured bottom seating error of 0.010" (0.025 mm).

To avoid bottom seating errors, a new procedure was developed to pre-seat the specimen while in the trimming ring during set up before the CRS cell is filled with permeant fluid.

7.2.3 Swelling and Void Ratio Errors

After resolution of the base seating error, there was often still a small discrepancy in the final specimen height measurement between the LVDT measurement and that measured using callipers upon removal of the specimen from the CRS device. This translated into a void ratio error between the two measurement methods. The change in measured final specimen height over a period of time was measured for the last two specimens tested. In one case the change in height was almost negligible, and in the other it was not insignificant. A plot of void ratio error vs. Cs, the slope of the swelling line, showed a clear relationship between the two parameters.

Therefore, it is likely that some of the void ratio errors, related to errors in specimen height, are related to specimen swelling that occurred between the time of load removal and specimen dimensioning using callipers. The LVDT measured specimen height is likely most correct and representative of the actual specimen height during hydraulic conductivity testing.

7.2.4 Hydraulic Conductivity Measurement Comparison

7.2.4.1 Ratio of CRS to Constant Head Hydraulic Conductivity Measurement

The CRS hydraulic conductivity measurement was either interpolated or extrapolated using the linear void ratio vs. log hydraulic conductivity trend for each specimen to determine the CRS hydraulic conductivity at the same void ratio as that of the constant head test. This was done to allow for comparison of the two measurement techniques. For resedimented specimens, the ratio of the CRS to constant head hydraulic conductivity was 1.00; for intact specimens this ratio was 0.94. This ratio ranged from 0.87 to 1.20 for resedimented specimens

and from 0.85 to 1.09 for intact specimens. For all specimens tested, the average ratio of the CRS to constant head hydraulic conductivity was 0.98 for a hydraulic conductivity range of 1 e-9 to 6 e-8 cm/s.

Therefore, the CRS hydraulic conductivity is neither higher nor lower than the constant head hydraulic conductivity. Given the small sample size, neither resedimented nor intact specimens have statistically different hydraulic conductivity measurements using the CRS and constant head techniques.

7.2.4.2 Effect of Non Uniformity

There were three specimens of intact material with naturally occurring non uniformities. Two of these non uniformities were in the form of coarser layers oriented perpendicular to the axial loading direction. One of these specimens resulted in a CRS hydraulic conductivity lower than the constant head hydraulic conductivity, and the other had the equally opposite result. The third non uniformity was a discolouration in a layer or zone of the specimen and resulted in equal CRS and constant head hydraulic conductivities.

The CRS and constant head techniques were found to measure the same average hydraulic conductivity for specimens with a non uniformity provided the non uniformity was continuous and is oriented perpendicular to the axial loading and flow direction.

7.2.4.3 Comparison with Interlaboratory Study Using a Flexible Wall Permeameter

The variability of three sets of measurements was compared by computing the ratio of the maximum to minimum measurement in each set. First, the ratio of the hydraulic conductivity measurements made in this research comparing the CRS technique to the constant head technique at the same void ratio was computed to be 1.11. This ratio was then compared to the ratio computed using the results from an interlaboratory study conducted by Benson et al (2010). This program used 12 labs to test specimens of 3 different soils including a low plasticity silt, a low plasticity clay and a high plasticity clay. Overall, across three tests on specimens of the same soil, the average ratio for a single laboratory in the interlaboratory study was 1.21. Finally, ratio of the hydraulic conductivity measurement made using different

applied hydraulic gradients on the same specimen during constant head testing in the CRS device was computed to be 1.04.

From these results, it is concluded that the CRS and constant head techniques for hydraulic conductivity measurement produce the same results. This conclusion is drawn primarily in comparison with the abilities of a single laboratory testing a single material using a single measurement technique, and also in comparison with the variability of the constant head test method measuring the hydraulic conductivity of the same specimen using different applied hydraulic gradients.

7.3 Recommendations for Future Work

The experimental analysis conducted for this research provided valuable insight into the potential agreement and/or disagreement between the CRS and constant head hydraulic conductivity measurement techniques. However, some problems were encountered in this research which would merit further study should the opportunity arise.

Firstly, the identification of the bottom seating error was an important discovery. However, despite modification of the set up procedure to pre-seat the specimen, errors in the final specimen height were still identified. This could be due to swelling, but insufficient data was collected in this study to fully determine the effect of swelling. Therefore, bottom seating could still be a concern, or another potential error source could be causing an error in measured specimen height. Any future research should attempt to more carefully track the specimen height during the test. This could be accomplished in a number of ways, including but not limited to:

1. More carefully measuring the location of the piston at the beginning of the test; the target location of the piston can be calculated by making careful measurements using a stainless steel dummy seated on the base porous stone. Knowing the target location of the piston and comparing it to the actual location can help identify if the specimen is properly seated.
2. Collecting sufficient data to compute the estimated specimen swell post load removal. The swell can be compared with the computed difference in specimen height between

the LVDT deformation measurement and the measured specimen height to get a true error estimate.

Secondly, more testing could be undertaken to identify the effects of non uniformities on the measured hydraulic conductivity. Only three non uniformities were included in this data set and the results were within the range of variability seen in the rest of the data set. More data is required to determine if non uniformities in intact specimens do have a significant effect on the measured hydraulic conductivity using either the CRS or constant head techniques. The effect of the type, size, location and continuity of the non uniformity could be investigated by the keen researcher.

An investigation into the causes of the instability in the void ratio vs. log hydraulic conductivity curve at the onset of loading and following removal of transient portions of the data set is necessary. A methodology to identify this portion of the data set and remove it would benefit further analysis. Investigation into the linkage between this instability and soil stiffness is merited.

Finally, increasing the size of the data set could help more solidly prove that the CRS and constant head techniques do measure the same hydraulic conductivity. There was not sufficient time to test statistical significance of the results. More materials should be tested, and the types of materials expanded to include a wider range of hydraulic conductivity, stiffness and plasticity.

REFERENCES

Abdulhadi, N. O. (2009). "An Experimental Investigation into the Stress-Dependent Mechanical Behavior of Cohesive Soil with Application to Wellbore Instability."

Allman, M. A., and Atkinson, J. H. (2010). "Mechanical properties of reconstituted Bothkennar soil." *Geotechnique*, 42(2), 289-301.

Anderson, G. R. (1991). "Physical Mechanisms Controlling the Strength and Deformation Behavior of Frozen Sand.", ScD Thesis, MIT, Cambridge, MA.

ASTM D4186 – 06 Standard Test Method for One-Dimensional Consolidation Properties of Saturated Cohesive Soils Using Controlled-Strain Loading

Benson, C. H., and Yesiller, N. (2010). *Interlaboratory Study to Establish Precision Statements for ASTM D5084-03, Standard Test Methods for Measurement of Hydraulic Conductivity of Saturated Porous Materials Using a Flexible Wall Permeameter.* Research Report: D18-1018, Committee D18 on Soil and Rock, Subcommittee D18.04 on Hydrologic Properties and Hydraulic Barriers

Burland, J. B. (1990). "On the compressibility and shear strength of natural clays." *Geotechnique*, 40(3), 329-378.

Cauble, D. F. (1996). "An Experimental Investigation of the Behavior of a Model Suction Caisson in a Cohesive Soil.", PhD Thesis, MIT, Cambridge, MA

Cotecchia, F., and Chandler, R. J. (1997). "The influence of structure on the pre-failure behaviour of a natural clay." *Geotechnique*, 47(3), 523-544.

Darcy, H. (1856). "Les Fontaines Publiques de la ville de Dijon." Paris.

Dewhurst, D., Brown, K., Clennell, M., and Westbrook, G. (1996). "A comparison of the fabric and permeability anisotropy of consolidated and sheared silty clay." *Engineering Geology*, 42, 253-267.

Germaine, J. T. (1982). "Development of the Directional Shear Cell for Measuring Cross Anisotropic Clay Properties.", ScD Thesis, MIT, Cambridge, MA

Germaine, J. T. (2009). "1.37 Geotechnical Measurements and Exploration Course Notes". Massachusetts Institute of Technology, Department of Civil and Environmental Engineering, Fall 2009.

Germaine, J. T., and Germaine, A. V. (2009). *Geotechnical Laboratory Measurements for Engineers*. John Wiley & Sons, Inc, Hoboken, New Jersey.

Gonzalez, J. H. (2000). "Experimental and Theoretical Investigation of Constant Rate of Strain Consolidation."

Gorman, C., Hopkins, T., Deen, R., and Drnevich, V. (1978). "Constant Rate of Strain and Controlled Gradient Consolidation Testing." *Geotechnical Testing Journal*, 1(1), 3-15.

Grennan, J. (2010). "Characterization of a Reconstituted Low Plasticity Silt." SM Thesis, MIT, Cambridge, MA

Hamilton, J., and Crawford, C. (1959). "Improved determination of preconsolidation pressure of a sensitive clay." *American Society of Testing Materials Special Technical Publication*, 254, 254-271.

Johnson, E. (1989). "Geotechnical Characteristics of the Boston Area." *Civil Engineering Practice, Journal of the Boston Society of Civil Engineers*, 4(1), 53-64.

Jones, C. A. (2010). "Engineering Properties of Resedimented Ugnu Clay from the Alaskan North Slope.", SM Thesis, MIT, Cambridge, MA

Ladd, C. C. 1996. "1.361 Advanced Soil Mechanics Course Notes". Massachusetts Institute of Technology, Department of Civil and Environmental Engineering, Fall 2009.

Ladd, R. S. (1965). *Use of Electrical Pressure Transducers to Measure Soil Pressure.* Cambridge, MA, 51.

Lee, K. (1981). "Consolidation with constant rate of deformation." *Geotechnique*, 31(2), 215-229.

Leroueil, S., Samson, L, Bososuk, M. (1983). "Laboratory and Field Determination of Preconsolidation Pressures at Gloucester." *Canadian Geotechnical Journal*, 20(3), 477-490.

Martin, R. T. (1982). "Suggested Method of Test for Determination of Soluble Salts in Soil." ASTM STP 476, 288-290.

Moriwaki, T., and Umehara, K. (2003). "Method for Determining the Coefficient of Permeability of Clays." *ASTM Geotechnical Testing Journal*, 26(1), 47056.

Ortega, O. J. (1992). "Computer Automation of the Consolidated-Undrained Direct Simple Shear Test.", SM Thesis, MIT, Cambridge, MA

Reynolds, R. T. (1991). "Geotechnical Field Techniques Used in Monitoring Slope Stability at a Landfill." *Proceedings of the 3rd International Symposium on Field Measurements in Geomechanics*, Balkema, Rotterdam, 883-891.

Sallfors, G. (1975). *Preconsolidation Pressure of Soft, Highly Plastic Clays*. Chalmers University of Technology, Goteburg, Sweden.

Seah, T. H. (1990). "Anisotropy of resedimented Boston Blue Clay.", ScD Thesis, MIT, Cambridge, MA

Sheahan, T. C. (1991). "An Experimental Study of the Time-Dependent Undrained Shear Behavior of Resedimented Clay Using Automated Stress-Path Triaxial Equipment.", ScD Thesis, MIT, Cambridge, MA.

Sheahan, T.C., and Watters, P. J. (1997). "Experimental verification of CRS consolidation theory." *Journal of Geotechnical and Geoenvironmental Engineering*, 123(5), 430-437.

Sheeran, D. E., and Krizek, R. J. (1971). "Preparation of homogeneous soil samples by slurry consolidation." *Journal of Materials*, 6(2), 356-373.

Skempton, A. W., and Jones, O. T. (1944). "Notes on the compressibility of clays." *Quarterly Journal of the Geological Society*, 100, 119-135.

Tavenas, F., Leblond, P., Jean, P., and Leroueil, S. (1983). "The permeability of natural soft clays. Part 1: Methods of Laboratory Measurement." *Canadian Geotechnical Journal1*, 20, 629-644.

Wissa, A., Christian, J., Davis, E., and Heiberg, S. (1971). "Consolidation Testing at Constant Rate of Strain." *ASCE Journal of Soil Mechanics and Foundations Division*, 97(10), 1393-1413.

Yoshikuni, H., Moriwaki, T., Ikegami, S., and Xo, T. (1995). "Direct Determination of Permeability of Clay from Constant Rate of Strain Consolidation Tests." *Proceedings of the International Symposium on Compression and Consolidation of Clayey Soils*, 609-614.

Znidarcić, D., Schiffman, R. L., Pane, P., Croce, P., Ko, H., and Olsen, H. W. (1987). "The theory of one dimensional consolidation of saturated clays: part V, constant rate of deformation testing and analysis." *Géotechnique*, 36(2), 227-237.

APPENDIX 1

CRS REDUCTION PROGRAM CODE

```
'*****************************************************
 ' Rev 1.08 programmed by JTG 6/28/00: add smoothing to pore pressure
 ' Rev 1.07 programmed by JTG 5/24/00: modify for large strain
 ' Rev 1.06 programmed by JTG 9/20/99: convert to quick basic
 ' Rev 1.05 programmed by JTG 8/01/97: app. comp. for new device
 ' Rev 1.04 programmed by jtg 3/10/97: apparatus compr. equation update
 ' Rev 1.03 programmed by DFC 1/28/96: apparatus compr. equation
 ' Rev 1.02 programmed by JTG 9/02/94: make output compatable with 123
 ' Rev 1.02 programmed by MPW 2/15/94: dU/T.Str and Total Work
 ' Rev 1.01 programmed by JVS 1/13/94: regression analysis for Cv and k
 '                          revised k equation
 ' Rev 1.0 programmed by JTG  rev date 6/27/90
 '*****************************************************
 ' v(i,j) is data reading array;i=1 time;=2 disp;=3 vert sts
 '        =4 pore pressure;=5 cell pressure ;=6 input voltage
 ' r(i,j) is results file
 'REM $DYNAMIC:  V, R
  rev$ = "CRS Rev 1.08"
100 DIM V(7, 2000), R(6, 2000), V.L(5, 30), A.D(5, 30), H$(30), zero(6), cf(6), ES(2000),
a.defl(2000), AC(4, 3)
110 FOR i = 1 TO 30: H$(i) = "": NEXT i
120 FOR i = 1 TO 7: P(i) = 1: NEXT i
130 CLS : PRINT
  PRINT "    **** This Program is part of the ****"
  PRINT "    *          MIT/WCC            *"
  PRINT "    *        GEOTECHNICAL         *"
  PRINT "    *       DATA ACQUISITION       *"
  PRINT "    *          SYSTEM            *"
  PRINT "    ************************************"
  PRINT "  This is the CRS TEST REDUCTION PROGRAM"; : PRINT rev$
  PRINT "        (last revised in June 2000)": PRINT
  PRINT "Please select from the following options"
  PRINT "       1...Create NEW Reduction File"
  PRINT "       2...Input Reduction data from disc"
  PRINT "       3...Edit Reduction File in Memory"
  PRINT "       4...Store Reduction File"
  PRINT "       5...Compute and Store Results"
  PRINT "       6...Print Headings, Data and Results (*)"
  PRINT "       7...Print Headings and Results (*)"
  PRINT "       8...Print Headings (*)"
  PRINT "       9...Read Program Notes (*)     (* = not completed)"
  PRINT "      10...End Program"
320 PRINT : INPUT "enter option:", x
  ON x GOTO 1350, 2670, 840, 2500, 2820, 130, 130, 130, 350, 6000, 320
  GOTO 130

350 REM program notes section

  CLS : PRINT : PRINT
  PRINT "This program computes STRESS,STRAIN,K ETC."
```

```
   PRINT "Apparatus deflection for CRS based on AJV 5/1/97 with rigid cap"
   PRINT "Data are smoothed for computation of Cv and Kv using input strain range"
   PRINT "    This moving average does not adjust for load reversals"
   PRINT "       therefore data should be removed for half the strain window"
   PRINT "       prior to reaching the hold stress point"
   PRINT "Additional smoothing using a moving window routine is applied to pore pressure"
   INPUT "press 'Enter' to continue", ANS$
   GOTO 130

440 REM this routine is to be used to input data from a data acq file

   PRINT "****************************************"
470 OPEN "I", #1, IFIL$(k)
480 INPUT #1, X1$, X2$, nch, X3$, X4$, X1, X2, x5$
490 FOR i = 1 TO nch + 1
500 INPUT #1, hed$(P(i))
   PRINT hed$(P(i));
510 NEXT i
   PRINT
520 FOR i = 1 TO nch + 1
530 INPUT #1, ch(P(i))
   PRINT ch(P(i));
540 NEXT i
   PRINT
550 FOR i = 1 TO nch + 1
560 INPUT #1, DUM(P(i))
   PRINT DUM(P(i));
570 NEXT i
   PRINT
580 FOR i = 1 TO nch + 1
590 INPUT #1, REF$(P(i))
   PRINT REF$(P(i));
600 NEXT i
   PRINT
610 FOR i = 1 TO nch + 1
620 INPUT #1, DUM(P(i))
   PRINT DUM(P(i));
630 NEXT i
   PRINT
   FOR i = 1 TO nch + 1
   INPUT #1, DUM(P(i))
   PRINT DUM(P(i));
   NEXT i
   PRINT
   INPUT #1, DUM$
   PRINT DUM$
   INPUT #1, DUM$
   PRINT DUM$
680 FOR i = 1 TO nch + 1
690 INPUT #1, RUTS$(P(i))
```

```
700 NEXT i
710 ON ERROR GOTO 780
   FOR j = 1 TO nch + 1
   INPUT #1, V(j, 1)
   NEXT j

720 i = 1
   m = 1
730 i = i + 1
  '****************************************
  '****************************************

   FOR m = 1 TO 1  'change m to skip readings
740 FOR j = 1 TO nch + 1
750 INPUT #1, V(j, i)
760 NEXT j

   NEXT m
  '**********************
  'IF V(1, i) > 100 AND V(1, i) < 160000 THEN i = i - 1
  ' IF m = -1 THEN i = i - 1
  ' m = m * -1
  '********************************************
  '********************************************

770 GOTO 730
780 RESUME 790
790 ON ERROR GOTO 0
800 CLOSE #1
810 nr = i - 1
820 PRINT "Data file "; IFIL$(k); " contains "; nr; " readings"
830 GOTO 3020

840 REM this section creates and edits the reduction file

870 CLS : EDT$ = "on"
880 PRINT " *** REDUCTION DATA ***"
890 PRINT ""
900 PRINT "   1. TEST NAME : "; TESTN$
910 PRINT "   2. DATE      : "; DR$
920 PRINT "   3. YOUR : "; OPR$
930 PRINT "   4. INITIAL SPECIMEN HEIGHT (cm) : "; H.INIT
940 PRINT "      HEIGHT OF SOLIDS       (cm) : "; HS
960 PRINT "   5. SPECIMEN AREA (sqr cm)      : "; AREA
970 PRINT "   6. APPARATUS INFORATION"
   PRINT "         Device Name: "; DEVICE$
980 PRINT
990 PRINT "   7. VERTICAL HEIGHT TRANSDUCER, Z:"
1000  PRINT "          ZERO(volts/volt): "; zero(2)
1010  PRINT "            CF  (cm/(v/v)): "; cf(2)
```

```
1020 PRINT "     VERT. STRESS TRANSDUCER :"
1030 PRINT "         ZERO(volts/volt): "; zero(3)
   PRINT "          Seating Value(volts/volt):"; sload
1040 PRINT "           CF  (kg/(v/v)): "; cf(3)
1050 PRINT "     PORE PRESSURE "
1060 PRINT "         ZERO(volts/volt): "; zero(4)
1070 PRINT "           CF (ksc/(v/v)): "; cf(4)
1080 PRINT "     CELL PRESSURE"
1090 PRINT "         ZERO(volts/volt): "; zero(5)
1100 PRINT "           CF (ksc/(v/v)): "; cf(5)
1110 INPUT "press 'Enter' for more"; ANS$
1120 CLS
1130 PRINT
1140 PRINT "  8. DATA POSITION IN FILE :"
1150 PRINT "       TIME.....column "; P(1)
1160 PRINT "       DISPLACEMENT...column "; P(2); "...channel "; x(2)
1170 PRINT "       VERTICAL STRESScolumn "; P(3); "...channel "; x(3)
1180 PRINT "       PORE PRESSURE .column "; P(4); "...channel "; x(4)
1190 PRINT "       CELL PRESSURE. column "; P(5); "...channel "; x(5)
1200 PRINT "       VOLTS IN.....column "; P(6); "...channel "; x(6)
1210 PRINT
1220 PRINT
1230 PRINT "   9.DAT FILE NAME"
1240 FOR i = 1 TO FILS
1250 PRINT "     "; IFIL$(i)
1260 NEXT i
1270 PRINT
1280 INPUT "  *** ARE THERE ANY CORRECTIONS (N or Item Number) "; m$
1290 IF m$ = "N" OR m$ = "n" OR m$ = "" GOTO 130
1300 ITNUM = VAL(m$)
1310 IF ITNUM > 11 THEN 1280
1320 CLS
1330 PRINT : PRINT
1340 ON ITNUM GOTO 1390, 1410, 1430, 1450, 1490, 1510, 1570, 2030, 1700, 2500, 2670
   GOTO 130
1350 REM following lines used only to create new reduction file

1360 CLS : PRINT "Enter the following information"
1370 PRINT "units must be in the kg and cm system"
1380 EDT$ = "off"

1390 INPUT "   1. TEST NAME : "; TESTN$
1400 IF EDT$ = "on" THEN GOTO 870
1410 INPUT "   2. DATE      : "; DR$
1420 IF EDT$ = "on" THEN GOTO 870
1430 INPUT "   3. YOUR NAME : "; OPR$
1440 IF EDT$ = "on" THEN GOTO 870
1450 INPUT "   4. INITIAL SPECIMEN HEIGHT (cm) : "; H.INIT
1460 INPUT "      HEIGHT OF SOLIDS       (cm) : "; HS
1480 IF EDT$ = "on" THEN GOTO 870
```

```
1490 INPUT "   5. SPECIMEN AREA (cm^2 )      : "; AREA
1500 IF EDT$ = "on" THEN GOTO 870
1510 PRINT "   6. SELECT THE TEST DEVICE FROM THE FOLLOWING :"
1520 PRINT "            1...Wissa"
   PRINT "           2...Trautwein"
   PRINT "           3...Penn State"
   PRINT
   : INPUT "         "; D
1530 IF D = 1 THEN DEVICE$ = "Wissa": GOTO 1560
1540 IF D = 2 THEN DEVICE$ = "Trautwein": GOTO 1560
   IF D = 3 THEN DEVICE$ = "Penn State": GOTO 1560
1550 GOTO 1510
1560 IF EDT$ = "on" THEN GOTO 870
1570 PRINT "   7. VERTICAL HEIGHT TRANSDUCER, Z:"
1580 PRINT "           ZERO(volts/volt): "; zero(2)
1581 INPUT "  value or <enter> to keep current value"; a$
1582 IF a$ = "" THEN GOTO 1590 ELSE zero(2) = VAL(a$)
1590 PRINT "            CF  (cm/(v/v)): "; cf(2)
1591 INPUT "  value or <enter> to keep current value"; a$
1592 IF a$ = "" THEN GOTO 1600 ELSE cf(2) = VAL(a$)
1600 PRINT "     VERT. STRESS TRANSDUCER :"
1610 PRINT "           ZERO(volts/volt): "; zero(3)
1611 INPUT "  value or <enter> to keep current value"; a$
1612 IF a$ = "" THEN GOTO 1614 ELSE zero(3) = VAL(a$)
1614 PRINT "           Seating Load (volts/volt): "; sload
   PRINT "    This is the load reading when the zero value"
   PRINT "     of the displacement transducer is recorded"
   INPUT "  value or <enter> to keep current value"; a$
   IF a$ = "" THEN GOTO 1620 ELSE sload = VAL(a$)
1620 PRINT "            CF  (kg/(v/v)): "; cf(3)
   INPUT "  value or <enter> to keep current value"; a$
   IF a$ = "" THEN GOTO 1630 ELSE cf(3) = VAL(a$)
1630 PRINT "     PORE PRESSURE "
   PRINT "           ZERO(volts/volt): "; zero(4)
   INPUT "  value or <enter> to keep current value"; a$
   IF a$ = "" THEN GOTO 1650 ELSE zero(4) = VAL(a$)
1650 PRINT "            CF (ksc/(v/v)): "; cf(4)
   INPUT "  value or <enter> to keep current value"; a$
   IF a$ = "" THEN GOTO 1660 ELSE cf(4) = VAL(a$)
1660 PRINT "     CELL PRESSURE"
   PRINT "           ZERO(volts/volt): "; zero(5)
   INPUT "  value or <enter> to keep current value"; a$
   IF a$ = "" THEN GOTO 1680 ELSE zero(5) = VAL(a$)
1680 PRINT "            CF (ksc/(v/v)): "; cf(5)
   INPUT "  value or <enter> to keep current value"; a$
   IF a$ = "" THEN GOTO 1690 ELSE cf(5) = VAL(a$)
1690 IF EDT$ = "on" THEN GOTO 870

1700 PRINT "    DATA INPUT FILES AND VERTICAL STRESS"
1710 CLS : PRINT
```

```
1720 PRINT "   two file input modes are available"
1730 PRINT "        1...enter first file name and program will increment"
1740 PRINT "          automatically (format yxx.dat)"
1750 PRINT "             y-name up to 6 characters"
1760 PRINT "             xx-sequence number entered separately"
1770 PRINT "             .dat-extension ,added automatically"
1780 PRINT "        NOTE..end sequence with stress =-1"
1790 PRINT "        2...enter each file separately "
   PRINT "          provide the complete file name"
   PRINT "          end sequence with 'Enter'"
1800 PRINT : INPUT "Please make selection "; S
1810 PRINT
1820 x = 1
1830 IF S = 1 THEN GOTO 1850
1840 IF S = 2 THEN GOTO 1880 ELSE GOTO 1800
1850 INPUT "enter the file name : "; F$
1860 INPUT "enter the starting sequence number : "; x
1870 EXT$ = ".dat"
1880 ON ERROR GOTO 1990
1890 i = 1
1900 IF x < 10 THEN x$ = "0" + RIGHT$(STR$(x), 1)
1910 IF x > 9 THEN x$ = RIGHT$(STR$(x), 2)
1920 IF S = 1 THEN IFIL$(i) = F$ + x$ + EXT$: GOTO 1950
1930 PRINT "enter the name for file number "; i; " : ";
1940 INPUT IFIL$(i)
1950 OPEN "i", #1, IFIL$(i)
1960 CLOSE #1
1970 i = i + 1: x = x + 1
1980 GOTO 1900
1990 FILS = i - 1
2000 RESUME 2010
2010 ON ERROR GOTO 0
2020 IF EDT$ = "on" THEN GOTO 870
2030 REM
2040 REM this routine is to be used to select sorting sequence
2050 REM programed by jtg 1/30/89
2060 REM
2070 OPEN "i", #1, IFIL$(1)
2080 INPUT #1, x$, IFIL$, nch, T$, D$, SC, UC, x$
2090 PRINT x$, IFIL$, nch, T$, D$, SC, UC, x$
2100 CLS : PRINT "YOU must select the proper channels for each reading"
2110 PRINT "    EVERY file must have the same format"
2120 PRINT "    The following inforamtion is based only on the first file"
2130 PRINT
2140 PRINT "this file was created under the name "; IFIL$
2150 PRINT "at "; T$; "on "; D$
2160 PRINT "by user number "; UC
2170 U = (V(3, i) - V(4, i))
2180 PRINT "using computer code number "; SC
2185 PRINT : INPUT "Hit <Enter> to continue..."; ZZ$
```

```
2186 CLS
2190 PRINT : PRINT "THE FILE CONTAINS THE FOLOWING CHANNELS"
2200 FOR i = 1 TO (nch + 1)
2210 INPUT #1, xdum$
2220 PRINT xdum$
2230 NEXT i
   INPUT #1, xdum
   PRINT
2240 FOR i = 2 TO nch + 1
2250 INPUT #1, ch(i)
2260 PRINT ch(i)
2270 NEXT i
2280 CLOSE #1: c = 0
2285 PRINT : INPUT "Hit <Enter> to Continue..."; ZZ$
2286 CLS
2290 REM
2300 REM the following lines are TEST specific
2310 EN$(1) = "TIME     ": EN$(2) = "VERT DISP": EN$(6) = "VOLTS IN "
2320 EN$(3) = "VERT.STRESS": EN$(4) = "PORE PRESSURE": EN$(5) = "CELL PRESSURE"
2330 PRINT :  PRINT "Select the channel number for.."
2340 INPUT "The vertical displacement ", x(2)
2350 INPUT "The vertical stress       ", x(3)
2360 INPUT "The Pore Pressure         ", x(4)
2370 INPUT "The Cell Pressure         ", x(5)
2380 INPUT "The input voltage (-1 if not recorded) ", x(6)
2390 REM
2400 REM sort channels by function
2410 P(1) = 1
2420 FOR i = 2 TO nch + 1
2430 FOR j = 2 TO nch + 1
2440 IF x(i) = ch(j) THEN P(i) = j: c = c + 1
2450 NEXT j
2460 NEXT i
2470 IF x(6) = -1 THEN P(6) = -1
2480 IF c <> 5 THEN PRINT "YOU HAVE A MISMATCH.. TRY AGAIN": c = 0: GOTO 2330
2490 IF EDT$ = "on" THEN GOTO 870 ELSE GOTO 130

2500 REM
2510 REM this section stores the reduction data
2520 REM

2530 CLS : PRINT : PRINT
2540 PRINT "This section stores the reduction data on disc"
2550 PRINT "the resulting file can be used for subsequent tests"
2560 PRINT "or be recalled during batch calculation"
2570 PRINT "note: the extension '.red' will be added to the file name"
2580 INPUT "enter the file name (8 character max) ", rfIL$
2590 rfIL$ = rfIL$ + ".red"
2600 OPEN "o", #1, rfIL$
```

```
2610 WRITE #1, rev$, rfIL$, DR$, TME$, OPR$, TESTN$, H.INIT, HS, SR, AREA, D, sload,
zero(2), cf(2), zero(3), cf(3), zero(4), cf(4), zero(5), cf(5), FILS, P(1), P(2), P(3), P(4), P(5), P(6), x(2),
x(3), x(4), x(5), x(6)
2620 FOR i = 1 TO FILS
2630 WRITE #1, IFIL$(i)
2640 NEXT i
2650 CLOSE #1
2660 GOTO 130

2670 REM
2680 REM this section retrieves the reduction file from disc
2690 REM

2700 CLS : PRINT "This section retrieves a reduction file from disc"
2710 INPUT rfIL$
2720 rfIL$ = rfIL$ + ".red"
2730 OPEN "i", #1, rfIL$
2740 INPUT #1, reva$, rfIL$, DR$, TME$, OPR$, TESTN$, H.INIT, HS, SR
2750 INPUT #1, AREA, D, sload, zero(2), cf(2), zero(3), cf(3), zero(4), cf(4), zero(5), cf(5), FILS,
P(1), P(2), P(3), P(4), P(5), P(6), x(2), x(3), x(4), x(5), x(6)
2760 FOR i = 1 TO FILS
2770 INPUT #1, IFIL$(i)
2780 NEXT i
2790 CLOSE #1
2800 IF D = 1 THEN DEVICE$ = "Wissa"
   IF D = 2 THEN DEVICE$ = "Trautwein"
   IF D = 3 THEN DEVICE$ = "Penn State"
2810 GOTO 130

2820 REM
2830 REM this routine computes values for consolidation tests
2840 REM

2850 CLS
2860 OPEN "O", #2, TESTN$ + ".res"
2870 RESTORE
2880 NR.MAX = 1
2900 '
2910 '*****COMPUTATIONS SECTION
2920 '
2930 CLS
2940 PRINT "This program uses a moving linear regression analysis in an "
2950 PRINT "attempt to provide representative values of Cv and k without"
2960 PRINT "being hindered by the problems associated with a high "
2970 PRINT "frequency of data acquisition."
2980 PRINT : PRINT
2990 PRINT " ENTER THE STRAIN INCREMENT TO BE USED FOR THE REGRESSION
ANALYSIS."
2991 PRINT "     Input it as a percentage, i.e. input '1.0' for 1% ."
2992 PRINT "     NOTE: 1.0 is usually a good value. Use a larger value to "
```

```
2993 PRINT "          'smooth out' your curves."
2994 INPUT " ENTER THE VALUE YOU CHOOSE "; INC

   CLS
2997 PRINT
   PRINT "This program allows you to smooth the pore pressure data"
   PRINT "  using a moving window.  The averaging replaces each data point"
   PRINT "  with an average of the points before and after.  There is no"
   PRINT "  separation based on loading, unloading, or secondary, so be careful"
   PRINT " "
   PRINT " ENTER the number of data points which defines the size of the moving"
   PRINT "   window.  This must be an ODD number"
   INPUT ; nwin
   IF nwin <= 0 THEN GOTO 2997
   IF (nwin - 1) / 2 = INT((nwin - 1) / 2) THEN GOTO 2998
   PRINT
   PRINT "This selection is not valid, Please try agian."
   GOTO 2997

2998 CLS


3000 LOCATE 11, 15: PRINT "Loading data into memory"

   'set up the compressibility parameters
   GOSUB 5000          'get the values
   sforce = (sload - zero(3)) * cf(3) + WP(D)
   IF sforce < .1 THEN sforce = .1
   REF.defl = AC(1, D) * sforce ^ AC(2, D)

3011 '
3012 FOR k = 1 TO FILS'loop over each file
3014   GOTO 440      'input data into v(l,m)
3020 PRINT "Data retrieval complete for "; IFIL$(k)

   PRINT "Smoothing Pore Pressure Data"
   IF nwin = 1 THEN GOTO 3090          'no smoothing required
   deln = (nwin - 1) / 2
    FOR i = 1 + deln TO nr - deln
    sumpp = 0
     FOR j = i - deln TO i + deln
     sumpp = sumpp + V(P(4), j)
     NEXT j
    ES(i) = sumpp / nwin      'using ES as tempory matrix
    NEXT i

    FOR i = 1 + deln TO nr - deln  'switch to original matrix
    V(P(4), i) = ES(i)
    NEXT i
```

```
3090   REM compute compressibility
3091 '
3100 '  IF NR < NR.MAX THEN GOTO 3101 ELSE L.NR = NR.MAX: C = 1'all ok

3110   REM compute strains
3120       FOR i = 1 TO nr
3130          m = 2
3140          FOR j = 2 TO 5
3150             V(P(j), i) = ((V(P(j), i) / V(P(6), i)) - zero(j)) * cf(j)
3220          NEXT j
3221          V(P(3), i) = V(P(3), i) - V(P(5), i) * AP(D) + WP(D)
3222          IF V(P(3), i) < .1 THEN a.defl = REF.defl: GOTO 3225
3224          a.defl = AC(1, D) * (V(P(3), i) ^ AC(2, D))
3225          c.defl = AC(4, D) * V(P(5), i)
           T.DEFL = REF.defl - a.defl - c.defl
3230          V(P(2), i) = (V(P(2), i) + T.DEFL) / H.INIT * 100  "ITS right here!!
3235          V(P(3), i) = V(P(3), i) / AREA

3240       NEXT i
3245   CLS
3255          CLS : LOCATE 10, 15: PRINT "STORING RESULTS AND PERFORMING
REGRESSION ANALYSIS"
3260          REM data storage
3270          WRITE #2, DATE$, TIME$, OPR$
           WRITE #2, "Reduction Program is ", rev$
3280          WRITE #2, IFIL$(k)
3284          WRITE #2, "    "
3285          WRITE #2, TESTN$, " CONSOLIDATION TEST RESULTS
Page"
3286          WRITE #2, "    "
3290          WRITE #2, "  Time  ", " Strain ", "Vert.Sts", "  Pore  ", "  Cell  ", "Eff.Sts.", "Void Rto", "
dU  ", "  K  ", "  Cv  ", "dU/TVSts", "Tot.Work"
3292          WRITE #2, " (sec)  ", "  (%)  ", " (ksc)  ", "  (ksc) ", "  (ksc) ", " (ksc)  ", "       ", "  (ksc)
", "(cm/sec)", "(cm2/sec)", "       ", "       "
3294          WRITE #2, "    "
3295          TOTWORK = 0
3296 '
3297 '***** DETERMINE BEGINNING AND ENDING POINTS FOR FULL WINDOW
PROCEDURE
3298 '
3299 FOR i = 1 TO nr
3300   IF (ABS(V(P(2), i) - V(P(2), 1))) > INC / 2 THEN BEGIN = i: GOTO 3302
3301 NEXT i
3302 FOR i = nr TO 1 STEP -1
3303   IF (ABS(V(P(2), nr) - V(P(2), i))) > INC / 2 THEN ND = i: GOTO 3305
3304 NEXT i
3305 '
3308          FOR i = 1 TO nr
3309               FLAG = 0
3310               E = (H.INIT - V(P(2), i) * H.INIT / 100 - HS) / HS
```

```
3320            U = (V(P(4), i) - V(P(5), i))
3321            ES(i) = V(P(3), i) - ((2 / 3) * U)
3322 '
3325            IF i = 1 THEN DT = 0: DK = 0: CV = 0: GOTO 3390
3326            IF i < BEGIN OR i > ND THEN FLAG = 1
3332 '
3338            GOSUB 3630
3350            LOCATE 12, 20: PRINT "Finished line "; i; " out of "; nr; "     "
3367 '
3380            UTVS = U / V(P(3), i)
3382             AVESTS = (ES(i) + ES(i - 1)) / 2
3384             DELSTRN = LOG((1 - (V(P(2), i - 1) / 100)) / (1 - (V(P(2), i) / 100)))
3386            INCWORK = AVESTS * DELSTRN
3388            TOTWORK = TOTWORK + INCWORK
3389 '
3390            WRITE #2, V(1, i), V(P(2), i), V(P(3), i), V(P(4), i), V(P(5), i), ES(i), E, U, DK, CV,
UTVS, TOTWORK
3400        NEXT i
3410 NEXT k
3420 CLOSE #2
3430 GOTO 130
3625 '
3630 '***** REGRESSION SUBROUTINE
3635 '
3640 '
3650 '***** DETERMINE LOCAL REGRESSION WINDOW LIMITS
3653 '
3654 '*****LIMITS FOR MAIN BODY OF DATA
3655 IF FLAG = 1 THEN GOTO 3728
3660        STRT = 0: FINISH = 0
3670   FOR BEFORE = i TO 1 STEP -1
3680        IF ABS(V(P(2), BEFORE) - V(P(2), i)) > INC / 2 THEN STRT = BEFORE + 1: GOTO
3700
3690   NEXT BEFORE
3700   FOR AFTER = i TO nr
3710        IF ABS(V(P(2), AFTER) - V(P(2), i)) > INC / 2 THEN FINISH = AFTER - 1: GOTO
3722
3720   NEXT AFTER
3722 '
3723        IF STRT = 0 THEN STRT = 1
3724        IF FINISH = nr + 1 THEN FINISH = nr
3725        IF STRT = FINISH THEN FINISH = STRT + 1
3726 GOTO 3756
3727 '
3728 '*****LIMITS FOR BEGINNING AND END OF DATA SET
3730        STRT = 0: FINISH = 0  'HALFINC=increment at start or end of data set
3732        IF i < BEGIN THEN STRT = 1: HALFINC = ABS(V(P(2), i) - V(P(2), 1)) ELSE GOTO
3746
3734        FOR AFTER = i TO nr
```

```
3740            IF ABS(V(P(2), AFTER) - V(P(2), i)) > HALFINC THEN FINISH = AFTER - 1:
GOTO 3753
3742        NEXT AFTER
3744 '
3746        IF i > ND THEN FINISH = nr: HALFINC = ABS(V(P(2), nr) - V(P(2), i))
3748        FOR BEFORE = i TO 1 STEP -1
3750            IF ABS(V(P(2), BEFORE) - V(P(2), i)) > HALFINC THEN STRT = i + 1: GOTO
3753
3752        NEXT BEFORE
3753        IF STRT = FINISH OR STRT >= nr AND i > ND THEN STRT = FINISH - 1
3754        IF STRT = FINISH AND i < BEGIN THEN FINISH = STRT + 1
3755 '
3756        WR = 0
3758 ' ***** DETERMINE LOCAL REGRESSION EQUATION
3760 '      WR=number of window readings
3770 '      TI=time, EI=strain, VSI=vertical stress, SUM before a variable indicates sum over
window range
3774 '
3780 '      TI2=TI^2
3790        WR = FINISH - STRT + 1
3800        AVGTI = 0: AVGEI = 0: SUMEI = 0: SUMTI = 0: SUMTIEI = 0: SUMTI2 = 0
3806        AVGVSI = 0: SUMVSI = 0: SUMTIVSI = 0
3810 '
3820   FOR CALC = STRT TO FINISH
3830        SUMTI = SUMTI + V(P(1), CALC)
3840        SUMEI = SUMEI + V(P(2), CALC)
3844        SUMVSI = SUMVSI + V(P(3), CALC)
3850        SUMTI2 = SUMTI2 + (V(P(1), CALC) * V(P(1), CALC))
3856        SUMTIEI = SUMTIEI + (V(P(1), CALC) * V(P(2), CALC))
3858        SUMTIVSI = SUMTIVSI + (V(P(1), CALC) * V(P(3), CALC))
3870   NEXT CALC
3880        AVGTI = SUMTI / WR
3890        AVGEI = SUMEI / WR
3891        AVGVSI = SUMVSI / WR
3892 '
3900 '
3910        BETA = 0
3920 ' *****SLOPE OF REGRESSION LINE GIVEN BT BETA
3930 '      BETAE=strain rate, BETAVS=stress rate
3935          IF (SUMTI2 - WR * (AVGTI) ^ 2) = 0 THEN BETAE = 1E+15: BETAVS = 1E+15:
GOTO 3960
3940        BETAE = (SUMTIEI - WR * AVGTI * AVGEI) / (SUMTI2 - WR * (AVGTI) ^ 2)
3950        BETAVS = (SUMTIVSI - WR * AVGTI * AVGVSI) / (SUMTI2 - WR * (AVGTI) ^ 2)
3960 '
3980 '
3982        DT = V(P(1), i) - V(P(1), i - 1)
          IF U = 0 THEN DK = 0: CV = 0: GOTO 3990
3984        DK = BETAE * (((1 - V(P(2), i) / 100) * H.INIT) * H.INIT) / U / 200000!
3986        CV = BETAVS * (((1 - V(P(2), i) / 100) * H.INIT) * H.INIT) / 2 / U
3990 RETURN
```

```
5000 ' ***** Apparatus Compressibility Parameters

   ' For the Wissa Device
     AC(1, 1) = .0031
     AC(2, 1) = .2351
     AC(3, 1) = 0
     AC(4, 1) = .001
     AP(1) = 3.37      'piston area
     WP(1) = 2.04      'piston weight
   ' For the Trautwein Device
     AC(1, 2) = .0103  'equation 0.0408(force)^0.578  was original
     AC(2, 2) = .1927   'power
     AC(3, 2) = 0
     AC(4, 2) = .0002
     AP(2) = 3.56
     WP(2) = 1
   'for Penn state device
     AC(1, 3) = 0
     AC(2, 3) = 0
     AC(3, 3) = 0
     AC(4, 3) = 0
     AP(3) = 0
     WP(3) = 0

   RETURN
6000 END
```